

Sheffield Hallam University

Microstructure and precipitation effects in inconel alloy 600.

GANE, Peter James

Available from the Sheffield Hallam University Research Archive (SHURA) at:

<http://shura.shu.ac.uk/3141/>

A Sheffield Hallam University thesis

This thesis is protected by copyright which belongs to the author.

The content must not be changed in any way or sold commercially in any format or medium without the formal permission of the author.

When referring to this work, full bibliographic details including the author, title, awarding institution and date of the thesis must be given.

Please visit <http://shura.shu.ac.uk/3141/> and <http://shura.shu.ac.uk/information.html> for further details about copyright and re-use permissions.

POLYTECHNIC LIBRARY
POND STREET
SHEFFIELD S1 1UB



Sheffield City Polytechnic Library

REFERENCE ONLY

ProQuest Number: 10694098

All rights reserved

INFORMATION TO ALL USERS

The quality of this reproduction is dependent upon the quality of the copy submitted.

In the unlikely event that the author did not send a complete manuscript and there are missing pages, these will be noted. Also, if material had to be removed, a note will indicate the deletion.



ProQuest 10694098

Published by ProQuest LLC (2017). Copyright of the Dissertation is held by the Author.

All rights reserved.

This work is protected against unauthorized copying under Title 17, United States Code
Microform Edition © ProQuest LLC.

ProQuest LLC.
789 East Eisenhower Parkway
P.O. Box 1346
Ann Arbor, MI 48106 – 1346

MICROSTRUCTURE AND

PRECIPITATION EFFECTS IN INCONEL ALLOY 600

by

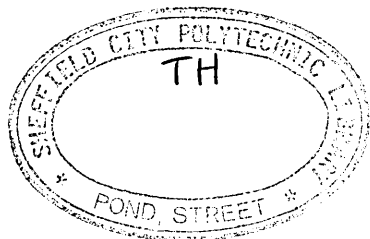
PETER JAMES GANE BSc

A thesis submitted in partial fulfilment of
the requirements of the Council for National
Academic Awards for the degree of Doctor of
Philosophy.

Sponsoring Establishment: School of Engineering
Materials Processing Division
Sheffield City Polytechnic
Pond Street
SHEFFIELD S1 1WB

Collaborating Establishment: Health and Safety Executive
HM Nuclear Installations
Inspectorate.

April 1992



Acknowledgements

I wish to thank the following establishments and people without whom this thesis would not have been possible:

H.M. Nuclear Installations Inspectorate for support through an SERC CASE Award.

Sheffield City Polytechnic School of Engineering for the provision of facilities.

Professor Brian Pickering for his guidance and support.

My parents for their long term support and anxious encouragement to complete this finished version.

Rolls-Royce plc, my current employers, and in particular Julie Clarke for her help and immense patience in preparing the text.

Peter James Gane

April 1992

Reading List/Postgraduate Courses Undertaken

1. Reading List

In addition to the references identified in the main text, the following books have been widely read:

- (i) The Plastic Deformation of Metals
- R.W.K. Honeycombe
Edward Arnold, 2nd edition reprinted 1985.

- (ii) The Fundamentals of Corrosion
- J.C. Scully
Pergamon International Library,
2nd edition 1981.

- (iii) Modern Physical Metallurgy
- R.E. Smallman,
Butterworths, 4th edition 1985

2. Postgraduate Courses

During the course of the research studies the following units from the MSc course 'Industrial Process Management' were undertaken at Sheffield City Polytechnic, September 1985 to June 1987:-

- Computing and Numerical Analysis
- Heat Treatments and Transformations
- High Temperature oxidation resistant materials
- Stainless Steels
- Corrosion.

Abstract

The microstructure and precipitation effects in Inconel Alloy 600

The main objectives of the project were to investigate the interactions of carbon, titanium and aluminium contents, grain size and cold working, with precipitation reactions which occur during heat treatments similar to those experienced as a consequence of commercial PWR Steam Generator (SG) tube processing.

In order to carry out this investigation commercial material was supplemented by a range of experimental casts.

The selected casts allowed the investigation of the following compositional variables:

- (i) the effect of C in alloys free from Ti or Al,
- (ii) the effect of C in alloys containing both Ti and Al, and
- (iii) the effect of Ti in alloys containing constant C and Al contents.

As a result of the experimental programme considerable progress has been made in clarifying the complex structure-property relationships which occur in Alloy 600.

The microstructures observed have been characterised and understood in terms of thermal and mechanical treatments. Studies involving analysis of the mechanical properties, have led to a clear understanding of the effects of grain size, precipitate type and distribution and residual cold work on mechanical behaviour. It has been shown that the activation energy for normal grain growth increases with increasing carbon and titanium contents. Explanations of the mechanical properties have been discussed in terms of grain size, dislocation hardening and solid solution hardening and it has been possible to understand the overall material properties with respect to these.

The kinetics of precipitation have been studied in depth, since it is the precipitation of chromium carbide which ultimately results in the principle mode of material degradation, namely, intergranular corrosion. A range of carbide precipitation 'C-curves' have been established and related to thermal and mechanical processing. Accelerated corrosion testing has provided an insight into the relationship between precipitation and structure on the stability of material in potentially corrosive environments.

C O N T E N T S

- 1 Introduction
- 2 Literature Survey
 - 2.1 Experience with Steam Generator Tube Materials
 - 2.2 Manufacturing Stages for Alloy 600 Steam Generator Tubes
 - 2.3 The Degradation of Alloy 600 Steam Generator Tubes in the Pressurised Water Reactor
 - 2.3.1 Secondary Side Degradation
 - 2.3.1.1 Tube Denting and Pitting
 - 2.3.1.2 Phosphate Wastage
 - 2.3.1.3 Vibration Induced Degradation
 - 2.3.1.4 Environmental Corrosion
 - 2.3.1.5 Controlling Secondary Side Tube Degradation
 - 2.3.2 Primary Side Degradation
 - 2.4 Stress Corrosion Cracking and Intergranular Attack of Alloy 600
 - 2.4.1 Environmental Variables
 - 2.4.1.1 Electrochemical Potential
 - 2.4.1.2 Environment
 - 2.4.1.3 Temperature
 - 2.4.1.4 Deformation
 - 2.4.2 The Effect of Metallurgical Variables
 - 2.4.2.1 Alloy Composition
 - 2.4.2.2 Grain Size
 - 2.4.2.3 Thermal and Mechanical Treatments
 - 2.4.2.4 Low Temperature Sensitisation
 - 2.5 The Optimisation of Variables to Reduce Service Degradation

- 3 **Experimental methods**
- 3.1 Selection of materials for study
- 3.2 Preparation of experimental alloys
- 3.3 Solution treatment of alloys
- 3.4 Cold rolling of experimental alloys
- 3.5 Thermal ageing studies
- 3.6 Hardness determinations
- 3.7 Mechanical property determinations
- 3.8 Optical metallography
- 3.9 Scanning electron microscopy
- 3.10 Transmission electron microscopy
- 3.11 Determination of time-temperature-precipitation
 'C' curves
- 3.12 Corrosion testing
- 4 **Experimental Results**
- 4.1 Evaluation of as-received commercial tubing
- 4.1.1 Identification of precipitate phases
- 4.1.2 Grain size - hardness relationships
- 4.2 Evaluation of solution treated alloys
- 4.2.1 Identification of inclusions in experimental
 alloys
- 4.2.2 Grain size - hardness relationships
- 4.2.2.1 Commercial tubing
- 4.2.2.2 Series I
- 4.2.2.3 Series II
- 4.2.2.4 Series III
- 4.2.3 Mechanical properties of experimental alloys
- 4.3 Evaluation of solution treated and thermally aged
 alloys
- 4.3.1 Hardness

- 4.3.1.1 Series I
- 4.3.1.2 Series II
- 4.3.1.3 Series III
- 4.3.2 Precipitation of carbides
 - 4.3.2.1 Series I
 - 4.3.2.2 Series II
 - 4.3.2.3 Series III
- 4.4 Evaluation of solution treated and cold rolled experimental alloys
 - 4.4.1 Hardness
 - 4.4.2 Tensile properties
- 4.5 Evaluation of solution treated, cold rolled and thermally aged experimental alloys
 - 4.5.1 Hardness
 - 4.5.2 Tensile properties
 - 4.5.3 Recrystallisation Kinetics
 - 4.5.4 Precipitation of carbides
- 4.6 Corrosion testing of experimental alloys
 - 4.6.1 Solution treated and thermally aged alloys
 - 4.6.2 Solution treated, cold rolled and thermally aged alloys
- 5 **Discussion**
 - 5.1 Identification of Precipitate Phases
 - 5.1.1 Carbide Phases present in As-Received, Solution Treated and Aged Commercial Alloys.
 - 5.1.2 Inclusions present in commercial and experimental alloys.
 - 5.1.3 Carbide phases present in solution treated and aged experimental alloys
 - 5.2 Structure and properties of as-received commercial tubing

- 5.2.1 Variability of grain size
- 5.2.2 Prediction of mill annealing temperatures
- 5.2.3 The effect of chromium carbide dispersion on the grain size
- 5.2.4 The effect of titanium on the grain size
- 5.2.5 Factors affecting the hardness of as-received commercial tubing
- 5.2.6 Petch relationships for solution treated commercial tubing
- 5.3 Effect of carbon content on structure and mechanical properties
 - 5.3.1 Alloys containing no titanium or aluminium
 - 5.3.2 Alloys containing 0.25/0.30% Al and 0.21/0.29% Ti
- 5.4 Effect of Titanium content on structure and mechanical properties
- 5.5 Grain boundary pinning particles
- 5.6 The effect of thermal ageing on microstructure and properties
 - 5.6.1 Hardness
 - 5.6.2 Precipitation of carbides
- 5.7 The effect of cold work prior to thermal ageing on microstructure and properties
 - 5.7.1 Hardness and tensile properties
 - 5.7.2 Precipitation of carbides
- 5.8 The influence of microstructure and properties on the corrosion response of Alloy 600
 - 5.8.1 Solution treated and thermally aged alloys
 - 5.8.2 Solution treated, cold rolled and thermally aged alloys.

- 6 **Conclusions**
- 6.1 Precipitation Reactions
- 6.2 Grain size control
- 6.3 Mechanical Properties
- 6.4 Corrosion behaviour
- 7 **Further work**

References

Tables

Figures

1 INTRODUCTION

Nickel-iron-chromium alloys of the nickel rich type are of considerable industrial importance. Chromium contributes good corrosion resistance whilst high nickel results in the retention of mechanical properties at elevated temperatures.

Inconel 600 Alloys, commonly known as Alloy 600, are based on the composition 76% nickel, 7% iron and 16% chromium. They were developed by introducing chromium into nickel using the most economic source, Ferro-chromium. Alloy 600 was originally utilised for the dairy industry due to its excellent resistance to corrosion by milk, but has now been replaced in this application by cheaper Austenitic Stainless Steels. Alloy 600 has found other important uses as a result of its good corrosion resistance in a variety of media, both acid and alkaline, oxidising and reducing. The selection of this material for pressurised water reactor (PWR) steam generator (SG) tubing was on the basis of its resistance to chloride stress corrosion cracking (SCC), coupled with its low rate of general corrosion in high purity water and boric acid solutions.

Pressurised water reactors have up to four steam generators, these being the means of heat exchange between the radioactive core and the turbines producing electricity. Steam generators are the second largest component in a nuclear steam supply system, being exceeded in size only by the reactor itself, Figure 1. Each SG unit contains several thousand relatively thin walled

(approximately 1 mm) tubes, which form the interface between the primary reactor coolant (relatively pure water contaminated with boric acid, acting as a neutron absorber and hydrogen added to suppress oxygen generation) and fluid in the secondary, or steam side (purified river, lake or sea water), these tubes being in an inverted 'U' configuration and sealed in a base plate to form a continuous loop. In this manner the primary coolant is continually recirculated.

Steam generators in PWRs experience a wide range of degradation problems on both primary and secondary sides of the tubing. On the primary side, water heated to approximately 325°C via contact with the core, is prevented from boiling by pressure applied to the sealed loop from pressuriser units. Problems associated with the primary side of SG tubes result from the presence of high levels of stress in a corrosive environment maintained at a high temperature. The principle degradation mode of Alloy 600 in such environments is stress corrosion cracking of the intergranular form (IGSCC). The superheated water circulating on the primary tube side heats water on the secondary side via conduction across the tube wall, the number of tubes being calculated to provide the necessary surface area for adequate heat exchange.

Water on the secondary side is not pressurised and therefore boils, producing steam which subsequently drives turbines to generate electricity. During boiling, non-volatile impurities present in the secondary side feedwater

can concentrate in stagnant regions such as crevices in the tube base plate and support plates, Figure 2. The concentration of contaminant impurities (salts) in crevices may lead to localised corrosion problems which account for a large proportion of secondary side tube degradation (1,2,3).

Efforts to reduce or eliminate all the SG tube degradation problems has resulted in modifications to plant design and integrity, water chemistry and metallurgical factors such as initial material selection and processing routes. Since the early 1980's PWR SG units have begun to use Alloy 600 tubes with a revised heat treatment condition. Tubes are now thermally treated (TT) after mill annealing (MA) and extensive testing has demonstrated an increased resistance to degradation by localised corrosion compared to the more usual 'MA' processed material (4).

2 LITERATURE SURVEY

2.1 Experience with Steam Generator Tube Materials

The worldwide experience with SG tube materials to the end of 1979 is presented below (5). The data shows that Alloy 600 was the most widely used material, accounting for some 74% of all tubes in service. The tube defect rates for Alloy 600 also show the highest occurrence, although most of the defect mechanisms are independent of the actual tube material, eg 'denting' of the tubes resulting from corrosion of the carbon steel base plate.

Tube Material	No of Reactors	No of Tubes in Service	% Tubes in Service	% Tubes with Defects	Failure* Mechanism
Alloy 600	69	974232	74	2.0	SCC, W, D, Fr, F
Monel 400	8	167700	13	0.2	SCC, Fr
Incoloy 800	8	101119	8	0.05	W
Austenitic Stainless	9	71922	5	0.9	SCC, W

* Abbreviation Key:-

D = Denting

SCC = Stress Corrosion Cracking

Fr = Fretting

F = Fatigue

W = Phosphate Wastage

A more recent analysis of worldwide tube performance, covering the period up to 1983-84, has been conducted by the same author (6). Figure 3 graphically depicts the way in which possible degradation mechanisms have accounted for actual or suspected tube failures over the period 1972 - 1984. Thermally treated Alloy 600 tubing has only been introduced since the early 1980's and so is not included in this data. The information relates to mill annealed material which is widely reported to have a significantly higher degradation rate.

For tabulating purposes, a steam generator tube defect (or failure) is defined as any tube plugged, to effectively isolate it from the steam system, for whatever reason. It is important to note that tubes which actually fail by developing a primary to secondary leak are a small proportion of the total number of tubes plugged. During 1983 and 1984, 1.1% and 1.3% respectively, of tubes plugged had actually leaked. Additionally, 0.6% and 1.0% respectively, represent tubes taken out of service (extracted) for metallurgical examination. The majority of tubes are plugged because they have been identified as potential future leakers by non-destructive testing, or because of their position in failure prone areas of some steam generators. Figure 4 details the number of reactors affected by tube failure as a result of the various degradation modes. These forms of degradation are discussed at length later in the survey. Figure 5 further analyses this information in terms of the actual number of tubes plugged as a result of the specific degradation modes.

2.2 Manufacturing Stages for Alloy 600 Steam Generator

Tubes

Tubing used for PWR steam generator application has an outside diameter of approximately 18 mm and a nominal wall thickness of 1.1 mm. Tube manufacture is by a combination of mechanical and thermal processes under strictly controlled conditions. Processing variables have a considerable effect on the structure and properties of the finished tubing and so must be clearly understood.

Improvements in material performance have resulted from a detailed study of the effects of these variables, at the various stages, on the final metallurgical condition of the tubing. A summary of the processing route as used by Vallourec (7) is presented below:-

Key Manufacturing Steps

Alloy Melting

(Vacuum Induction Route)

Bar Forging

(Approximately 220 mm Diameter)

Hot Extrusion to Hollow Shell

(Approximately 90 mm OD x 12 mm ID)

Cold Reduction to Final Dimensions via

Cold Pilgering Process

Multiple Step Operation with Intermediate

Mill Anneals

Final Cold Reduction to Finished Size Via
Cold Pilger or Drawing Process
Drawing used for Strictest Dimensional
Requirements

Final Mill Anneal

Roll Straightening

Surface Preparation

Blasting on ID and Grinding on OD

Non-Destructive Examination

Eddy Current and Ultrasonic Techniques

Special Thermal Treatment (TT)

(Optional)

Bending of 'U' Sections

Stress Relieving of Tight U-Bends

Final Inspection and Packing

The successful production of tubing suitable for PWR steam generators relies on the strict control of each processing stage. The method of manufacture and condition of supply are arrived at via discussion with the customer and an in-depth appreciation of the final service requirements.

The cold pilgering operations, to reduce the hollow extruded shell (90 mm OD x 12 mm ID) to the final tube size (18 mm OD x 16 mm ID), in conjunction with the intermediate and final mill annealing operations, largely determine the service structure of the material. Intermediate and final mill anneals allow the cold worked alloy to recrystallise, and so control the grain structure and chromium carbide distribution and morphology. The introduction of a special thermal treatment has provided an additional means of modifying the crucial morphology and distribution of the carbides, and has been a major factor in increasing the resistance to degradation of the tubing in service.

The manufacturing route has evolved to produce tubing suitable for the service environment. PWR steam generator tubing must have adequate tensile strength at the elevated service temperature in conjunction with excellent resistance to the various forms of corrosion degradation. The control of alloy composition, grain size and carbide distribution are critical in developing an acceptable product. The use of non-destructive examination, by ultrasonic testing, ensures the rejection of any defects resulting from the manufacturing process. Residual stress, particularly from U-bending and straightening operations, must be relieved or both tensile and corrosion properties would suffer.

In spite of the tight controls imposed for tube manufacture there will always be some degree of process variability. In service, variability of Alloy 600 steam generator tubing

is widely reported and is due to manufacturing variability, resulting in a distribution of structures and properties, as well as variations in operating environments.

The introduction of an additional heat treatment, following the non-destructive examination, was developed as a response to a new problem in more or less pure water which was termed 'Coriou' cracking (8). Simultaneous research was also undertaken to find a microstructure with an increased resistance to intergranular stress corrosion cracking (IGSCC). The presence of residual stress resulting from manufacture, and a microstructure sensitive to Coriou type and intergranular stress corrosion cracking, were identified as key parameters affecting in-service tube degradation (9).

An early attempt to desensitise the microstructure involved reducing the mill annealing temperature, in order to allow recrystallisation to occur without dissolving the chromium carbides. This approach produced a recrystallised microstructure with chromium carbides inherited from the hot worked structure, hence intergranular carbides were largely avoided. Intergranular sensitisation should therefore no longer be a feature which could lead to IGSCC. However, extensive environmental testing revealed that such a microstructure was unsatisfactory since, although precipitation sites would principally be at the preexisting intragranular carbides, a structure consisting of large discrete intragranular carbides and smaller highly sensitised grain boundary carbides would be produced.

Another alternative evaluated was to increase the alloy's resistance to SCC by lowering its yield strength. Modifications to cast chemistry (principally carbon) and processing (mill annealing temperature) brought about this change. However, this approach proved unacceptable due to the mechanical property requirements by the users. The possibility of shot peening to ensure compressive surface stresses was also considered, but deemed to be difficult to control within very tight limits and therefore unreliable.

The final decision was to move to a thermal solution to the problem which would simultaneously relieve residual manufacturing stresses and fully desensitise the microstructure. The selection of a special thermal treatment, consisting of 15 hours at 704°C was arrived at, after consideration of the process of desensitisation and the requirement for stress relieving without introducing distortion. Desensitisation relies upon the alloy being held for a sufficient time period inside the precipitation domain where chromium carbides form. Initially, carbon held in solid solution (from the final mill anneal) will precipitate as chromium carbides, principally at sites of greatest diffusion rate such as grain boundaries and grain boundary triple points, with an initial surrounding depletion of the matrix chromium level. Additional time at temperature allows further chromium diffusion to occur and a 'healing' of depleted regions surrounding the carbides. The end result is a microstructure which is stress free and consists of relatively few intragranular carbides remnant from mill annealing, with fully desensitised carbides located mainly at the grain boundaries.

2.3 The Degradation of Alloy 600 Steam Generator Tubes in the Pressurised Water Reactor

A survey of the published literature concerning Alloy 600 SG tubes in PWRs reveals a wide range of types of degradation in service. Section 2.1. of this survey indicates the extent of the general problem with the distinction being made between primary and secondary sides of the steam generation loop. This present survey follows this convention and, where possible, categorises degradation against it's prime area of attack, that is the primary or secondary side of the tubing. Crevice type corrosion on the secondary side of the tubing can be neatly categorised, whilst other modes of degradation such as stress corrosion cracking, affect both primary and secondary sides. A detailed consideration of purely secondary side modes of degradation is presented before moving on to discuss primary side attack and mechanisms common to both sides of the tubing.

2.3.1 Secondary Side Degradation

Leaving aside stress corrosion cracking (SCC) and Intergranular Attack (IGA), which topics will be discussed in detail later, secondary or steam side degradation problems owe as much to the steam generator design as to the material susceptibility. These problems largely result from design features such as:-

(i) The selection of a 12 inch thick tube base plate. This base plate is a ferritic steel forging and may suffer from an expansive corrosion product, leading to crushing or 'denting' of the SG tubes.

(ii) The existence of a 'Crevice', where the tubes are sealed into the base plate and where they pass through support plates positioned along their length, Figure 2.

(iii) Vibration of the tube bundle (each SG contains several thousand tubes, Figure 1), which is a consequence of compromising the necessary tube configuration against the attainment of adequate secondary fluid flow, to ensure satisfactory heat extraction.

2.3.1.1 Tube Denting and Pitting

Corrosion of the tube base plate results in local crushing of the tubes and is termed 'Denting'. Widespread examination of tube base plate intersections removed from operating steam generators has confirmed this mechanism (10).

The occurrence of substandard feedwater conditions, arising from the presence of sea, river or lake water salts, ingressing via leaking condensers in the turbine plant, has allowed the concentration of corrosive salts to occur in the tube base plate crevice. Such concentrations have caused corrosion of the ferritic steel base plate and resulted in tube denting. The cause of denting is well

explained by Potter - Mann (11) type linear accelerated corrosion in which a non-protective oxide layer, magnetite (Fe_3O_4), is formed as corrosion progresses. The magnetite corrosion product, which occupies about twice the volume of the parent metal, grows in the base plate crevice. The large volume expansion causes considerable radial stresses to be exerted on the tubing and base plate which can result in the simultaneous deformation of both. As denting progresses both tube and base plate can crack. Denting produces non-uniform deformation, with the resultant strain level in the tubing being determined by the shape and extent of the corrosion product.

It has been shown (10) (12) that chlorides are the most likely salts to cause denting and also that copper chloride is the most aggressive of all chlorides that may be present. The denting phenomena has been experienced where sea, lake and river water are used as the secondary side coolant (13).

An additional problem in terms of feedwater chemistry is the combination of high oxygen concentrations and relatively low pH levels which lead to corrosion of components in the turbine plant. Simultaneous with tube denting, localised pitting corrosion can occur. Oxygen is not the only oxidising species that promotes localised pitting corrosion and evidence suggests that copper and nickel oxides are also responsible. Chloride anions and copper cations have been reported to play the most detrimental role in pit nucleation and growth (14) (15).

The presence of metallic copper on top of magnetite deposits is well known in conventional boilers where copper alloy components are widely used in feedwater pipework. The detrimental presence of copper emphasises the need to consider all possible corrosion consequences for the steam/water system as a whole when materials are selected for any individual component.

Acid attack, either generally or locally, can be inhibited by the addition of an alkali, such as sodium hydroxide or phosphate, which prevents the accumulation of acid chloride concentrations (16). During the mid 1970's PWR plant operators responded to the widespread problem of tube denting (and localised pitting) and began to introduce phosphates into the bulk secondary side water in an attempt to combat the effects of contaminant acid salts. PWR stations in the USA opted for phosphate levels significantly higher than their European counterparts. However, the introduction of phosphate water treatment, whilst overcoming tube denting, did itself result in a new form of secondary side corrosion, termed 'phosphate wastage', where the alkali additions became the cause of corrosion.

2.3.1.2 Phosphate Wastage

Subsequent to the introduction of phosphate water treatment to control tube denting, it was discovered that a generalised thinning of the tubes was occurring where sludge built up in the base plate and tube support plate

crevices. The phosphates added to control acid corrosion were themselves concentrating to corrosive levels, causing tube degradation. Phosphate induced tube thinning, or wastage, was sometimes widespread and could occasionally be accompanied by stress corrosion cracking (SCC) (5).

As the sludge (a combination of phosphates and metal oxides) builds up in crevice locations, a critical height is reached where liquid can no longer penetrate to the lower sludge region to replace liquid being vapourised by boiling during steam generation. These processes are essentially the same as those postulated for the concentration of acid salts in the tube base plate crevice which results in denting. At large sludge heights a steam blanketing condition probably exists near to the base and support plate which allows no liquid to circulate and hence no associated build-up of solids to occur. The temperature in this region approaches the primary coolant temperature. Near the upper surface of the sludge, adequate circulation of liquid exists and no concentration of aggressive phosphates occurs. The most corrosive region is judged to be the intermediate region where alternate wetting and drying occurs, figure 2. It soon became noticeable that the adoption of phosphate treatment was proving unsatisfactory in the prevention of tube sheet corrosion, since it brought about its own corrosion problems. As a result, the industry opted to reduce ion ingress from the feedwater by using an all volatile treatment (AVT) chemistry.

The all volatile water chemistry is based on the use of ammonia and hydrazine which, whilst neutralising acid salts, do not themselves concentrate in crevice locations. Thus, for phosphate wastage, the cause was determined to be an aggressive environment, and the corrective action involved a change in the environmental additions from a phosphate chemistry to AVT.

Simultaneous with the introduction of AVT, control of the general secondary side water chemistry and the importance of strict control of the entire system became a priority. Condenser leaks were traced and repaired whilst air ingress positions, responsible for high oxygen levels, were sealed. The control of secondary water was improved with a marked decrease in allowed impurity levels. The introduction of AVT and condenser demineralisation (CD) resulted in a dramatic reduction in the occurrence of tube wall thinning (wastage) and this mode of degradation is no longer considered to be a serious problem (5). The use of AVT and CD has resulted in these reactors showing a low incidence of tube defects because of corrosion from the secondary side.

2.3.1.3 Vibration Induced Degradation

The principle cause of vibration in steam generators is the constantly recirculating secondary side water. The dynamic processes of water circulation and boiling on the secondary tube side produces vibrations which are usually of a small amplitude and high oscillatory frequency in nature. Such vibrations cause local rubbing or 'fretting' between the

tubes and their support plates situated along the tube bundle length. Fretting will result in detrimental local metal loss, thus reducing the tube wall thickness, and can also leave these regions highly susceptible to fatigue cracks (17). It has been observed that under such conditions fatigue cracks can be initiated close to the tube surface at very low stresses, well below the fatigue limit for non-fretted material.

In the recirculating steam generators the most likely regions for vibration and possible fatigue failure to occur is the inlet region above the tube sheet and in the U-bend region where velocities are highest with fluid flow transverse to the tubes. Fatigue cracking has not been reported in these areas of PWR steam generators, but cracking has occurred in once through units where secondary side coolant is discharged after steam has been raised, and considerably greater operating experience exists for such cases (17) (18). Additional factors which may affect such failures include entrained water (flow loading), uneven flow distribution and bowing of lance tubes (bending stresses), where lance tubes are incorporated to facilitate the mechanical removal of built-up sludge in static flow regions. Turbine valve testing, auxiliary feedwater injection and water hammer are further factors leading to cyclic tube stresses (19)(20). Evidence presented by the CEGB (21) concludes that vibration induced damage is not a problem on model 'F' steam generators (as designated for Sizewell 'B'), due to the introduction of anti-vibration bars which effectively damp out operating and transient vibrations.

2.3.1.4 Environmental Corrosion

Alloy 600 SG tubes removed from operating PWR stations have shown extensive forms of intergranular corrosion on the secondary side. The majority of corrosion has been confined to crevice locations, but it should be noted that actual tube leaks are very rare (4). Stress corrosion cracking (SCC) and intergranular attack (IGA) are the corrosion modes affecting the secondary side of the tubes. Some fourteen reactors were affected in 1982 by such corrosion (22).

In the case of stress corrosion cracking, the corrosion morphology consists of a single or multiple major crack with minor to moderate amounts of branching. Cracks propagate along intergranular paths in the majority of cases. It is now widely accepted that a high stress level is necessary in order for intergranular stress corrosion cracking (IGSCC) to propagate rapidly. The second form of intergranular corrosion affecting the secondary side has been described as general intergranular attack (IGA) or volumetric IGA. Its morphology is characterised by a uniform or relatively uniform attack of all grain boundaries over the surface of the tubing. A distinguishing feature between IGA and IGSCC is the lack of any evidence for a stress contribution to the morphology of IGA. The two degradation mechanisms are often grouped together, since they frequently occur at the same location and are believed to be caused by an alkaline environment. A third form of intergranular corrosion, termed intergranular penetration (IGP) has been variously

described as a mixture or hybrid between the other two forms.

The most important locations for all the above forms of corrosion are (i) the tube/tube sheet crevice and (ii) the tube/tube support plate crevice. In eleven of the reactors surveyed by Tatone and Pathania in 1984 (22), tube degradation occurred in the deep tube to tube sheet crevice, while in two other reactors, support plate crevices were primary sites.

A short term solution to secondary side SCC/IGA has been to install sleeves within the affected tubes, thus preventing possible loss of coolant due to tube rupture. Additional means include removal of sludge build up by mechanical or chemical means, although the effectiveness of this remedy is unclear.

A detailed consideration of SCC and IGA mechanisms occurring on the secondary side will follow in Section 2.4 of this review. Environmental and metallurgical factors affecting SCC and IGA on the primary side will be discussed at the same time.

2.3.1.5 Controlling Secondary Side Tube Degradation:

Proposed Design Modifications

The various mechanisms which result in secondary side tube degradation can be combated by modifications to the design and operating conditions of the steam generator unit.

Tube denting was a significant problem during the 1970's and by 1977 had resulted in the formation of the Steam Generator Owners Group in the USA (23). As previously discussed, denting at tube sheet and support plate crevice locations has largely been controlled by the introduction of an all-volatile plus condenser demineralisation water regime, thus preventing expansive corrosion products being produced in crevices, strict control of deleterious oxygen ingress and a change in the support plate material (23) (24) (25) (26).

The substitution of carbon steel support plates by 12% Cr ferritic stainless steel alternatives resulted from laboratory tests which concluded that such a stainless steel is effectively resistant to corrosion in the water environment as controlled by AVT. However, evidence has been presented which suggests that whilst corrosion of a stainless steel support plate will be significantly lower than for the carbon steel equivalent, there is still some possibility of denting over long periods of time (10). Such a possibility will become more likely at higher salt concentrations, therefore strict water chemistry control will remain a vital priority.

The problem of denting of the base plate crevices cannot currently be resolved by a similar material substitution. The requirements for the base plate to be some twelve inches thick and produced from a forging, imposes forgeability problems if ferritic stainless steel was to be used. The control of tube denting in these regions must

therefore be by alternative means which utilise feedwater chemistry control and a reduction of the tube sheet crevice.

Methods of reducing the tube sheet crevice are via full depth hydraulic expansions and mechanical rolling of the tubes into the base plate.

Full depth hydraulic expansion has been proposed in order to reduce the crevice to a small region not greater than 6.3 mm deep. While such a modification will reduce the crevice and produce a more uniform level of stress, a small crevice will always persist. The nature of the denting phenomena requires only a small crevice for its initiation and so it may still occur and ultimately lead to circumferential cracking. Long term data supporting the beneficial effect of a reduced crevice is not available, but evidence does suggest that mill annealed Alloy 600 can be affected by localised IGA in such regions (27). In contrast to full length hydraulic tube expansion, as favoured in the USA, French PWRs have opted to use mechanical rolling to effect a reduction in the tube sheet crevice (9).

In France mechanical rolling is used to expand and seal tubes into the tube sheet. This causes considerable deformation, from the action of the helical rolling, but produces a very tight fit with only a negligible residual crevice. In the USA, where hydraulic expansion is used, the result is a lower and more uniform level of deformation

and stress, but produces a 'looser' fit with the possibility of a small crevice. The French technique may therefore leave tubes more susceptible to SCC, due to the higher level of induced stress, whilst the American techniques may result in the concentration of aggressive contaminants in the residual crevice and hence the occurrence of denting over extended time periods.

A further proposed modification to reduce the possibility of contaminant sludge build-up at support plate intersections is to replace drilled holes with broached holes of the quatrefoil configuration. This modification, to be incorporated in the model 'F' steam generators for Sizewell 'B', will promote high velocity flow along the tubes thus sweeping away impurities and preventing detrimental sludge build-up (28).

Corrosion tests have indicated that corrosion (IGA/SCC) and tube denting are both reduced as the heat flux decreases, leading to the possibility that at some reduced, but finite heat flux such forms of degradation may not begin or are arrested (29). The effect of temperature on both primary and secondary side corrosion will be discussed at length in later sections of this review.

A review of Japanese practices revealed ten instances of steam generator tube leakage in the period up to 1984. However, leakage rates in Japanese PWRs have been kept to a minimum owing to a strict adherence to the following measures (30):-

(i) When degradation is encountered in even a single tube, all tubes in each steam generator affected are inspected over the full length.

(ii) All tubes with defect indications are replaced by either introducing a thermal sleeve or isolating the tube by plugging (sealing off). In practice it is usually so difficult to make qualitative judgements on the basis of non-destructive evaluation indications (Eddy Current) that all such 'suspect' tubes are either plugged or sleeved.

(iii) Rigorous water chemistry regimes are strictly adhered to.

(iv) Impurities which cause degradation, such as metal oxide sludge accumulation on the secondary side, are removed during annual outages.

The adoption of these 'common sense' procedures has resulted in a very low occurrence of tube ruptures in service.

2.3.2 Primary Side Tube Degradation

Degradation of SG tubes on the primary, or pressurised circuit, side is by the mechanism of stress corrosion cracking. The reported occurrence rate of primary side SCC is comparable to that of the principle secondary side mechanisms of SCC and IGA. The absence of any coolant boiling on the primary side indicates that this form of

degradation arises from the susceptibility of stressed Alloy 600 to SCC in high temperature water (up to 325°C). The principle areas affected by SCC are the most highly stressed locations, such as the tight U-bends in the innermost rows, and the locally expanded regions where the tubes are sealed into the tube sheet.

It is possible to identify the generic factors which will lead to SCC of Alloy 600 on both primary and secondary tube sides. These factors are:-

(i) a 'sensitised' material condition, which equates to the as mill annealed state.

(ii) the presence of 'high' stress levels with a surface tensile component.

(iii) the presence of a corrosive environment. On the primary side this relates to relatively pure water at high temperature, and on the secondary side to salt concentration at lower temperatures.

Temperature has been identified as the major environmental factor which influences the initiation of SCC from the primary side (29). The effect of temperature will be discussed later, but the trend is for a reduction in the rate of occurrence of SCC as the temperature is decreased. It has been reported that less corrosion is seen at the outlet leg ('cold') of SG U-tubes than at the inlet leg ('hot') location.

The microstructural aspects of SCC, ie the 'sensitivity' of the material, is related to the final mill annealing temperature and any subsequent thermal treatments. The most susceptible microstructures are those produced using low mill annealing temperatures (less than 980°C) which develop a fine grain size (ASTM 9-11) and contain a copious quantity of intragranular carbide (4). The grain boundaries of these materials usually contain little, if any, carbide (31) (32). Grain boundary carbides, therefore, appear to be beneficial in terms of reducing primary side SCC. Coriou (32) was the first to publish results which indicated that material which received a heat treatment to precipitate grain boundary carbides, had improved resistance to SCC in high temperature water.

Later work by Domain et al (33) and EPRI (34) confirmed this, with the added comment that an improvement in primary side SCC was found to be associated with grain boundary precipitation with or without any grain boundary chromium depletion. An in-depth consideration of the effects of microstructure and SCC will be presented in Section 2.4 of this review.

The main source of stress is residual stress inherent from the design of the steam generator, the tube manufacturing process and from installation. Stresses arising from water pressure and thermal gradients can also provide significant stress effects, and so increase the susceptibility to SCC. Apart from modifying the microstructure, corrective actions have also been aimed at reducing the level of residual

stress. Laboratory tests have indicated that in-situ stress relief of the inner-row U-bends is practicable, using resistance heaters pulled up to and around the bend (29). Airey (4) evaluated the effect of in-situ annealing on highly susceptible mill annealed tubing. Material in the tight U-bend configuration was annealed in the 593°C to 816°C temperature range for times up to one hour, and exposed to pure water and caustic environments. SCC was only observed in U-bends annealed at the lowest temperature for the shortest time (593°C for one minute). It was concluded that the SCC resistance of stressed Alloy 600 U-bends can be readily improved by an in-situ anneal in the 593°C to 816°C temperature range for a comparatively short time (15 minutes recommended). There was little discernible microstructural modification associated with these annealing parameters and it can be concluded that the beneficial effect is due to a reduction in the residual stress level. This conclusion has been confirmed by x-ray residual stress measurements and additional microstructural investigations (35).

The annealing of tubing prior to bending has also been shown to reduce the level of U-bend residual stress (36). The effectiveness of this treatment prior to bending is attributed to the recovery of a surface layer deformed during tube manufacture. The surface component of residual stress, arising from the finishing stages of tube manufacture (section 2.2), is relieved prior to bending and so the overall stress level is reduced. It is apparent that the reduction in the surface residual stresses from tube manufacture is as important as the reduction of

stresses produced during bending and installation. The post mill anneal thermal treatment ensures that residual stresses are relieved, as well as modifying the grain boundary microstructure to reduce SCC susceptibility.

The reduction of residual stress in the expanded tube sheet locations has been investigated in relation to counteracting the induced tensile stress by applying a compressive stress via shot peening (36). The use of shot peening is widespread in engineering to counter operating tensile stresses and so increase loading potential. Shot peening has the advantage of accessibility via specially designed lances, and so can reach awkward locations such as the inside diameter of SG tubes expanded into the tube sheet. However, it is necessary that the balance is maintained between the induced inside diameter compressive stresses and the resultant outside diameter tensile stresses. The possibility of a resultant increase in the rate of secondary side SCC needs to be evaluated in relation to Water Chemistry and possible sludge pile accumulation.

The existence of a corrosive environment on the secondary tube side is readily comprehensible, but the existence of 'pure' water acting as a corrosive medium on the primary side is less obvious. Primary water usually contains approximately 650 ppm boron as boric acid (acting as a moderator), trace levels of lithium hydroxide to inhibit SCC by producing borate anions and a hydrogen over pressure sufficient to prevent the generation of oxygen gas (37).

The effect of environment on SCC susceptibility will be considered in subsequent sections with an emphasis on identifying the controlling mechanisms and assessing their industrial significance.

The occurrence of primary side SCC relies upon the simultaneous existence of the three generic factors previously identified. If any one of these factors could be removed then SCC would not occur. The following survey considers the factors which lead to SCC in Alloy 600 with the distinction being made between primary and secondary tube side mechanisms where possible. Environmental factors can be categorised in this way, but microstructural susceptibility, and its control, will have implications for both primary and secondary side SCC.

2.4 Stress Corrosion Cracking and Intergranular Attack of Alloy 600

2.4.1 Environmental Variables

Data presented in Section 2.1 of this review indicates that SCC is a significant cause of the degradation on both primary and secondary sides. Almost all the SCC failures of Alloy 600 tubes in SG service prior to 1975 originated from the secondary side. The only instances of SCC originating from the primary side were in regions of high residual stress, such as the tight inner-row U-bends and tube expansions (38). The occurrence of SCC on the primary side during the 1970's was a rare event, and so most of the early research concentrated on Secondary Side SCC which was thought to be due to the build-up of caustic environments in areas of poor circulation.

In 1976 a tube failure was located at the apex of a tight U-bend and was attributed to primary side initiated SCC. During subsequent years further failures occurred which originated from the primary side, often in locations where secondary side denting had increased the local concentration of residual stress (such as tube support plate locations). There have also been instances of Primary Side SCC in areas which do not suffer from Secondary Side denting (39). The recognition of SCC as a failure mode, from which a single tube rupture could force a complete shut-down, has directed efforts to understand the mechanism of SCC in Alloy 600 in both primary and secondary water environments.

2.4.1.1 Electrochemical Potential

It has been widely reported that electrochemical potential is of key importance in the cracking behaviour of Alloy 600 in both primary and secondary water environments. Van Rooyen's review in 1975 (40) indicated that Alloy 600 can be rendered susceptible to SCC under certain electrochemical potentials where the protective oxide film is unstable in the test environment. Anodic dissolution of the surface oxide in conjunction with mechanical tearing and cleavage can result in this form of localised corrosion.

The use of controlled electrochemical potential testing is important since it is possible to assess material SCC susceptibility using discretely controlled parameters which are known to result in maximum SCC. In essence this form

of controlled testing will allow the relative SCC susceptibility of various material conditions to be ranked one against the other. The environmental conditions of water composition, pH and temperature, in conjunction with the material heat treatment condition and level of stress need to be identified.

In service Alloy 600 SG tubes are coupled to the Carbon Steel base plate, and as a result of the different electrochemical potentials of the two materials an electrochemical cell is formed which will have a measurable circuit potential. The susceptibility of Alloy 600 to SCC will then depend upon the influence of this cell potential upon the surface oxide stability in the water environment. The stress state of the material, resulting from combinations of residual stress from manufacture and fabrication along with contributions from active service deformation (such as tube crushing or 'denting'), will alter the cell potential and may effect the oxide stability and SCC susceptibility. Although the stability of the protective oxide film will be a function of the electrochemical potential and water environment, the initiation and propagation of SCC will depend upon the existence of microstructural effects and applied stress. This concept has previously been described, and it is important to note that accelerated electrochemical potential testing relies upon the existence of these contributing parameters in order to assess relative levels of SCC susceptibility.

The effect of coupling Alloy 600 to other metals has been investigated by Coroiu and Blanchet (32). The precise experimental conditions were not reported but it was found that coupling to gold suppressed SCC in pure water, whereas coupling to stainless steel had a neutral effect, and coupling to low carbon steel accelerated SCC. The tests were repeated in water with the pH adjusted to 11.5 by the addition of LiOH (a constituent of primary water). The harmful effect of coupling to low carbon steel persisted, whilst no trace of SCC was detected as a result of coupling to gold or stainless steel. Although the electrochemical potentials were not reported, it is evident that these experiments demonstrate the importance of this parameter for controlling SCC in Alloy 600. Furthermore, the important effect of water chemistry adjustments is highlighted and indicates that it may be possible to reduce SCC occurrence by this means.

The use of controlled electrochemical testing as a means of material SCC susceptibility evaluation will be referenced in subsequent sections of this review. The understanding of Alloy 600's sensitivity to environmental factors is important and can result in the optimisation of service performance.

2.4.1.2 Environment

In the context of this review, 'environment' refers to the primary and secondary water chemistries. The exact analysis of primary and especially secondary water depends

upon the individual plant preferences and locality. The evaluation of SCC susceptibility has concentrated on the effect of minor constituent variations, such as dissolved oxygen and boric acid levels, with and without the contributory effects of other factors identified as increasing SCC, such as deformation, heat treatment condition and electrochemical potential.

The primary coolant consists of borated water (less than 4400 ppm boron) with a trace of lithium hydroxide (0.2 to 1.0 ppm Li) and a H₂ overpressure of approximately 0.1 MPa. Airey (31) evaluated the effect on the protective surface oxide and SCC susceptibility in pure water and primary water chemistries with and without hydrogen present. The advanced analytical techniques used showed differences between coupons exposed in autoclaves operating with or without a hydrogen overpressure. The oxide film composition varied between the two tests and the conclusion that hydrogen affects the oxide film in a detrimental manner was made.

The findings of Airey supported those of Bulischeck (37) who reported that SCC initiation times are shorter in hydrogenated primary water compared with pure water. A possible comment on these findings is that a reduction in hydrogen levels should be considered, but this proposal must be carefully evaluated against the need to suppress oxygen generation. An additional conclusion from Bulischeck's study was that there was no significant difference between the behaviour of Alloy 600 in either primary or pure water at 365°C in the absence of hydrogen.

The effect of lead as a contaminant in high temperature water has been studied (41). This is probably because lead residues have been detected in conventional boiler systems and so evaluations of its effect on alloy 600 was considered useful. The failure mode changed from intergranular for annealed materials to transgranular for sensitised material at 316°C when lead or lead compounds are present. A change in the SCC mode from intergranular, for mill annealed and very low carbon materials (less than 0.006%), to transgranular for thermally treated materials (649°C/1 hour), in lead doped water at 323°C has also been observed (4). A conclusion would be that the presence of lead in the primary water does not result in SCC which follows the areas of grain boundary chromium depletion present in sensitised materials, where material thermally treated at 649°C/1 hour will be in a sensitised condition. The significance of lead in PWR systems is unclear with contamination being only a very remote possibility from back-up steam plant or nuclear fuel.

Copson and Dean (42) studied the possible effect of fluoride contamination in pure water, a situation which may arise due to the industrial practice of pickling tubing. No evidence of cracking was found following a 10 week exposure test in a 0.5% NaF aerated solution at 315°C using U-bend samples. The effect of oxygen concentration on SCC of Alloy 600 in pure water at 316°C has been evaluated by Copson and Economy (43). It has been shown that the propensity for intergranular SCC increases with an increasing oxygen concentration when a crevice is present.

The absence of a crevice and/or the presence of hydrogen as the gas phase did not result in cracking. These studies indicate that the pickling of tubing would not be expected to accelerate SCC, and that the presence of oxygen in the gas phase will only increase SCC if it can concentrate in crevice locations. This later conclusion indicates that a critical oxygen concentration is required for the initiation of SCC.

The study of caustic concentrations on the SCC of Alloy 600 has been extensive because occurrences have been widely reported on the secondary side, and until the mid 1970's this was where the vast majority of SCC occurred. The concentration of caustic species in stagnant regions on the secondary side may result from the leakage of alkali-producing impurities from the Condenser, from the use of phosphate water chemistries and from the hydrolysis of such active or remnant phosphate treatments. Berge et al (44) studied the behaviour of mill annealed tubing in deaerated caustic solutions with concentrations in the range 4 to 500 g/l NaOH at 350°C. Analysis of results from C-ring and U-bend tests revealed that the crack propagation rate decreased from approximately 5 $\mu\text{m}/\text{h}$ to 0.3 $\mu\text{m}/\text{h}$ as the NaOH concentration was reduced from 100 g/l to 4 g/l. Overall, the conclusion was that NaOH has only a small influence on the cracking of Alloy 600 under the test conditions.

Pathani (45) tested Alloy 600 in the form of pressurised capsules (hoop stress approximately 55% of the yield strength at room temperature) and C-rings (stressed to 150%

of the room temperature yield strength). The pressurised capsules tested at 300°C showed an increasing incidence of cracking as the caustic concentration rose from 40 to 200 g NaOH/Litre H₂O. The C-ring tests at 290°C showed a peak incidence of cracking at 100 g NaOH/Litre H₂O. An EPRI study conducted by Airey (4) complicated the picture, with the results of his study using mill annealed and thermally treated samples tested at 315°C in the range 10 to 50 Wt% NaOH solutions. Mill annealed samples showed a large scatter of results, but the trend was for a reduction in the crack depth as the deaerated NaOH concentration increased from 10 to 50%. Thermally treated samples showed considerably less scatter and a reversed trend so that the crack depth, although at a much lower level than for mill annealed material, increased as the deaerated NaOH concentration increased.

The same EPRI investigation chose to study the effect of silica on the caustic test environment since it had previously been indicated that it could have a deleterious effect on caustic SCC. It was found that a mixture of Silica and Sodium Hydroxide was less aggressive than Sodium Hydroxide alone (46). The addition of silica to a 10% NaOH solution at 316°C improved SCC resistance. However, the addition of silica to a 50% NaOH solution at 327°C decreased the SCC resistance. These seemingly contradictory results can be reconciled by the differences in test environment. It is reasonable to suggest that maximum SCC propagation occurs at a maximum corrosion rate. At 316°C and a 10% NaOH solution a critical corrosion rate

exists whereas at 50% NaOH the solution is too aggressive. The addition of the inhibiting silica therefore reduces the corrosion rate for 10% NaOH below the critical level and hence reduces SCC propagation. A similar inhibiting effect at 50% NaOH brings this solution into a critical corrosion rate domain and produces an increase in SCC propagation. These results confirm the inhibiting nature of silica addition to caustic environments but highlight the difficult balance which must be maintained for it to be effective in this role.

In summary the effect of environment chemistry on both primary and secondary cracking is difficult to quantify because of the wide diversity of test conditions used. On the primary side the detrimental effect of hydrogen has been well demonstrated, and indications suggest a further harmful effect of dissolved oxygen. On the secondary side it is well reported that the concentration of caustic sludge in stagnant flow areas can lead to tube degradation. The detrimental effect of copper contamination, possibly from the boiler system, appears to be conclusive. Additional environments and contaminants have produced variable results, and so their effect on SCC susceptibility is unclear. Section 2.4.1.1 of this review discussed the importance of electrochemical potential on SCC susceptibility due to its importance as regards the stability of the oxide film. The variability of the test results and inconclusiveness of the results can in most cases be rationalised in relation to the following:-

(i) there can be a significant variation in a batch of material which has been nominally processed under identical conditions.

(ii) the effect of test solutions on the electrochemical potential of the material has largely not been reported. The exact test conditions can affect the material susceptibility and protective oxide film at the start of the test.

It is suggested that further studies should seek to clarify this unclear situation by undertaking a systematic study of environmental chemistry variations.

2.4.1.3 Temperature

It is widely known that active corrosion processes are temperature sensitive. The role of temperature on stress corrosion cracking must be related to the activity of the corrosive species, the stability of the protective oxide film and the alloys yield strength. All of these factors are temperature dependant, and so it can be anticipated that the SCC rate will increase as the test temperature is raised.

Cowan and Gordon (47) studied the effect of temperature in deaerated pure water for Alloy 600. The results indicated that a temperature increase from 290°C to 340°C (50°C) resulted in at least a five fold decrease in the measured time for cracking to be observed. A later study by

Bulischek et al (48) recorded an increase in the intergranular cracking rate with increasing temperature. Bulischek also tested in pure deaerated water, but loaded samples using a constant strain rate of approximately $3 \times 10^{-7} \text{ s}^{-1}$. Subsequent analysis of failed samples, by scanning electron microscopy, showed that 60%, 39% and 1.5% of the fracture resulted from intergranular crack propagation at 365, 345 and 325°C respectively. The remainder of the fracture path consisted of ductile failure which was generally unassociated with grain boundaries.

Phipps (49) reviewed laboratory and service data for mill annealed Alloy 600 in an attempt to establish a time - temperature relationship in primary water. Widespread predictions are that primary water SCC will become evident during the first 2 or 3 cycles of full temperature operation for mill annealed tubing. The performance of thermally treated tubing is predicted to be 'significantly' improved relative to mill annealed tubing, but no further quantification is given.

In addition to microstructure, Phipps highlights the importance of stress level for SCC. Cracking develops in stressed areas, primarily; the tube to base plate expanded zone, the adjacent transition zone and the innermost rows of U-bends. Failure in the tube-base plate area has been observed within 12 months operation, and through wall cracking in the adjacent transition zone by 18 months. Leakages in the U-bend region of inner rows has occurred over periods of four years.

Examination of tubes pulled from steam generators has shown that intergranular attack in addition to SCC occurs at the tube-base plate and tube-support plate locations where a crevice exists. This secondary side phenomenon has previously been discussed, and Phipp's review confirms the importance of the overall steam generator design.

Phipps also revealed that SCC occurred predominantly on the SG tube hot leg, with some cracked areas related to out of tolerance manufacturing defects. The possibility of reducing the overall operating temperature of the steam generator so that the hot leg decreases from 325°C to 293°C (current cold leg) and the cold leg decreases from 293°C to 261°C may be an approach to reduce the occurrence of SCC. Any reduction in the operating temperature must be at the detriment of power output, but where a power station is not required to operate at full capacity this may not adversely affect economic considerations. Indeed for a plant experiencing active SCC, and so undergoing costly repair shut-downs, this approach may be viable. Out of tolerance manufacturing defects can be avoided by improved inspection techniques prior to tube installation.

Theus (50) evaluated the cracking rate of Alloy 600 in AVT water covering the temperature range 329°C to 428°C. A strong temperature dependence was found with a log linear increase in crack growth rate occurring when the temperature increased from 329°C to 428°C. Airey (4) reported a significant detrimental influence of temperature on the crack depth in caustic solutions for both mill

annealed and thermally treated material. The temperature range investigated was 316°C to 343°C, and despite considerable scatter a general trend is evident. This trend, of increasing crack depth with increasing temperature, is most pronounced for thermally treated material.

In summary, the literature indicates a definite effect of temperature on SCC of Alloy 600. The results show variable levels of scatter, which in some cases prevents the identification of firm trends. However, other results, especially in pure deaerated water and for thermally treated samples, show a strong influence of temperature which is indicative of a thermally activated process. A proposed mathematical expression to describe this influence is; log time to initiate cracking is proportional to the reciprocal of absolute temperature (T), ie $\exp(-Q/KT)$, the Arrhenius equation; where Q is the activation energy and K is the Boltzman constant (51). The discrepancies apparent in some data, and between researchers, may be attributable to material variations. These material variations can arise from cast chemistry variations and the effect that 'minor' differences in thermal and mechanical processing have on microstructure and residual stress levels. It has been widely reported that SCC in Alloy 600 is sensitive to these factors, and it is probable that environmental conditions during the tests would have a significant effect on the electrochemical potential and hence the stability of the oxide film.

2.4.1.4 Deformation

Steam generator tube locations which are subject to residual stress and/or plastic deformation during service account for the majority of instances of SCC in operating PWR's. The contribution of stress to stress corrosion cracking is universally accepted, and so studies of this factor, and accelerated testing utilising stressed samples, are pertinent to developing an understanding of this phenomena.

Yonezawa and Onimura (52) carried out a series of experiments to elucidate the SCC resistance of cold worked nickel base alloys in PWR primary water. The stress and strain dependency of SCC resistance was evaluated with constant load or constant strain specimens.

The results for constant strain SCC tests for mill annealed Alloy 600, using pre-strained reverse U-bend specimens, showed a decrease in the SCC test time from 10^4 to 10^2 hours as the stress at the top of the U-bend (measured by x-ray diffraction) increased from 50 to 85 MPa. At the same ratio of the applied stress to the 0.2% proof stress after cold working, the SCC resistance decreased with an increased cold working ratio. Additional testing showed that the SCC resistance of the cold worked Alloy 600 increased as the cold working ratio increased, at the same applied stress level. These findings indicate that it is

both the applied stress and the relative proof stress of the material that are important for assessing the SCC resistance. That is, for a constant yield strength an increase in cold work reduces the SCC resistance.

Comparative tests with thermally treated Alloy 600 (15 hours 700°C) revealed that the SCC resistance of the thermally treated Alloy 600 is higher than that of the mill annealed material at each stress level. Metallographic assessments of these material conditions indicated that there appeared to be no correlation between SCC resistance in high temperature water and the grain boundary segregation of impurity elements (B, S, P) and chromium depletion near the grain boundaries. However, it was noted that thermally treated material had microstructures with semi-continuous grain boundary carbides and isolated intragranular carbides, whereas mill annealed material contained only isolated carbides situated primarily intragranularly. It was suggested that thermal treatment resulted in increased grain boundary precipitation which accounted for the reduced SCC susceptibility compared to mill annealed material of the same composition.

Foster and Taylor (53) and Theus (50) have confirmed the findings of Yonezawa and Onimura. Foster and Taylor reported that cold deformation of the order of 15-20% appeared capable of increasing the incubation time for crack initiation even in the presence of high applied stress. Theus reported that in the range 0 to 35% prestrain, in both primary and secondary environments, an

increase in the time to failure occurred as the prestrain increased. The conclusion is that, all other factors being equal, the resistance to SCC initiation increases as the 0.2% proof stress increases. This effect would be expected because any given constant level of stress will have a lesser proportionate effect on the yielding of the material as the yield stress increases.

Congleton and Parkins (54) undertook an extensive programme of slow strain rate tests on Alloy 600 in order to try and reproduce cracking experienced during steam generator operation. Overall they found that, based on the results of strain rates in the order of 10^{-6} s^{-1} , Alloy 600 SG tubing was difficult to crack in typical PWR primary water at 300°C. Tests at 340°C have shown that the tubing is more susceptible to SCC on the inner surfaces than on the outer surfaces, although no explanation was offered. Testing at very low strain rates was considered to be of only marginal advantage in producing SCC. Indeed strain rates in the order of 10^{-6} s to 10^{-8} s^{-1} are practically equivalent to static load tests, and for such strain rates it would be the time at load rather than the strain rate which controls any cracking.

These experiments were some of the few where the cell potential was carefully controlled. The test conditions were chosen as those where the polarisation curves obtained at fast and slow sweep rates, when plotted on the same graph, were most widely separated. This condition should have represented the electrochemical potential where SCC

was most likely, but the results were largely inconclusive. It is argued that cyclic loading on plain or pre-cracked specimens may be a more profitable approach in assessing the cracking susceptibility.

An investigation by Bulischeck and Van Rooyen (37), which predated that by Congleton and Parkins, reported substantially more conclusive results. The investigations showed that when Alloy 600 was subjected to slow deformation rates, such as those that may be experienced by actively denting tubes, failure occurred more rapidly than is indicated by constant deflection - type specimens. It was assumed that a slip step emergence - film rupture mechanism was responsible for minimising the crack initiation period. Preliminary test results indicated that the activation energy for crack initiation is related to the carbon content of the material, with low carbon content materials having lower activation energies. Susceptible 'heats' of material exhibited SCC in a strain rate range of 10^{-6} and 10^{-8} s^{-1} at 365°C and 290°C respectively. Crack propagation rates for slightly cold worked material ranged from 10^{-7} mms^{-1} at 290°C to $3 \times 10^{-6} \text{ mms}^{-1}$ at 365°C . It was estimated that as received (not cold worked) material would exhibit crack growth rates approximately half of these for cold worked material. Cyclic loading did not appear to initiate SCC faster than constant loads, and no effect of frequency was noted in the range 10 to 10^{-3} Hz .

In conclusion it is pertinent to suggest that the occurrence of SCC could be reduced by eliminating all sources of residual and active stress on the SG tube bundle. Active deformation and cold worked materials should be eliminated and avoided wherever possible.

2.4.2 The effect of metallurgical variables

The susceptibility of Alloy 600 to SCC arises as a result of the interaction of metallurgical factors. The alloy composition, within the specification range, is vital, as is the thermal and mechanical processing history which largely develops the final material structure and properties. Alloy 600 is not precipitation hardenable, and so its mechanical strength can only be developed by controlling the thermal and mechanical processing. Alloy composition, grain size, cold work and carbide morphology and distribution must all be recognised as the key metallurgical variables. As a result of extensive evaluation it has largely been possible to optimise these factors in order to reduce SCC susceptibility. However, further elucidation of the controlling mechanisms and their interactions will improve the material utilisation and dependability.

2.4.2.1 Alloy composition

The selection of Alloy 600 for PWR SG tubes resulted from its excellent inherent corrosion resistance. The combination of approximately 75% Nickel and 15% Chromium allowed the possibility of developing a 'self-healing'

corrosion resistant material with good strength retention at elevated temperatures.

The chemical composition range of Alloy 600 is shown below (55):-

Nickel (plus cobalt)	72.0% min
Chromium	14.0 - 17.0%
Iron	6.00 - 10.00%
Carbon	0.15% max
Manganese	1.00% max
Sulphur	0.015% max
Silicon	0.50% max
Copper	0.50% max

Inco Alloys do not report levels of phosphorus, but analysis of commercial Alloy 600 indicates usual contents of 0.007% to 0.011%.

Alloy 600, with its high Nickel content, has a lower carbon solubility than conventional austenitic steels. Decreased carbon solubility leads to increased precipitation of chromium carbide, mainly at grain boundaries, which can result in the occurrence of intergranular SCC. The relationship between carbon content and SCC has been widely evaluated by many researchers.

McIlree (56) found no effect of carbon on SCC at 316°C in high purity water. Blanchet et al (8) concurred with this finding when testing material with carbon levels of 0.002% and 0.04% at 350°C also in high purity water. Similar work by Wilson and Aspden (38), using 0.03% and 0.06% carbon material tested at 315°C in caustic solutions, further substantiated this finding.

Apparently contradictory results concerning the effects of carbon level on SCC are also reported. McIlree (56) further found that the combination of annealing, at 1120°C for one hour, plus thermal treatment, at 675°C for 2 hours, did show a detrimental effect of high carbon on SCC when tests were carried out at 316°C in 50% NaOH. Theus (57) evaluated the cracking susceptibility of varying carbon content alloys in heat treated conditions equating to mill annealing at 289°C in 10% NaOH. The results clearly showed that high carbon material (0.06%) cracked less severely than lower carbon material (0.02%). However, the influence of carbon on SCC was not detectable when samples were mill annealed plus thermally treated. Later work by Crum (58) and Bulischek (37) confirmed Theus's findings.

In summary it appears that, despite experimental scatter in the reported data, carbon is a key element with respect to controlling SCC in Alloy 600. Material in the mill annealed condition shows a decreasing SCC susceptibility with increasing carbon content when tested under caustic conditions at typical operating temperatures. This result can be rationalised in terms of an increasing activation

energy for SCC as the carbon level increases, ie the SCC resistance increases as the level of carbon in solid solution increases. This effect appears not to be apparent in pure deaerated water, a fact which emphasises the importance of reporting the test environment. The introduction of the thermal treatment transforms the situation since most of the dissolved carbon will now be precipitated, primarily at grain boundaries. The greater the level of chromium carbide precipitation, resulting from the dissolved carbon, the greater will be the SCC susceptibility in a corrosive environment. This effect has been reported for tests in 50% NaOH at 316°C but not for tests in pure deaerated water at the same temperature.

In practice Alloy 600 is reported to contain small titanium contents (59) which could modify the effects of carbon, and lead to a reduction in the amount of chromium carbide precipitation and consequently result in a degree of stabilisation against intergranular corrosion. Titanium also has a high affinity for nitrogen and so particles of titanium nitride (TiN) as well as carbonitride (TiCN) will form. This will increasingly occur as the titanium to carbon ratio increases, but extensive microstructural surveys confirm that the majority of carbon is still precipitated as chromium carbides. Clearly, although titanium has a higher affinity for carbon than chromium the formation of carbides depends upon the overall content of each element and competitive processes of precipitation.

The iron content of Alloy 600 arises because the material evolved from the addition of ferro-chrome to nickel. The available literature does not discuss the role of iron on SCC susceptibility, but its influence must be related to its effect on solid solution hardening and possibly stacking fault energy. Iron will slightly decrease the SFE and so aid planar slip and promote anodic dissolution and possibly hydrogen embrittlement. However this effect will be minimal and the iron content is controlled within levels defined as a result of the alloy's empirical development.

The role of manganese, silicon and copper has not been reported in the literature, but reference to their effects in commercial austenitic stainless steels may be relevant (59). Manganese is usually present in austenitic stainless steels in the order of 1 to 2 %. Its effect on SCC susceptibility is variable, but above approximately 2% it has been shown to enhance SCC in chloride solutions. Silicon is known to improve chloride SCC resistance, probably by the formation of a surface protective layer of manganese silicate when the steel is exposed to $MgCl_2$ solutions. The levels of 1% max for Mn, 0.5% for Cu, and 0.5% max for Si are likely to be due to conservatism regarding the alloy's compositional development as much as to strictly defined metallurgical effects. All these elements will contribute to solid solution hardening and have an influence on SFE. However, due to their minor alloying levels, any effects will be extremely negligible and provided no significant detriment is attributable to their presence it is sufficient to define the known benign limits.

Residual elements such as sulphur and phosphorus are usually considered to be detrimental in steels, since they are known to form low melting point phases at grain boundary locations. The segregation of these elements to grain boundaries can lead to a local loss of ductility, known as 'temper embrittlement' in low alloy transformable steels.

The quantitative effect of sulphur and phosphorus grain boundary segregation in Alloy 600 on SCC is unclear. Coriou et al (32) detected the presence of sulphur rich precipitates in the propagation zone of an intergranular crack. It was suggested that a possible relationship existed between the detrimental presence of grain boundary sulphur and the resulting SCC. Blanchet et al (8) reported that alloys containing 75 to 77% nickel can be embrittled at grain boundaries by precipitates of manganese and nickel sulphides, this occurring for a sulphur content as low as 0.0009%. These compounds, which are probably unstable in water at 350°C, led to the formation of a strongly sulphurous medium in the small volume at the bottom of the crack. This region would then be susceptible to a rapid point by point dissolution of the nickel rich alloy. Precipitates found on the flanks of the crack would be a witness to this reaction. The maximum grain boundary contents of sulphur were observed following thermal ageing at 600°C. However the effects varied significantly at the mill annealing temperature changed. Thermal treatments which promote diffusion, such as high mill annealing temperatures and extended treatment times, will result in

the greatest degree of grain boundary sulphur segregation.

Airey (4) did not detect an increase in grain boundary sulphur content during thermal treatment at 700°C. However, the concentrations of phosphorus and boron were seen to increase. Since thermal treatment at 700°C for 15 hours has been shown to offer the greatest improvement in SCC resistance, it was concluded that the presence of these elements was not detrimental. Yonezawa et al (52) studied the segregation differences of sulphur, phosphorus and boron between mill annealed and thermally treated materials. They observed no difference in the levels of these residual elements at grain boundaries, and concluded that they did not affect the SCC resistance of Alloy 600. The analytical technique of fracture surface material removal by Argon sputtering further revealed that phosphorus and boron were present as segregated layers rather than being incorporated into grain boundary precipitates, as was the case for sulphur.

2.4.2.2 Grain Size

The grain size of Alloy 600 SG tubes depends upon alloy composition and thermal and mechanical process history. It is unrealistic to consider the effects of these variables on SCC in isolation. The carbon content will determine the volume fraction of chromium carbide precipitates available at any given processing temperature. In conjunction with the thermal and mechanical processing, the carbides can play a major part in determining the final grain size.

Blanchet et al (8) examined specimens with grain sizes

ranging from 20 μm to 300 μm . Stressed samples in demineralised water at 350°C all showed evidence of cracks intergranularly. However, the appearance of some intragranular cracks was noted with larger grain sized samples. Foster and Taylor (53) reported that fine grained material was more resistant to SCC than coarse grained material in deaerated water at 350°C. However, Blanchet (8) and Wilson (38) found no significant effect of grain size in deaerated water at 350°C and 10% NaOH at 315°C. Exposure to 50% NaOH was sufficient to reveal increased susceptibility to SCC at 315°C.

As previously discussed, the activation energy for SCC increases as the carbon content increases for mill annealed material. An increasing carbon content will result in a decreasing grain size, and so the resultant observation of an improvement in SCC resistance may be linked to both factors. Additionally, the thermal and mechanical history will determine the level of carbide precipitation, final grain size and dislocation structure, which in turn will contribute to the SCC susceptibility.

A general observation can be offered that a fine grain size is beneficial in reducing SCC susceptibility if all other metallurgical factors are constant. SCC follows intergranular paths in Alloy 600, and a reduction in grain size means an increase in grain boundary area per unit volume, Sv. As the grain size is reduced the concentration of impurities per unit Sv will reduce which in turn will increase SCC resistance.

2.4.2.3 Thermal and Mechanical Treatments

The processing history of Alloy 600 SG tubes follows the basic schedule detailed in section 2.2. of this review. Tubing in the mill annealed condition has a thermal and mechanical history of hot and cold extrusion and pilgering followed by a final anneal 'in-situ' i.e. mill annealed. Widespread evaluation has been made of tubing which has also been subjected to an additional thermal treatment after the mill anneal. The parameters used during the combination of mechanical forming and thermal mill annealing will determine the material grain size, microstructure and level of carbon held in solution. All these metallurgical features contribute to the SCC susceptibility, as previously discussed. The post mill anneal thermal treatment will then affect the final precipitate distribution and morphology. Additionally the thermal treatment will stress relieve the material, this factor having an important influence on SCC as previously discussed.

Bulischek et al (48) studied the effects of simulated mill annealing heat treatments on cold worked material (the material condition following final cold pilgering or cold drawing). The results indicated that there was a strong connection between SCC in high temperature pure or primary water and processing history. Airey (60) has reported that the importance of processing history on SCC susceptibility is not usually apparent following a thermal treatment of 15 hours at 704°C

Vallourec are manufacturers of Alloy 600 SG tubing and have extensively studied the relationship between composition, processing parameters, microstructure and corrosion resistance (7) (61). The range of permissible carbon contents must satisfy the microstructural and mechanical property requirements, and these in turn are related to the processing parameters. For mill annealed tubing, a minimum carbon content is one that produces intergranular carbides (0.029%), and for thermally treated tubing a maximum carbon content is one which avoids the existence of a significant level of intragranular carbides (0.035%).

The selection of an annealing temperature (on the mill) is important because it directly affects the form of carbide precipitates as well as grain growth and mechanical properties. As high an annealing temperature as possible is desired since this will allow full solution (ie a solution anneal) and results in a low level of intragranular precipitation. However, this must be balanced with the requirement for mechanical properties since, for a fixed carbon content, increasing the annealing temperature (above approximately 980°C) will cause grain growth and a reduction in mechanical properties.

In the case of tubing for Sizewell 'B', the Alloy 600 material must meet minimum tensile properties of a 0.2% proof stress of 300 MPa, which is achieved by drawing the tubing through a continuous furnace at 2 feet per minute (62). The specified mill anneal temperature of 980°C for 2 minutes will produce an adequate grain size and mechanical properties. However, because of kinetic factors affecting

carbide dissolution, this relatively short time may not result in the intended degree of precipitates taken into solution and an unspecified effect on SCC susceptibility may remain. The mill annealing schedule further specifies an additional treatment where the actual metal temperature must reach 948°C for 3 to 5 minutes. This treatment represents a compromise between SCC resistance and tensile properties. A higher temperature will increase SCC resistance, by allowing a fuller solution anneal, but would result in reduced (possibly unacceptable) mechanical properties. Indeed evidence exists to suggest that 3-5% cold work is necessary to produce the required mechanical properties in finished tubes. Any such cold work will increase the SCC susceptibility because of residual stress, but it may also decrease the SCC crack growth rate because the tensile properties will have been increased. This effect has been discussed in section 2.4.1.4 of the review.

The release of mill annealed Alloy 600 tubing is based jointly on mechanical properties and corrosion resistance. Tubing is evaluated for corrosion resistance via immersion in 25% HNO₃ for 48 hours (modified 'Huey' test). For mill annealed tubing a maximum weight loss of 0.01% must not be exceeded. However, although the Huey test is a good indicator of general corrosion resistance its applicability in determining susceptibility to SCC is less certain. Indeed, Vallourec (61) report that Huey test results are not sensitive to carbon or to annealing temperature, and that the only detectable factor appears to be the cooling rate from the mill annealing temperature. The reasons for

this are not discussed, but the effect may be due to the increased susceptibility of slowly cooled tubing resulting from the increased tendency for chromium depletion adjacent to the grain boundary chromium carbides.

Airey (4) has extensively studied the relationship between the mill annealing schedule and the subsequent material microstructure following thermal treatment. The final annealing temperature was found to be the principle factor contributing to a satisfactory thermal treatment (704°C for 15 hours), although carbon content was also important. The mill annealing temperature controls the level of carbon in solution prior to the thermal treatment, and it is this carbon which will be precipitated as chromium carbides at grain boundary locations.

The Airey study evaluated four heats of tubing with carbon contents in the range 0.011 to 0.048%. A mill annealing temperature of 982°C to 1010°C for 1 to 5 minutes was identified as producing a semi-continuous grain boundary decoration of chromium carbides following thermal treatment. This schedule also minimised the existence of grain boundary chromium depletion and provided acceptable mechanical properties. The degree of grain boundary chromium depletion following thermal treatment (at 704°C) was found to increase with increasing annealing temperature for a given heat of material. The degree of chromium depletion reached a maximum after thermal treatment for 1 hour at annealing temperatures of 927°C and 982°C, and after 5 hours for tubing annealed at 1038°C.

The conclusions from the Airey study are that for material annealed up to 982°C there is no evidence of grain boundary chromium depletion after the full thermal treatment (indeed no evidence was found for times greater than 5 hours at 704°C). However, material annealed at 1038°C contained a layer of chromium depletion even after 15 hours at 704°C. Furthermore, the degree of grain boundary chromium depletion increased with increasing annealing time for a given annealing temperature prior to thermal treatment. The effect also increased with increasing carbon content for a given mill annealing schedule. The widely reported beneficial effect of thermal treatment on the corrosion resistance of Alloy 600 tubing is a function of the modified grain boundary precipitation and any associated chromium depleted zones. The absence of such depleted zones is considered to be beneficial for SCC resistance, although this has not been fully quantified for all test environments.

The Airey study reported a reduced level of SCC, after testing in 10% deaerated NaOH at 343°C for material annealed at the bottom end of the production temperature range. SCC was present to a greater extent for material with the highest carbon content (0.048%) for the same heat treatment schedules. The SCC depth of attack then increased with decreasing mill annealing temperature. These observations confirm the importance of carbon content and mill annealing temperature prior to thermal treatment. The high carbon material which has experienced a low

temperature mill anneal (below 980°C) will contain extensive amounts of intragranular carbide prior to thermal treatment. During thermal treatment only a very limited amount of grain boundary carbide will precipitate, since the majority of the carbon is accounted for as large discrete intragranular precipitates. The absence of semi-continuous grain boundary precipitates will offer a path of low resistance to intergranular SCC in a susceptible media such as NaOH. Similarly, Crum (63) found that the caustic resistance of thermally treated Alloy 600 can be less for a high carbon heat of material. This occurs when the annealing temperature and carbon content produce thermally treated material which contains extensive intragranular carbide precipitation and only minimal grain boundary precipitation. The presence of appreciable grain boundary precipitation can be as important as the absence of an associated chromium depleted zone for the purposes of preventing SCC propagation.

In summary, the thermo-mechanical processing of Alloy 600 tubing in conjunction with the material composition sets the balance between mechanical and corrosion properties.

The grain size is developed by recrystallisation resulting from the combination of either cold work and annealing or dynamic recrystallisation during hot working. Grain growth does not occur until about 980°C, when finely dispersed carbide particles, which pin the grains, begin to grow. Solution of the carbides begins at around 1040°C, with treatments for 1 to 2 hours at 1090°C to 1150°C

sufficient to dissolve all carbides and result in grain growth. In general, material with a fine grain size is preferred because it has improved corrosion resistance and imparts high tensile, fatigue, toughness and ductility levels. The final mill anneal, following the cold pilger or draw to size, will control the chromium carbide distribution and morphology as well as the level of carbon held in solution and the grain size. A post mill anneal thermal treatment, 15 hours at 704°C, can, result in the precipitation of semi-continuous grain boundary chromium carbides, which are free from any associated chromium depletion zones, as well as having an effective stress relieving effect.

2.4.2.4 Low Temperature Sensitisation

A concern exists that Alloy 600, which is initially resistant to SCC, may become sensitised as a result of prolonged exposure to steam generator operating temperatures. If such a mechanism were to occur then it would undermine the validity of production release corrosion data and could lead to the necessity for a restrictive life limitation being placed on the tubing. The descriptive term 'low temperature sensitisation' (LTS) has been adopted during investigations into this possible effect.

Wagner et al (64) reported evidence of LTS in Alloy 600 tubes removed from service after approximately 25,000 hours (3 years). Comparative SCC tests performed with samples removed from service tubes and others from the same tubes but heat treated to ensure no chromium depletion at the

grain boundaries showed a greater incidence of cracks for the non-heat treated material. However, these findings are not conclusive since no detailed prior processing history is discussed and the test medium (aerated caustic) is not representative of the SG operating environment. In this instance it is proposed that grain boundary chromium carbide precipitation had occurred with an associated chromium depleted zone. If such a mechanism did occur at approximately 300°C then it would be vital to understand the previous processing treatments prior to service. It would be considered highly unlikely that any such effect could occur for thermally treated tubing, since the 15 hours at 704°C will have healed the chromium carbide associated chromium depletion zones.

Substantiation of any microstructural change associated with Wagner's findings have not been forthcoming. Perment and Graham (65) did not, detect with electron microscopy, any microstructural changes in laboratory specimens exposed for 16,000 hours at 330°C in deaerated water. Domain et al (33) confirm the lack of microstructural change for samples removed from testing after 14,000 hours at 343°C in AVT water. It was concluded that grain boundary microstructural changes are unlikely to occur over a period of 40 years at steam generator operating temperatures.

In comparison, type 304 austenitic stainless steels do experience LTS in comparable time periods to those evaluated for Alloy 600. This difference in behaviour can be attributed to differences in carbon solubility as well

as carbon and chromium diffusion rates, with Alloy 600 having lower solubility and diffusion rates than type 304 stainless steel. Further to this comparison, Airey (4) evaluated the effect of small amounts of deformation on LTS. Low levels of deformation have been shown to decrease the time for LTS in austenitic stainless steels, with such levels of deformation equating to damage that may occur as a result of straightening or polishing of equivalent Alloy 600 SG tubes. However no increase in LTS was observed in Alloy 600 samples.

In summary, there is only very limited evidence to suggest that any detectable level of chromium carbide precipitation can occur at SG operating temperatures. Hence, there will be no associated chromium depleted zone and no contribution to intergranular SCC susceptibility. However, it has been widely reported that SCC susceptibility is not solely related to chromium depleted zones. As discussed in section 2.4.2.1 the segregation to grain boundaries of residual elements (principally sulphur) may lower the SCC resistance. The possibility of such segregation occurring during SG operation has not been fully evaluated or reported.

2.5 The Optimisation of Variables to Reduce Service

Degradation

Alloy 600 PWR SG tubes are subject to a spectrum of degradation modes, all of which result from the interaction of a susceptible material condition and a hostile environment. The means of reducing these modes of degradation can only be achieved by increasing the material resistance and/or decreasing the hostility of the service environment.

The reduction of secondary side degradation has largely resulted from modifications to the water chemistry and plant design. The once serious problem of tube denting has been eliminated by strict control of the secondary water and improved fabrication techniques to limit the existence of crevice locations adjacent to the tubing.

In addition to water chemistry control, by filtering and all-volatile treatment additions, the replacement of ferritic steel by ferritic stainless steel support plates and the increased use of anti-vibration bars has been important. As a result support plate corrosion which leads to tube denting, and fatigue damage from vibrations have been greatly reduced.

The alloy composition has been controlled to tight limits within the commercial specification range. The necessary balance between mechanical properties and corrosion resistance has been achieved based on an understanding of the interaction between material composition and processing parameters. It has been possible to specify carbon levels and tube manufacturing parameters which result in a microstructure with optimised properties. The tubing in the final mill annealed condition, prior to any thermal treatment, should have a microstructure with a semi-continuous decoration of all grain boundaries with chromium carbides. The subsequent thermal treatment may increase the density of grain boundary precipitation, heal any chromium depleted zone and stress relieve the tubing. The service microstructure will then contain only occasional intragranular carbides with a fairly heavy decoration of semi-continuous fully equilibrated intergranular chromium carbides (M_7C_3).

The superior service performance of thermally treated Alloy 600 SG tubing can also be related to the low level of residual stress, which will allow rapid repassivation if the protective surface oxide is ruptured. The semi-continuous grain boundary precipitates will provide an effective barrier to intergranular crack propagation.

Tube degradation on the primary side is also due to susceptible material in a corrosive environment. Stress corrosion cracking is the principle concern with efforts being taken to reduce the corrosive nature of the primary water and increase the material resistance. The material optimisation has been discussed and the importance of reducing the residual stress level, especially important for stress corrosion cracking, has been identified. The possibility of lowering the service temperature for SG units experiencing tube degradation has been suggested. This would be at the expense of operational efficiency but, where plant shutdown may be necessary to carry out refitting of tubes, it may offer an advantage in terms of an extended life between outages.

The effects of minor water additions, to the level of ppm, on electrochemical potential and the stability of the oxide film have been introduced. This is one area however which still requires further clarification by quantitative study. Alloy 600 remains the specified steam generator tube material for Britain's first pressurised water reactor. The Sizewell 'B' PWR will take advantage of all the design improvements to reduce service degradation and utilise Alloy 600 in the thermally treated condition. The vast majority of world wide research indicates that the thermal treatment of Alloy 600, which has undergone the optimised mill annealing schedule, is beneficial in terms of resisting intergranular cracking. However, there is presently only limited operating experience with Alloy 600 in this condition, and although no in-service degradation

has been reported, the variability in accelerated testing results makes it difficult to have absolute confidence in the materials performance over the proposed 40 year life span. This variability may be inevitable with a single steam generator containing several thousand tubes originating from a number of casts and processed with some degree of variation.

Despite the persisting doubts regarding variability, Alloy 600 steam generator tubes in the thermally treated condition have been specified for recent PWR's in France and the USA, as well as for Sizewell 'B'. A possible future development may be the move to an alloy with an increased chromium content. Inconel Alloy 690 has approximately 25% chromium, compared with Alloy 600's 15%, and so has a more resistant protective oxide film and is virtually immune to chromium depletion zones associated with precipitation of chromium carbides at grain boundaries. Additionally Alloy 690 is reported as showing negligible service variability. The future use, after extensive evaluations, of a steam generator material such of Alloy 690, may increase the margin of safety and reliability of steam generator tubes as compared with the optimised Alloy 600. However, Alloy 600 still accounts for some 74% of all PWR steam generator tubes currently in service, and so all efforts to elucidate the interacting roles and effects of composition, manufacturing variables and service parameters remains pertinent.

3.1 Selection Of Materials For Study

Inconel Alloy 600 in the form of commercially manufactured steam generator tubes (18 mm diameter, approximately 1.1 mm wall thickness) was supplied with four variations in composition, Table 1. In addition, three of the four commercial casts had undergone the 'thermal ageing treatment', consisting of 15 hours at 704°C, following mill annealing.

Initial experimental work was to characterise as-received tubing in terms of hardness, structure and grain size. Materials HT 2682 (TT) and HT 2697 (MA), the lowest and highest carbon contents respectively, were further selected to investigate the effect of mill annealing temperature in the range 900° - 1200°C, which covered possible industrial treatment temperatures, on the grain size and hardness of the austenite, and the solution of the carbides.

In order to supplement the commercial casts of Alloy 600 which were available, a series of experimental materials were produced. These casts cover the range of commercial

material compositions but incorporate variations in carbon, titanium and aluminium contents. Table 1 also gives the full chemical analysis of the selected commercial and experimental alloys which allow the investigation of the following compositional variables:

- (i) the effect of C in alloys free from Ti or Al (Series I).

 - (ii) the effect of C in alloys containing both Ti and Al (Series II)
- and
- (iii) the effect of Ti in alloys containing constant C and Al contents (Series III).

The alloy series detailed in Table 1 were selected for characterisation.

3.2 Preparation of Experimental Alloys

The experimental alloys were made as 5 Kg vacuum melted casts. The small ingots produced were surface dressed and any pipe was discarded. Hot rolling was carried out from a soaking temperature of 1150°C, using a number of reductions with reheating to 1150°C between each rolling pass to prevent edge cracking. The final hot rolled strip thickness was 2 mm, which was similar to the tube wall thickness and yet sufficient to allow further cold rolling required to study the effect of cold working on precipitation reactions. The edges of the hot rolled strip were then removed and coupons for solution treatment cut

from the remaining width of the strip.

Due to the cooling of the thinner strip being more pronounced as rolling progressed, the actual rolling temperature was considerably lower than 1150°C, but the as-rolled grain size was very comparable with that observed for the commercial tube materials. However, it should be recorded that for cast numbers 4 and 5, the cooling had been such that full recrystallisation had not occurred during rolling. There was also evidence in cast number 7 of some slight residual banding. This was due to the small original ingot size and consequent relatively smaller overall reduction compared with that experienced by commercial tube material.

3.3 Solution Treatment Of Alloys

Commercial casts 2682 (TT) and 2697 (MA) were solution treated in the temperature range 900° - 1200°C to cover possible mill annealing temperatures. Quarter sections of tubes, approximately 40 mm long, were sealed in silica tubes under a partial pressure of argon (about 100 mm Hg) in order to prevent any atmospheric pick up during the heat treatment.

The silica tube encapsulated specimens were given the following solution treatments:

- (i) 900° - 1200°C for 30 minutes at 50°C intervals followed by water quenching, the silica tubes being broken under water.

(ii) 900° - 1200°C for 30 minutes at 50°C intervals followed by air cooling after breaking the silica tubes to allow ingress of air.

Solution treatment of the selected experimental casts followed an identical schedule to the commercial alloys, except that the coupons were heat treated in an argon atmosphere furnace to prevent nitrogen pick-up.

3.4 Cold rolling Of Experimental Alloys

The effects of cold work, introduced via cold rolling, on solution treated experimental alloys was investigated. In order to study the effect of cold working on the thermal ageing response and corrosion behaviour of Alloy 600, experimental alloys representing extremes of composition and structure were selected. These extremes in terms of variation in carbon and titanium are covered by experimental alloys 4 and 5, Table 1.

The alloys, in the form of 2 mm thick strip, were solution treated at 1150°C for 30 minutes and water quenched. The solution treated materials were subsequently cold rolled to achieve a nominal reduction in strip thickness of 25% and 50%. The rolling was carried out using a small two roll mill, with successive reductions in the roll gap until the required strip thickness was achieved. As a result of Alloy 600's elasticity and the control limits of the rolling mill, it was not possible to achieve exactly the aim reductions in thickness. However, the deviations were considered minor with the final strip thickness, and

uniformity, being assessed with a micrometer.

3.5 Thermal Ageing Studies

Alloys comprising series I, II and III which had been solution treated at 950°C, 1050°C and 1150°C, followed by air cooling for the thin walled commercial tubing and water quenching for the thicker experimental alloys, were given prolonged thermal ageing treatments. In addition cold rolled experimental alloys were also thermally aged for selected times.

The thermal ageing treatments were 500-1000°C (500°C, 600°C, 640°C, 700°C, 800°C, 900°C and 1000°C) for times up to 100 hours. All samples were sealed in evacuated silica tubes, under a pressure of argon of approximately 100 mm Hg, to prevent nitrogen pick-up and oxidation. Following thermal ageing all samples were water quenched, with the silica tubes being broken under water.

3.6 Hardness Determinations

(i) Commercial Tubing

In all cases hardness measurements were taken on the outside surface of the tube using a 20 Kg load with a Vickers diamond indenter hardness testing machine. The samples were mounted in bakelite and the surface was polished back to a 600 grit surface finish. Extreme care was taken when polishing due to the contour, ie the curve of the tube, and the work hardening characteristics of the alloy. Excessive polishing could result in non-uniform thinning of some areas and possible work hardening of the

surface due to these austenitic alloys showing a high work hardening rate. A minimum of 3 hardness indentations were taken on each specimen.

(ii) Experimental Laboratory Casts

The 2 mm strip thickness of these alloys enabled hardness indentations to be made on the central, through thickness, region of the strip. The samples were mounted in bakelite before being polished to at least 600 grit surface finish. Vickers hardness indentations were then carried out using a 20 Kg load and a minimum of 3 indents for each sample.

In all cases the hardness value quoted is an average value.

3.7 Mechanical Property Determinations

Experimental alloys covering series I, II and III were selected for investigation of structure - property relationships. Flat tensile specimens to BS18:Part 3 (1971) were produced from strips of experimental alloys covering the range of thermal and mechanical process treatments. All testing was carried out at room temperature.

Prior to machining of the tensile test pieces the strips were descaled in a boiling solution of 50:50 H_2SO_4 and HNO_3 . Careful monitoring was required to ensure that no detrimental surface attack occurred once the heat treatment scale had been removed. The tensile test samples were tested on an Instron 5000 KN capacity machine using a

calibrated full scale deflection of 1000 Kg. Testing of the samples followed standard practice with initial sample dimensions being recorded and stress-strain graphs being taken and used to subsequently calculate tensile properties. The tensile properties determined were 0.2% proof stress (0.2%PS) and the ultimate tensile strength (UTS).

3.8 Optical Metallography

Optical metallography was used for two main objectives, namely the study of precipitate phases and the determination of the austenite grain size.

Mounted and polished samples, with a surface finish of at least 1 micron (1/4 micron finishes being used on occasion) were etched in Schaftmeisters reagent (1 part HNO_3 to 10 parts HCl and 10 parts H_2O) to reveal preferentially the precipitate distribution. This technique allowed optical studies of as-received and solution treated alloys. It is recognised that the distribution of carbides revealed by optical microscopy is not necessarily a good indication of the susceptibility to IGA, but it is possible to show gross differences such as those between Alloy 2682 and 2697 in the as-received condition, figures 6 and 7.

To reveal the austenite grain sizes all the samples were polished to one micron surface finish and electrolytically etched in 10% oxalic acid. Great care was taken to ensure that the grain sizes revealed were from the same region used in hardness testing, in order for valid structure property relationships to be determined. The mean linear

intercept of grain size was determined in the usual manner. A knowledge of the average grain diameter (d) and the number of grains measured allowed the 95% confidence limits to be determined.

3.9 Scanning Electron Microscopy (SEM)

Scanning electron microscope studies of etched specimens together with energy dispersive x-ray analysis (EDX) allowed the study of precipitate phases and identification of inclusions in the alloys.

Samples were mounted in conductive bakelite, polished to 1/4 micron surface finish and etched in Schaftmeisters reagent, to preferentially dissolve the matrix thus leaving precipitate phases in relief.

The SEM enables high magnification and high resolution studies of precipitate phases, to a practical magnification of x 50,000, to be undertaken. This compares with the best possible optical magnification of approaching x 1000. The SEM enabled detailed studies of precipitate distribution and size to be carried out and for this reason extensive use was made during the investigation.

Large inclusions present in the alloys can effectively be analysed with the EDX system (these were usually large, angular Ti(CN) particles). Smaller carbides however are not so easily analysed. The limitation of the EDX system on bulk samples is the excitation of a fairly large area and a volume which penetrates below the sample surface.

Since the region from which characteristic x-rays are produced is larger than the electron beam it follows that the analysis is not sensitive enough even for a qualitative assessment of small carbides, whose composition is similar to that of the matrix. Larger inclusions however can be analysed since a greater proportion of the collected x-rays originate from the inclusion itself, and its composition is readily distinguishable from that of the surrounding matrix.

3.10 Transmission Electron Microscopy (TEM)

Thin foils and carbon extraction replica techniques have been used with some utilisation of the EDX analysis system. In this case the EDX system can positively identify the composition of small carbides, since there is no bulk sample, but only for extracted carbides on a layer of carbon. Selected area electron diffraction (SAED) has been used on thin foils and carbon replicas to identify the structure of the phases present.

The direct carbon extraction replicas were prepared in the conventional manner, using an initial light etch in Schaftmeisters reagent, the extraction etch also using the same etching reagent. Thin foils were prepared by mechanical thinning specimens from the tube walls, these specimens first being spark machined using a copper-tungsten electrode. The circular sections were gradually mechanically thinned on silicon carbide paper until they were approximately 0.20 mm thick. The thinned discs were then electrochemically polished and dished (to

produce the 'transparent' region of material) in a Struers electropolishing cell using an electrolyte of 6% perchloric acid in glacial acetic acid at room temperature and a current density of 1.7 mA/cm^2 .

The specimens were examined in a JEOL 100 CX electron microscope, the carbides being identified by SAED and EDX. Both dark and bright field micrographs were prepared to identify the positions in the microstructure at which the identified carbides were observed.

These techniques have been extensively utilised for the experimental alloys following solution treatment, and for all the alloys following thermal ageing treatments. It is only in the TEM that the point at which carbides first nucleate can be observed, and it is this which will determine the boundary of the time-temperature-precipitation C-curves.

3.11 Determination of Time-Temperature-Precipitation 'C'

Curves

Construction of the precipitation C-curves was achieved by extensive microstructural studies to determine the combinations of thermal ageing temperature and time which resulted in the formation of chromium carbides. Samples were initially solution treated at 1150°C followed by thermal ageing for times up to 100 hours (with and without prior cold working).

The boundaries of the precipitation domain were identified

by microstructural examination using SEM and TEM techniques. The SEM studies revealed the presence of precipitated chromium carbides, and subsequent TEM evaluation, utilising SAED and EDX, identified the precise combinations of time and temperature which resulted in the precipitation. It was largely possible to distinguish between M_7C_3 and $M_{23}C_6$ type chromium carbides using these techniques.

Construction of the time-temperature-precipitation diagram, by plotting temperature versus log time, resulted in 'C' type curves. The form of the 'C' curve is typical of a nucleation and growth process. At high temperatures the driving force for nucleation (degree of carbon supersaturation) is low but the carbide growth rate (diffusion dependant) is high. As a result, precipitation only becomes detectable after relatively long ageing times. A lowering of the ageing temperature leads to an increase in the driving force for precipitation but a reduction in the growth rate. The reduced growth rate is more than offset by the increased driving force, and overall precipitation occurs after relatively shorter ageing times. As the ageing temperature is further reduced a point is reached where the increasingly sluggish growth rate, because of slower diffusion of the carbide particle is no longer offset by the increased driving force for nucleation. This combination of ageing time and temperature produces the 'nose' of the precipitation curve, with subsequent lowering of temperature resulting in longer ageing times prior to the formation of precipitates. This

mechanism explains the resultant 'C'-curve shape which outlines the time and temperature boundaries of the precipitation domain. The presence of deformation (cold work) in the samples would be expected to affect this nucleation and growth process, and so a limited evaluation has been made of material cold rolled prior to thermal ageing.

3.12 Corrosion Testing

In order to investigate the effect of various thermal and mechanical treatments on the corrosion behaviour of selected samples, a straight forward yet commercially pertinent test was required. The corrosion test criteria were as follows:-

(i) to provide a measure of intergranular corrosion susceptibility.

(ii) to allow some degree of material ranking to occur in terms of susceptibility as a result of thermal and mechanical treatments.

To satisfy these criteria a modified Huey test was chosen which coincided with the Westinghouse release test. The modified Huey test (ASTM type C) utilises a boiling solution of 25% (by volume) HNO_3 . Samples were placed in conical flasks fitted with cold finger condensers, and held clear of the base by glass supports. Sample weight loss measurements were taken every 48 hours, as in the Westinghouse procedure, with up to 4 exposure periods

starting with fresh solutions of nitric acid for each exposure.

In order to study the effect of localised cold deformation following thermal ageing, selected samples were bent through 67° about their mid-length position. A hydraulic press was utilised for this operation with 67° selected because it was readily produced on the available equipment and more importantly represented a level of deformation akin to severe tube denting.

Samples representing a wide range of processing conditions were corrosion tested. Detailed examination was carried out after each exposure period to evaluate the degree of attack. If the samples had suffered from severe or catastrophic attack then no further testing was undertaken. The test conditions used proved to be very severe for material in susceptible conditions and many tests were terminated before the fourth exposure period. All samples were retained for optical and SEM examination.

4 EXPERIMENTAL RESULTS

4.1 Evaluation of As-Received Commercial Tubing

Commercial PWR SG tubing, with compositions detailed in Table 1, was made available by the Nuclear Installations Inspectorate (NII). Tubing from casts 2682 and 2697 were selected to form part of the investigation into compositional variables, and were incorporated along with experimental alloys into series II and III alloys. The evaluation of commercial tubing however utilised all the available commercial casts, namely casts 2683 and 2686 in addition to 2682 and 2697. The final heat treatment condition of the tubing covered both the mill annealed and mill annealed plus thermally treated conditions.

Tubing from casts 2682 and 2697 only was selected for the identification of precipitate phases; inclusions and carbides. The full range of commercial casts were utilised for the determination of grain size - hardness relationships.

4.1.1 Identification of Precipitate Phases

Optical microscopy showed the overall distribution and morphology of inclusions and carbide phases for cast 2682 and 2697, figures 6 and 7 respectively. It can clearly be seen that as-received 2682 (thermally treated) had a markedly different distribution of carbides than 2697 (mill

annealed) in term of inter and intra granular precipitation.

The inclusions present in commercial alloys 2682 and 2697 were identified by scanning electron microscopy (SEM) and energy dispersive x-ray analysis (EDX). Studies of etched specimens, to preferentially dissolve the matrix, revealed a number of angular particles which were shown to be titanium - rich. The majority of these particles were identified as Ti(CN), the chromium and nickel present in the EDX spectrum originating from the surrounding matrix, figure 8. Occasionally, as shown in figure 9, there was magnesium sulphide associated with the Ti(CN), magnesium often being present in small quantities in these alloys originating from alloy manufacture. There was also evidence of a small amount of phosphorus associated with the magnesium sulphide. There was no discernible difference between the inclusions present in commercial alloys 2682 (TT) or 2686 (MA) and it is recognised that these are original melt related phases which remain unaffected by tube manufacture.

Optical microscope studies were sufficient to reveal the gross differences in carbide distribution between as-received Alloy 2682 (TT) and 2697 (MA), figures 6 and 7. The thermally treated material 2682 (TT), besides containing large angular inclusions left undissolved at the mill annealing temperature, also contained many grain boundary carbides which morphologically were consistent with their being precipitated during thermal treatment,

which conventionally is at about 700°C. Typical grain boundary carbides present in thermally treated material are shown in figure 10. These carbides have been identified as $M_{23}C_6$ type, figure 11. The dislocations may have resulted from carbide precipitation, or because the as-received thermally treated material was under-mill annealed or subjected to some form of physical straightening/sizing operation. These possibilities will be discussed later. In either case the residual dislocations will augment the hardness level of the material.

Thermally treated material also contained intragranular carbides, figure 12, which have been identified as M_7C_3 , figure 13. These carbide precipitates will not have been precipitated during thermal treatment, but will have formed during previous mill anneal treatments.

Optical and electron microscope studies of as-received cast 2697 (MA) showed that in the mill annealed condition there were many precipitates within the grains together with some at the boundaries. The intragranular carbides were angular in morphology and remained undissolved at the mill annealing temperature. These carbides were identified as M_7C_3 , figures 14 and 15. The few grain boundary carbides had morphologies indicative of precipitation during cooling from the mill annealing temperature, probably due to the fairly rapid cooling rate of these thin walled tubes. The grain boundary carbides were plate-like in nature and identified as $M_{23}C_6$, figures 16 and 17. Some smaller carbides are also observed within the grains, together with

a general dispersion of very fine carbides, figure 18, and some of these were distinctly angular in nature. The electron diffraction pattern indicated that the fine carbide dispersion is TiC, figure 19. The postulated influence of a fine dispersion of titanium carbide will be discussed later.

4.1.2 Grain Size - Hardness Relationships for As-Received Commercial Tubing

The study of grain size-hardness relationships for selected casts 2682 (thermally treated) and 2697 (mill annealed) has been supplemented by information on all the commercial tubing received, Table 2 and figure 20. Data for both mill annealed and mill annealed plus thermally treated conditions conformed well to the Petch analysis. Gradients of the lines, ie K_y in the Petch equation, were the same for both heat treatment conditions. However, the hardness of the mill annealed material was consistently about 15HV harder than mill annealed and thermally treated material from the same cast. This will be discussed later.

4.2 Evaluation of Solution Treated Alloys

Alloys comprising series I, II and III were evaluated in the solution treated condition in terms of identification of precipitate phases and grain-size - hardness relationships.

4.2.1 Identification of Inclusions Present In Experimental Alloys

Experimental alloys were hot rolled to strip,

approximately 2 mm thick, in multiple passes with a reheat temperature of 1150°C, as discussed in section 3.2. Metallographic examination revealed that not all the experimental alloys had completely recrystallised following this processing route, but it is in this condition that the assessment for melt related inclusions was carried out. The recrystallisation of experimental alloys will be discussed later.

Experimental alloys 1B and 4, which contained no titanium (and very little aluminium) were found to contain angular aluminium - rich inclusions, figure 21. These are probably aluminium oxide inclusions with the composition Al_2O_3 .

Alloys 5, 6 and 7, all of which contained varying levels of titanium and aluminium, were found to contain titanium rich inclusions. Alloys 6 and 7 contained angular titanium-rich inclusions which were also associated with aluminium and magnesium, a typical EDX spectrum is shown in figure 22. These inclusions will most probably be oxides of composition Al_2O_3 and a spinel of MgO/Al_2O_3 . Alloy 6, however, revealed only titanium-rich, Ti (CN) inclusions, figure 23.

4.2.2 Grain size - Hardness Relationships

Commercial and experimental alloys were subjected to solution treatment temperatures in the range 900°C to 1200°C. In order to investigate the effect of this treatment, which simulates the final mill anneal, the grain size and hardness level for each alloy was determined.

4.2.2.1 Commercial Tubing

The Petch relationships for the solution treated and air cooled casts 2697 and 2682 are shown in figure 24. It can be seen that the slopes of the Petch relationships are identical. From the comparison of the data on all the solution treated commercial tubing both air cooled and water quenched, with the as-received material, given in figure 25, it is clear that the slopes of the Petch relationships are all virtually identical.

The results fall into a general pattern in which:

- (a) the lower carbon cast 2682 has a higher hardness than the high carbon cast 2697.
- (b) the solution treated and air cooled material is harder than the solution treated and water quenched material.
- (c) the mill annealed as-received tubing is harder than either the as-received thermally treated tubing, and considerably harder than the solution treated material.

These effects will be discussed later.

4.2.2.2 Series I

Effect of Varying Carbon Content in Alloys Containing Neither Aluminium or Titanium

For this work, the two extremes of carbon content in the aluminium and titanium free experimental casts were used, namely casts 1B and 4 containing 0.02% and 0.08% respectively. Specimens were solution treated at temperatures between 900°C and 1200°C followed by either

air cooling or water quenching. The high carbon cast 4 had not fully recrystallised during the hot rolling, and did not recrystallise completely until the solution treatment temperature exceeded 1050°C, figures 26 (a) and (b). Moreover the incompletely recrystallised structures showed very variable grain size, figure 26 (a). On the other hand the low carbon cast 1B was completely recrystallised during rolling and showed uniform recrystallised grain sizes at all solution treatment temperatures, figure 27 (a) and (b).

The effect of solution treatment temperature and rate of cooling on the grain size is shown in Table 3 and figures 28 and 29. It can be seen that up to 1050°C the grain size was independent of carbon content, and only showed a slight coarsening with increasing temperature. Above 1050°C the high carbon alloy coarsened much more than the low carbon alloy, and this unusual result is due to recrystallisation occurring during solution treatment. This will be discussed later. Moreover, figure 28 also shows that at the higher solution treatment temperatures, above about 1100°C, the air cooled material had a coarser grain size than the water quenched material. This may indicate some further grain growth during the slower air cooling compared with water quenching.

The effect of solution treatment temperature and rate of cooling on the hardness is shown in Table 3 and figure 30. There was virtually no difference between the hardness of water quenched and air cooled specimens. At solution treatment temperatures above 1100/1150°C the hardness was

independent of carbon content, but below 1100°C the higher carbon alloy was much harder than the low carbon alloy, due to it being incompletely recrystallised. In the low carbon alloy, increasing the solution treatment temperature caused little or no change in hardness until the highest temperatures were reached, and even then the decrease in hardness was only slight. Because the high carbon material was incompletely recrystallised at the lower solution treatment temperatures, the hardness does not reflect solely the grain size, but also comprises a significant contribution from remnant dislocation strengthening and from the sub-grain size of the polygonised structures in recovered specimens.

Only fully recrystallised specimens with hardness values below 130 HV have been used for the Petch relationships shown in figure 31. The data therefore covers a small range of low hardness and $d^{-1/2}$ values. For the low carbon cast 1B the slopes of the Petch relationships were somewhat less than those for the commercial tubing in figure 25, and the water quenched material was marginally (4 HV) harder than the air cooled material. There was no difference between the water quenched and air cooled data for the high carbon cast 4, the hardness of which was about 8 HV greater than that of the low carbon cast at the same grain size. The slope of the Petch relationship for the high carbon material was virtually the same as that for the commercial tubing.

4.2.2.3 Series II

Effect of Varying Carbon Content in Alloys Containing 0.25/0.30% Al and 0.21/0.29% Ti

For this work commercial casts 2682 and 2697, together with experimental alloy 7 were used. Specimens were either air cooled or water quenched from solution treatment temperatures between 900°C and 1200°C, and details of hardness and grain size are given in Table 4. The microstructures of the experimental alloy 7 are shown in figure 32 from which it can be seen that recrystallisation had been complete during rolling. The effect of solution treatment temperature on the grain size is shown in figure 33 from which a clear pattern can be seen. Whilst there was some variation between the different carbon content materials at low solution treatment temperatures, due to variations in the initial processing of the alloys, with increasing carbon content:

- (a) the grain size at the high solution treatment temperatures, progressively decreased.
- (b) the temperature for the commencement of grain coarsening increased.

In general there was no systematic difference in grain size between the air cooled and water quenched conditions.

The effect of solution treatment temperature on the hardness is shown in figure 34. Due to the complex interaction of grain size, carbon in solution, dispersion strengthening, by undissolved carbides, and dislocation strengthening, there was no clearly defined effect of carbon content nor of the rate of cooling. The results clearly show however that grain size had an overriding effect, the

hardness decreasing with increasing solution treatment temperature.

The Petch relationships for the alloys are shown in figure 35. All the relationships had virtually the same slope which was the same as for the commercial materials shown in figures 20 and 24. An interesting feature was the absence of dependence of the hardness on the grain size for the 0.04%C and 0.08C alloys at the coarsest grain sizes, ie at the highest solution treatment temperatures. This will be discussed later. Also noticeable was the higher hardness of the air cooled condition compared with the water quenched condition for the 0.02%C and 0.04%C alloys, but not for the 0.08%C alloy.

4.2.2.4 Series III

Effect of Titanium Content in Alloys Containing 0.02/0.04%C and 0.23/0.25% Al

The carbon content was chosen as being typical of commercial alloy 600, and titanium contents in the range 0.15% and 0.40% were used in conjunction with 0.23/0.25% Al. For the experimental alloys, alloy 5, containing 0.15% Ti, had not recrystallised completely during hot working, but had recrystallised after solution treatment at temperatures above 950°C. The other experimental alloy, alloy 6 containing 0.40% Ti, was completely recrystallised during hot working and at all solution treatment temperatures. Assuming, reasonably, that all the nitrogen is combined with titanium as TiN, the effective titanium in the alloys will be reduced slightly, but even so all were

hyperstoichiometric, having Ti:C ratios greater than the stoichiometric ratio for TiC, namely 3.99. The effect of titanium on the structure and properties will be discussed later.

Details of the hardness and grain size of specimens either air cooled or water quenched from solution treatment temperatures between 900°C and 1200°C are given in Table 5. The effect of solution treatment temperature on the grain size is shown in figure 36. It can be seen that the 0.22% Ti commercial alloy 2697 had an appreciably smaller grain size at low temperatures compared with the 0.15% Ti and 0.40% Ti alloys, which were experimental alloys. This may be due to differences in the hot working of commercial and experimental materials. There was no clearly defined effect of titanium on the grain coarsening temperature, nor of the rather limited variation in carbon content. However, at temperatures above the grain coarsening temperature increasing the titanium content progressively and markedly increased the grain size. These effects will be discussed later.

The effect of solution treatment temperature on the hardness is shown in figure 37, from which it can be seen that the effect of titanium on the hardness was not very great or consistent at high solution treatment temperatures. At low solution treatment temperatures, however, the 0.22% Ti commercial material was consistently harder than the 0.15% and 0.40% Ti experimental alloys. This was due to the finer grain size of the commercial

material, which is shown by the Petch relationships in figure 38. The Petch relationships will be discussed later.

4.2.3 Mechanical Properties of Experimental Alloys

The effect of solution treatment temperature, in the range 950 to 1150°C, on tensile properties was investigated. Experimental alloys were room temperature tensile tested.

Series I Alloys

Section 2.4.2.2 detailed grain size - hardness results for the alloys which contain neither aluminium or titanium. This information has been supplemented by tensile tests for each alloy covering the same solution treatment range.

Table 6 and figure 39 present the tensile results for alloy 1B, containing 0.02% C, and alloy 4, containing 0.08% C. Alloy 1B shows a reduction in 0.2% proof stress and UTS with increasing solution treatment temperature. Alloy 4 shows a similar but more pronounced trend. These results will be discussed later in terms of cast chemistry, recrystallisation and grain growth.

Series II Alloys

As for series I alloys the tensile results complement the grain size hardness information presented in section 2.4.2.3. Series II alloys contain varying carbon contents for approximately constant levels of Ti and Al. Reference to Table 1 reveals that the only experimental alloy in

series II is alloy 7, and hence this is the only alloy for which tensile results are available.

Table 7 presents the tensile information for alloy 7, and figure 39 shows this information in graphical form. Although a direct comparison with other series II alloys is not possible, the tensile results will be discussed with reference to series I and III alloys. Alloy 7 is fully recrystallised at 900°C and therefore grain growth occurs with further increases in the solution treatment temperature without the effect of recrystallisation.

Series III Alloys

These alloys contain varying levels of titanium for approximately constant levels of aluminium and carbon. The hardness - grain size information presented in section 2.4.2.4 is complemented by tensile results presented in Table 8 and figure 39.

Alloy 5 containing 0.15% Ti had not fully recrystallised following hot working but had recrystallised following solution treatment above 950°C. Alloy 6 containing 0.40% Ti however was fully recrystallised prior to solution treatment at all temperatures. Figure 39 shows that the proof stress and UTS for both alloys falls with increasing solution treatment temperature, with alloy 6 retaining the higher tensile properties.

4.3 Evaluation of Solution Treated and Thermally Aged Alloys

The effect of thermal ageing in the range 500°C to 1000°C for times ranging from 10 minutes to 100 hours has been evaluated in terms of hardness, tensile properties and carbide precipitation. Selected corrosion tests were also undertaken and these will be presented and discussed later.

4.3.1 Hardness

The effect of thermal ageing on mechanical properties has been monitored in terms of hardness for all alloys. Section 4.3.2 covers the microstructural changes, primarily in terms of carbide precipitation, which occur during these ageing treatments.

4.3.1.1 Series I

The hardness results for alloys 1B and 4, solution treated at 1150°C water quenched, following thermal ageing are presented in Tables 9 and 10. The results for alloy 1B, reveal no appreciable hardness change over the entire ageing range. Indeed the small degree of variation between the results is concluded to be due to the inherent initial hardness variation of the material. The results for alloy 4 show significant hardness changes during ageing treatments and these are graphically presented in figure 40. The increase in hardness during ageing is clearly dependant upon both the time and temperature, with the maximum hardness level, approximately 170 HV, occurring following ageing at 700°C for 8 hours. The hardness results indicate a precipitation hardening process for this alloy. The correlation of this hardness change with carbide precipitation will be discussed later.

4.3.1.2 Series II

Alloys 2682, 2697 and 7 constitute Series II. The commercial alloys 2682 and 2697 were solution treated at 950, 1050 and 1150°C prior to ageing, whereas experimental alloy 7 was solution treated at 1150°C only and then aged. The hardness test results are presented in Tables 11 to 17 inclusive, and it can be seen that the full range of ageing was not undertaken on alloy 2682 because of limited material availability. The results for alloys 2682 and 2697, tables 11 to 16 inclusive, show that there has been no appreciable hardness change during ageing from any of the solution treatment temperatures.

The results for alloy 7, 0,08% C and 0.28% Al/0.29 Ti, does show an appreciable effect of ageing on the hardness level. The results presented in Table 17 are graphically shown in figure 41. A comparison between the results for alloy 7 and alloy 4 (figure 40) reveal an equivalent peak hardness level achieved following ageing at 650/700°C. It can be seen that alloy 7 maintains the peak aged hardness for an appreciably longer time at 700°C (100 hours) than alloy 4 (8 hours). This age hardening effect will be discussed in terms of alloy composition and carbide precipitation.

4.3.1.3 Series III

Alloys 5, 2697 and 6 constitute Series III. The hardness test results are presented in Tables 14 to 19 inclusive. The effect of ageing on alloy 2697 has already been

reported in terms of no appreciable change. The same is true for alloys 5 and 6, Tables 18 and 19 respectively, with no significant change in hardness during ageing. There is no discernible influence of the varying titanium level for approximately constant carbon. The results for alloys 5 and 6, 0.02% C / 0.15% Ti and 0.03% C and 0.40% Ti respectively are almost identical. This indicates that titanium alone, at these levels, does not result in a hardness change during ageing. However, reference to the results for alloys 4 and 7 does indicate that titanium at 0.29% in conjunction with carbon at 0.08% does produce significant hardness increase during ageing. The effect of titanium on age hardening would appear to be that it stabilises the carbide precipitates which cause the ageing response. The effect of composition on hardness and precipitation will be discussed later.

4.3.2 Precipitation of Carbides

Detailed microstructural studies were carried out to determine the onset and extent of precipitation which occurs during the ageing treatments. The precise conditions which resulted in the initiation of precipitation were determined by transmission electron microscopical techniques. It has been possible in most cases to construct time-temperature-precipitation 'C' curves which define the precipitation domain arising from thermal ageing.

4.3.2.1 Series I

Examination of the microstructures following solution treatment, 1150°C water quenched, revealed an absence of any detectable precipitation, figure 42 (a) and (b). The onset of precipitation was then studied and the precipitates analysed by electron diffraction. In all cases the precipitates were identified as chromium carbide of the $M_{23}C_6$ type.

The first detectable precipitates always appeared on the grain boundaries initially as thin plate like particles. Typical examples are presented in figures 43 (a) and (b) for alloy 1B aged 650°C 1 hour and alloy 4 aged 650°C 30 minutes. It is apparent that a higher level of carbon, 0.08% for alloy 4 compared to 0.02% for alloy 1B, results in both earlier and a greater degree of precipitation during ageing.

Extended ageing affected the morphology and distribution of the precipitates for both alloys. As ageing progressed alloy 1B exhibited a coarsening of discrete grain boundary carbides, figure 44 (a), and the formation of bands of fine rod-like precipitates both inter- and intra-granularly, figure 44 (b). As indicated in section 4.3.1.1 there was no appreciable hardness change associated with either the onset of precipitation or its subsequent growth. Clearly extended ageing results in the precipitation of solid solution carbon as chromium carbides, primarily at the grain boundaries, and for a 0.02% level of carbon there is no appreciable change in hardness.

Alloy 4 however, with 0.08% carbon, does show a significant hardness change with extended ageing. Figure 40 shows the maximum age hardening response to result from ageing at 650°C for 100 hours. The effect of extended ageing is clearly shown in figure 45, where the transition from thin plate to larger discrete precipitates being shown. In this case there is a distinct relationship between hardness and precipitation. Figure 46 shows the $M_{23}C_6$ precipitation from material aged at 650°C for 100 hours. There are numerous rod like precipitates which form bands running adjacent and perpendicular to the grain boundaries. The precipitates have nucleated and grown in the high diffusion rate areas of grain boundaries and dislocations piled-up perpendicular to those boundaries.

The precipitation C-curves for series I alloys are presented in figure 47. The actual observation points (SEM/TEM) used for construction of the C-curves have been omitted to avoid confusion. Continuous lines representing 0% (ie the onset of) precipitation have been used in all cases. It can be seen that alloy 4 (0.08%C) precipitates carbide faster than alloy 1B (0.02% C). These effects will be discussed later.

The effect of composition and ageing treatments on microstructure and hardness will be discussed later.

4.3.2.2 Series II

Series II alloys comprise alloys 2682, 2697 and 7. Following microstructural studies it was revealed that alloy 2682 had grain boundary $M_{23}C_6$ precipitates present

following solution treatment at all the temperatures evaluated. This effect is clearly shown in figure 48. Consequently it was not possible to study the effect of ageing on carbide precipitation for alloy 2682. The reasons for the presence of carbides in this alloy will be discussed later but may be due to precipitation during cooling from the solution treatment temperature. Alloys 2697 and 7 did not contain any precipitates following solution treatment above 1000°C and were therefore incorporated into this study. The precipitation C-curves for alloys 2697 and 7 solution treated at 1150°C and aged are presented in figure 49.

Comparison of the precipitation C-Curves indicates that alloy 7 has a faster rate of precipitation compared to alloy 2697. This effect results from the higher carbon content of alloy 7, although additional influences may well be due to the material grain size and prior processing history. The grain size of alloy 7 is approximately 60 microns whilst for alloy 2697 approaches 130 microns, the significance of this will be discussed later. A further comparison between alloy 7 and alloy 4, figures 47 and 49 respectively, reveals a faster rate and larger precipitation domain for alloy 7. Both alloys have an equivalent level of carbon, but alloy 7 also contains 0.29% Ti and 0.28% Al with an appreciably smaller grain size of 60 microns compared to 160 microns for alloy 4. The interaction between composition, grain size and precipitation will be discussed later.

As for alloy 4 the hardness results revealed a significant age hardening response for alloy 7. It has been possible to correlated this effect with the precipitation reactions. Figure 41 indicates that the maximum age hardening response occurs following ageing at 650°C for 100 hours (as for alloy 4). Figure 50 shows the distribution and morphology of precipitates, identified as $M_{23}C_6$ Chromium Carbide, following this optimum ageing. It can be seen that the precipitates are rod like in nature and are interacting with dislocations. The effect of strain induced in the matrix must also contribute to the hardening effect. The precipitates are located at the grain boundaries and within the grains. In comparison, alloy 2697 does not display this type of precipitation, ageing results in the coarsening of discrete grain boundary chromium carbides and eventually limited precipitation within the grains. As previously stated there is no detectable hardness change during ageing for alloy 2697.

4.3.2.3 Series III

Alloys 5, 2697 and 6 comprise Series III which cover chemistry variation of 0.15 to 0.40% Ti for 0.02/0.04% C and 0.23/0.25% Al. The precipitation C-Curves for alloys 5 and 6 are presented in Figure 51, whilst figure 49 covers alloy 2697. All three alloys have grain sizes in the range 95 to 125 microns with varying carbon and titanium levels. Inspection of the C-curves reveals the largest precipitation domain for alloy 2697 with 0.04% C and 0.22% Ti.

The lowest carbon content alloy 5, has the smallest precipitation domain and contains 0.02% C and 0.15% Ti. Comparing alloys 5 and 6 it can be seen that the higher level of carbon and titanium, in alloy 6, results in a larger precipitation domain. These effects will be discussed later.

As previously discussed there was no appreciable hardness change during the ageing of any Series III alloys. Microstructural studies revealed mainly grain boundary precipitates which became discrete and coarsened as a result of extended ageing. Figure 52 shows this effect for alloy 5 following ageing at 600°C for 64 hours. There is a distinct difference between the precipitation occurring in alloys 5 and 6 following this ageing treatment. Figure 53 shows the grain boundary precipitation effects in alloy 6 aged at 600°C for 64 hours. In this case there is no discrete grain boundary chromium carbides but a band of very fine precipitates which have been identified as TiC. There is also evidence of chromium carbide in this precipitation band but to a lesser extent than the titanium carbide. The slightly smaller precipitation domain shown in figure 51 may be a result of diminished levels of $M_{23}C_6$ chromium carbide due to the presence of titanium carbide. These effects will be discussed later.

4.4 Evaluation of Solution Treated and Cold Rolled

Experimental Alloys

This study utilised experimental alloys 4 and 5. The choice of these alloys was made because they represented

the extremes of the available compositions. Alloy 4, Series I, contains 0.08% C with no Al or Ti, whilst Alloy 5, Series III, contains 0.02% C with 0.23% Al and 0.15% Ti. The initial evaluation was in terms of the effect of cold rolling on the mechanical properties which were monitored via hardness and tensile testing. Additional evaluation considered the influence of cold rolling on subsequent thermal ageing and the important corrosion response. The solution treatment temperature used for both alloys was 1150°C (water quenched).

4.4.1 Hardness

The effect of cold rolling on hardness is shown in Table 20 and figure 54. It can be seen that, from initially equivalent solution treated hardness levels, alloy 4 work hardens at a marginally faster rate and finally achieve a significantly higher final hardness level than alloy 5. The mechanism of work hardening responsible for these hardness increases will be discussed later in terms of composition and dislocation strengthening.

4.4.2 Tensile properties

Table 21 and figure 55 (a) and (b) present tensile properties associated with the hardness levels reported in 4.4.1. It can be seen that alloy 4 achieves higher levels of proof stress and UTS than alloy 5.

There is agreement between the effect of cold rolling on hardness and tensile properties, and an indication that the higher carbon content alloy (alloy 4) will work harden at a slightly faster rate and ultimately achieve higher property

levels than the lower carbon content alloy (alloy 5). As previously discussed both alloys 4 and 5 did not contain any precipitated carbide in this solution treated condition.

4.5 Evaluation of Solution Treated, Cold Rolled and Thermally Age Experimental Alloys

In order to further understand the effects of cold work on structure and properties, an investigation was undertaken to determine the subsequent thermal ageing response. Alloys 4 and 5 were used for this study, for the reasons discussed in section 4.4., and the evaluation was in terms of hardness, tensile properties, precipitation and corrosion behaviour. It has also been possible to study the effect of thermal ageing on the recrystallisation behaviour of the alloys.

4.5.1 Hardness

Hardness determinations were made following solution treatment at 1150°C (WQ) and cold rolling with approximately 25% and 50% reductions in thickness. This was followed by ageing in the temperature range 500°C to 1000°C for times from 10 minutes to 100 hours.

The hardness test results are presented in Tables 22 to 29 and displayed graphically for ageing in the range 500°C to 900°C in figures 56 to 61. It is clearly evident that significant changes in the hardness levels for both alloys occurs during ageing. The reasons for these changes are revealed from structural studies where the effect of ageing

on recrystallisation can be seen. These hardness results do not allow a detailed correlation to be established between the simultaneously occurring mechanisms of precipitation and recrystallisation (including the prerequisite stage of recovery), but do provide a means of monitoring these changes. An interpretation of the recrystallisation kinetics will be given in section 4.5.3.

As expected, material cold worked by approximately 50% had a higher hardness than material cold worked by 25%. Alloy 4 had a higher hardness level than alloy 5 for both levels of cold work. This situation was maintained until ageing at 700°C resulted in the dramatic hardness decrease of alloy 5 (50% reduction) following ageing for 8 hours. Recrystallisation was occurring for this material condition.

As ageing continues there is progressive recrystallisation of all four alloys. It can be predicted from earlier studies that carbide precipitation is also occurring during ageing. This effect will be reported in section 4.5.4. In general, for equivalent levels of cold work, the higher carbon cast (alloy 4) maintains a slightly higher level of hardness both before and after recrystallisation than the lower carbon cast (alloy 5).

4.5.2 Tensile Properties

Due to the limited availability of test material it was decided to restrict this study to Alloys 4 and 5, with approximately 50% cold work, and aged at 700°C, only. This

ageing temperature was chosen because of the commercially important thermal treatment (16 hours at 700°C) following mill annealing.

Table 30 presents the tensile results for material solution treated, cold worked by 50% and thermally aged at 700°C for 1 to 100 hours. It can be seen that both alloys undergo a significant reduction in tensile properties during ageing at 700°C. As discussed in section 4.5.1 these alloys are undergoing recrystallisation and carbide precipitation. The results show that alloy 5 begins and completes recrystallisation before alloy 4 for reasons that will be discussed later. These tensile results support the hardness data previously discussed and clearly reveal the effect of recrystallisation on mechanical property levels.

4.5.3 Recrystallisation Kinetics

Thermal ageing caused all four conditions, namely alloys 4 and 5 cold rolled to approximately 25 and 50% reduction in thickness, to recrystallise. The combination of ageing time and temperature which leads to recrystallisation depends upon the level of internal strain (from the cold work) as well as the grain size and microstructure of the material. Hence it is to be expected that material with 50% cold work will recrystallise before that with 25% cold work. The different rate of recrystallisation between alloy 4 and alloy 5, for the same level of cold work, is a function of the grain size, microstructure and composition.

Examination of figures 56 to 61 reveal an order of recrystallisation, with the alloy condition which recrystallises most readily, as; alloy 5-50% cold reduction, alloy 4-50% cold reduction, alloy 5-25% cold reduction and alloy 4-25% cold reduction. The values of cold reduction are approximate, but the increased tendency for alloy 5 to recrystallise before alloy 4 is evident. Table 20 gives the actual % cold reductions for each alloy and the as-rolled hardness values. Tables 3 and 5 give the grain sizes for each alloy prior to cold rolling, with alloy 4 at 81 microns and alloy 5 at 94 microns M.L.I.. These grain sizes are very similar and indicate that this would not be a significant factor in determining the order of recrystallisation. Figures 54 and 55 show that the two alloys work harden at slightly different rates, with alloy 4 attaining a higher final hardness value. Section 4.5.1 indicates that this is related to the alloy composition with the higher hardness occurring for the higher carbon content.

It can be surmised that alloy 4 shows a greater resistance to recrystallisation than alloy 5 for equivalent levels of cold reduction. It is suggested that this effect may be partly due to the titanium containing alloy (alloy 5) having a distribution of stable TiC/TiN precipitates which generate dislocations during cold working and accelerate subsequent recrystallisation during ageing. These effects will be discussed later.

Figure 62 shows a grain structure typical for both alloys 4

and 5 in the fully recrystallised condition following ageing. The presence of distinct precipitates marking 'ghost' boundaries of deformed grains overlaid on a fully recrystallised structure can be seen. There is little evidence of grain boundary precipitation on the recrystallised boundaries, which indicates that recrystallisation occurs below the carbide solvus temperature. This observation is important because of the effect of precipitate location and distribution on stress corrosion cracking. Such a structure has previously been observed as offering a low resistance to SCC (61). The relationship between cold work, thermal ageing and SCC will be discussed later.

4.5.4 Precipitation of Carbides

As for section 4.3.2 a study of the onset of precipitation can only effectively occur if the alloy is initially free from precipitates prior to ageing. This condition was observed for alloys 4 and 5 with both levels of cold reduction. The onset of precipitation was studied by optical and electron microscopy, with the latter technique being used to determine the crystal structure of the precipitates.

Figures 63 and 64 show the time-temperature-precipitation C-Curves for the cold rolled and aged alloys 4 and 5. In all cases the precipitates were identified as $M_{23}C_6$ chromium carbides with the onset of precipitation occurring at grain boundaries.

Figure 63 for alloy 4 shows only a slightly increased tendency for precipitation as the level of cold reduction increases from 25 to 50%. Similarly figure 64 for alloy 5 indicates very little change in the precipitation rate or domain as a result of increasing the level of cold reduction. However, comparison with the C-curves for no cold work indicates significant increases in the precipitation rate and domain as the level of cold work is increased from 0 to 50%.

These results suggest that precipitation is occurring both during and after recrystallisation. If full recrystallisation occurred before precipitation then cold work would not affect its rate or temperature domain. However it is clear that cold work does influence precipitation and so both reactions must be occurring simultaneously. This effect will be discussed later.

4.6 Corrosion Testing of Experimental Alloys

To conclude the experimental studies a corrosion test programme was undertaken to study the effects of various thermal and mechanical treatments on the corrosion behaviour. Analysis of the corrosion test results reveals trends and effects related to all the preceding treatments and additionally to the effect of localised post ageing cold deformation (ie bent samples).

4.6.1 Solution Treated and Thermally Aged Alloys

The accumulative weight loss results for alloys 4 and 5 following exposure for up to four periods of 48 hours immersion are given in Table 31. A significant number of samples failed to survive beyond the first or second immersion period because of extensive IGC which resulted in disintegration of the samples. Figures 65 and 66 display the weight loss results after one period of 48 hour immersion.

Figure 65 indicates that alloy 4 was in a highly sensitive condition to corrosion following ageing for 100 hours at 500 and 600°C. Both flat and bent samples showed a catastrophic increase in corrosion from 100 hours at 500°C through to 1 hour at 700°C. Continued ageing at 700°C beyond 1 hour resulted in a divergence of behaviour. The flat samples had a reducing corrosion rate for ageing beyond 1 hour. The bent samples were catastrophically corroded up until ageing for 100 hours, at which time the susceptibility fell to the comparable low level recorded for the flat samples. These results support the mechanism of sensitisation as a consequence of grain boundary precipitation. These effects will be discussed later.

Figure 66 shows the results for alloy 5 following ageing. The results reveal significantly lower levels of corrosion than alloy 4 for all aged conditions. Both flat and bent samples follow the same pattern, and show that corrosion

susceptibility rises as the ageing temperature increases from 500°C to 700°C for an ageing time of 1 hour. Continued ageing at 700°C for up to 100 hours results in a much reduced level of weight loss. These reduced weight losses are comparable with the lowest levels observed for alloy 4.

The intergranular nature of the corrosion evident in both alloys is shown in figures 67 and 68. Alloy 4 suffers extensive grain boundary attack and the loss of entire grains, especially following ageing at 500°C for 100 hours. The same aged condition for alloy 5 resulted in localised 'fingers' of corrosion for the flat sample. Extensive intergranular attack and grain loss are evident as shown in figure 69. Such localised corrosion was not seen on the bent sample, but general IGC did occur, figure 70. It is possible that corrosion 'fingers' occur because of concentrations of critical strain, and once initiated the corrosion takes the form of localised fingers. This effect will be discussed later.

To further investigate the phenomena of localised 'fingers' of corrosion observed in alloy 5, a series of microhardness traverses were taken at positions corresponding to the middle of the 'fingers' and midway between them. As an approximation the 'fingers' were between 1 and 1.5 mm wide and spaced in the order of 6 and to 15 mm apart.

The averaged results from three hardness surveys are shown in Table 33. There appears to be some correlation between areas of localised corrosion and increased hardness levels. This was consistent for all hardness traverses but the effect was only observed on a single flat sampled aged at 500°C for 100 hours. These results support a local strain theory for corrosion and will be discussed later.

4.6.2 Solution Treated, Cold Rolled and Thermally Aged Alloys

The accumulative weight loss per unit surface area for alloys 4 and 5 with approximately 50% cold work prior to ageing are presented in Table 32. Comparison with the results from non-cold rolled material, Table 31, reveals a significant difference in corrosion rate. The cold rolled material has weight loss results an order of magnitude lower than non-cold worked material. With all samples surviving over the entire series of five exposure periods. Figures 71 and 72 display the accumulated weight loss results for alloys 4 and 5 respectively. It should be noted that this study was limited to material aged at 700°C.

Comparison of figures 71 and 72 indicates very similar results for both alloy 4 and alloy 5. This is contrary to material which had not been cold rolled prior to ageing, figures 65 and 66, where alloy 4 showed significantly greater corrosion weight loss in all heat treated conditions except 100 hours at 700°C. It has been proposed that alloy 4 (0.08% C) is far more influenced by grain

boundary sensitisation and precipitation than is alloy 5 (0.02% C).

In general for alloy 4 the corrosion rate falls as ageing time increases. This trend is clearly shown for the bent samples, whereas for flat samples the corrosion results following ageing for 100 and 16 hours are anomalous but at a lower level than those following ageing for between 1 and 8 hours. The bent samples have a slightly increased corrosion rate compared to the flat samples.

The corrosion results for alloy 5, as shown in figure 72, show a different trend to alloy 4. The corrosion rate is at its greatest following ageing for 100 hours at 700°C. The bent samples showed very similar corrosion results to the flat samples, which indicates that localised cold work did not appreciably effect corrosion in these samples.

Proposed reasons for the differing corrosion response between casts and material conditions will be discussed later, with the influences of carbide distribution and volume fraction being particularly important.

Introduction

The experimental results presented in Section 4 will be discussed in order to attempt to explain the behaviour of the material in response to combinations of thermal and mechanical treatments. The resulting structure and properties of the material will be explained, where possible, in relation to the processing route and its significance to commercial PWR tubing production.

5.1 The Identification of Precipitate Phases5.1.1 Carbide Phases Present in As-Received, Solution Treated and Aged Commercial Alloys

The present results have shown that two distinct forms of chromium rich carbide can exist in Alloy 600, namely M_7C_3 and $M_{23}C_6$. Other work (67) has confirmed these findings with M_7C_3 typically containing 96% Cr, 2% Fe and 2% Ni whilst $M_{23}C_6$ contains 87% Cr, 3% Fe, 10% Ni.

The M_7C_3 occurs primarily within the grains as quite large particles which have formed during production of the tube. Some of these particles are present on grain boundaries because boundaries have migrated to them and become pinned. They will therefore act as grain boundary pinning particles and as such will help to control the grain size. However their pinning effect is not expected to be very great in this respect because of the relatively large particle sizes. This will be discussed later.

Since M_7C_3 is the stable carbide at high temperatures in these alloys, they persist to quite high solution treatment temperatures. The solvus temperatures were calculated to be, under equilibrium conditions, 941°C and 1032°C for casts 2682 and 2697 respectively. With increasing solution treatment temperature, if M_7C_3 was primarily responsible for the loss of pinning at grain boundaries and grain growth, then it would be expected that the activation energy for grain growth would be that for Cr diffusion through the matrix or the self diffusion of vacancies. In fact, as will be discussed later, the activation energy for grain growth is considerably lower than these mechanisms suggest (68). It may be inferred that the growth of M_7C_3 possibly occurs by grain boundary diffusion between particles situated on such boundaries, the overall Ostwald Ripening occurring as boundaries become unpinned and migrate from particle to particle. This could only be substantiated by detailed kinetic studies of the growth of Cr_7C_3 .

The $M_{23}C_6$ chromium carbide occurs almost exclusively on grain boundaries. In the mill annealed and thermally treated condition there were many more precipitates of this type than in the mill annealed condition. This is because $M_{23}C_6$ precipitates and grows on grain boundaries during the thermal treatment of 15 hours at 704°C . $M_{23}C_6$ was however observed on grain boundaries of material which had been mill annealed. This had most probably formed during cooling from the mill annealing temperature. The same form of carbide occurred in solution treated material after high solution treatment temperatures and relatively slow rates

of cooling. In this condition most of the carbides had been dissolved and the degree of supersaturation and the tendency for precipitation during cooling was at its greatest.

For thermally treated commercial material, the time at 704°C had been sufficient for grain boundary $M_{23}C_6$ carbides to grow. In all these cases the grain boundary $M_{23}C_6$ was semi-continuous. Models have been proposed for the precipitation of $M_{23}C_6$ (68) indicating that Cr diffusion normal to the grain boundary is the rate controlling step for nucleation. Once nucleation has occurred grain boundaries will be primary nucleation sites for the precipitation of $M_{23}C_6$. It is widely acknowledged that the growth of $M_{23}C_6$ is controlled by grain boundary diffusion of chromium.

Titanium in Alloy 600 has been shown to produce quite large cubic Ti(CN) or Ti(N) particles, often associated with MgS. In the present work there is also evidence of a fine dispersion of TiC. It is possible that, despite the small volume fraction of TiC, its small particle size enables it to play a significant role in the control of grain size by acting as effective grain boundary pinning particles. Evidence has not been obtained to show clearly how solution treatment temperature influences the occurrence of TiC, if at all, or its growth.

Commercial material which had undergone solution treatment and subsequent thermal ageing contained precipitates very similar to those present in thermally treated material.

This result is as expected and confirms the understanding of the precipitating phases which can be formed. The effect of ageing on solution treated commercial tubing will be discussed later.

5.1.2 Inclusions Present in Commercial and Experimental Alloys

Commercial materials contained angular titanium-rich particles approximately 5 microns in diameter. These were undoubtedly Ti(CN) and although not numerous were easily detected. In some cases magnesium sulphide was associated with these Ti(CN) particles. Magnesium is sometimes used in Alloy 600 as an addition which helps promote hot workability by its scavenging action on impurities. It is also interesting to note that some phosphorus was associated with the magnesium sulphide.

Experimental alloys 1B and 4, comprising Series I, were found to contain only aluminium-rich inclusions, which varied in size from 1 to 3 microns in diameter. Since Series I alloys contain no titanium and aluminium, the residual aluminium content (<0.05%) must account for these inclusions. Series II and III alloys, which contain titanium and aluminium, have inclusions rich in titanium (Ti(CN)) and aluminium. These angular inclusions were approximately 5 microns in diameter and occasionally associated with magnesium, which has impurity (S,P) scavenging effects.

5.1.3 Carbide Phases Present in Solution Treated and Aged Experimental Alloys

Two forms of chromium carbide may occur, namely M_7C_3 and $M_{23}C_6$. All experimental alloys solution treated up to 1050°C contained a small number of isolated intragranular M_7C_3 and a greater degree of grain boundary $M_{23}C_6$. The reason for these precipitates and their distribution has previously been discussed. All alloys solution treated at 1150°C showed no evidence of any chromium carbide present in the microstructure. These carbide free structures were then chosen as the condition for subsequent detailed studies of precipitation following thermal ageing.

The precipitation of chromium carbides as a result of thermal ageing will be discussed in detail later, but in all cases the detected carbides were of the $M_{23}C_6$ type occurring primarily at grain boundaries.

5.2 Structure and Properties of the As-Received Commercial Tubing

5.2.1 Variability of Grain Size

An interesting feature in commercial materials was the finer grain size towards both the inner and outer surfaces of the tubes. This may have been due to the concentration of cold work in the surface regions during tube drawing, particularly from sizing passes or straightening operations prior to the final mill anneal. This would cause recrystallisation to be confined towards tube surfaces. However, the smaller grain size near to the tube surfaces may also have been influenced by rate of heating and cooling during mill annealing, although for thin walled

tubing this would be of relatively less significance than variations in the degree of cold work.

As shown in Table 2, the mill annealed and mill annealed plus thermally treated material from the same cast did not have precisely the same grain size. It would not be expected that a thermal treatment at 700°C would alter the grain size of material which had been mill annealed at about 950°C. This clearly suggests that there is variability in the mill annealing conditions from tube to tube from the same cast. This variability in the mill annealing schedule will be discussed later.

In order to investigate further the grain size variation from tube to tube within a batch, five individual tubes were examined from the mill annealed material of alloy 2697. The grain sizes obtained, with the corresponding hardness values, were as follows:

Tube No	Grain Size (μm) and 95% CL	$d^{-\frac{1}{2}}$ ($\mu\text{m}^{-\frac{1}{2}}$)	Hardness (HV)
1	13.4 (\pm 1.3)	0.273	221
2	16.4 (\pm 0.9)	0.247	210
3	17.1 (\pm 1.2)	0.242	222
4	15.1 (\pm 1.2)	0.258	224
5	15.6 (\pm 1.1)	0.253	217

The grain size variations exceed the overlap of 95% confidence limits in several cases, and it would therefore seem that the mill annealing temperature was not consistent even within the tubes from a given batch, let alone from batch to batch. The results for the different tubes from alloy 2697, shown in the above table, confirm the finding

that mill annealed material is harder for the same grain size than mill annealed and thermally treated material. It should also be noted that even within the same batch there was some 10HV variation in hardness for the same grain size. This will be discussed later.

5.2.2 Prediction of Mill Annealing Temperatures

Using data obtained from the solution treatment experiments and the grain sizes observed in the as-received commercial materials, it is possible to attempt to estimate the mill annealing temperature used in commercial practice. As can be seen from figure 25, the rate of cooling had little effect on the grain size - hardness relationship for solution treated materials. It may be assumed that the rate of cooling from the mill annealing temperature, which is quite rapid and of the order of 450°C/minute, will be not too dissimilar from those used in the current experimental work. It is also assumed that the 700°C thermal treatment and any additional stress relief will not affect the grain size developed after mill annealing.

Accepting these assumptions, and using the data given in Table 4 and figure 33, it can be estimated that cast 2682 (TT) was mill annealed somewhat below 900°C, whilst cast 2697 (MA) was mill annealed at just about 900°C. Both casts were therefore apparently mill annealed below the recommended temperature. Evidence suggests that material was 'under-annealed' which may have resulted in incomplete annealing out of dislocations. This analysis confirmed the experience reported in discussions with CERL who also have evidence to suggest lower than specified mill annealing

temperatures (62). The net result is variability in grain size and hardness of commercial tubing.

5.2.3 The Effect of Chromium Carbide Dispersion on The Grain Size

The data in Table 2 shows that cast 2682 had a considerably coarser grain size than any of the other commercial casts in both heat treated conditions. It is significant that cast 2682 had the lowest carbon content of 0.02% compared with 0.03/0.04% for the other casts examined. The solubility of carbon as chromium carbide in Inconel 600 is given by the following equation (62) (69):

$$\log (C) = \frac{T(^{\circ}\text{C}) - 1456}{302.8} \dots\dots\dots (1)$$

Where (C) is the mass % C dissolved in the alloy at T°C.

This indicates that at a mill annealing temperature of 950°C some 0.021% C would be dissolved, ie all the carbides would be dissolved in cast 2682. This alone could account for the considerably coarser grain size, there being no grain boundary pinning particles. But cast 2682 in the mill annealed condition did contain undissolved carbides, and this is further evidence that the mill annealing temperature was lower than the specified 950°C. In fact it was estimated previously that cast 2682 was mill annealed somewhat below 900°C, on which basis and using equation (1) it can be calculated that only about 0.015% C would be

dissolved. This would agree with the microstructural observation that undissolved carbides were present in the mill annealed condition. It can therefore be concluded that in the lowest carbon content cast, 2682, there were insufficient carbides undissolved to maintain a very fine grain size by grain boundary pinning, whereas in the 0.03% C and 0.04% C alloys (casts 2683 and 2697 respectively) there were sufficient undissolved carbides to maintain a much finer grain size than in cast 2682.

It is possible to estimate the grain size from the Zener equation:

$$R = \frac{4}{3} \cdot \frac{r}{f} \dots\dots\dots (2)$$

Where R is the grain radius, r the radius of the grain boundary pinning particles and f the volume fraction of the pinning particles.

It can reasonably be assumed that the volume fraction (f) of the undissolved carbides which act to pin the grain boundaries is proportional to the %C undissolved in the alloy (C_u) at the mill annealing temperature, and that C_u is the difference between the dissolved and the total carbon contents of the alloy. Using a mill annealing temperature of about 900°C as predicted in the previous section for casts 2682 and 2697, which would give C_u values of 0.005% C and 0.025% C respectively, it can be calculated that for the observed grain sizes the carbide particle size in cast 2697 should be about 2.7 times as large as those in

cast 2682. Whilst no systematic measurements of carbide particle size have been made, an inspection of the representative optical micrographs indicates that the carbides were both larger and more numerous in cast 2697 than in cast 2682. This analysis confirms the widely acknowledged fact that the greater the volume fraction of undissolved carbides, the coarser they are (67) (70).

It can be concluded that during mill annealing the carbides in the high carbon cast 2697 coarsened more than those in the low carbon cast 2682.

There is a critical undissolved particle radius (r_c) above which the particles do not exert a pinning effect, which has been defined as (71).

$$r_c = \frac{6 R_o f}{\pi} \cdot \left(\frac{3}{2} - \frac{2}{Z} \right)^{-1} \dots\dots\dots (3)$$

Where R_o is the matrix grain radius, f the volume fraction of undissolved particles and Z a heterogeneity factor for grain size.

Assuming constancy of R_o and Z , r_c will increase as f increases and therefore the higher f value in the high carbon cast 2697 compared with the low carbon cast 2682 will mean a higher r_c value for the high carbon cast 2697. Allowing for the difference in matrix grain size between the two casts, it can be calculated that the critical particle radius above which grain coarsening can occur in cast 2697 is about 2.7 times greater than for cast 2682.

The use of these theoretical models confirms that the greater the volume fraction of undissolved carbides the larger their particle size will be. Additionally as the volume fraction and particle size increases so does the grain size that can be effectively pinned. In conclusion this provides an explanation for the finer grain size of high carbon material compared to low carbon material. The low carbon alloy contains few small precipitates which readily lose their pinning effect as they grow, resulting in rapid grain growth during heat treatment. The higher carbon alloy however has a greater number of larger precipitates that grow more rapidly but also effectively retain their grain pinning characteristics for longer as the temperature increases.

The Zener equation presupposes that the actual grain size is a function of the reciprocal of the volume fraction of the pinning particles. This assumption can be tested if the mass fraction (f_m) is substituted for the volume fraction, since grain size should be proportional to $1/f_m$. Figure 73 plots this data for chromium carbide, Cr_7C_3 , and shows that no clearly distinguishable relationship is evident. However, the data available may not be fully representative since alloys containing only carbon (ie no titanium) are pinned by precipitates that must be chromium carbide. In alloys containing titanium it is suggested that titanium carbide, TiC , has a significant effect, and although little experimental support is available a Zener analysis will be discussed latter.

5.2.4 The Effect of Titanium On the Grain Size

Commercial Alloy 600 contains some 0.20% Ti. The grain size appears to be related to the presence of chromium carbides, the solubility of which is given by equation (1), rather than the more stable and less soluble TiC and TiN. An explanation for this relationship may well be due to the nitrogen content of the alloy. TiN is considerably more stable than TiC, and has an exceedingly low solubility in austenite. The titanium will combine preferentially with the nitrogen and, because the alloys are hyperstoichiometric with respect to the Ti:N ratio (3.42) all the nitrogen will be combined as TiN. This lowers the effective titanium content available for the formation of TiC precipitates.

For example, using a fairly typical composition for a commercial alloy containing 0.02% C, 0.20% Ti and 0.005%N, combining the titanium with all the nitrogen lowers the effective titanium content to about 0.18%. This will be available for combination with carbon, but using the solubility equation for TiC in austenitic steels (72):-

$$\log [\text{Ti}] [\text{C}] = \left(\frac{-6780}{T(\text{k})} \right) + 2.97 \dots\dots (4)$$

it can be calculated that all the TiC would be dissolved at about 980°C, ie only just above the mill annealing temperature. There would be very little TiC undissolved at the mill annealing temperature and probably insufficient to cause grain boundary pinning. The volume fraction of TiN would be small, and because it forms at high temperatures

its particle size would be large, so that it also would not cause grain boundary pinning. The presence of TiN has not been detected but is likely to exist for the reasons discussed. For 0.03% C the solvus temperature of chromium carbide may well be above that for TiC so that chromium carbide forms preferentially to TiC especially as kinetically it precipitates more rapidly than TiC. However increasing the titanium and/or carbon contents above those normally found in commercial alloys may well cause TiC to be present at the mill annealing temperature in sufficient quantity to affect the grain size. The determination of which carbides control the grain size will be further discussed later.

As discussed in section 5.2.3 the Zener equation indicates that the actual grain size is proportional to the reciprocal of the mass fraction of carbides. Applying this to TiC reveals interesting results. Figure 74 plots the relevant data for all casts studied and shows that a correlation does exist for titanium containing alloys. There is a difference between experimental and commercial alloys, but in both cases as the mass fraction of TiC increases then the grain size decreases. Clearly TiC must be having a significant influence in controlling grain size during solution treatment. This is an important finding, not previously reported in the literature, and could be of industrial significance in achieving the balance between grain size, mechanical and corrosion properties.

5.2.5 Factors Affecting The Hardness of 'As-Received'

Commercial Tubing

Figure 20 shows that mill annealed material was consistently some 20 HV harder than mill annealed and thermally treated material. This is most probably due to solid solution hardening resulting from increased carbon in solution at the mill annealing temperature compared with the thermal treatment temperature. Moreover this solid solution hardening would not be dependent on the carbon content of the alloy because all the alloys contained undissolved carbides at the apparent mill annealing temperature of about 900°C, as shown by the calculated chromium carbide solvus temperatures using equation (1).

CAST NO	C% OF ALLOY	CALCULATED CARBIDE SOLVUS TEMPERATURE (°C)
2682	0.02	941
2683	0.03	994
2686	0.03	994
2697	0.04	1032

It is interesting to see whether the difference in hardness between mill annealed and mill annealed and thermally treated tubing is entirely due to carbon in solution. There is no quantitative structure-property relationship data for Alloy 600, but much data is available on austenitic stainless steels which may well be applicable. A typical equation for the tensile strength (73) is:

$$\begin{aligned} \text{TS (MPa)} = & 447 + 540 (\%C) + 847 (\%N) + 37 (\%Si) + 1.7 (\%Ni) \\ & + 18.5 (\%Mo) + (\%Mo) + 77 (\%Nb) + 46(\%Ti) + 18.5 (\%Al) \\ & + 2.2 (\% \text{ delta ferrite}) + 12.6 d^{-\frac{1}{2}} \dots\dots (5) \end{aligned}$$

Where () is the mass % of element dissolved in the austenite and d is the mean linear intercept of grain size in mm.

Equation (5) can be tested to see whether it would correctly predict the tensile strength of mill annealed Alloy 600. Using data from figure 20, a hardness of 210 HV is observed at approximately $d^{-\frac{1}{2}} = 0.24 \mu\text{m}^{-\frac{1}{2}} = 7.58 \text{mm}^{-\frac{1}{2}}$. Using a typical commercial composition for Alloy 600 (Table 1) of 0.004 % N and the balance 74% Ni, virtually all the N would be as undissolved TiN leaving some 0.20% Ti in solid solution. At the normal mill annealing temperature of 950°C, about 0.021% C would be dissolved according to equation (1) and there would of course be no delta ferrite. Using equation (5) the predicted tensile strength would be 714 MPa. The hardness for the grain size observed was 210 HV which can be converted by standard tables (74) to an equivalent tensile strength of 708 MPa. The agreement is excellent, and gives confidence in using equation (5) to calculate the solid solution hardening by carbon. From figure 20 and using a grain size of $d^{-\frac{1}{2}} = 0.24 \mu\text{m}^{-\frac{1}{2}}$, ie ($d = 0.0174 \text{mm}$) the mill annealed material is 19 HV harder than the mill annealed and thermally treated material.

At these hardness levels this can be converted (74) (75) to an increase in tensile strength of 73 MPa. Equation (1) shows that material mill annealed at 950°C contains 0.018% more carbon dissolved than does material thermally treated at 700°C, whilst equation (5) shows that this difference in

dissolved carbon would lead to a carbon solid solution strengthening of 10 MPa. With the lower mill annealing temperatures of about 900°C, which have been indicated previously, even less carbon would be dissolved (about 0.015%) which would decrease the carbon solid solution strengthening to only 6 MPa. Consequently the difference in hardness between mill annealed and thermally treated material was much greater than can be attributed only to differences of carbon in solution. As carbon solid solution strengthening only accounted for less than 10% of the 74 MPa difference in hardness between the two standard commercial heat treatment conditions, by far the greatest difference was due to some other strengthening mechanism. Dislocation strengthening brought about by the straightening process applied to tubes after mill annealing is the most likely cause.

Hardness data for mill annealed cast 2697 showed that for a constant grain size there was a variation of 13HV between tubes, this equates to a variation in tensile strength of 50 MPa. This could not conceivably be due to differences in the dissolved carbon content resulting from variations in the mill annealing or thermal treatment temperatures. It must be concluded therefore that there were considerable differences in the degree of work hardening during straightening from one tube to another in the same cast.

5.2.6 Petch Relationships For Solution Treated

Commercial Tubing

As shown in figure 25, the Petch relationships for the solution treated commercial tubing were all approximately parallel. This means that the value of k_y in the Petch equation is constant:

$$H = h_i + k_y d^{-\frac{1}{2}} \dots\dots\dots(6)$$

where H is the hardness (HV) and h_i is a constant analogous to the friction stress σ_i in the normal Petch equation.

Because the different grain sizes were produced by varying the solution treatment temperature, which would dissolve different amounts of carbon, it is interesting to examine whether this affected the results in figure 25. The higher solution treatment temperatures gave the larger grain sizes, ie small $d^{-\frac{1}{2}}$ values, and more carbon in solution, ie more solid solution hardening by carbon. Hence it is possible that the values of k_y in equation (6) were rather less than the true grain size dependence of hardness due to h_i being greater at the smaller $d^{-\frac{1}{2}}$ values. The maximum difference in carbon dissolved in the commercial tubing at the highest solution treatment temperatures would be 0.02% which would give an increase in hardness of only 3HV (75). This has virtually no effect on the value of k_y , which therefore entirely reflects the grain size.

It is evident from figure 25 that the material air cooled after solution treatment was always harder than water quenched material. It is suggested this is due to more carbides precipitating during the slower air cool than the faster water quench. Precipitated carbides together with any undissolved carbides at the lower solution treatment temperatures generated dislocations which caused some dislocation hardening. It is well known that carbides can generate dislocations by the volume changes associated with their formation and also by the differences in thermal coefficient of expansion between the carbide and the matrix (76).

Some support for this explanation is afforded by the greater difference in hardness (ΔH) between air cooled and water quenched material in the high carbon cast 2696 (0.04%C, $\Delta H = 24HV$) compared with the low carbon cast 2682 (0.02%C, $\Delta H = 13HV$). The higher carbon material will precipitate more carbides during air cooling with a consequently greater tendency for associated generation of dislocations. Solution treatment will remove any effects of cold working and as can be seen in figure 25 as-received mill annealed material was at least 20HV harder than the hardest solution treated material (cast 2682 AC). Consequently, bearing in mind the effect of dislocations generated by carbides in the solution treated material, it may be concluded that the straightening operation produced a work hardening effect equivalent to an increase in hardness of about 30HV.

An unexpected effect, also shown by figure 25, is the consistently higher hardness of the lower carbon cast 2682 compared with the higher carbon cast 2697. No satisfactory explanation can be given for this but a contributory factor may be that in the higher carbon material there were more and larger undissolved carbides, as already reported. In the higher carbon material it is possible that any carbides formed during cooling from the solution treatment temperature are precipitated on existing undissolved carbides. Consequently a smaller number of carbide particles will be precipitated than in lower carbon material, and fewer dislocations will be generated. However such an effect would only be applicable at the lower solution treatment temperatures below the carbide solvus of $\sim 1030^{\circ}\text{C}$ for alloy 2697 with 0.035% C. Clearly some other mechanism must also be operative, at present not understood. Changes in solid solution hardening resulting from carbide formation cannot be the reason for the lower carbon material being harder than the higher carbon material.

5.3 Effect of Carbon Content on Structure and Mechanical Properties

5.3.1 Alloys containing no titanium or aluminium

A noticeable feature is the much large grain size of the high carbon cast 4 at solution treatment temperatures above 1050°C . This arises because the as-rolled material had not fully recrystallised.

Recrystallisation was not complete below 1050°C possibly because there were sufficient carbide particles pinning the recovered sub-grain boundaries. Above 1050°C, when carbide re-resolution and particle growth occurred, recrystallisation took place rapidly and was accompanied by marked grain growth of the recrystallising grains. This may be because some sub-grain boundaries became unpinned before others, resulting in selective sub-grains growing to form the nuclei for recrystallised grains.

There would be relatively few such recrystallisation nuclei which would grow rapidly due to the difference in stored energy between the recrystallised grains and the unrecrystallised matrix. Hence very large recrystallised grains would occur. This process is not dissimilar from that which occurs during the recrystallisation of cold worked mild steels which precipitate AlN during the recovery process. The temperature at which the recrystallised grain size increased rapidly, 1050/1100°C, is a little below the solvus temperature for the chromium carbide in this 0.08% alloy, which from equation (1) is calculated to be 1123°C. This confirms the effect was associated with the growth of precipitates to a size at which they no longer pinned the recovered sub-boundaries (77) rather than with complete solution of the pinning carbides. This effect is shown in figure 75.

It should be emphasised however that this behaviour is not typical of normal grain growth for the alloy, as shown by figure 29, in which the logarithm of the average grain

size is plotted against the reciprocal of the absolute temperature. Normal grain growth may be represented ideally by the equation (78):

$$D = kt^{\frac{1}{2}} \exp \frac{-Q}{2RT} \dots \dots \dots (7)$$

where D is the grain size, t the heating time at temperature T(K), R the gas constant and Q the activation energy for the grain growth process.

For a constant time at temperature, log D should be a linear function of the reciprocal of the temperature, and this is shown to be the case for the low carbon material, figure 29, which shows normal grain growth characteristics up to about 1100°C, but the slope of the curve increased at temperatures above 1100°C. For high carbon material, there is a change in mechanism at about 1050°C as a consequence of recrystallisation which is taking place. It is therefore difficult to draw conclusions as to how carbon influences grain size during the process of recrystallisation.

The Petch relationship for the high carbon cast, alloy 4, had an identical slope to those for commercial materials, but for the low carbon cast, alloy 1B, the slope was shallower. However considering the very restricted ranges of both $d^{-\frac{1}{2}}$ and hardness, and the low level of hardness for which experimental scatter can introduce considerable variations, the differences in gradient assume less

significance. On the other hand, the water quenched low carbon material was about 4HV harder than the average for the 0.02%C cast. Assuming that the water quenched material retained all its carbon in solution, whereas the carbon was precipitated as carbide during air cooling, then on the basis of equation (5) and the equivalence of 1 MPa in tensile strength = 0.3HV at the hardness level observed (74) (75), the above differences in hardness would be predicted to be 3HV and 10HV respectively. The agreement is quite good in as much as 4 HV lies in the range 3 to 10 HV.

Application of equation (5) to the tensile properties for alloys solution treated at 950°C predicts that alloy 4 will have a UTS level approximately 30 MPa above that for alloy 1B. This agreement is very close to the actual difference of 37 MPa, although the predicted UTS values do show significant variation from the actual results reported in Table 6.

Figure 39 shows the UTS and proof stress properties to be higher for the higher carbon alloy (alloy 4) than the lower carbon alloy (alloy 1B). This is true over the entire solution treatment range from 950°C to 1150°C. As the solution treatment temperature is increased so the level of carbon in solution increases as a consequence of dissolving carbides. Grains become unpinned and the grain size increases causing a reduction in proof stress and UTS. Additionally, fewer carbides will generate fewer dislocations and this effect will further cause the proof

stress and UTS to decrease as the solution treatment temperature increases.

5.3.2 Alloys containing 0.25/0.30%Al and 0.21/0.29%Ti

It is clear from figure 33 that increasing the carbon content not only refined the grain size at any solution treatment temperature above 950°C, but also increased the temperature at which grain coarsening commenced. Grain coarsening commenced at temperatures rather below the chromium carbide solvus temperature, calculated from equation (1), as seen from figure 75. Using a grain size of about 25 μm to define the grain coarsening temperature, the relationship between the chromium carbide solvus and grain coarsening temperatures is shown in figure 75. It is evident that the grain coarsening temperature falls further below the carbide solvus temperature as the carbon content increases

It should be noted that the grain coarsening temperature was also below the TiC solvus, and it is possible, as discussed in section 5.2.4, that TiC has a marked influence on the grain coarsening temperature. Indeed in titanium containing alloys this is most likely to be the case, with the grain size being controlled by a combination of chromium and titanium carbides.

Using equation (7) which describes the process of normal grain growth, figure 76 shows a graph of $\log D$ against $1/T$ (K). It can be seen that in the 0.02%C alloy, normal grain

growth was occurring with no boundary pinning by undissolved particles at temperatures above 950°C. This confirms the results in figure 75, with the grain boundary pinning occurring between 900-950°C being shown by the horizontal section in figure 76. The 0.04%C and 0.08%C casts show even more clearly the change in mechanism from one involving complete grain boundary pinning at low temperatures, below the grain coarsening temperature, to one involving normal grain growth at higher temperatures. These results confirm those shown in figures 33 and 75. It is also interesting to observe that the slope of the line for normal grain growth increases with increasing carbon content. The activation energies calculated from figure 76 (for the 0.25/0.30%Al, 0.21/0.29%Ti, casts) and from figure 29 (for the casts free from Al and Ti) were as follows:

Cast No.	Composition			Activation Energy for Grain Growth KJ.mol ⁻¹
	C	Al	Ti	
2682	0.02	0.30	0.21	124
2697	0.04	0.25	0.22	163
7	0.08	0.28	0.29	276
1B	0.02	<0.05	<0.05	82
4	0.08	<0.06	<0.05	138

The results show that irrespective of whether the casts contain aluminium and titanium, increasing carbon increases

the activation energy for grain growth. The reason for this is unclear, but it should be noted that, as the carbon increased, so did the titanium. An effect may be due to titanium and/or TiC/TiN precipitates. The introduction of aluminium and titanium markedly increases the activation energy for grain growth at any given carbon content. This is likely to be the result of additional solute drag impeding grain boundary movement. This is likely to be predominantly due to the titanium addition, which in the context of controlled rolling of HSLA steels is known to interact markedly with boundaries to retard recrystallisation (79). Alternatively TiC/TiN may be having a pinning effect on the grain boundaries, as previously discussed.

The Petch relationships, whilst having more or less the same slope irrespective of carbon content and cooling rate, figure 35, show a constant hardness for the 0.04% and 0.08%C alloys at the coarsest grain sizes. This is associated with the highest solution treatment temperature and is a result of the complete solution of carbides. Carbon solid solution hardening offsets the loss of hardness due to grain growth. In order to obtain a measure of the different levels of hardness of the Petch relationships for the different materials, the hardness corresponding to a typical mean $\bar{d}^{-\frac{1}{2}}$ value of 0.020 microns^{-1/2} ($\bar{d} = 25$ microns) has been plotted in figure 77 against carbon content.

Air cooled material was harder than the water quenched material for both 0.02%C and 0.04%C casts. This has been

explained tentatively as being due to the precipitation of carbides during air cooling causing the generation of dislocations and hence dislocation strengthening. In the 0.08%C alloy, however, there was virtually no difference between the water quenched and air cooled hardness values because any precipitation during air cooling occurred on the many undissolved carbides in this high carbon alloy. The other features shown in figure 77 are the decrease in hardness, in both air cooled and water quenched conditions, when the carbon content increased from 0.02% to 0.04% and the subsequent increase in hardness when the carbon content increased further to 0.08%. Again a tentative explanation is offered to explain the lower hardness of the 0.04%C cast compared to the 0.02% C cast. It is possible that precipitation during cooling occurs on undissolved carbides in the 0.04%C cast, which results in fewer carbides and consequently fewer dislocations being generated with a reduction in the hardening effect.

The hardness increase revealed as the %C rose from 0.04% to 0.08% is probably due to the larger number of undissolved carbides in the 0.08% C alloy, compared with the 0.04% C alloy, which generated more dislocations on cooling and thus gave more dislocation hardening.

Cast No	%C	Temp for d = 25µm (°C)	Chromium carbide solvus temp °C	% C as undissolved Cr carbides	% C dissolved	Carbon Solid solution hardening HV
2682	.02	950	941	0	0.02	3
2697	.04	1000	1032	0.009	0.031	5
7	.08	1050	1123	0.027	0.053	9

It should be pointed out that there will be different amounts of carbon dissolved in the alloys at the temperatures for a grain size of 25 µm. As shown in the table above this would give different amounts of solid solution hardening in the water quenched condition in which minimal precipitation occurs during cooling. Correcting for this solid solution hardening, however, makes very little difference to the effect of carbon on the hardness, figure 77.

Only experimental alloy 7 of the series II alloys was tensile tested after solution treatment. Comparison of 0.2% Proof Stress and UTS between Series I and Series III alloys, figure 39(a) and (b), reveals that alloy 7 had the highest levels of UTS and proof stress. Reference to equation (5) confirms the importance of carbon, aluminium and titanium on the UTS for solution treated alloys. The actual tensile results confirm the empirically predicted influence of composition and grain size.

5.4 Effect of Titanium Content on Structure and Mechanical Properties

There is no clearly defined effect of either titanium or carbon on the grain coarsening temperature, figure 36, which was in the temperature range 1000/1050°C. From the solvus temperature data given previously, and from figure 75, alloys containing between 0.02% C and 0.04% C would grain coarsen at or below 1000°C if chromium carbide is pinning the grain boundaries. It is possible that the 0.04% C, 0.22% Ti cast, with the lowest Ti:C ratio, has grain boundaries pinned by chromium carbides at temperatures up to the grain coarsening temperature. This cannot be the case for the 0.02% C/0.15% Ti and 0.03% C/0.40% Ti casts since the grain coarsening temperatures are too high compared to the solvus for chromium carbide. It must be concluded that for low carbon (high Ti:C ratio) TiC is acting to pin the grain boundaries. However, an effect due to TiN cannot be excluded from consideration.

At temperatures below the grain coarsening temperature the 0.04%C 0.22%Ti alloy had the smallest grain size (20 μm) compared with the lower carbon alloys (35 μm).

As it has previously been indicated that this 0.04% C alloy contains mainly chromium carbide pinning particles. It may also be suggested that some TiC particles must be contributing to the pinning effects. In fact, in figure 33 it was shown that in a 0.012% C, 0.21% Ti cast (2682)

there was a two stage grain coarsening effect. The lower temperature of coarsening may well be due to the loss of pinning by chromium carbide, whilst the higher temperature of coarsening may be due to the loss of TiC pinning.

If, however, the effect of titanium content on the grain size below the grain coarsening temperature is examined, it can be seen, figure 78, that with increasing titanium content the grain size first decreases and then increases up to a titanium content of 0.40%. This is precisely the effect which has been observed in High Strength Low Alloy Steels grain refined by either niobium or vanadium (80) in which the pinning particles were NbC and VN respectively. This evidence tends to suggest that TiC is the major grain boundary pinning particle in all these alloys with an additional effect from chromium carbide.

At temperatures above the grain coarsening temperature, where all the chromium carbide has dissolved, the grain size increases with increasing Ti content, figure 36. Since as all the TiC would be dissolved above 1100°C, this effect cannot be due to any effects of undissolved particles. It may be explained by reference to figure 79, which is the conventional plot of $\log D$ against $1/T(K)$. Apart from confirming the effects already discussed, figure 79, also shows that at high solution treatment temperatures the activation energy for grain growth increased with increasing titanium content. This is confirmed by the following data which also includes the alloys used to investigate the effect of carbon in the presence of aluminium and titanium.

Cast No	Analysis m/o		Activation Energy for Grain Growth at High Temperatures (KJ mol ⁻¹)
	% C	% Ti	
5	.02	.15	136
2682	.02	.21	124
2697	.04	.22	163
7	.08	.29	276
6	.03	.40	253

In the discussion of that work it was concluded that carbon increased the activation energy, but this was unexpected and no explanation could be advanced. However, the results from the alloys free from aluminium and titanium indicated that the effect of carbon was quite small. Because the titanium content increased together with the carbon in the aluminium-titanium alloys, the effect ascribed to carbon may well be due to titanium.

Figure 80 plots the Ti to C ratios against activation energies and reveals that a minimum occurs at a ratio of approximately 9:1. This minimum activation energy occurs at a much higher Ti/C ratio than stoichiometry (4:1), but it is suggested that this level may practically result in all the available carbon being combined with titanium to form TiC. It is well known that competition exists between Ti and Cr for C to form carbides, and that although Ti has the greater affinity for C, the actual formation of precipitates is strongly influenced by kinetic considerations. The complete tie-up of all Ti and C would minimise their solute drag effect and so reduce the activation energy for grain growth. However the presence of a dispersion of TiC would inhibit grain growth as already discussed.

It is clear from figure 81, which also includes data for alloys containing less than 0.05% Ti, that increasing titanium markedly increased the activation energy. Additionally carbon had a generally similar but less pronounced effect (except for the 0.03% C cast). These effects are to be expected, because normal grain growth is diffusion controlled, and the activation energy for diffusion is known to increase with increasing solute concentration (81). Also it is suggested that titanium may interact with carbon by forming clusters which further act to increase the activation energy. This increase in activation energy means that the temperature dependence of grain size is greater, and so more rapid grain growth occurred with increasing temperature as the titanium content increased, which may explain why the grain size at high temperatures increased with increasing titanium content.

The Petch relationships for alloys with varying titanium contents all had virtually the same gradient, figure 38. In the 0.22% Ti alloy the air cooled specimens were harder than those water quenched, and this has been explained previously. In the 0.15% Ti alloy, however, there was no difference between the air cooled and water quenched hardness values. This cast also contained a low level of carbon at 0.02%, so that the potential for precipitation during cooling was very small, and thus any dislocations generated by such precipitated carbides would be few and the hardening effect small. On the other hand, in the 0.40% Ti alloy the air cooled specimens were unexpectedly softer than the water quenched specimens. A possible but

speculative explanation for this is that this cast contained the largest amount of undissolved TiC so that any precipitation during air cooling occurred on these undissolved carbides. Consequently there was a negligible effect on the level of dislocation hardening. Thus, the larger thermal stresses induced by rapid water quenching generated more dislocations from the many undissolved carbides present at temperatures below 1100°C, so that the hardness was greater than for the more slowly air cooled specimens.

Using a typical $d^{-\frac{1}{2}}$ value of 0.14 (50 μm) in figure 38, and data from casts 7 and 2682, the effect of titanium on the general hardness level can be assessed from the following results:

Cast No	Analysis m/o			Ti m/o in solution	Ti:C ratio	Hardness HV	
	C	Ti	N			AC	WQ
5	.02	.15	.005	.133	6.65	138	138
2682	.02	.21	.004	.196	9.80	151	140
2697	.04	.22	.004	.206	5.15	143	122
7	.08	.29	.004	.276	3.45	122	140
6	.03	.40	.005	.383	12.76	132	143

There is no clearly defined effect of either the titanium content or the Ti:C ratio, on the hardness level. Using equation (5), and the equivalence between tensile strength and hardness, it can be shown that increasing the titanium content from 0.15% to 0.40% would cause solid solution hardening of less than 4HV, which would be largely undetectable. Consequently, because grain size variations have been discounted in the above data, any differences in

hardness are likely to be due to precipitation effects, dispersion hardening by undissolved carbides and dislocation hardening.

Table 8 and figures 39(a) and (b) present the proof stress and UTS tensile results for solution treated alloys 5 and 6. The 0.40% Ti alloy (alloy 6) has a higher UTS level than the 0.15% Ti alloy (alloy 5). These results are consistent with equation 5 for approximately similar grain sizes over the solution treatment range of 950°C to 1150°C.

Structural studies revealed that alloy 5 only fully recrystallised following solution treatment at about 950°C, where as alloy 6 was fully recrystallised at this temperature. It is evident that recrystallisation accounts for the major effect on proof stress and hardness levels. Hardness and proof stress follow the same trend with increasing solution treatment temperature. Clearly any effect of carbon and titanium on these properties will be masked by the effect of recrystallisation, especially in alloy 5. The UTS results however do confirm the importance of solid solution hardening resulting from carbon and titanium.

A possible explanation for the slower recrystallisation of the 0.15% Ti cast compared to the 0.40% Ti cast is that at 0.40% Ti there will be more undissolved Ti(CN) to produce dislocations as a result of cold work. Therefore an increase in the rate of recrystallisation would occur which would be further stimulated by precipitates acting as nucleation sites.

5.5 Grain Boundary Pinning Particles

Evidence has been presented and interpreted to indicate that either chromium carbide or TiC, possibly both, act to pin the grain boundaries and thus control the grain size. It has been shown that the undissolved chromium carbide at temperatures above 900°C is Cr₇C₃. It is possible to analyse the present results in order to assess whether Cr₇C₃ or TiC are likely to have the predominant pinning effect. Using the solubility equations for Cr₇C₃ (equation 1) and for TiC (equation 4) and the compositions of the alloys, the mass fraction of undissolved pinning particles f_m , can be calculated for temperatures below the grain coarsening temperature. The pinned grain size can then be related to the mass fraction of undissolved pinning particles, by means of the Zener equation (equation 2) assuming a constant particle size. The volume fraction of pinning particles is directly proportional to their mass fraction. Hence the pinned grain size below the grain coarsening temperature should be linearly related to the reciprocal of the mass fraction of undissolved pinning particles.

The appropriate data is given in Table 34 and plotted in figures 73 and 74 in which, because of errors associated with the calculation of the mass fraction of undissolved carbides, only values of f_m greater than 0.0005 have been used. A number of features are shown:

- (a) there is no clearly defined relationship for Cr_7C_3
- (b) there is a very well defined relationship for TiC
- (c) the commercial alloys had much finer grain sizes for a given mass fraction of pinning particles than did the experimental alloys.

From this it is concluded that the effective pinning particles are TiC rather than Cr_7C_3 in the alloys containing titanium. Also it would appear that the TiC particle sizes in the commercial alloys are about one third the size of those in the experimental alloys. This helps to explain the differences in grain size for the same mass fraction of undissolved particles, and is most probably due to differences during processing.

In the alloys containing less than 0.05% Ti, the nature of any grain boundary pinning particles cannot be decided from the results obtained, but must be Cr_7C_3 .

The low titanium content alloys, such as cast 1B, have Ti:N ratios in the order of 10:1, whilst high titanium content alloys, such as alloy 6, have high Ti:N ratios in the order of 80:1. These ratios suggest that TiN would form in all alloys probably during the solidification cool. Assuming equilibrium conditions exist then all the nitrogen would be tied-up as TiN in all alloys. For typical N levels of 0.005% this would leave approximately 0.045% and 0.395% Ti available in the lowest and highest Ti content alloys respectively. It is evident that subsequent TiC formation will have a significant effect in high Ti content alloys,

and as previously discussed will influence grain size control. In the low Ti content alloys however there will be only 0.045% Ti available for TiC formation which must compete with chromium carbide precipitation during processing. As a result the low Ti casts will not have grain boundaries pinned by TiC, but rather will contain large TiN particles and grain size controlling Cr_7C_3 .

5.6 The Effect of Thermal Ageing on Microstructure and Properties

Solution treated and thermally aged casts have been evaluated in terms of hardness, microstructure and corrosion behaviour. Due to the limited availability of material, tensile testing was not undertaken. The correlation between corrosion response and heat treatments will be discussed later.

5.6.1 Hardness

It is evident that the commercial casts (alloys 2682 and 2697) have a different response to ageing than the experimental casts, tables 9 to 19. Tables 11 to 16 show an approximately constant level of hardness, for both casts 2682 and 2697 during ageing. This effect occurs for solution treatment temperatures between 950°C and 1100°C , and hence varying levels of precipitation and carbon in solution. No single explanation based on either precipitation hardening or the generation of dislocations associated with precipitates can be made. It is possible that constant hardness is maintained because the material is in the fully softened condition prior to ageing and no

significant age hardening occurs. The precipitation and growth of grain boundary chromium carbides will not affect hardness and with few pre-existing or generated dislocations and no grain growth the overall hardness level is approximately constant.

The change in hardness during thermal ageing was negligible for all alloys except alloy 4 and alloy 7. These two alloys show a significant response to ageing in terms of a hardening reaction followed by eventual softening. Figures 40 and 41 show the hardness changes which occur and clearly reveal the ageing and subsequent over ageing effects. An explanation for these ageing effects lies in the material's chemical composition. Both alloys have a 0.08% carbon content, which is at least twice that of all the other casts studied. Alloy 7 begins with, then attains, and finally retains, a higher hardness level than alloy 4. The significant compositional variation between the two alloys is the level of aluminium and titanium in alloy 7 (0.28% and 0.29% respectively) but absent in alloy 4. These elements appear to stabilise the hardening reaction probably because of titanium carbide precipitation as discussed in Section 5.4. Associated microstructural studies will be discussed later.

It is known that ageing in the range 500°C to 1000°C produces carbide precipitation in solution treated alloy 600. This hardness study has shown that only when the carbon content is at a level considered extremely high for commercial casts, 0.08%, will precipitation result in a significant hardness increase.

5.6.2 Precipitation of Carbides

The study of carbide precipitation in alloy 600 is the key to developing an understanding of how material composition and processing variables interact to affect mechanical properties and corrosion behaviour.

Series I Alloys

In the absence of Al and Ti it is clear that as the carbon increases from 0.02% to 0.08% the precipitation rate and temperature domain are extended. This effect is shown in figure 47. The effect of grain size on precipitation is considered to be insignificant between the alloys studied because they had similar average grain sizes in the range 70 to 80 microns. As the level of carbon in solid solution prior to ageing increases so the volume fraction of carbides formed during ageing will increase. There is also a difference in carbide distribution and morphology as the carbon content increases.

At a carbon level of 0.02%, ageing up to 650°C produced fine discrete grain boundary carbides which then coarsened with little evidence of additional intragranular precipitation. Ageing at 700°C resulted in a band of fine grain boundary carbides and occasional discrete intragranular carbides, figure 44(b). This effect appears to be anomalous to the general trend of coarsening grain boundary carbides, but it is suggested that variations in strain level may have resulted in localised recrystallisation. The result is successive rows of fine precipitates which mark the position of migrated grain boundaries, figure 44 (b). Occasional intragranular carbides may also have formed at areas of high dislocation density as a

consequence of prior processing. This further reinforces the finding that processing of alloy 600 often results in an inhomogenous microstructure. The relatively low volume fraction of carbides for a carbon content of 0.02% and an absence of dislocations has not resulted in a precipitation hardening effect.

Increasing the carbon content to 0.08% significantly effects carbide precipitation. Comparison between figure 44 (a) and figure 46 reveals a marked change in the morphology and distribution of precipitates. Extensive carbide precipitation has resulted in an interaction between carbides and dislocations and generated high levels of associated internal strain. The overall effect is a precipitation hardening response dependant upon ageing time and temperature. The peak hardness level corresponds to a structure with numerous rod like precipitates running adjacent and perpendicular to the grain boundaries. It can be seen that dislocations piled-up perpendicular to the boundaries have acted as areas of increased diffusion and hence precipitation, Figure 46.

It is clear that increasing the carbon content increased carbide precipitation. The effect has been marked with the high carbon alloy showing a precipitation hardening response to thermal ageing. It is anticipated that these distinct differences in precipitation will be reflected in the corrosion behaviour. This effect will be discussed in section 5.8.

Series II Alloys

Increasing the carbon from 0.04% to 0.08% with 0.25/0.30% Al and 0.21/0.29% Ti extended the precipitation domain, figure 49.

The rate of precipitation also increased slightly, the nose of the curve being at shorter times, as the carbon content increased. As for series I alloys this difference is largely due to the carbon content with a faster rate and increased volume fraction of carbide precipitation occurring as the carbon content increases. In this instance a significant difference in grain size existed between the two alloys studied. At 0.08% C the grain size was 60 microns compared to 130 microns at 0.04% C. The reasons for this have already been discussed but an influence on precipitation during ageing will also occur. The smaller grain size of the high carbon alloy will aid nucleation and growth of carbides because of the relatively shorter distances for diffusion. However the major effect is thought to be due to the difference in carbon level rather than grain size.

Directly comparing the precipitation C-Curves for casts with 0.08% C with and without Al and Ti (ie Series I and Series II) reveals an interesting effect, figures 47 and 49. The presence of 0.029% Ti and 0.28% Al further extends the precipitation temperature domain. It is concluded that Al and Ti increase the tendency for $M_{23}C_6$ type chromium carbides and/or a more stable titanium carbide is being formed, before $M_{23}C_6$ at temperatures above 1000°C. The later explanation may be the case as it has not been possible in most cases to distinguish between TiC and $Cr_{23}C_6$ at the onset of precipitation. These findings further support the discussion presented in Section 5.2.4.

As discussed in section 5.6.1 both Series I and Series II alloys with 0.08% C displayed a precipitation hardening response. The Series II alloy contained precipitates very similar to the Series I alloys following optimum ageing (relating to peak hardness at 650°C for 100 hours, figure 50). Numerous rod like precipitates formed adjacent and perpendicular to grain boundaries. The interaction of these precipitates with dislocations and the generation of internal matrix strain gave rise to the hardening effect.

Commercial alloy 2682, with 0.02% C, was excluded from this study because it contained carbide precipitates following solution treatment at 1150°C prior to ageing. This effect is anomalous in comparison to the 0.08% C cast where all the carbon is in solid solution at 1150°C. The explanation may be in the cooling rate from solution treatment, since experimental alloys were water quenched and commercial alloys air cooled. The batch of material allocated for this study may have experienced a particularly slow air cool giving rise to carbide precipitation. This cannot have been the case for commercial alloy 2697, with a higher carbon content of 0.04%, which was free from carbides following solution treatment at 1150°C.

It is clear that the difference in precipitation behaviour between experimental and commercial casts is difficult to explain. The causes must be a combination of mechanisms arising from the material's sensitivity to processing. As previously discussed, experimental evidence supports the suggestion that cooling rate is a major variable. The pre-existence of chromium or titanium carbides and carbo-nitrides will also affect

precipitation patterns and hardness reactions. Minor variations between the time held at the solution treatment temperature plus differences in cooling rate may result in significant variations in precipitation. The solution treatment soak time will be of even more importance for commercial alloys which contained extensive amounts of precipitation as a consequence of prior processing.

Series III Alloys

The effect of thermal ageing on alloys containing variations of 0.15% to 0.40% Ti for 0.02/0.04% C and 0.23/0.25% Al shows a significantly different precipitation response compared with series I and II alloys.

The three alloys which form this series have broadly similar grain sizes, approximately 95 - 125 microns, prior to ageing. It is not considered that this variation would account for the differences in precipitation response. There was no appreciable hardness change during ageing for any Series III alloy indicating that the volume, distribution and type of carbides did not induce high levels of internal strain directly or by interaction with dislocations. Based on the carbon contents this result is not surprising, since both Series I and II alloys showed no age hardening response for carbon contents less than 0.08% C.

The measured onset of precipitation is determined by the detection of chromium carbides, principally $M_{23}C_6$, using electron diffraction. It has already been discussed that titanium has a higher affinity for carbon than chromium, therefore it is to be expected that titanium and chromium carbides will be in competition where both elements are present.

Figure 51 presents the onset precipitation C-Curves for experimental Series III alloys. There is an increase in the precipitation temperature domain as carbon increases from 0.02% to 0.03% and titanium increases from 0.15% to 0.40%. As previously discussed it is likely that both titanium and chromium carbides occur in these alloys. The precipitation curves are likely to be an amalgamation of Cr_{23}C_6 and TiC precipitates, with difficulty in distinguishing between them being experienced in practical studies. TiC has a higher temperature stability than Cr_{23}C_6 , and so it is likely to account for the higher temperature carbides. This is supported by reference to the chromium carbide solvus temperature calculated in section 5.2.5. The solvus temperature rises from 941°C for 0.02% C to 994°C for 0.03% C. It would therefore be unlikely that the carbides detected following ageing at 1000°C for 100 hours would be chromium carbides. Instead TiC is much more likely.

The effect of titanium on grain size control, mechanical properties and precipitation are evident from the experimental studies already presented. Its influence on the corrosion behaviour will be discussed later.

5.7 The Effect of Cold Work Prior to Thermal Ageing on Microstructure and Properties

It has been commented upon many times that alloy 600 in the form of commercial PWR tubing is not generally homogenous in terms of structure or properties. It is possible that tube bending, straightening and handling following the final mill anneal and prior to thermal treatments are the main causes. The thin wall section of the tubing (approximately 1 mm) may mean that

significant amounts of cold work can be introduced. The inclusion of cold work prior to ageing into the experimental casts allowed these effects to be studied. Reductions of 25% to 50% are large but are considered representative of actual local deformation that could be introduced during manufacture. The interaction between cold work, precipitates and corrosion response are key areas to be elucidated.

5.7.1 Hardness and Tensile Properties

Cold rolling after solution treatment resulted in significant work hardening. The 0.08% C cast (alloy 4) work hardened at a faster rate, and to a greater extent, than the 0.02% C, 0.15% Ti, 0.23% Al cast (alloy 5), figure 54. Since all of the carbon is in solution this must influence the work hardening response. The grain sizes are similar in the range 80 to 90 microns, and therefore will not contribute to the different work hardening responses.

The greater work hardening rate for the 0.08% C cast compared to the 0.02% C, 0.15% Ti must be due to the effect of solid solution hardening and solute drag effects. The higher level of carbon in solution has an increased effect on impeding dislocation mobility thereby giving rise to increased work hardening. The effect of carbon on stacking fault energy (SFE) is considered small, since whilst the SFE will increase as carbon increases this will be more than offset by the effect of chromium which reduces the SFE. The effect of chromium in lowering the SFE may partly contribute to the higher work hardening rate for the higher carbon alloy.

Thermal ageing studies of cold worked material revealed a different response compared to non cold worked material. The

ageing range of 500°C to 1000°C can be sufficient to recrystallise cold worked material. Recrystallisation can occur before, after or simultaneously with carbide precipitation. If recrystallisation occurs before the onset of precipitation then it does not affect the resultant precipitation. However if precipitation occurs prior to recrystallisation then cold work is likely to accelerate the formation and growth of carbides. If precipitation and recrystallisation occur simultaneously then the effect of cold work will be minimal but carbides forming on grain boundaries would tend to impede grain growth.

Tensile results from material aged at 700°C, figure 55, further show the process of recovery and recrystallisation.

5.7.2 Precipitation of Carbides

In the fully recrystallised condition both alloys have microstructures consisting of equiaxed grains with carbides marking the positions of previously deformed grains. The presence of carbides on 'ghost' grain boundaries, figure 62, confirms that precipitation has occurred before full recrystallisation at 700°C. The evidence suggests that the larger number of precipitates on deformed boundaries the greater will be the resistance to recrystallisation due to pinning. This supports the finding that the high carbon alloy (0.08% C) recrystallises later than the low carbon alloy (0.02% C).

The presence of intragranular precipitates may also partly be due to recrystallisation under certain processing conditions. Clearly during commercial tube manufacture a local region of material may experience deformation sufficient to result in recrystallisation during thermal treatment at 700°C. In such

cases precipitates will mark prior deformed grains and be located inside the recrystallised structure.

The absence of grain boundary chromium carbides in favour of intragranular precipitates was suggested as a means of reducing stress corrosion cracking susceptibility. This approach could be successful but for the fact that not all the carbon will be precipitated on the deformed boundaries. Sufficient carbon is usually still available for carbides to be nucleated on the recrystallised boundaries resulting in adjacent regions being denuded in chromium and so susceptible to SCC.

The effect of cold work prior to ageing has been discussed in Section 5.7.1. There was only a very slight, and unquantifiable, difference in the range 25% to 50% cold work, but a clear difference compared to material in the solely solution treated condition. Precipitation will occur at locations of high dislocation density, because of enhanced diffusion, which may occur near to boundaries. Hence carbides precipitate more rapidly in cold worked material. This conclusion is important with respect to commercial tubing because variations in cold work in the material may give rise to varying precipitation reactions. Consequently the distribution and density of carbides will not be homogenous and variations in mechanical properties and corrosion resistance will occur.

5.8 The Influence of Microstructure and Properties on the Corrosion Response of Alloy 600

The correlation between microstructure, mechanical properties and corrosion is necessary to an understanding of the service response of alloy 600 SG tubing. Based on such an understanding it should be possible to improve the materials commercial properties. The test media used in the experimental study was boiling 25% (vol) HNO_3 solution which is known to produce intergranular corrosion (IGC) in susceptible material.

5.8.1 Solution Treated and Aged Alloys

Alloy 4 (0.08%C) was highly susceptible to corrosion when aged between 500°C and 700°C, figure 65. Ageing at 700°C for between 16 hours and 100 hours desensitised the material. Samples with localised cold deformation (ie bent samples) showed an increased susceptibility compared to flat samples, figure 65. Alloy 5 (0.02% C, 0.15% Ti) showed an increased corrosion rate as the ageing temperature increased for 500°C to 700°C. Extended ageing at 700°C then resulted in a general reduction in susceptibility, figure 65.

It is evident that although extended ageing at 500°C did not give rise to detectable carbides in either alloy 4 or alloy 5, it did produce sensitised material. This effect, shown in figure 65 for alloy 4, is most pronounced where the test samples contained deformation. Although no chromium carbides were detected it is proposed that chromium and carbon were diffusing to nucleate and form precipitates located primarily on grain boundaries. Adjacent areas would therefore be denuded in chromium and as a result sensitive to SCC. This sensitised condition remained even when carbides were clearly detectable, and only began to diminish

after extended ageing when back diffusion of chromium into denuded zones occurred. Depending on the samples (bent or flat) ageing at 700°C for between 8 hours and 100 hours was required to fully desensitise the structure.

Alloy 5 with its much lower carbon content, 0.02%, had an almost identical precipitation domain to alloy 4, figures 47 and 51. In comparison with the high carbon cast, alloy 5 was significantly less prone to corrosion as a result of ageing between 500°C and 700°C. It is suggested that the significantly lower volume fraction of carbides produced for 0.02% C compared to 0.08% C account for the lower corrosion rate. Fewer carbides reduce the volume of matrix denuded in chromium and hence susceptibility decreases.

The results show that the lower the carbon content of the material the lower will be the corrosion rate in boiling nitric acid. This can be related to the volume fraction of carbides and susceptibility arising because of chromium denudation. The corrosion rate achieved after extended ageing is more or less independent of the carbon content, since once the matrix has been 'healed' of chromium denuded zones it is the inherent resistance of alloy 600 which inhibits further attack. The results indicate that a significantly longer ageing time is required to achieve desensitisation as the carbon content is increased from 0.02% to 0.08%. The weight loss results support the precipitation C-curves since both corrosion and precipitation are extended over temperature and time as the carbon content increases.

The intergranular nature of the corrosion is seen in all material conditions, figure 67 and 68. This further supports the mechanism of attack being due to chromium denuded zones surrounding grain boundary carbides. Local deformation increased the rate of attack due to the increased level of matrix strain, resulting from dislocation interactions, in areas cold worked.

The 0.02% C, 0.15% Ti cast (alloy 5) revealed localised 'fingers' of corrosion following extended ageing at 500°C. No carbides were detected but the attack was localised and intergranular in nature, figure 69. This sample demonstrated variations in grain size and hardness, with the regions of fine grain size and high hardness coinciding with these localised 'fingers' of corrosion. It is suggested that the fine grain regions may have preferentially recrystallised and left intragranular chromium carbides located on the 'ghost' boundaries of deformed grains.

5.8.2 Solution Treated, Cold Rolled and Thermally Aged Alloys

Material cold worked by 50% prior to ageing at 700°C had corrosion rates an order of magnitude lower than unworked material. Far from accelerating corrosion the effect of the cold work has been to significantly reduce it. Structural studies show that both alloys undergo recrystallisation during ageing at 700°C simultaneously with the precipitation of chromium carbides. The resultant structure consists principally of intragranular carbides within the recrystallised structure and marking the boundaries of the prior deformed grains. The absence of grain boundary carbides is proposed as the reason for the reduced corrosion rate.

Earlier discussions identified that such structures may not necessarily reduce corrosion since grain boundary sensitisation can still occur. Extended ageing at 700°C resulted in a general decrease in the corrosion rate as the ageing time increased from 1 hour to 100 hours. Ageing for between 16 hours and 100 hours resulted in corrosion rates approximately equivalent to those for non-cold worked samples aged for an equivalent time. It is clear that in the desensitised condition there is no difference between cold worked and unworked alloys.

Localised deformation had no appreciable effect on the corrosion rate, although slightly more extensive corrosion was seen in the region of the deformed material.

This study has confirmed that it is the volume fraction and distribution of chromium carbides which have the predominant effect on corrosion in boiling nitric acid. Cold worked material, which recrystallises during ageing, can be less prone to intragranular corrosion because of the absence of grain boundary zones of chromium depletion. However if the degree of cold work allows full precipitation to occur before recrystallisation, then grain boundary sensitisation of the newly formed strain-free structure will occur during subsequent thermal treatments. In general the corrosion rate falls as the ageing time extends beyond that required to precipitate the carbides. Cold work prior to ageing at 700°C can produce structures resistant to IGC, but it would be difficult in commercial practice to accurately and consistently control the means of deforming the tubing. Hence the generation of homogeneous structures would be difficult to reliably produce.

6 Conclusions

All the conclusions reached from the experimental studies help explain the interaction between composition and thermo-mechanical treatments on the precipitation reactions, grain size control, mechanical properties and corrosion behaviour. In general, the aims of the investigation have been achieved.

6.1 Precipitation Reactions

1 Commercial tubing contains chromium carbides which are mainly intergranular $M_{23}C_6$ and occasionally intragranular M_7C_3 . The grain boundary carbides occur primarily as a result of precipitation during thermal ageing at $700^{\circ}C$ for 15 hours. There is evidence that a fine dispersion of titanium carbide, TiC , also exists in titanium containing casts.

2 Experimental alloys contained the same carbides as commercial alloys, with the type and amount of each depending on the alloy composition and the thermal treatment experienced. Rapid cooling from solution treatment temperatures resulted in isolated M_7C_3 , whilst additional thermal treatments gave rise to extensive grain boundary precipitation of $M_{23}C_6$ carbides.

- 3 Experimental alloys with carbon contents of 0.08% produced a significant precipitation hardening response during thermal ageing. Extensive grain boundary $M_{23}C_6$ was formed which interacted with and/or generated dislocations. In the absence of recrystallisation, this resulted in a hardness increase.
- 4 Alloys with 0.08%C and 0.29%Ti maintained peak precipitation hardness levels longer than Ti free alloys. Titanium is either stabilising the chromium carbide against overageing or giving rise to a double precipitation hardening peak.
- 5 Cold work prior to thermal ageing can increase the rate of precipitation and extend the temperature range over which the precipitates occur. Where precipitation takes place before recrystallisation the matrix strain aids the nucleation and growth of carbides. However, if recrystallisation is complete before precipitation, then cold work has no influence on the formation of carbides.
- 6 Localised variations in cold work can give rise to corresponding variations in carbide precipitation. It is suggested that such variations help to explain the service variability of Alloy 600, and also the localised "fingers" of corrosion which have been observed in this work and by other workers (62).

6.2 Grain Size Control

- 1 In titanium containing alloys there is clear evidence that TiC controls the grain size. In alloys free from titanium it must be chromium carbides, principally $M_{23}C_6$, which control the grain size. An increasing carbon content refined the grain size and increased the grain coarsening temperature. In the absence of titanium it has not been possible to show clearly how carbon affects grain size, although control must be due to chromium carbides, principally $M_{23}C_6$, pinning the grain boundaries.

- 2 Grain growth studies have shown that variability exists in the mill annealing temperature for commercial tubing. This variability occurs within and between batches, which were all processed in nominally the same way.

- 3 Commercial tubing materials have finer grain sizes than experimental alloys. This is a consequence of the smaller grain boundary pinning particles, for a given volume fraction, in commercial materials. This difference is tentatively attributed to differences in the hot processing conditions, although it has not been possible to identify the reasons for this.

- 4 Commercial tubing showed a significant variation in grain size across the wall thickness, with a finer grain size occurring towards the surface regions. It is proposed that the concentration of deformation in these regions has resulted in small recrystallised grains relative to the sub-surface larger grains which have grown during hot processing.

5 In alloys containing titanium and aluminium the activation energy for normal grain growth increased with increasing titanium. This has been explained in terms of a fine distribution of TiC which acts to impede grain growth.

6 Material left unrecrystallised after hot working could show anomalously large grain sizes if recrystallisation takes place during subsequent solution treatment. This is because carbides will be located on the worked grain boundaries and so will not exert a grain boundary pinning influence on the recrystallised structure.

6.3 Mechanical Properties

1 There was a difference in hardness between mill annealed and thermally treated commercial tubing. Carbon in solid solution would account for only about 10% of this difference, and it is concluded that work hardening produced by straightening the tubing accounts for the remaining 90%.

2 There was clear evidence of variations in the degree of work hardening in commercial tubing both within and between batches. A critical amount of work occurring before the final mill anneal could account for the finer surface grain sizes as a result of localised recrystallisation.

3 The pre-existence of carbides and the rate of cooling controls the hardness of solution treated material. Slow air cooling can result in carbide precipitation and dislocation generation, so that air cooled material is harder than water quenched material. However, if pre-existing carbides are present then any further carbides

precipitated will tend to occur on existing precipitates and so minimise associated dislocation generation. In this case water quenching will produce harder material because of the additional thermal stresses produced by the rapid water quench.

4 Thermal ageing initially reduces the hardness because it acts as a stress relief for mill annealed and solution treated materials. If the volume fraction of carbides is sufficient, ie 0.08% C in these studies, then the precipitation of $M_{23}C_6$ chromium carbides can give rise to a significant age hardening effect. The peak hardness occurs after ageing at 650°C for 100 hours, since in this condition the precipitate size interacts with dislocations to an optimum degree.

5 Work hardening has a major effect in Alloy 600. The rate of work hardening has been shown to increase with an increase in the carbon content. This effect is largely due to the effect of solute drag on dislocation mobility. There may also be a slight lowering of the SFE as chromium is taken into solution, which offsets the slight rise in SFE due to increasing the carbon in solution.

6 Recrystallisation occurs as a result of deformation prior to thermal ageing. Increasing the degree of cold deformation, up to 50% reduction in thickness, results in earlier and faster recrystallisation. As expected strain free recrystallised material has significantly lower mechanical properties than cold worked material.

6.4 Corrosion Behaviour

- 1 The corrosion response of thermally aged material supports the mechanism that chromium carbide precipitation and chromium denudation controls intergranular corrosion. Initial ageing at 700°C resulted in the precipitation of chromium carbides with adjacent chromium denuded zones. In this condition material is highly susceptible to corrosion. Extended ageing allows the back diffusion of chromium into the denuded zones, with corrosion resistance recovering to its maximum level.
- 2 Corrosion paths follow the pattern of chromium carbides. Where precipitation has occurred in fully recrystallised material, with carbides situated on grain boundaries, then in sensitised material the corrosion path will be intergranular. Grain boundary chromium carbides in fully desensitised material can act as a physical barrier to effectively block the progress of intergranular corrosion cracks.

If the material recrystallised after carbide precipitation then zones adjacent to the carbides will be desensitised. Carbides will be located intragranularly on 'ghost' boundaries from the worked structure. No intergranular carbides will be present and so corrosion is at a minimum level. However, it is not recommended that this approach be used in commercial practice to produce corrosion resistant structures, because of the difficulty in consistently controlling the necessary thermo-mechanical treatments.

- 3 Variability in the level of localised deformation prior to ageing is common in commercial practice. This affects precipitation and recrystallisation and so can influence the corrosion behaviour. Localised regions of fine grain size and high hardness can occur and have been shown to cause distinct 'fingers' of corrosion. IGA is increased within these 'fingers' which contain intergranular carbides along with a recrystallised structure and increased hardness. The reason for the increased hardness is unclear but may be due to the finer grain size.
- 4 The introduction of localised cold work after thermal ageing increased IGA in the deformed regions. This simulates deformation introduced as a result of tube expansion into the base plate as well as tube denting. It is clear that deformation introduced prior to or during service is detrimental to the corrosion resistance.
- 5 In summary, it is clear that corrosion in nitric acid is at a minimum level when; (i) full precipitation has occurred before recrystallisation (ii) ageing has allowed any chromium denuded zones to be healed by back-diffusion, and (iii) when all post ageing deformation is avoided. In commercial practice this will be a difficult balance to achieve along with the mechanical property requirements.

7. Further Work

The following areas of study should be considered to extend the current understanding:-

- (1) A detailed analysis of the commercial manufacturing techniques for SG tubes in Alloy 600 type materials. Attention should be given to post mill anneal operations to better understand the service variability of the tubing.
- (2) An in-depth electron microscopy study of the exact composition of carbides present following mill annealing and thermal treatment. Titanium and Chromium carbides need to be distinguished and their contribution to the structure and properties quantified.
- (3) The factors leading to susceptibility in various corrosive environments need to be further studied. The current work shows a very strong link between chromium carbide precipitation and the corrosion rate. Published literature continues to speculate whether it is denuded chromium zones and/or trace element segregation (S,P,B) which cause susceptibility. Detailed studies using AUGER analysis would determine trace element concentrations and quantify their effect on corrosion.
- (4) It has been proposed that material which recrystallises during thermal treatment will be less susceptible to corrosion. This is confirmed to some extent by the current work but a programme of studies is required to further elucidate this effect.

(5) The effect of in-service ageing on structure and properties needs to be studied. In particular the low temperature segregation of trace elements and chromium should be studied. It is anticipated that these factors would further help to optimise the service response.

References

- 1 J P N Paine and S Green. Nuclear Technology, Vol 55, p10, 1981.
- 2 J P N Paine. Corrosion/82 NACE, preprint No 204, Houston, Texas, 1982.
- 3 S J Green and J P N Paine. "Steam Generator Materials - Experience and Prognosis", Proc Int Sym Environmental Degredation of Materials in Nuclear Power Systems - Water Reactors. NACE : Houston, Texas, P53, 1984.
- 4 G P Airey. EPRI Research Project 1708-1. 'Optimisation of Metallurgical variables to improve corrosion resistance of Inconel Alloy 600'. Final Report. Palo Alto, Calif, Electric Power Research Institute, July 1983, NP 3051.
- 5 O S Tatone and R S Pathania. Nuclear Safety, Vol 22, No 5, p636, 1981.
- 6 O S Tatone, Nuclear Engineering International, p81, June 1981.
- 7 Research discussion with P J Gane, March 1987
D Vuillume, R D Monbard, Vallourac Industries, France
PWR Steam Generator Tubes in Alloy 600. Key Manufacturing Steps and their Influence
- 8 J Blanchet and H Coriou
Reprint No G13, Confr, on "SCC and Hydrogen Embrittlement", NACE, HOUSTON, June 1977.
- 9 Framatome, Tour Fiat, Paris, France
Research Discussion with P J Gane, March 1987.
- 10 A R Vala et al, Materials Performance, NACE, p9, Feb 1980.
- 11 E C Potter and G M V Mann, Br Corrosion J, Vol 1, p 26-35 1965.

- 12 J W Oldfield and W H Sutton, Br Corrosion J, Vol 13, No 3, p104, 1978.
- 13 D Van Rooyen and J R Weeks, BNL-NUREG-50 778, Jan 1978.
- 14 A K Agrawal et al, EPRI Final Report, Battelle Columbus Laboratories, Nov 1982.
- 15 J R Park, Proc 2nd Int Symp "Environmental Degradation of materials in Nuclear Power Systems - Water Reactors", p456, Monterey, Calif, 1985.
- 16 R Garnsey. 'The chemistry of Steam Generator Corrosion', CEGB Research, June 1979, pp12-23.
- 17 P L Ko, 'Experimental Studies of the Tube Fretting in Steam Generators and Heat Exchangers', ASME paper 78-PVP-22.
- 18 W J Heikler and R Q Vincent, paper presented at the ASME Nuclear Engineering Division Conference, San Francisco, Aug 1980.
- 19 J C Watkins and R A Berry. 'A state-of-the-Art Literature Survey of Water Hammer', RE-A-79-044, April 1979.
- 20 E O Marchand et al, Paper Presented at the ASME Nuclear Engineering Div, Conf, San Francisco, Aug 1980.
- 21 J E Newell, Sizewell 'B' Power Station Public Enquiry, Nov, 1984, CEGB/P/15.
- 22 O S Tatone and R S Pathania, Nuclear Engineering International, Jan 1985, p36.
- 23 Sizewell 'B' Power Station Public Enquiry, Nov, 1984, CEGB/P/15 (Add 3)
- 24 S J Green et al, Proc of "Century 2 Nuclear Engineering" Conf ASTM 80-C2/NE-8, Calif, 1980

- 25 WCAP-9922, "Reliability and Safety of the Westinghouse Model F Steam Generator", Part 1, Executive Summary, Oct 1981.
- 26 Ibid Part 2 - "Reliability Evaluations", Oct 1981.
- 27 EPRI NP 2092 "Nuclear Unit Operating Experience, 1978 and 1979". Update Final Report Oct 1981.
- 28 B Hemsworth: Nuclear Installations Inspectorate, "Structural Integrity of the Westinghouse Model F Steam Generator", Revision R, May 1982.
- 29 S J Green. 'Methods for Preventing SG Failure or Degradation', Electric Power Research Institute, Presented at POST SMIRT Conference, ISPRA, Italy, August 26-27, 1985.
- 30 Y Togo and N Mori 'Preventing Tube Degradation in Japan', Nuclear Engineering International, p43, Feb 1985.
- 31 G P Airey. Proc of the International Symposium on "Environmental Degradation of Materials in Nuclear Power Systems - Water Reactors". Myrtle Beach, South Carolina, Aug 22-25, 1983, NACE. p262
- 32 H Coriou, J Blanchet et al Jnl of Nuclear Materials, 2975, Vol 55, p187 1976.
- 33 H Domain et al, 'Effect of Microstructure on Stress Corrosion Cracking of Alloy 600 in High Purity Water', Corrosion, 1977. Vol 33, p26.
- 34 "Stress Corrosion Cracking of Alloy 600 and Alloy 690 in Steam Generators", Owners Group Research Project S192-2, Final Report. Palo Alto, Calif, Electric Power Research Institute, May 1983, NP-3061. p156.

- 35 G J Theus et al,
'SCC Tests of Monel 400 SG Tubing'
Paper 209 in "Corrosion 1982"
Houston, TX, NACE (1982)
- 36 G Frederick and P Hernalsteen 'Generic Preventative
Actions for Mitigating MA Inconel Alloy 600
Susceptibility to Pure Water Stress Corrosion
Cracking'.
Presented at Specialist Meeting on Steam Generators,
Stockholm, Oct 1-5, 1984.
- 37 T S Bulischek, D Van Rooyen
Nuclear Technology, Vol 55, p383, 1981.
- 38 I L Wilson and R G Aspden.
"Caustic Stress Corrosion Cracking of Iron-Nickel-
Chromium Alloys". International Conference on "SCC
and Hydrogen Embrittlement of Iron Based Alloys",
NACE, Houston, June 1977, p179.
- 39 W D Fletcher
"Summary of Operating Plant Experience Related to U-
bends Incidents". EPRI-WS-80-0136, Denver, Aug 1980.
- 40 R Van Rooyen
"Review of the SCC of Inconel 600"
Corrosion 1975, Vol 31, p327
- 41 H R Copson et al,
"Stress Corrosion Behaviour of Ni-Cr-Fe Alloys in
High Temperature Aqueous Solutions". Procs, 5th
International Congress on Metallic Corrosion,
NACE, Houston, 1974. p202.
- 42 H R Copson and S W Dean
"Effects of Contaminants on Resistance to SCC of Ni-
Cr Alloy 600 in Pressurised Water", Corrosion, 1965,
Vol 21, p1.

- 43 H R Copson and G Economy
"Effects of Some Environment Conditions on SCC
Behaviour of Ni-Cr-Fe Alloys in Pressurised Water"
Corrosion, 1968, Vol 24, p55.
- 44 Ph Berge et al
"Caustic SCC of Fe-Cr-Ni Austenitic Alloys"
Corrosion, 1977, Vol 33, p425.
- 45 R S Pathani
"Caustic Cracking of Steam Generator Tube Materials"
Corrosion, 1978, Vol 34, p149.
- 46 I L Wilson et al
"Caustic SCC Behaviour of Fe-Ni-Cr Nuclear Steam
Generator Tubing Alloys".
Nuclear Technology, 1976, Vol 31, p70.
- 47 R L Cowan and G M Gordon
"Intergranular SCC and Grain Boundary Composition of
Fe-Ni-Cr Alloys"
Procs, Int Confr on "SCC and Hydrogen Embrittlement of
Iron Base Alloys", NACE, Houston 1977. p27
- 48 T S Bulischek et al,
"SCC of Inconel 600 Tubing in Deaerated High
Temperature Water".
NUREG/CR-0858, June 1979.
- 49 C R Phipps
"Review of Temperature Relationships to SCC in Inconel
600 Tubes of 'Westinghouse Type' Steam Generators".
EPRI report Summary; 1986.

50 G J Theus

"Summary of the Babcock and Wilcox Company's SCC
Test of Alloy 600".

EPRI WS-60-0136, EPRI Workshop on Cracking of Alloy
600 U-Bend Tubes in Steam Generators, Denver,
August 20-21, 1980

51 R Bandy and D Van Rooyen

"SCC of Inconel Alloy 600 in High Temperature Water
- An Update".

Corrosion - NACE, Vol 40, No 8, 1984.

52 T Yonezawa and K Onimura

"Materials for Nuclear Core Applications"

BNES, London, 1987.

53 G C Foster and J W Taylor

"SCC of Inconel 600 Heat Exchanger Tubing in High
Temperature Water".

Procs, Effect of Environment on Materials Properties
on Nuclear Systems, Paper No 8, Institute of Civil
Engineers, London, July 1971.

54 J Congleton and R N Parkins

"Stress Corrosion Cracking of Alloy 600 in High
Temperature Water"

"Nuclear Engineering and Design" p103 (1987) NED00693.

55 Inco Alloys International

'Inconel Alloy 600'

Company Publication 1987.

- 56 A R McIlree et al
"Effects of Variations of Carbon, Sulphur, and
Phosphorus on the Corrosion Behaviour of Alloy 600"
"Corrosion Problems in Energy Conversion and
Generation", p442, New York, 1974, The Electro
Chemical Society Inc
- 57 G T Theus
"Caustic SCC of Inconel 600, Incoloy 800 and Type 304
Stainless Steel". Nuclear Technology, 1976, Vol 28,
p388.
- 58 J R Crum
Paper No 24 Presented at Symposium "Corrosion/81",
April
6-10, Toronto, 1981.
- 59 H E Hanninen
International Metals Reviews
Vol 24, No 3, 1979.
- 60 G P Airey
"Microstructural Aspects of the Thermal Treatment of
Inconel Alloy 600"
Metallography, 1980, Vol 13, p21.
- 61 G Perrat and D Vuillum
"Selection of Annealing Temperatures for TT Alloy 600
and 690 Tubing".
As reference 7.
- 62 Technical Discussions with CEGB Research (CERL),
Leatherhead, Surrey
P J Gane, 1985/6.

- 63 J R Crum
"Effect of Composition and Heat Treatment on SCC of Alloy 600 SG Tubes in Sodium Hydroxide"
Corrosion, 38, p40, 1982
- 64 C H Wagner et al
Written Discussion on Reference 38, 1977.
- 65 F W Perment and N A Graham
"SCC in High Purity Water"
"Corrosion Problems in Energy Conversion and Generation", p423, New York, 1974, The Electrochemical Society, Inc.
- 66 K W Andrews, D J Dyson and S R Keown
'Interpretation of Electron Diffraction Patterns',
Adam Hilger Ltd, 1971
- 67 D R Johns, F R Beckitt and R A E Hooper
'The characterisation and Intergranular Corrosion Resistance of Alloy 600 for the Nuclear Installations Inspectorate' British Steel Corporation Contract Report No RSC/7171/84, 7 August 1984.
- 68 D Sinigaglia et al
Corrosion - NACE, Vol 38, No 2, Feb 1982, p92.
- 69 R C Scarberry, S C Pearman and J R Crum
"Corrosion" - NACE, Vol 32, No 10, p401 Oct 1976
- 70 J W Martin and R D Dohery
in 'Stability of Microstructure in Metallic Systems',
1980, p191-193, Cambridge University Press.
- 71 T Gladman
Proc. Roy. Soc. 1966, A294, p298
- 72 T M Williams and D R Harries
in 'Creep Strength in Steels and High Temperature Alloy'. 1974, p152, The Metals Society (London).

- 73 F B Pickering
in 'MICON 78 - Optimisation of processing, properties
and service through Microstructural Control'. STP
672, ASTM 1979, p281
- 74 D Tabor
'The Hardness of Metals', Oxford University Press
- 75 'The Making, Shaping and Treating of Steel', 1957,
United Steel Corporation
- 76 S R Keown and F B Pickering
in 'Creep Strength in Steels and High Temperature
Alloys', 1974, p134, The Metals Society (London)
- 77 T Gladman and F B Pickering
JISI, 1967, 205, p653
- 78 R E Reed-Hill
Physical Metallurgy Principles, 1964, Van Nostrand
- 79 M K Akben and J J Jonas in 'HSLA Steel - Technology
and Applications' Ed M Korchynsky, 1984, p149,
American Soc for Metals
- 80 R K Amin and F B Pickering in 'Thermomechanical
Processing of Microalloyed Austenite', Eds A J DeArdo,
G A Ratz and P J Wray, 1982, Met Soc of AIME, p1
- 81 L H Van Vlack 'Materials Science for Engineers', 1971,
Addison - Wesley, p171

Table 1
Chemical Compositions of the Commercial and
Experimental Casts Used for the Investigation

Alloy Series	Cast No	Chemical Composition m/o (Balance Ni)												
		C	MN	Si	Fe	Cr	Cu	Co	S	P	B	Al	Ti	N
Commercial Tubing	2682	.02	.25	.30	9.29	15.50	.28	.05	.001	.010	.003	.30	.21	.004
	2683	.03	.29	.26	9.58	15.66	.39	.06	.002	.011	.003	.23	.21	.004
	2686	.03	.38	.21	8.89	15.97	.24	.06	.003	.011	.003	.22	.23	.004
Series I Varying C	2697	.04	.27	.16	9.72	14.85	.26	.03	.002	.010	.003	.25	.22	.004
	1B*	.02	.26	.09	9.07	14.84	.23	.03	.002	.007	.002	.05	.05	.005
	4*	.08	.26	.10	9.05	14.72	.23	.10	.001	.007	.005	.05	.05	.004
Series II Varying C	2682	.02	.25	.30	9.29	15.50	.28	.05	.001	.010	.003	.30	.21	.004
	2697	.04	.27	.16	9.72	14.85	.26	.03	.002	.010	.003	.25	.22	.004
	7*	.08	.26	.10	9.00	14.58	.23	<.10	.002	.007	.005	.28	.29	.004
Series III Varying Ti	5*	.02	.26	<.10	9.09	14.94	.23	<.10	.002	.007	<.005	.23	.15	.005
	2697	.04	.27	.16	9.72	14.85	.26	.03	.002	.010	.003	.25	.22	.004
	6*	.03	.27	.10	9.13	14.90	.23	.01	.002	.007	.005	.23	.40	.005

* Experimental Casts

Table 2

Hardness and Grain Size Data for As-Received Commercial Tubing

Condition	Cast No	Hardness (HV 20)	MLI of grain size (μm)	$d^{-\frac{1}{2}}$ ($\mu\text{m}^{-\frac{1}{2}}$)
Mill Annealed	2682	200	24.5 (\pm 2.0)	0.202
	2683	221	13.3 (\pm 0.9)	0.274
	2697	221	13.4 (\pm 1.3)	0.273
Mill Annealed and Thermally Treated	2682	190	17.75 (\pm 1.9)	0.237
	2683	212	11.07 (\pm 0.9)	0.300
	2686	207	12.05 (\pm 1.0)	0.288
	2697	205	12.90 (\pm 1.3)	0.278

() indicate 95% Confidence Limits of grain size

Table 3

Hardness and Grain Size of Solution Treated Alloys

Containing Varying Carbon Contents and no Aluminium or Titanium

Solution Treatment Temp °C	Cast 1B 0.02%C				Cast 4 0.08%C							
	Air Cooled		Water Quenched		Air Cooled		Water Quenched					
	HV	d (µm)	d ^{-½} (µm ^{-½})	HV	d (µm)	d ^{-½} (µm ^{-½})	HV	d (µm)	d ^{-½} (µm ^{-½})			
900	127	38.7±2.9	.161	125	53.1±3.7	.137	153	34.5±2.7	.170	162	41.4±2.8	.155
950	125	43.4±3.0	.152	128	55.9±3.9	.134	157	32.8±2.3	.175	156	51.9±3.9	.139
1000	128	45.0±3.4	.149	125	57.9±4.4	.131	158	35.6±2.4	.168	157	55.1±4.0	.135
1050	124	55.2±3.7	.135	126	65.4±4.9	.124	152	54.1±3.6	.136	152	52.9±3.7	.137
1100	121	59.4±3.8	.130	127	68.3±5.0	.121	126	90.5±6.4	.105	142	68.9±4.8	.120
1150	122	85.1±6.4	.108	123	67.7±5.2	.122	119	157.7±13.2	.080	126	81.4±6.1	.111
1200	116	102.0±7.4	.099	122	90.1±8.3	.105	115	216.5±19.0	.068	123	150.5±13.3	.082

95% Confidence limits of grain size given

Table 4
Hardness and Grain Size of Solution Treated Alloys Containing Varying Carbon Contents With
0.28/0.30% Al and 0.21/0.29% Ti

Cast No	% C	Solution Treatment Temperature °C	Air Cooled			Water Quenched		
			Hardness (HV)	d (µm)	$d^{-\frac{1}{2}}$ (µm ^{-½})	Hardness (HV)	d (µm)	$d^{-\frac{1}{2}}$ (µm ^{-½})
2682	.02	900	176	22.8+1.9	.210	166	22.3+1.7	.212
			172	21.4+1.7	.216	159	23.1+1.7	.208
			146	62.9+6.5	.126	131	70.5+6.2	.119
			147	64.8+7.1	.124	132	72.2+6.2	.118
			142	85.7+7.6	.108	133	89.6+8.2	.106
			136	119.5+11.0	.092	125	144.7+16.3	.083
2697	.04	1200	124	236.6+22.1	.065	105	265.0+27.9	.061
			193	14.2+1.0	.265	173	12.5+1.0	.283
			191	15.3+1.4	.256	162	14.0+1.3	.267
			166	27.9+2.2	.189	155	16.3+1.4	.248
			146	40.1+3.7	.158	125	46.5+5.9	.147
			136	56.0+5.1	.134	117	71.9+10.4	.118
7	.08	1150	117	125.0+10.9	.090	111	91.2+7.8	.105
			125	175.6+17.2	.075	112	215.0+19.0	.068
			162	29.5+2.0	.184	168	25.8+1.7	.197
			168	21.8+1.4	.214	163	28.4+1.9	.188
			161	26.4+1.8	.195	165	23.7+1.4	.205
			156	26.3+1.7	.195	163	24.1+1.4	.204
			153	29.3+1.8	.185	155	33.5+1.6	.173
			129	79.5+5.2	.112	143	56.8+3.8	.133
			131	148.9+12.4	.082	129	161.7+13.4	.079
			900					

Table 5

Hardness and Grain Size of Solution Treated Alloys Containing 0.02/0.04% C, 0.23/0.25% Al and Varying Titanium Contents

Cast No	% C	Solution Treatment Temperature °C	Air Cooled			Water Quenched		
			Hardness (HV)	d (µm)	$d^{-\frac{1}{2}} - \frac{1}{2}$ (µm ^{-½})	Hardness (HV)	d (µm)	$d^{-\frac{1}{2}} - \frac{1}{2}$ (µm ^{-½})
5	.02	900	154	30.5±2.0	.181	149	32.5±2.2	.175
		950	149	32.4±2.2	.176	145	35.7±2.5	.167
		1000	142	35.5±2.5	.168	146	36.2±2.3	.166
		1050	140	45.2±3.1	.149	138	37.2±2.1	.164
		1100	137	55.7±3.5	.134	132	59.1±3.9	.130
		1150	121	112.2±8.4	.094	129	93.4±6.5	.103
		1200	123	120.5±8.6	.091	129	124.5±8.6	.089
		900	193	14.2±1.0	.265	173	12.5±1.0	.283
		950	191	15.3±1.4	.256	162	14.0±1.3	.267
		1000	166	27.9±2.2	.189	155	16.3±1.4	.248
2697	.04	1050	146	40.1±3.7	.158	125	46.5±5.9	.147
		1100	136	56.0±5.1	.134	117	71.9±10.4	.118
		1150	117	125.0±10.9	.090	111	91.2±7.8	.105
		1200	125	175.6±17.2	.075	112	215.0±19.0	.068
		900	137	34.1±2.5	.171	148	38.5±1.6	.161
		950	141	35.6±2.4	.168	147	44.4±3.1	.150
		1000	138	36.7±2.5	.165	148	47.3±3.5	.145
		1050	130	59.7±3.9	.129	139	53.2±3.9	.137
		1100	130	74.1±5.0	.116	132	66.8±4.6	.122
		1150	116	162.2±13.2	.079	125	106.2±8.4	.097
1200	109	316.9±29.6	.056	118	276.8±26.3	.060		
6	.03	900	137	34.1±2.5	.171	148	38.5±1.6	.161
		950	141	35.6±2.4	.168	147	44.4±3.1	.150
		1000	138	36.7±2.5	.165	148	47.3±3.5	.145
		1050	130	59.7±3.9	.129	139	53.2±3.9	.137
		1100	130	74.1±5.0	.116	132	66.8±4.6	.122
		1150	116	162.2±13.2	.079	125	106.2±8.4	.097

95% Confidence Limits of Grain Size Given

Table 6

The Effect of Solution Treatment Temperature on the Mechanical Properties of Series I Alloys

Alloy	Solution Treatment Temp °C	0.2% Proof Stress (MPa)	UTS (MPa)
1B	950	212	563
	1050	206	542
	1150	193	515
4	950	231	600
	1050	213	554
	1150	200	561

Table 7

The Effect of Solution Treatment Temperature on the Mechanical Properties of Series II Alloys

Alloy	Solution Treatment Temp °C	0.2% Proof Stress (MPa)	UTS (MPa)
7	950	246	683
	1050	241	630
	1150	221	624

Table 8

The Effect of Solution Treatment Temperature on the Mechanical Properties of Series III Alloys

Alloy	Solution Treatment Temp °C	0.2% Proof Stress (MPa)	UTS (MPa)
5	950	233	596
	1050	211	560
	1150	195	553
6	950	222	601
	1050	211	574
	1150	213	569

Table 9

Effect of Thermal Ageing on Hardness (HV) of Solution Treated (1150°C WQ) Alloy 1B

Ageing Time	Temperature (°C)							
	500	600	650	700	750	800	900	1000
30 mins	123	121	122	126	120	121	124	126
1 hour	118	125	122	121	123	127	122	118
4 hours	121	125	123	120	124	123	124	122
8 hours	115	124	119	118	122	121	124	122
16 hours	119	122	124	119	122	122	119	120
64 hours	122	121	119	119	121	117	123	122
100 hours	123	125	120	120	116	120	119	124

Solution Treated Hardness = 123 HV

Table 10

The Effect of Thermal Ageing on the Hardness (HV) of Solution Treated (1150°C WQ) Alloy 4

Ageing Time	Temperature (°C)							
	500	600	650	700	750	800	900	1000
30 mins	128	121	123	121	131	149	140	133
1 hour	124	123	123	120	131	163	148	131
4 hours	119	123	121	151	168	154	138	129
8 hours	119	125	138	171	163	151	141	129
16 hours	118	127	150	160	163	149	133	126
64 hours	117	138	162	157	155	144	139	110
100 hours	125	155	168	160	147	144	132	113

Solution Treated Hardness = 126 HV

Table 11

The Effect of Thermal Ageing on the Hardness (HV) of Solution Treated (950°C) Alloy 2682

Ageing Time	Temperature (°C)							
	500	600	650	700	750	800	900	1000
30 mins	189	193	197	198	198	195	-	-
1 hour	204	203	191	186	191	190	-	-
4 hours	210	198	196	186	191	194	-	-
8 hours	194	197	198	196	194	190	-	-
16 hours	194	196	195	184	191	193	-	-
64 hours	199	198	200	197	189	195	-	-
100 hours	200	193	201	203	191	196	-	-

Solution Treated Hardness = 172 HV

Table 12

The Effect of Thermal Ageing on the Hardness (HV) of Solution Treated (1050°C AC) Alloy 2682

Ageing Time	Temperature (°C)							
	500	600	650	700	750	800	900	1000
30 mins	165	161	160	160	163	161	-	-
1 hour	161	162	167	161	165	168	-	-
4 hours	170	156	157	154	173	172	-	-
8 hours	164	159	172	167	175	168	-	-
16 hours	167	157	166	166	174	172	-	-
64 hours	164	157	166	173	170	174	-	-
100 hours	159	157	175	177	176	175	-	-

Solution Treated Hardness = 147 (HV)

Table 13

The Effect of Thermal Ageing on the Hardness (HV) of Solution Treated (1150°C AC) Alloy 2682

Ageing Time	Temperature (°C)		
	650	700	750
30 mins	153	150	156
1 hour	149	156	151
4 hours	159	152	155
8 hours	158	149	157
16 hours	156	154	159
64 hours	159	156	156
100 hours	153	169	169

Solution Treated Hardness = 136 (HV)

Table 14

The Effect of Thermal Ageing on the Hardness (HV) of Solution Treated (950°C AC) Alloy 2697

Ageing Time	Temperature (°C)							
	500	600	650	700	750	800	900	1000
30 mins	205	205	198	200	202	198	203	171
1 hour	217	203	210	200	207	194	199	166
4 hours	212	220	215	199	212	205	202	172
8 hours	211	193	210	201	206	210	204	160
16 hours	211	218	217	194	206	204	200	162
64 hours	220	201	211	203	205	204	207	162
100 hours	218	206	208	214	216	201	209	159

Solution Treated Hardness = 191 HV

Table 15

The Effect of Thermal Ageing on the Hardness (HV) of Solution Treated (1050°C) Alloy 2697

Ageing Time	Temperature (°C)							
	500	600	650	700	750	800	900	1000
30 mins	162	162	164	165	169	164	166	159
1 hour	173	171	166	163	169	168	170	170
4 hours	168	168	166	168	174	175	172	167
8 hours	168	163	174	178	177	174	167	154
16 hours	175	168	166	169	181	182	165	161
64 hours	172	162	177	185	178	179	164	163
100 hours	176	165	183	185	183	173	166	161

Solution Treated Hardness = 146 HV

Table 16

The Effect of Thermal Ageing on the Hardness (HV) of Solution Treated (1150°C AC) Alloy 2697

Ageing Time	Temperature (°C)							
	500	600	650	700	750	800	900	1000
30 mins	154	147	149	150	146	141	153	155
1 hour	143	143	148	150	153	155	151	147
4 hours	159	157	169	165	158	150	151	146
8 hours	149	149	163	152	153	160	150	145
16 hours	153	157	151	154	158	156	154	148
64 hours	156	152	167	170	162	160	157	151
100 hours	160	155	163	175	162	161	157	143

Solution Treated Hardness = 117 HV

Table 17

The Effect of Thermal Ageing on the Hardness (HV) of Solution Treated (1150°C WQ) Alloy 7

Ageing Time	Temperature (°C)							
	500	600	650	700	750	800	900	1000
30 mins	137	137	137	138	135	142	151	145
1 hour	131	137	138	136	151	159	146	140
4 hours	136	140	136	150	177	161	154	141
8 hours	131	136	140	162	166	156	154	135
16 hours	138	132	158	169	167	164	140	139
64 hours	138	142	174	165	167	156	147	132
100 hours	135	148	174	173	158	152	142	131

Solution Treated Hardness = 143 HV

Table 18

The Effect of Thermal Ageing on the Hardness (HV) of Solution Treated (1150° WQ) Alloy 5

Ageing Time	Temperature (°C)							
	500	600	650	700	750	800	900	1000
30 mins	125	122	117	124	119	121	123	118
1 hour	118	123	122	124	119	121	122	112
4 hours	120	122	118	119	123	123	124	116
8 hours	120	121	121	126	122	122	116	119
16 hours	121	121	121	123	122	121	115	119
64 hours	119	118	126	124	123	120	117	114
100 hours	116	120	124	121	120	119	117	117

Solution Treated Hardness = 129 HV

Table 19

The Effect of Thermal Ageing on the Hardness (HV) of Solution Treated (1150°C WQ) Alloy 6

Ageing Time	Temperature (°C)							
	500	600	650	700	750	800	900	1000
30 mins	120	117	121	119	122	120	118	123
1 hour	126	117	119	119	117	124	118	118
4 hours	120	122	120	116	119	121	122	116
8 hours	115	122	119	119	120	119	119	116
16 hours	118	116	119	116	119	122	116	114
64 hours	122	122	119	120	118	120	120	115
100 hours	119	116	118	120	119	120	111	116

Solution Treated Hardness = 125 HV

Table 20

The Effect of Cold Rolling on the Hardness of Alloys 4 and 5

Alloy	Solution Treated Hardness (HV)	% Cold Reduction in Thickness	Hardness (HV)
4	126	26	288
		51	340
5	130	28	287
		47	300

Table 21

The Effect of Cold Rolling on the Tensile Properties of Alloys 4 and 5

Alloy	Soln Treated tensile Properties		% Cold Reduction in Thickness	Tensile Props	
	0.2% Proof Stress (MPa)	UTS (MPa)		0.2 ps (MPa)	UTS (MPa)
4	200	561	26	347	746
			51	478	933
5	195	553	28	290	702
			47	402	878

Table 22

Hardness (HV) for Cold Rolled Alloys Aged at 500°C

Ageing Time	Alloy 4 25% CR	Alloy 5 25% CR	Alloy 4 50% CR	Alloy 5 50% CR
10 mins	267	251	341	320
30 mins	259	234	330	306
1 hour	254	243	339	299
4 hours	243	230	337	299
8 hours	248	241	340	309
16 hours	253	238	336	308
64 hours	274	240	341	309
100 hours	272	246	345	315

CR = Cold rolled reduction in thickness prior to ageing

Table 23**Hardness (HV) for Cold Rolled Alloys Aged at 600°C**

Ageing Time	Alloy 4 25% CR	Alloy 5 25% CR	Alloy 4 50% CR	Alloy 5 50% CR
10 mins	279	236	325	290
30 mins	248	239	336	290
1 hour	270	238	347	288
4 hours	258	241	319	294
8 hours	270	235	322	284
16 hours	271	243	316	285
64 hours	247	220	281	276
100 hours	251	224	289	270

Table 24**Hardness (HV) for Cold Rolled Alloys Aged at 650°C**

Ageing Time	Alloy 4 25% CR	Alloy 5 25% CR	Alloy 4 50% CR	Alloy 5 50% CR
10 mins	276	233	319	286
30 mins	268	325	325	286
1 hour	260	236	326	280
4 hours	267	238	314	273
8 hours	245	226	284	272
16 hours	243	223	280	273
64 hours	237	210	261	251
100 hours	235	214	275	238

CR = Cold rolled reduction in thickness prior to ageing

Table 25**Hardness (HV) for Cold Rolled Alloys Aged at 700°C**

Ageing Time	Alloy 4 25% CR	Alloy 5 25% CR	Alloy 4 50% CR	Alloy 5 50% CR
10 mins	272	225	307	277
30 mins	245	221	306	269
1 hour	249	218	287	264
4 hours	243	219	279	257
8 hours	228	212	280	245
16 hours	228	213	258	221
64 hours	233	201	245	161
100 hours	225	197	251	144

Table 26**Hardness (HV) For Cold Rolled Alloys Aged at 750°C**

Ageing Time	Alloy 4 25% CR	Alloy 5 25% CR	Alloy 4 50% CR	Alloy 5 50% CR
10 mins	248	210	285	260
30 mins	246	214	284	239
1 hour	241	213	264	200
4 hours	238	198	251	149
8 hours	235	189	242	146
16 hours	222	196	236	141
64 hours	209	179	193	138
100 hours	205	183	183	141

CR = Cold rolled reduction in thickness prior to ageing

Table 27

Hardness (HV) for Cold Rolled Alloys Aged at 800°C

Ageing Time	Alloy 4 25% CR	Alloy 5 25% CR	Alloy 4 50% CR	Alloy 5 50% CR
10 mins	234	199	271	188
30 mins	226	199	240	149
1 hour	227	197	241	146
4 hours	220	196	200	140
8 hours	207	187	195	140
16 hours	206	177	186	137
64 hours	201	140	175	135
100 hours	205	129	163	132

Table 28

Hardness (HV) for Cold Rolled Alloys Aged at 900°C

Ageing Time	Alloy 4 25% CR	Alloy 5 25% CR	Alloy 4 50% CR	Alloy 5 50% CR
10 mins	208	153	175	136
30 mins	199	127	166	137
1 hour	192	135	163	134
4 hours	190	131	154	137
8 hours	184	125	148	131
16 hours	181	135	149	130
64 hours	159	135	148	132
100 hours	149	128	147	129

CR = Cold rolled reduction in thickness prior to ageing

Table 29

Hardness (HV) for Cold Rolled Alloys Aged at 1000°C

Ageing Time	Alloy 4 25% CR	Alloy 5 25% CR	Alloy 4 50% CR	Alloy 5 50% CR
10 mins	153	139	160	140
30 mins	150	133	160	134
1 hour	152	131	153	136
4 hours	143	127	151	132
8 hours	144	127	148	130
16 hours	140	131	142	129
64 hours	133	130	142	124
100 hours	124	126	126	125

CR = Cold rolled reduction in thickness prior to ageing

Table 30

The Effect of Ageing at 700°C on the Tensile properties of 50% Cold Rolled Alloys 4 and 5

Alloy	Ageing Time (hours)	0.2% Proof Stress (MPa)	UTS (MPa)
4	1	696	826
	16	512	725
	24	439	736
	100	343	665
5	1	657	767
	16	263	640
	24	236	631
	100	271	647

Table 31
Accumulative Weight Loss per Unit Surface Area For Alloys
4 and 5, Solution Treated and Thermally Aged

* = Sample Disintegration

Alloy	Condition: Ageing temp/time (hours)	Accum Weight Loss (mg/cm ²)			
		1 x 48 hours	2 x 48 hours	3 x 48 hours	4 x 48 hours
4	500°C/100 (flat)	7.32	27.67	*	*
4	500°C/100 (bent)	8.98	85.90	*	*
4	600°C/100 (flat)	37.80	*	*	*
4	600°C/100 (bent)	23.63	*	*	*
4	700°C/1 (flat)	*	*	*	*
4	700°C/1 (bent)	*	*	*	*
4	700°C/8 (flat)	0.78	8.79	*	*
4	700°C/8 (bent)	19.84	*	*	*
4	700°C/16 (flat)	0.27	0.59	1.01	1.66
4	700°C/16 (bent)	*	*	*	*
4	700°C/100 (flat)	0.12	0.25	0.33	0.54
4	700°C/100 (bent)	0.14	0.28	0.36	0.54
5	500°C/100 (flat)	0.17	0.33	1.00	1.61
5	500°C/100 (bent)	0.19	0.51	1.10	1.72
5	600°C/100 (flat)	0.73	1.69	4.31	9.40
5	600°C/100 (bent)	0.21	0.92	3.41	9.46
5	700°C/1 (flat)	4.92	*	*	*
5	700°C/1 (bent)	7.93	*	*	*
5	700°C/8 (flat)	1.72	22.24	*	*
5	700°C/8 (bent)	3.37	*	*	*
5	700°C/16 (flat)	7.08	*	*	*
5	700°C/16 (bent)	5.03	*	*	*
5	700°C/100 (flat)	0.48	0.75	1.01	1.25
5	700°C/100 (bent)	0.60	0.90	1.07	1.30

Table 32Accumulative Weight Loss Per Unit Surface Area For Alloys 4 and 5, Solution Treated, Approximately 50% Cold Work and Thermally Aged

Alloy	Condition Ageing temp/time (hours)	Accum Weight Loss (mg/cm ²)			
		1 x 48 hours	2 x 48 hours	3 x 48 hours	4 x 48 hours
4	700°C/1 (flat)	0.16	0.46	0.80	1.34
4	700°C/1 (bent)	0.22	0.60	0.96	1.61
4	700°C/8 (flat)	0.41	0.67	0.99	1.29
4	700°C/8 (bent)	0.24	0.74	1.01	1.53
4	700°C/16 (flat)	0.10	0.28	0.43	0.58
4	700°C/16 (bent)	0.22	0.48	0.65	0.84
4	700°C/100 (flat)	0.14	0.42	0.60	0.80
4	700°C/100 (bent)	0.07	0.29	0.43	0.58
5	700°C/1 (flat)	0.13	0.35	0.65	0.99
5	700°C/1 (bent)	0.19	0.42	0.73	1.01
5	700°C/8 (flat)	0.21	0.43	0.53	1.09
5	700°C/8 (bent)	0.17	0.32	0.53	0.78
5	700°C/16 (flat)	0.26	0.48	0.75	0.98
5	700°C/16 (bent)	0.30	0.54	0.80	1.05
5	700°C/100 (flat)	0.25	0.62	1.40	1.81
5	700°C/100 (bent)	0.28	0.64	1.00	1.27

Table 33

Microhardness Survey For Alloy 4 Aged 500°C 100 hours
and Corrosion Tested for 48 hours

<u>Position</u>	<u>Microhardness (HV)</u>
Mid corrosion 'finger' (1)	201
Midway between (1) and (2)	143
Mid corrosion 'finger' (2)	229
Midway between (2) and (3)	162
Mid corrosion 'finger' (3)	272
Midway between (3) and (4)	200
Mid corrosion 'finger' (4)	224
Midway between (4) and (5)	168
Mid corrosion 'finger' (5)	214

TABLE 34

Mass Fractions of Undissolved Carbides at 900°C to 1100 °C

CAST No.	ANALYSIS m/o		SOLN. TREAT. TEMP. °C	Cr ₇ C ₃		TiC		GRAIN SIZE	
	C	Ti		f _m	1/f _m	f _m	1/f _m	AC (μm)	WQ (μm)
1B	.02	<.05	900	.00055	1818	-	-	38.7	53.1
4	.08	<.05	900	.00722	139	-	-	34.5	41.4
			950	.00655	153	-	-	32.8	51.9
			1000	.00544	184	-	-	35.6	55.1
			1050	.00343	291	-	-	54.1	52.9
			1100	.00131	763	-	-	90.5	68.9
5	.02	.15	900	.00055	1818	.00037	2702	30.5	32.5
			950	-	-	.00006	16667	32.4	35.7
2682	.02	.21	900	.00055	1818	.0006	1667	22.8	22.3
			950	-	-	.0003	3333	21.4	23.1
2697	.04	.21	900	.00378	265	.0013	769	14.2	12.5
			950	.00211	474	.0010	1000	15.3	14.0
			1000	.00100	1000	.0007	1428	27.9	16.3
7	.08	.29	900	.00722	139	.00280	357	29.5	25.8
			950	.00655	153	.00250	400	21.8	28.4
			1000	.00544	184	.00215	465	26.4	23.7
			1050	.00343	291	.00174	575	26.3	24.1
			1100	.00131	763	.00124	806	29.3	33.5
6	.03	.40	900	.00167	599	.00125	800	34.1	38.5
			950	.00100	1000	.00106	943	35.6	44.4
			1000	-	-	.00087	1150	36.7	47.3

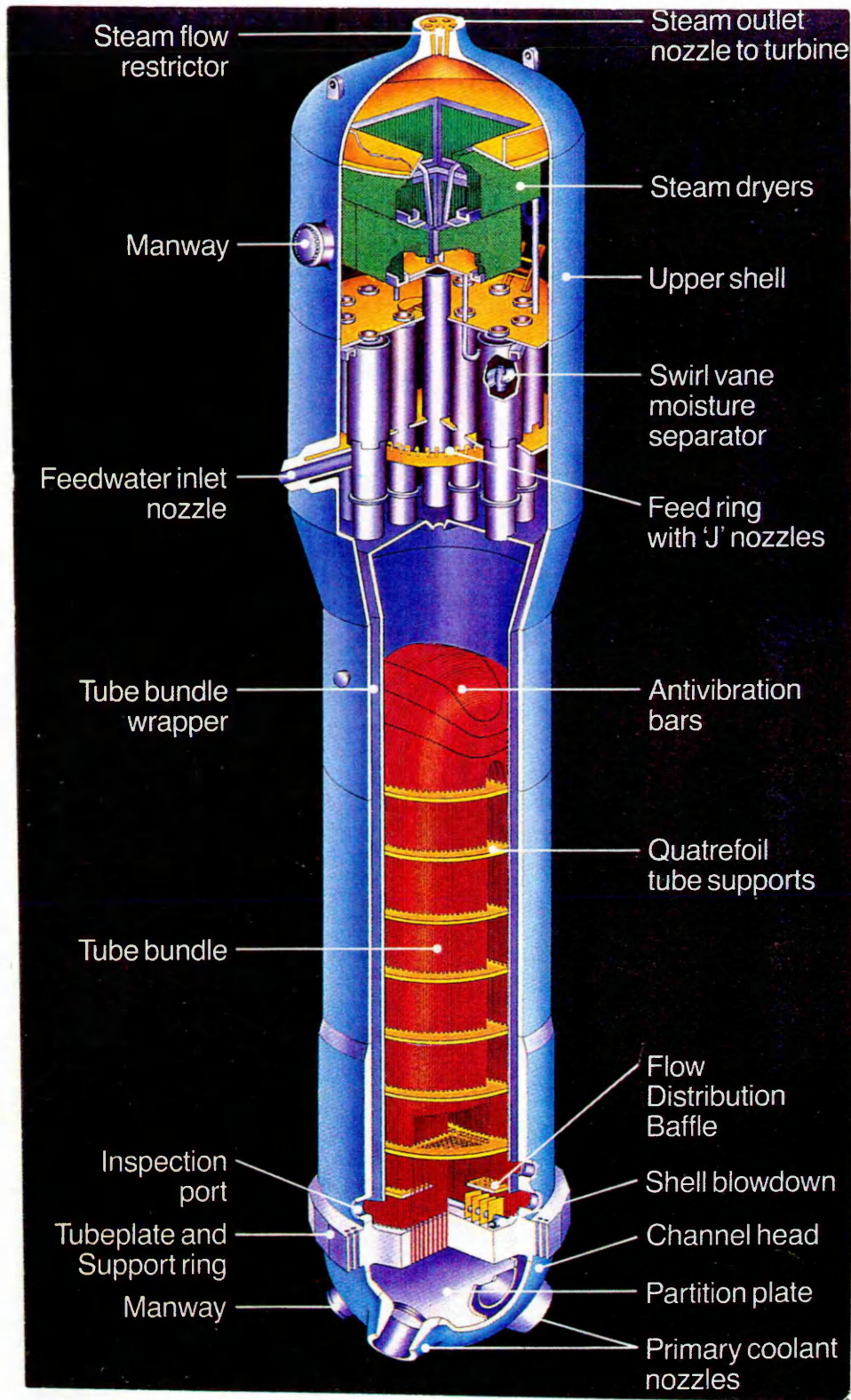


Figure 1

This figure shows one of the four Steam Generators attached to the Central Pressure Vessel. The 'F' Type steam generator is a development of earlier versions and has been designed to overcome corrosion problems that have been experienced on some plants.

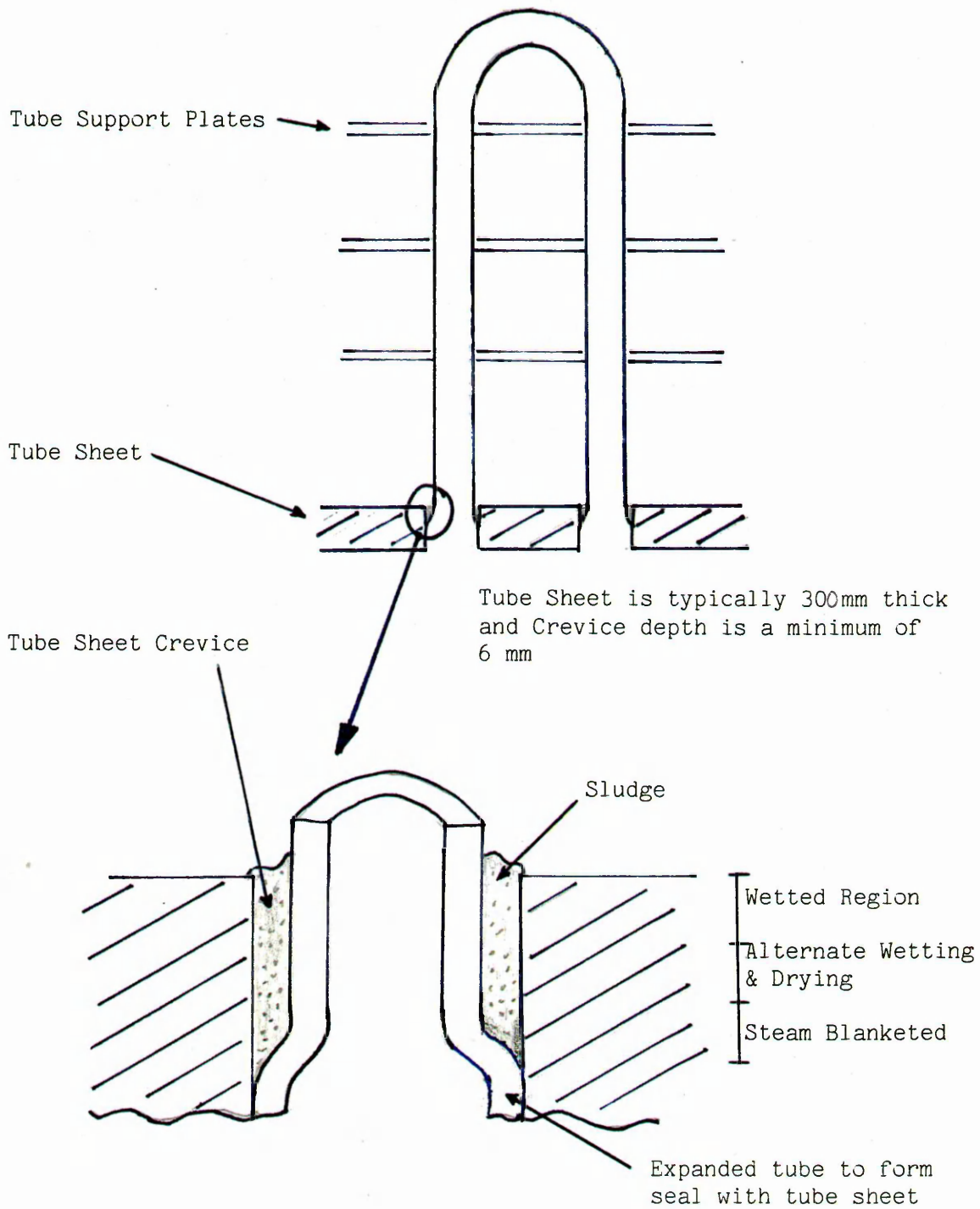


Figure 2 Schematic Diagram of SG Tube System and detail of Tube Sheet Crevice.

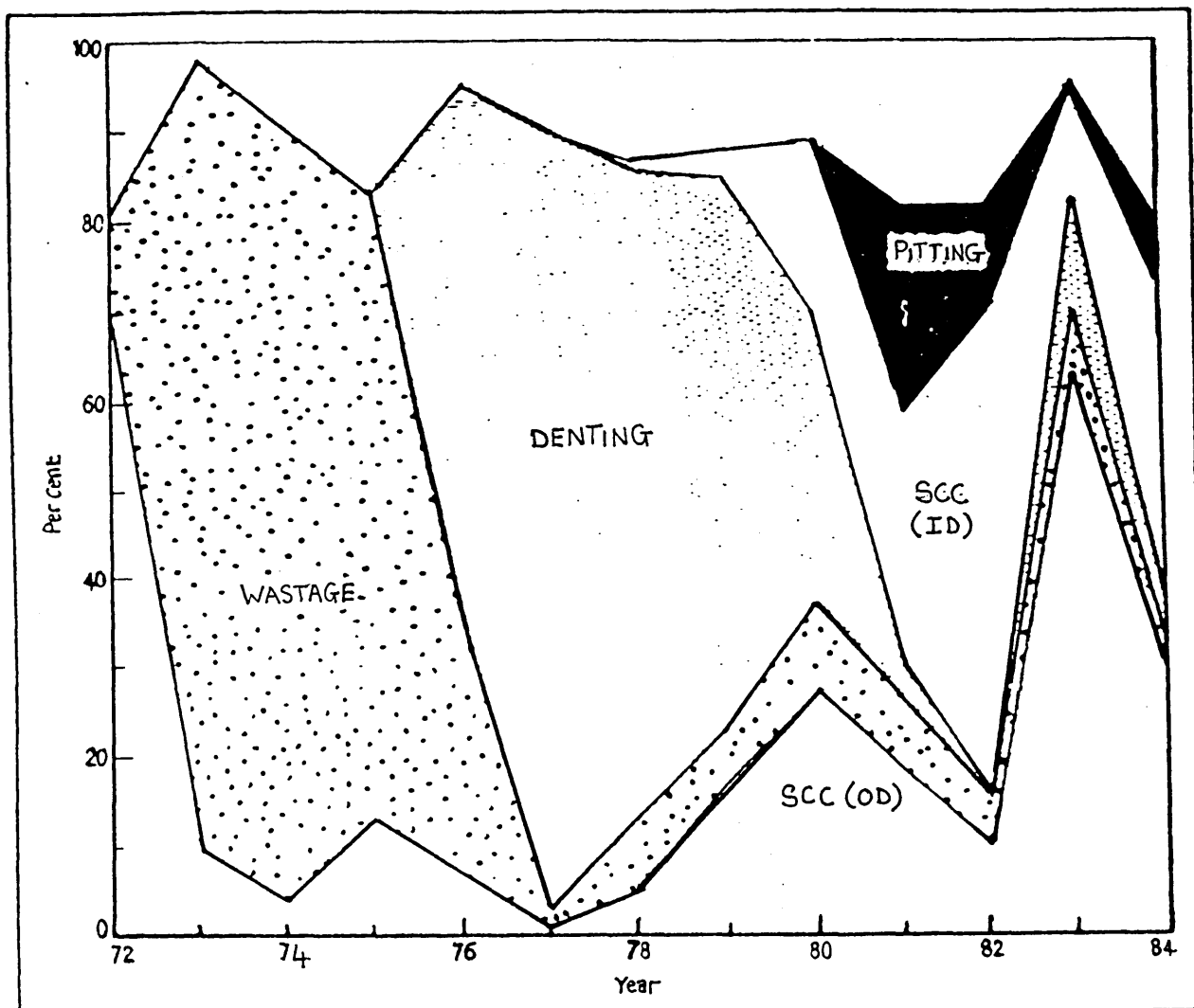


Figure 3 History of Tube Failure Mechanisms

More than 80% of defects are due to corrosion. SCC (OD) is secondary side stress corrosion and intergranular attack. SCC (ID) is primary side stress corrosion cracking.

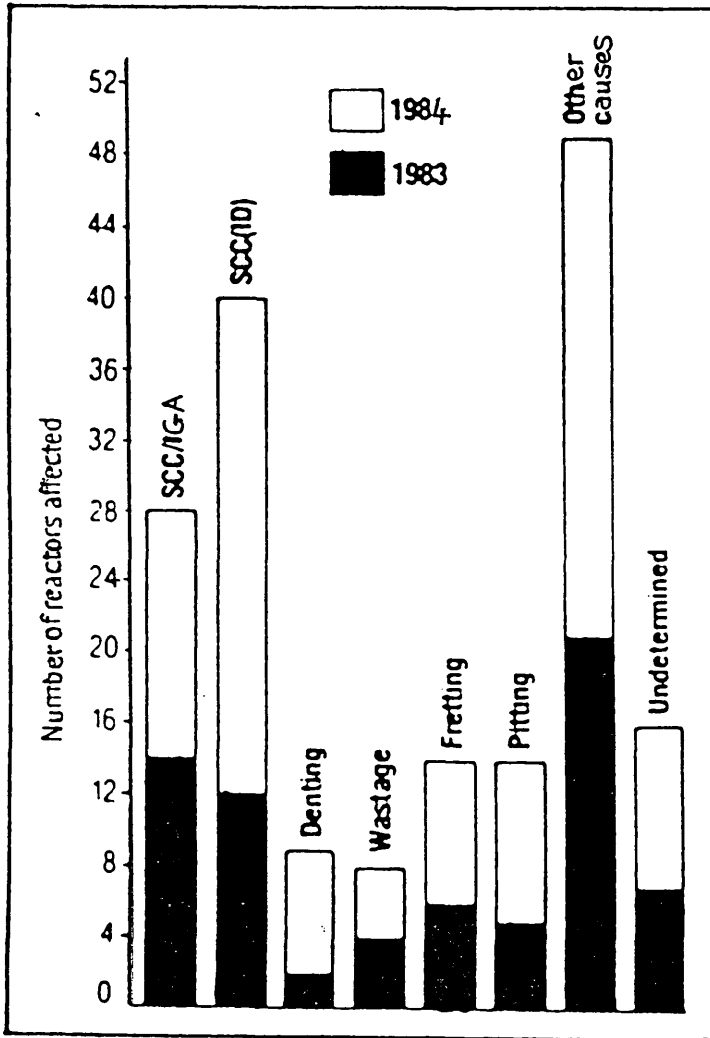


Figure 4 Number of Reactors at which Tubes were plugged in 1983/1984, and mechanisms responsible for plugging. (148 reactors in 1984)

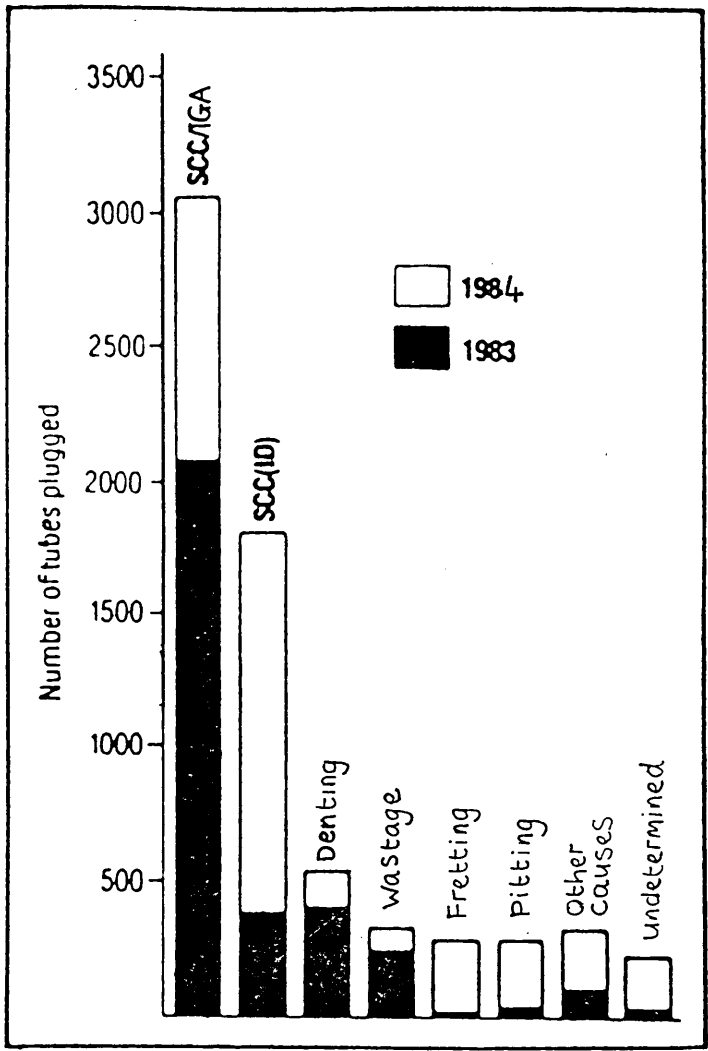
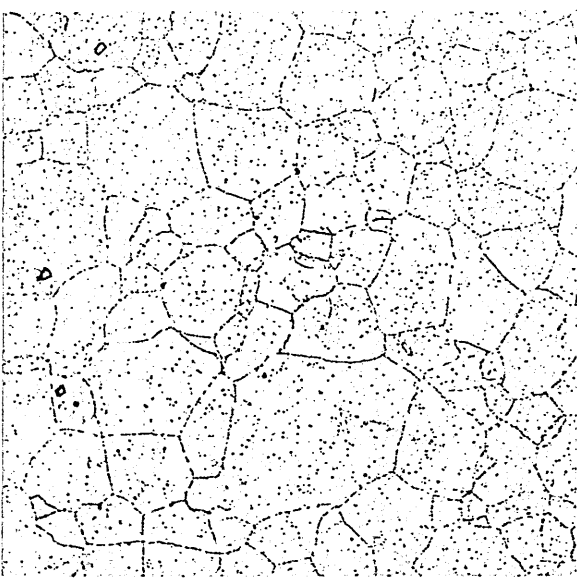
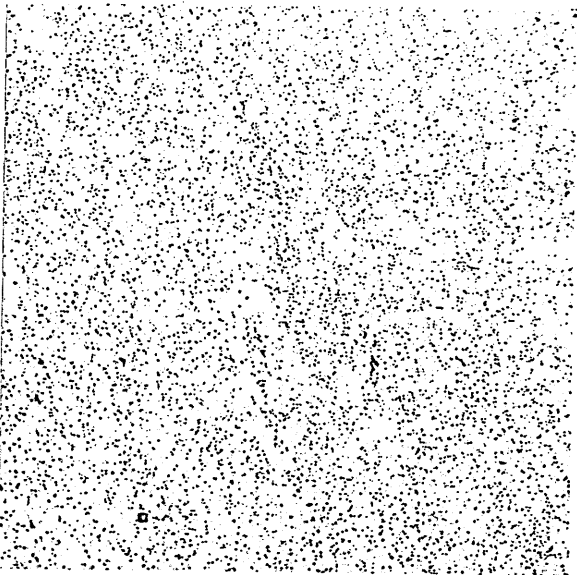


Figure 5 Number of Tubes plugged in 1983/1984 and mechanisms responsible for plugging.
 (2.1 x 10⁶ tubes in service in 1984)



x 200

Figure 6 Microstructure of cast 2682
Thermally Treated - As Received



x 200

Figure 7 Microstructure of cast 2697
Mill Annealed - As Received

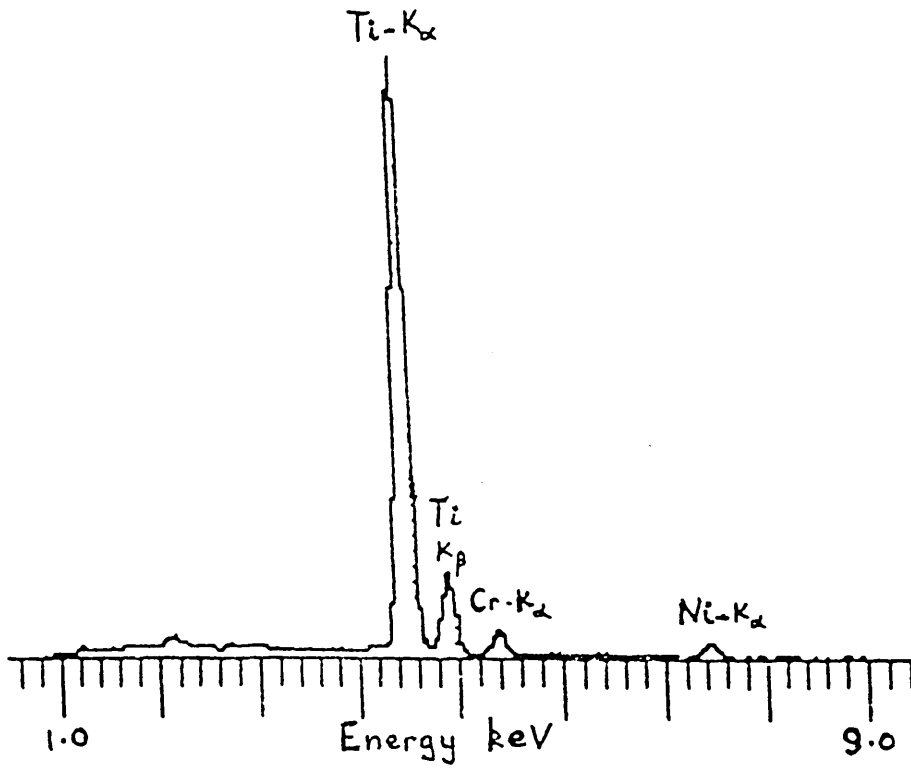


Figure 8 E.D.X Spectrum from angular
Ti(CN) particle in Cast 2697(MA)

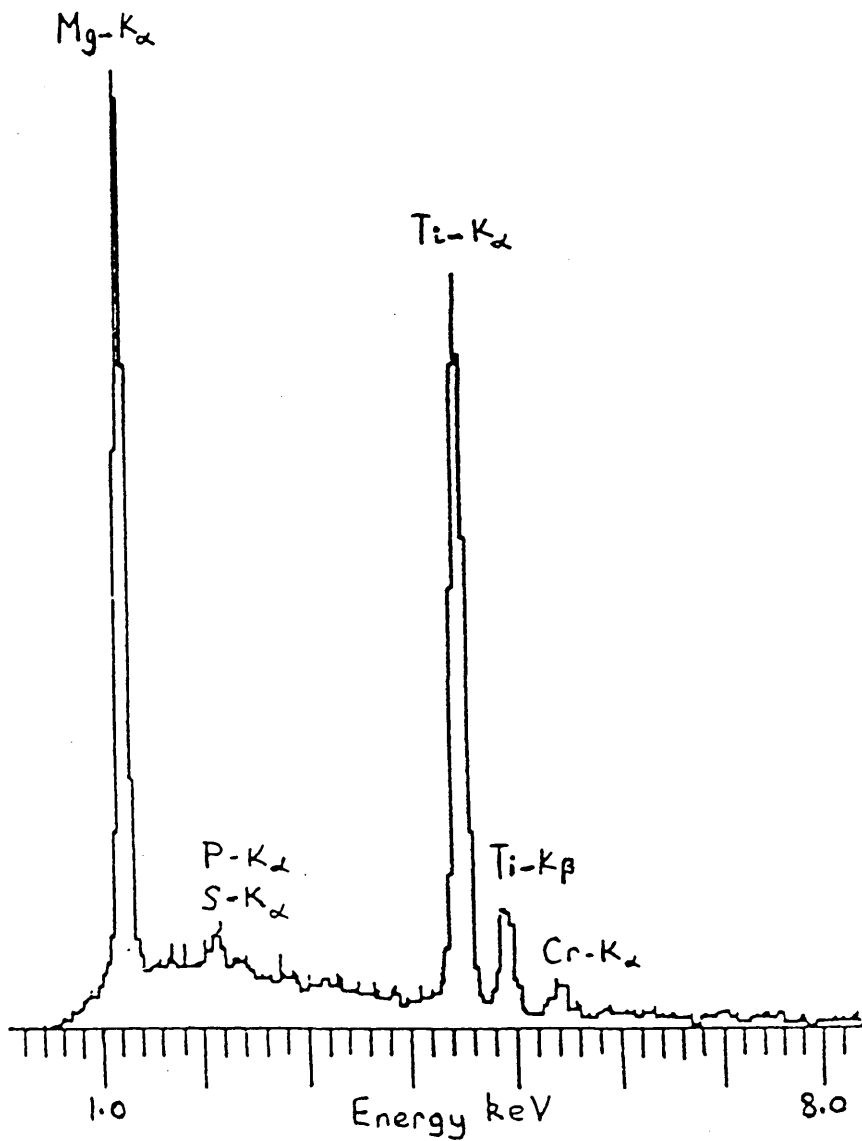


Figure 9 E.D.X Spectrum from angular Ti(CN) associated with MgS in cast 2682(TT)

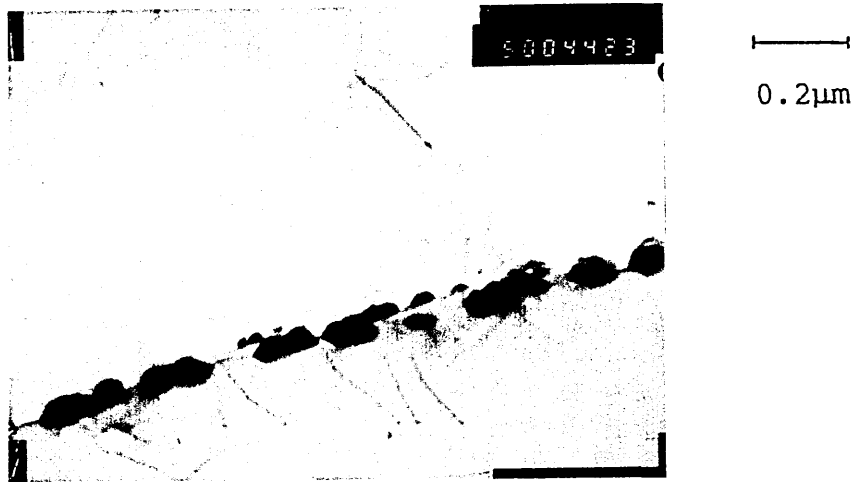


Figure 10 Electron Micrograph of Cast 2682
Thermally Treated - Extensive Grain
Boundary Carbides



Figure 11 Electron Diffraction Pattern
from Grain Boundary Carbides
Shown in Figure 10 - Crystal
Structure determined as $M_{23}C_6$

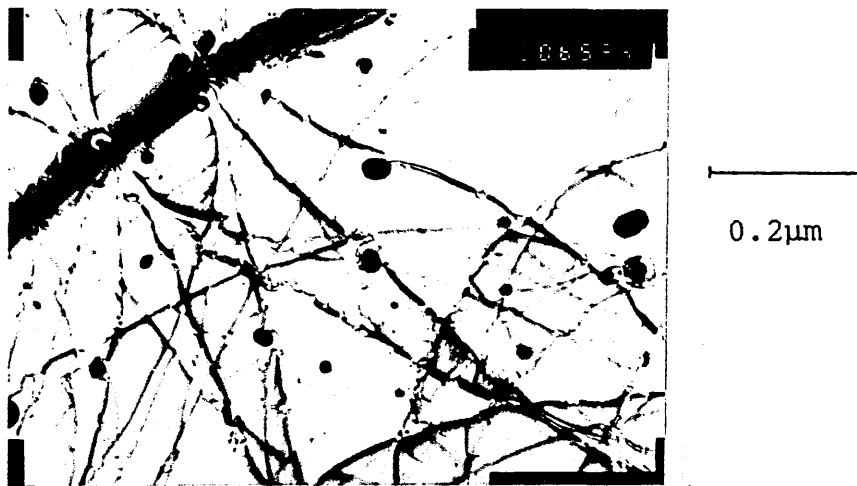


Figure 12 Electron Micrograph of Thermally Treated Cast 2682

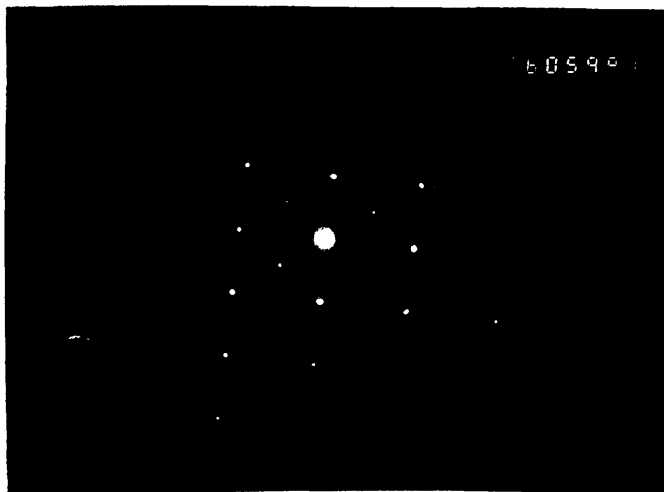


Figure 13 Electron Diffraction Pattern from Intragranular Carbides shown in Figure 12. Crystal Structure determined as M_7C_3 .

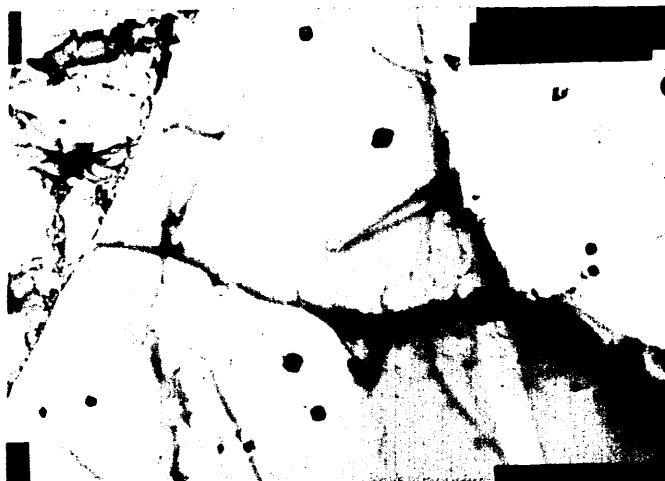


Figure 14 Thin foil electron Micrograph of
cast 2697 mill annealed As - Received



Figure 15 Electron Diffraction Pattern from
Intragranular Carbides shown in
figure 14 - crystal structure
determined as M_7C_3



Figure 16 Carbon Extraction Replica of cast 2697 showing the thin 'plate - like' nature of grain boundary precipitates.

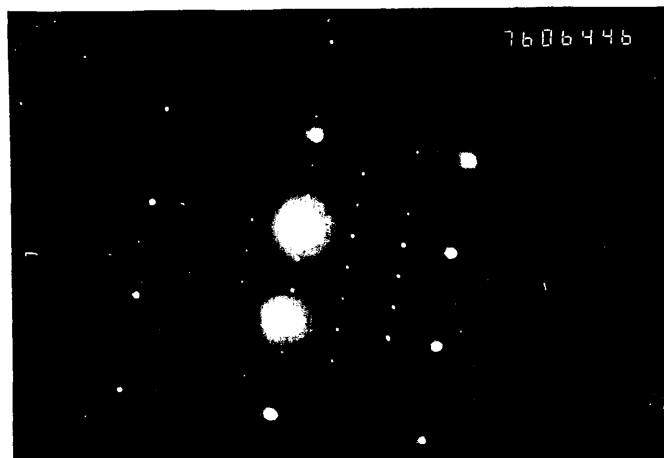


Figure 17 Electron Diffraction Pattern from grain boundary Carbides shown in figure 16 - crystal structure determined as $M_{23}C_6$.

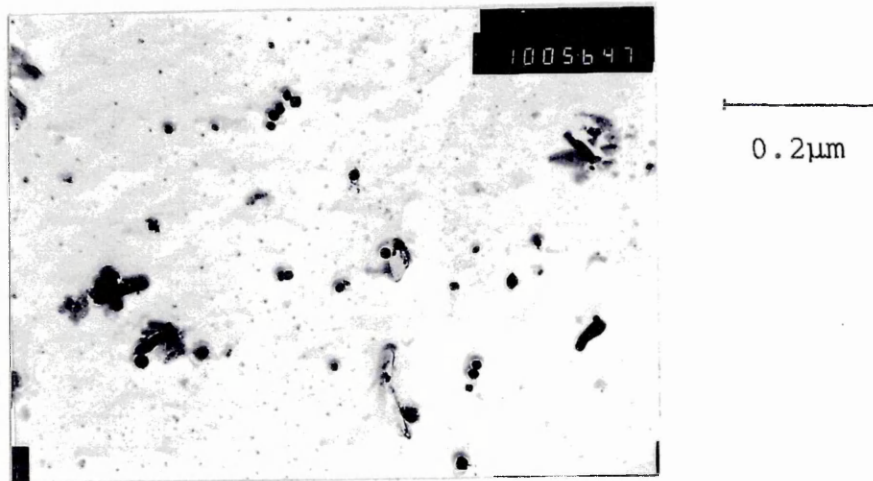


Figure 18 Carbon extraction replica of cast 2697 mill annealed showing mainly intragranular carbides.



Figure 19 Electron diffraction pattern from smaller intragranular Carbides shown in figure 18 - structure determined as Titanium Carbide (TiC)

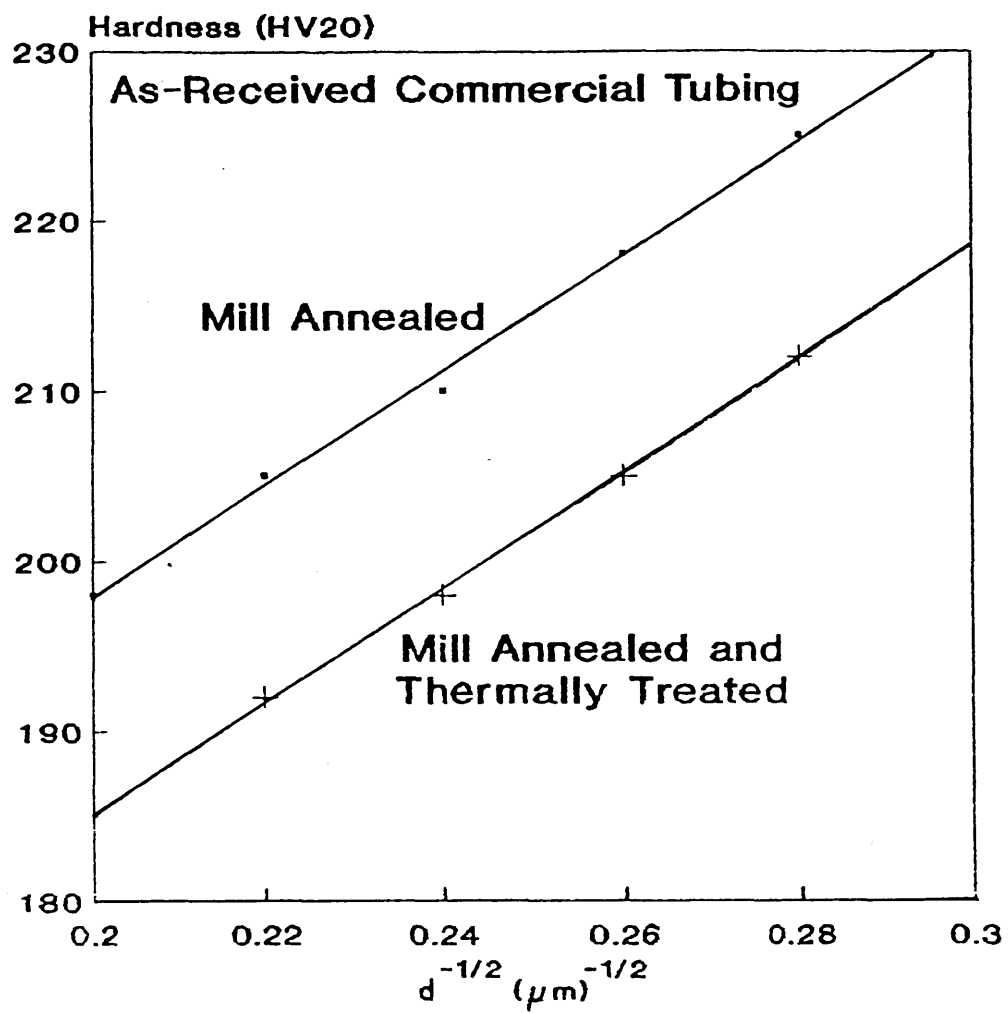


Figure 20

Petch Relationship for As-Received Commercial Tubing

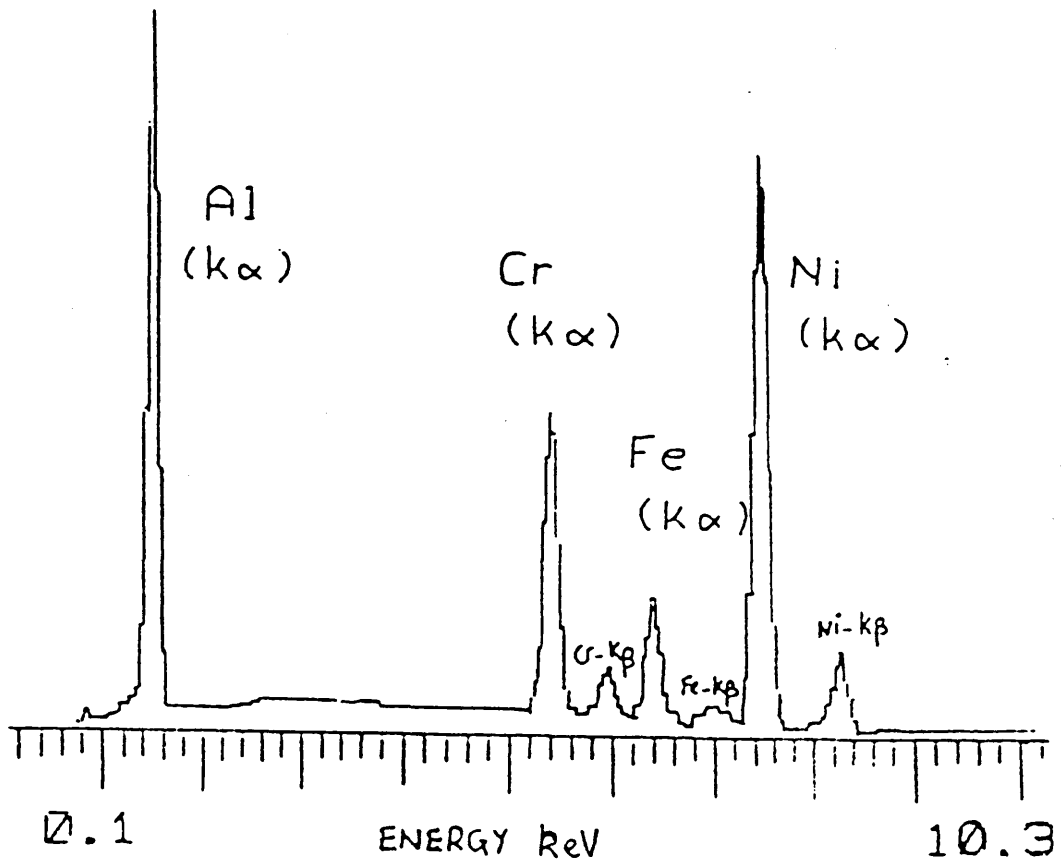


Figure 21 E.D.X. Spectrum from globular Al - rich inclusion in Alloy 4.

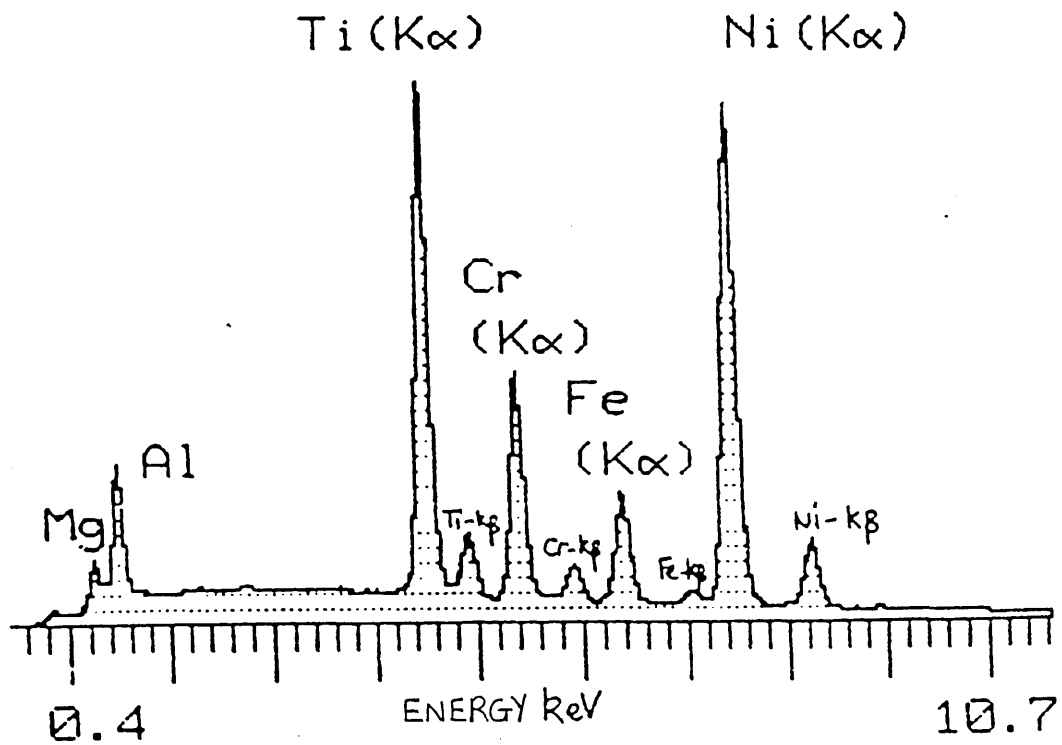


Figure 22 E.D.X. Spectrum From angular
 Ti(CN) inclusion associated with
 Mg and Al in Alloy 7

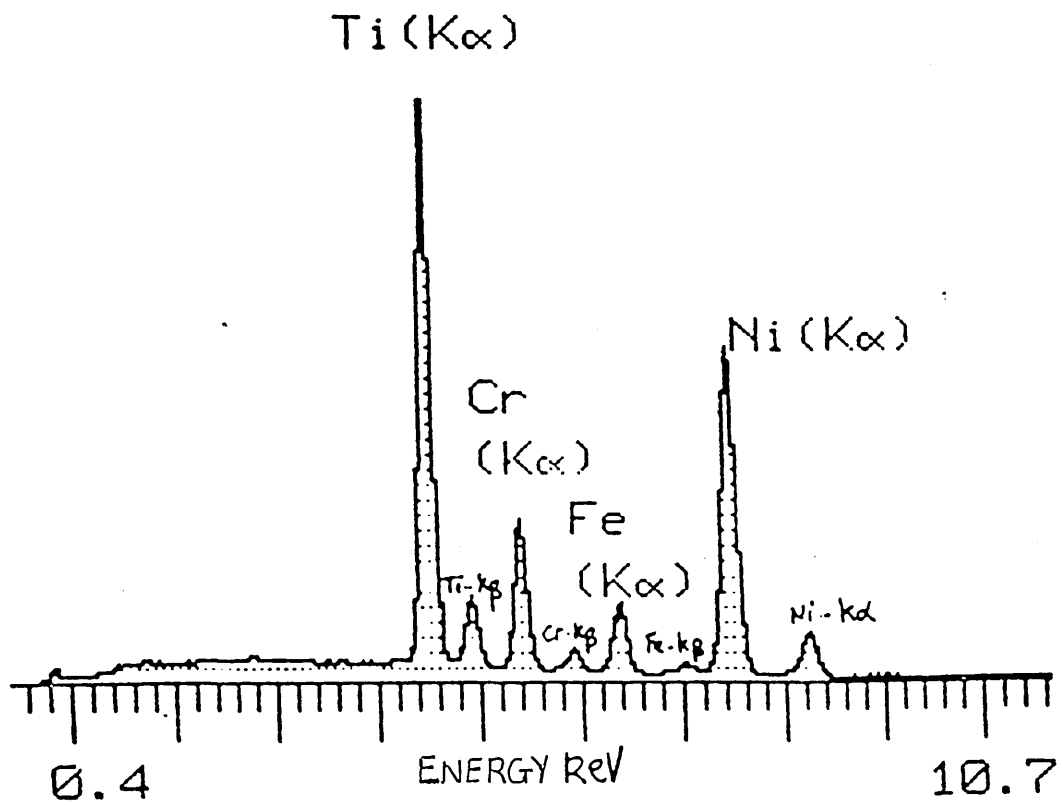


Figure 23 E.D.X. Spectrum From An angular
Ti(CN) inclusion In Alloy 6

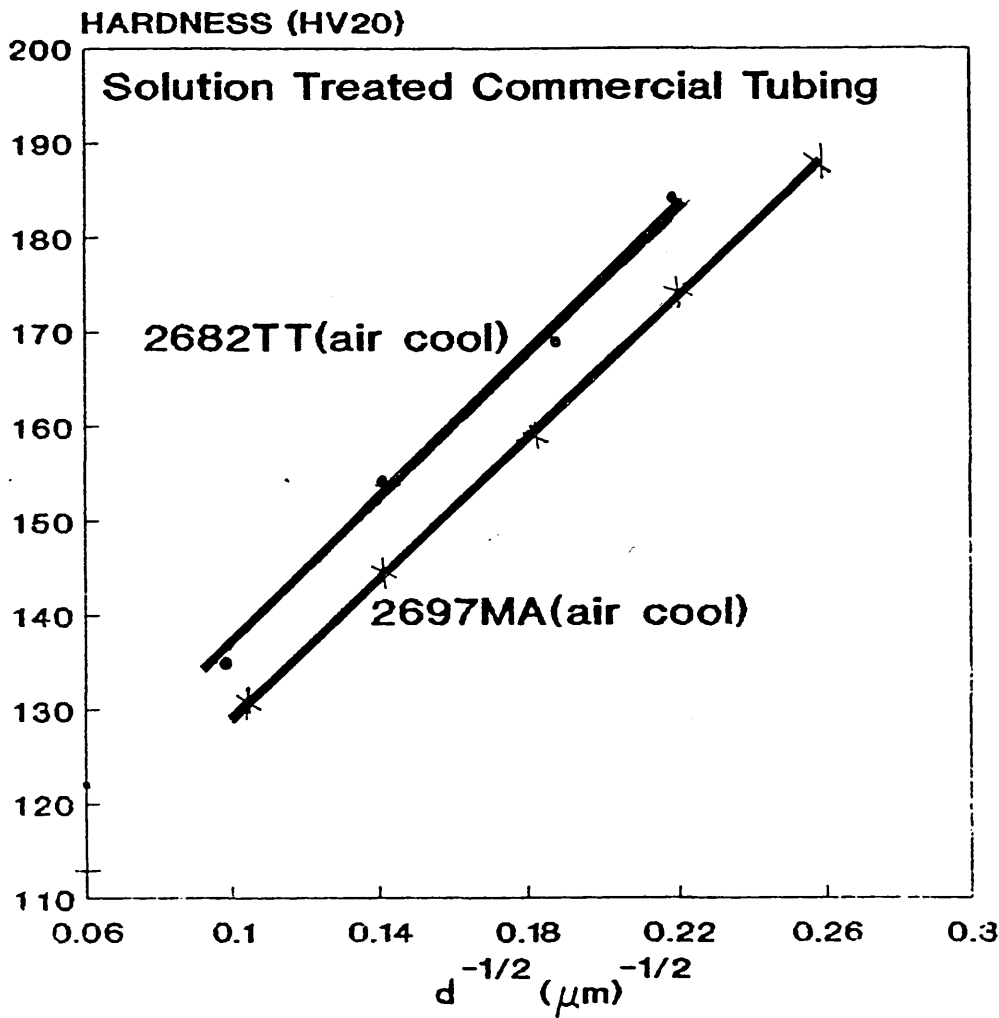


Figure 24 Petch Relationship for Mill
 Annealed and Thermally Treated
 Casts 2697 and 2682 following
 Solution Treatment

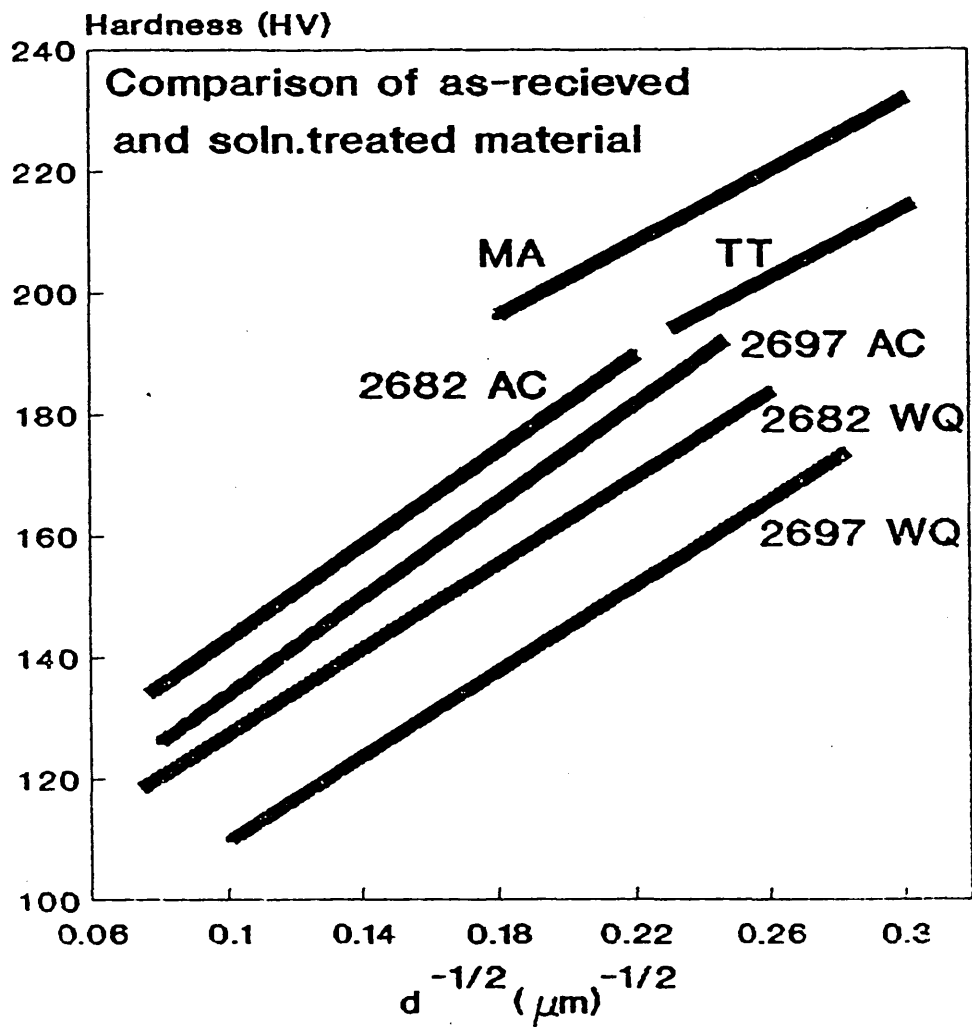


Figure 25 Petch Relationship for As-Received
Commercial Casts following
Solution Treatment



(a) x 52



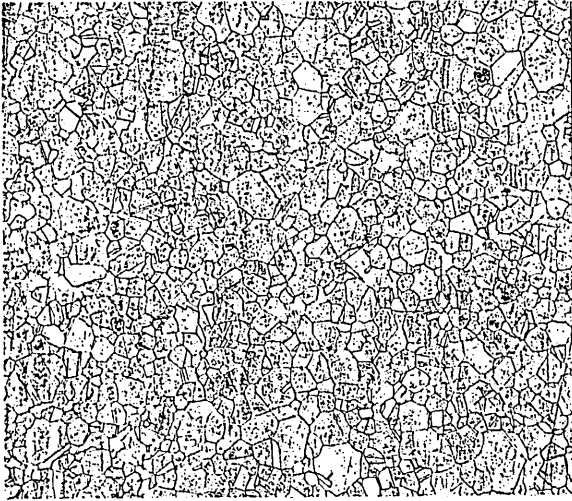
(b) x 52

Figure 26

Grain Structure of Series I Alloy 4 following Hot Rolling
and Solution Treatment

(a) Alloy 4 ST 900°C Air Cool

(b) Alloy 4 ST 1200°C Air Cool



(a) x 52



(b) x 40

Figure 27

Grain Structure of Series I Alloy 1B following Hot Rolling
and Solution Treatment

(a) Alloy 1B ST 900°C Air Cool

(b) Alloy 1B ST 1200°C Air Cool

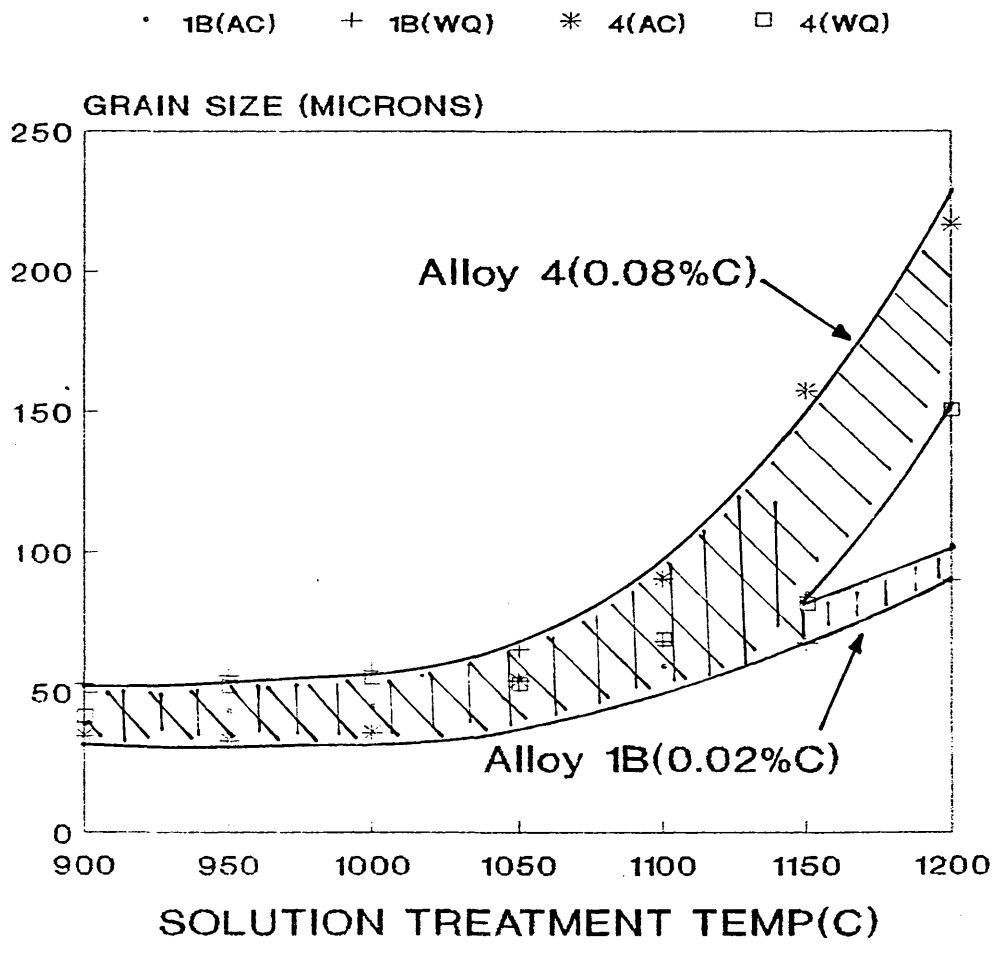


Figure 28 Series I Alloys: Effect of
 Solution Treatment Temperature
 and Rate Of Cooling on Grain
 Size

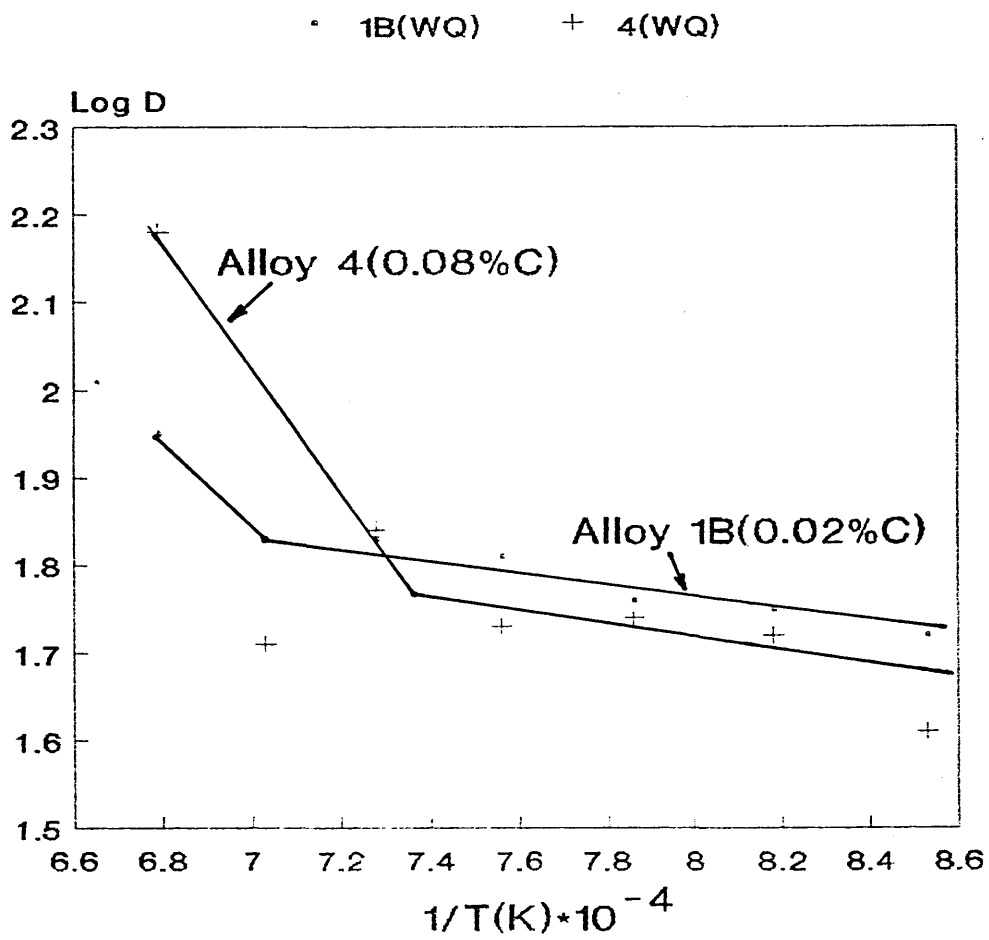


Figure 29 Temperature v Log Grain Size for
 Series I Alloys after Solution
 Treatment (WQ)

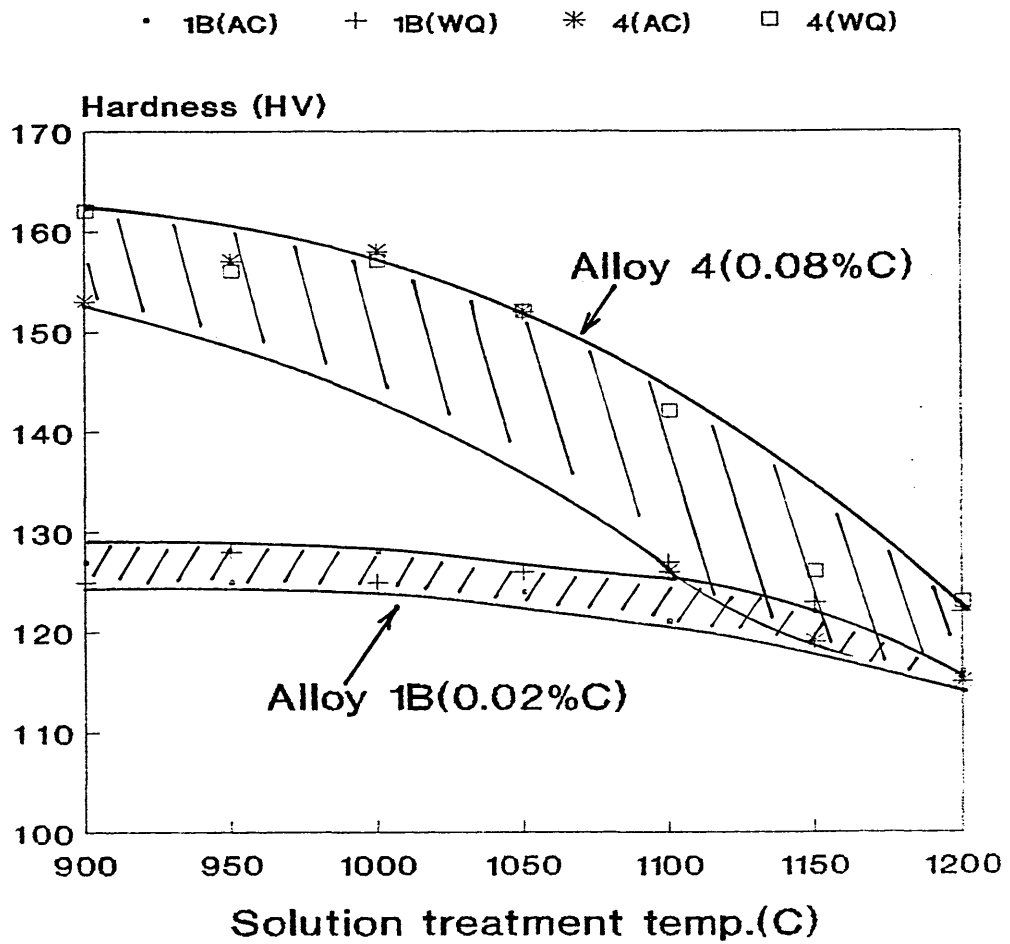


Figure 30 Series I Alloys: Effect of
 Solution Treatment Temperature
 and Rate Of Cooling on
 Hardness

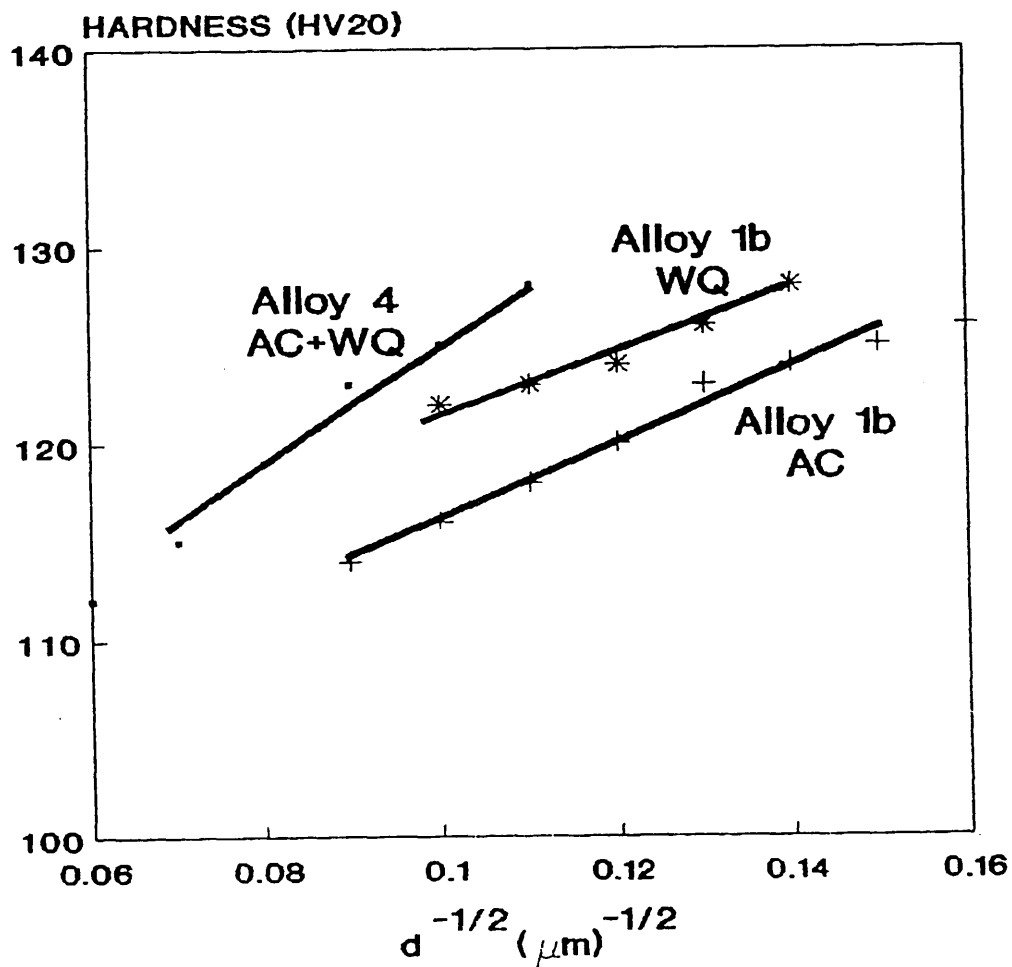
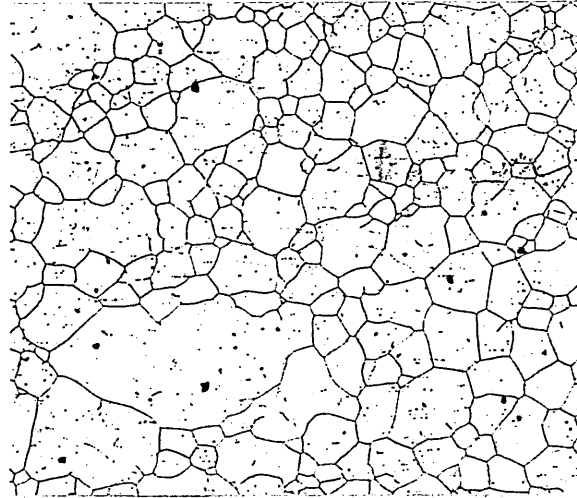


Figure 31 Petch Relationship for Series I
 Alloys after Solution Treatment -
 Fully Recrystallised conditions
 only



(a) x 52



(b) x 52

Figure 32

Grain Structure of Series II Alloy 7 following Hot Rolling
and Solution Treatment

(a) Alloy 7 ST 900°C Air Cool

(b) Alloy 7 ST 1200°C Air Cool

• 2682(AC)	+ 2682(WQ)	* 2697(AC)
□ 2697(WQ)	× 7(AC)	◇ 7(WQ)

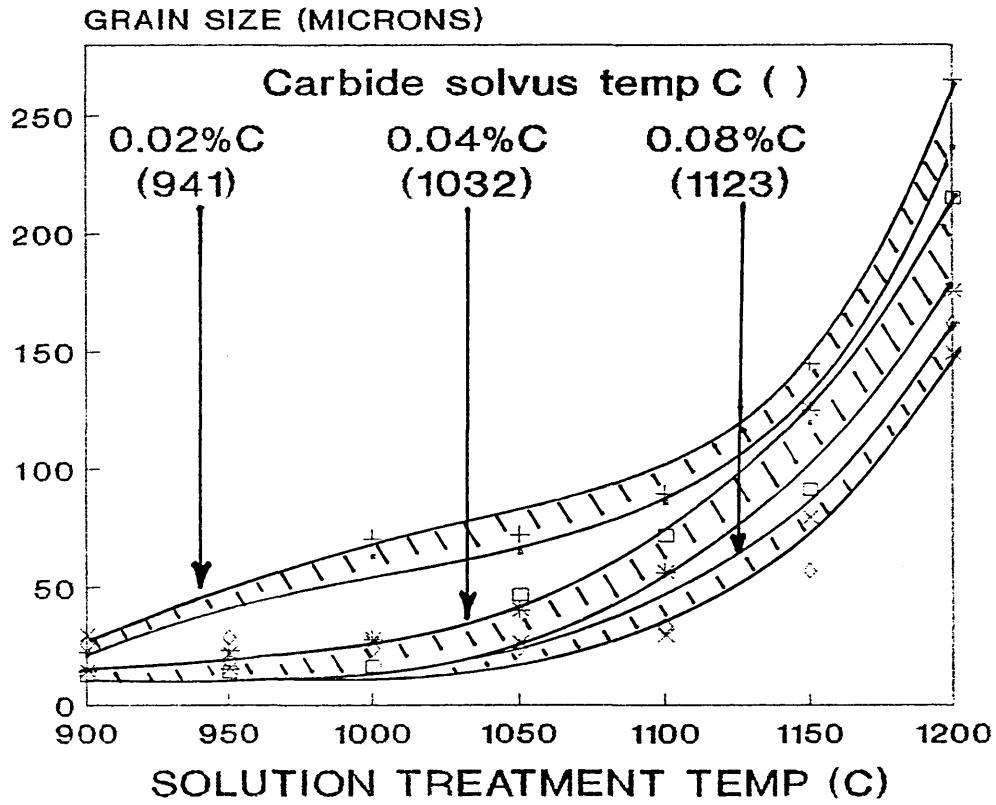


Figure 33 Series II Alloys: Effect of solution treatment temperature and rate of cooling on grain size

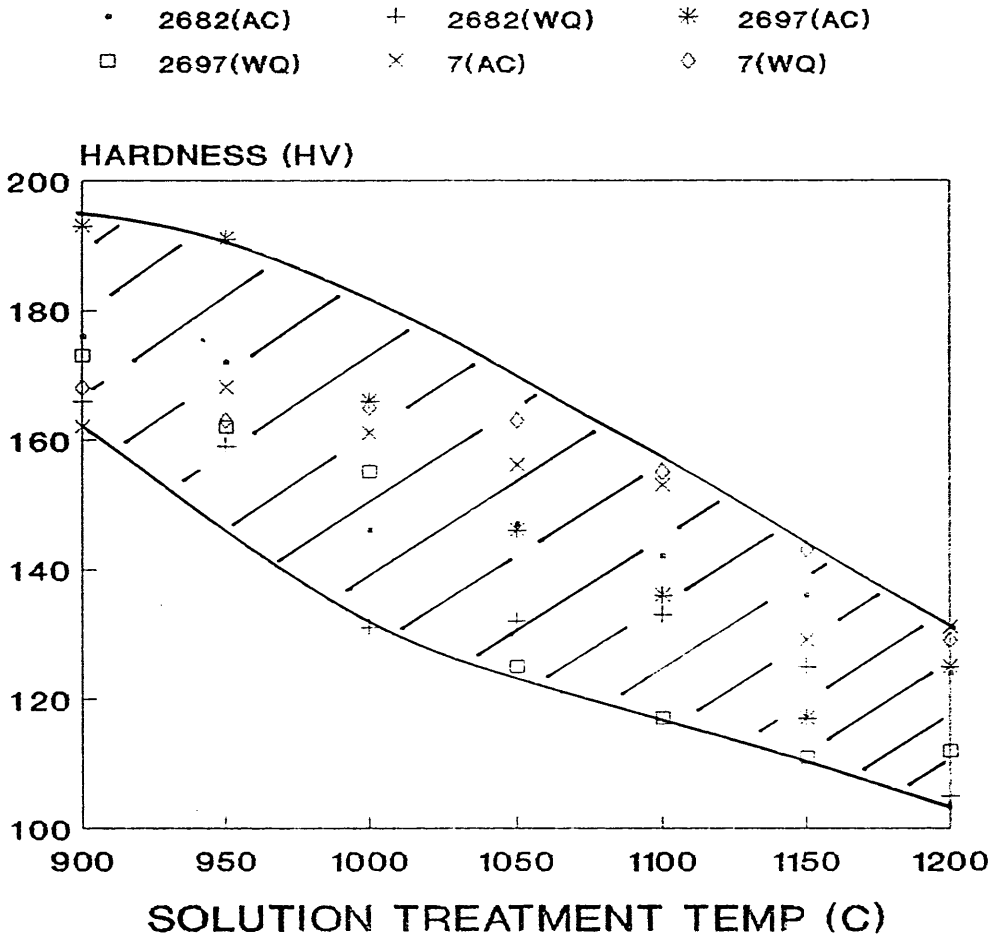


Figure 34 Series II Alloys: Effect of solution treatment temperature and cooling rate on hardness

• 2682 AC	+ 2682 WQ	* 2697 AC
□ 2697 WQ	× 7 AC	◇ 7 WQ

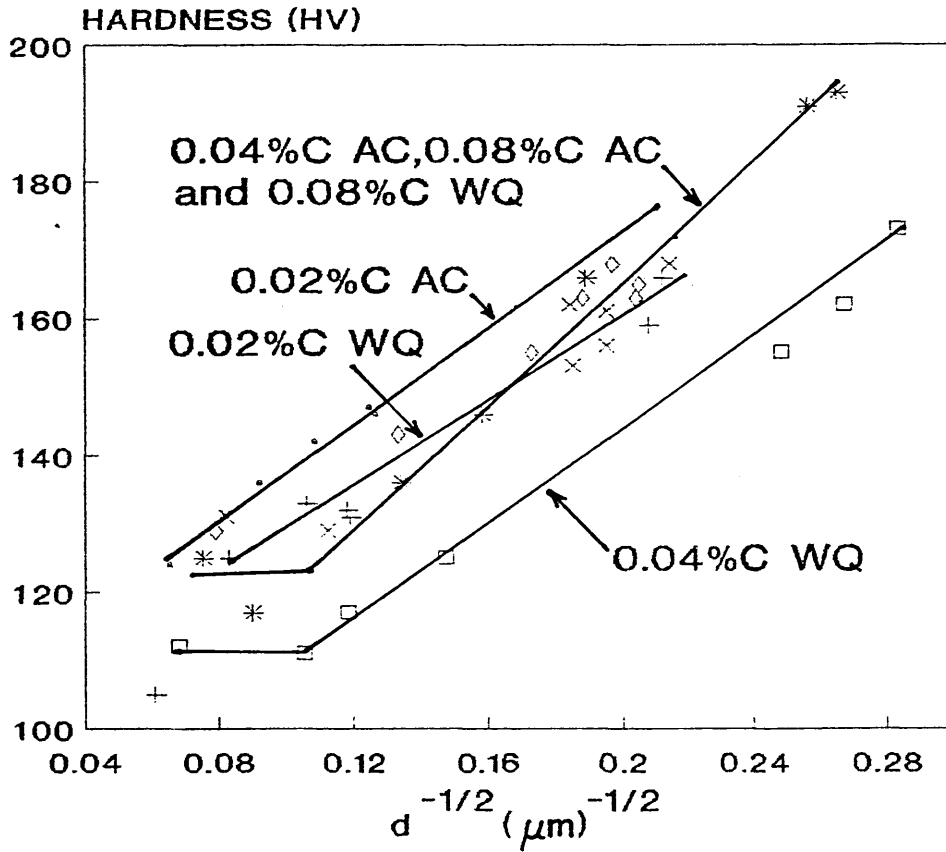


Figure 35 Patch Relationship for Series II
Alloys after Solution Treatment

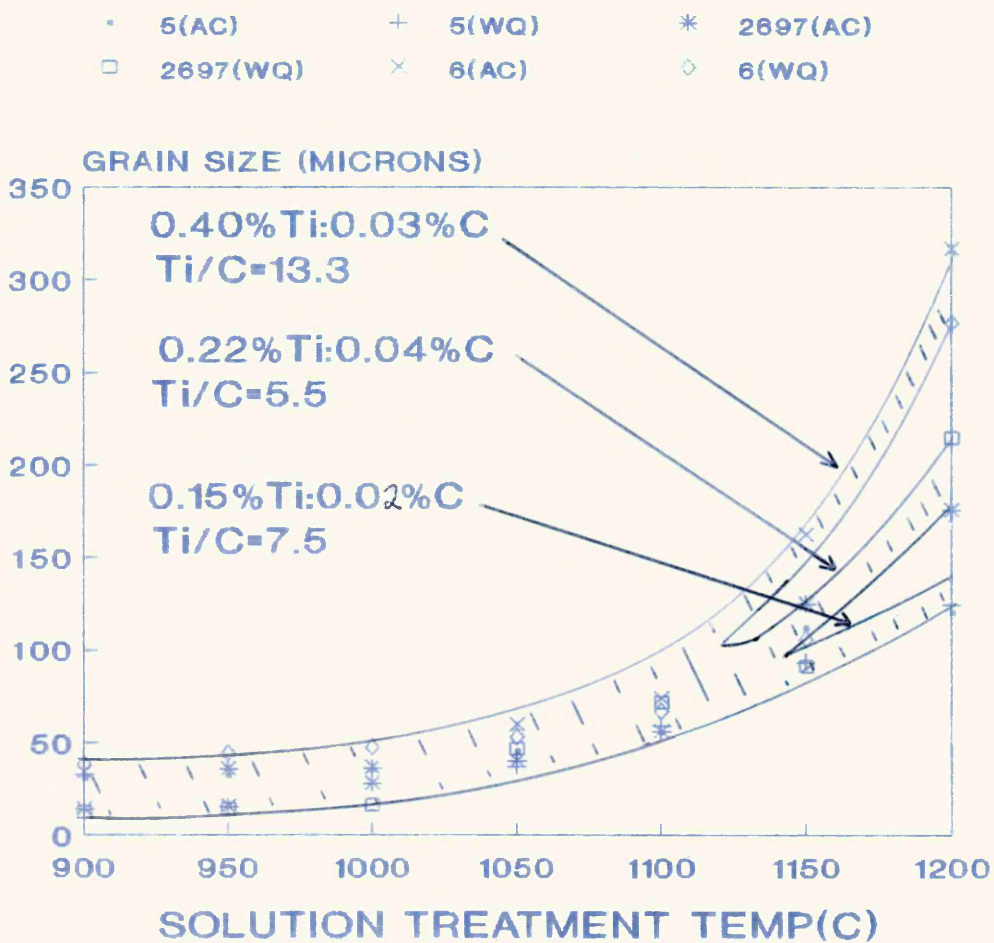


Figure 36 Series III Alloys : Effect of solution treatment temperature and rate of cooling on grain size

• 5(AC)	+ 5(WQ)	* 2697(AC)
□ 2697(WQ)	× 6(AC)	◇ 6(WQ)

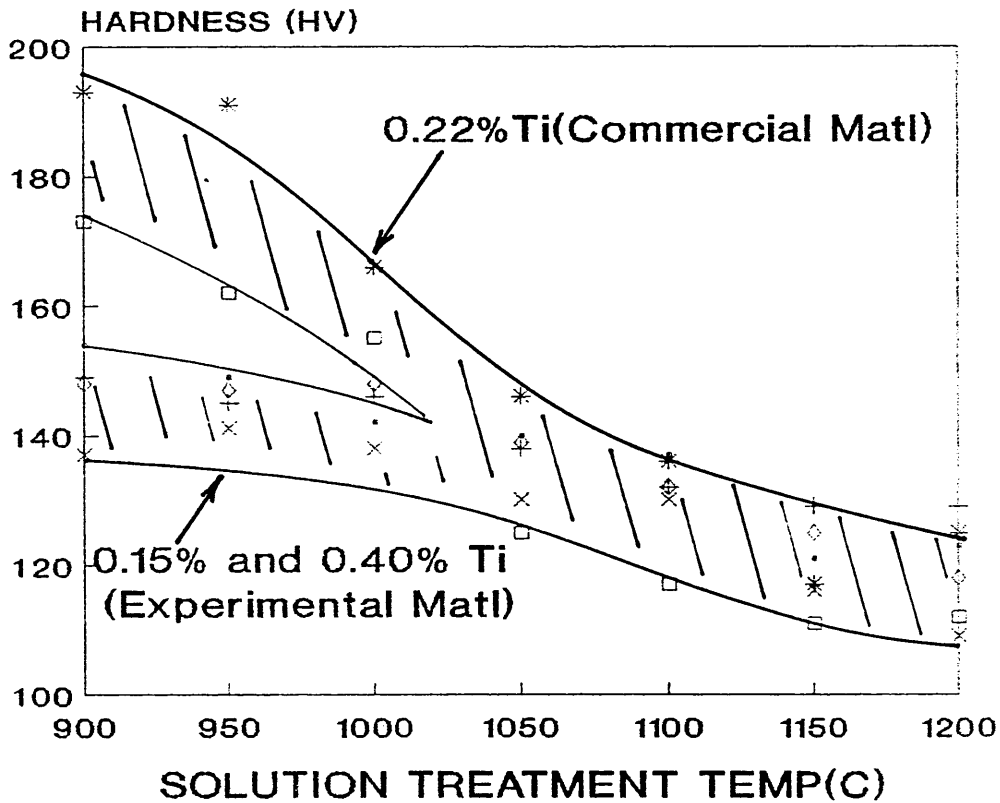


Figure 37

Series III Alloys: Effect of solution treatment temperature and rate of cooling on hardness

• 0.15% Ti(AC) + 0.15% Ti(WQ) * 0.22% Ti(AC)
 □ 0.22% Ti(WQ) × 0.40% Ti(AC) ◇ 0.40% Ti(WQ)

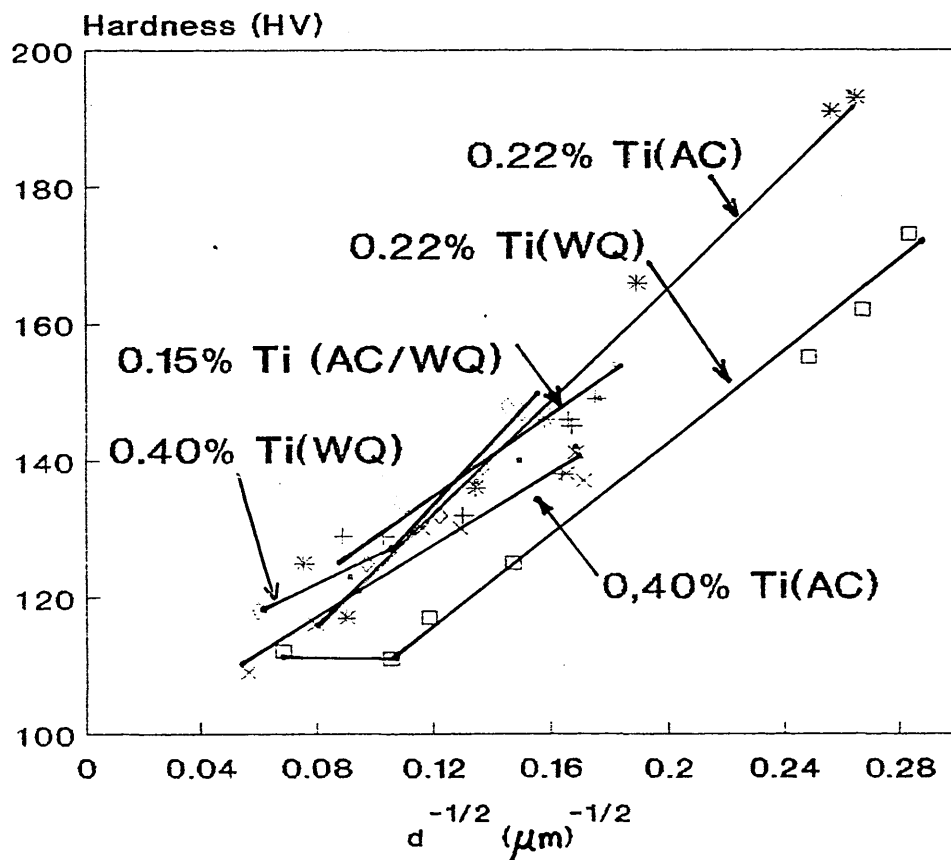


Figure 38 Petch Relationship for Solution
 Treated Series III Alloys

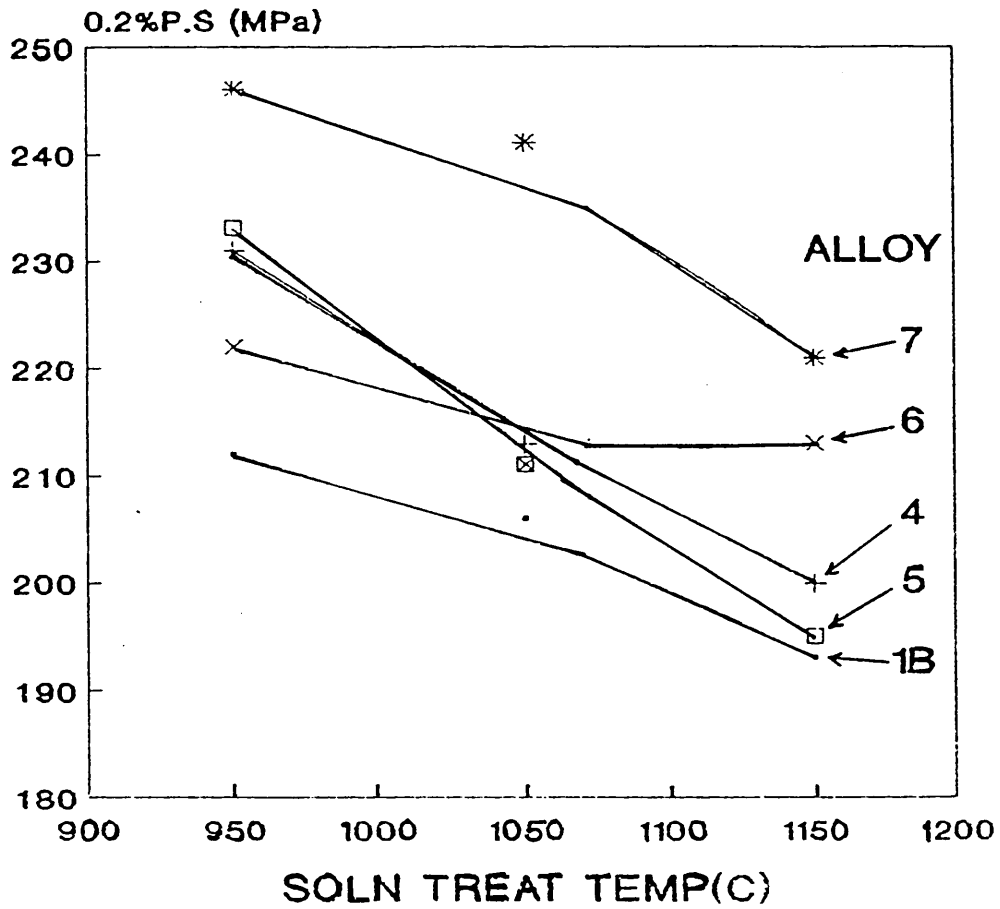
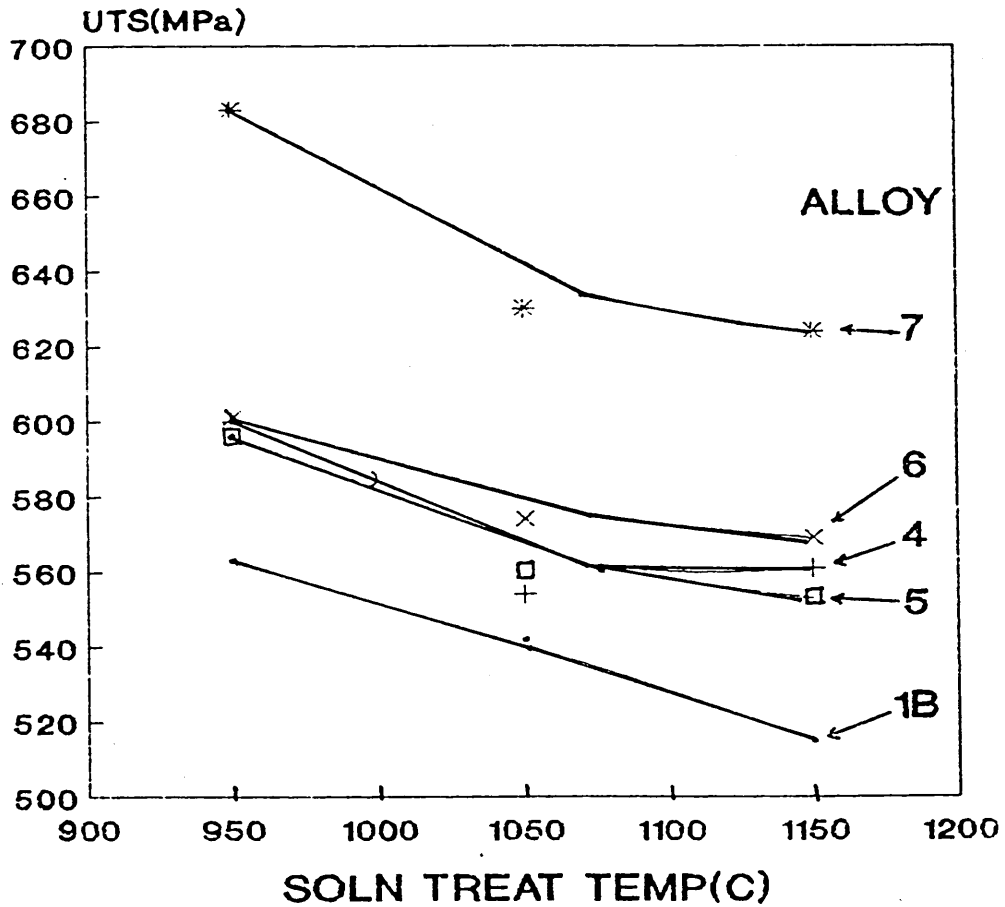


Figure 39 Effect of Solution Treatment Temperature on the 0.2% Proof Stress and UTS of Experimental Alloys



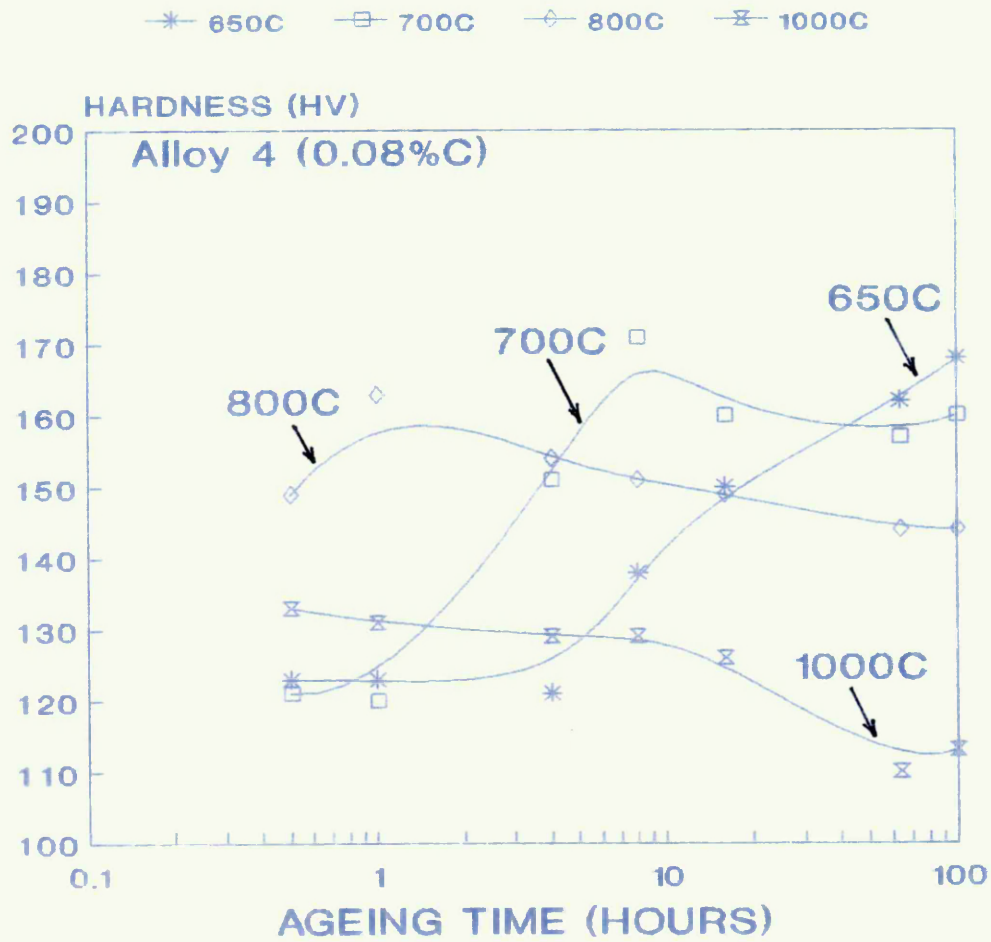


Figure 40 Effect of Thermal Ageing on the
Hardness of Series I Alloy 4

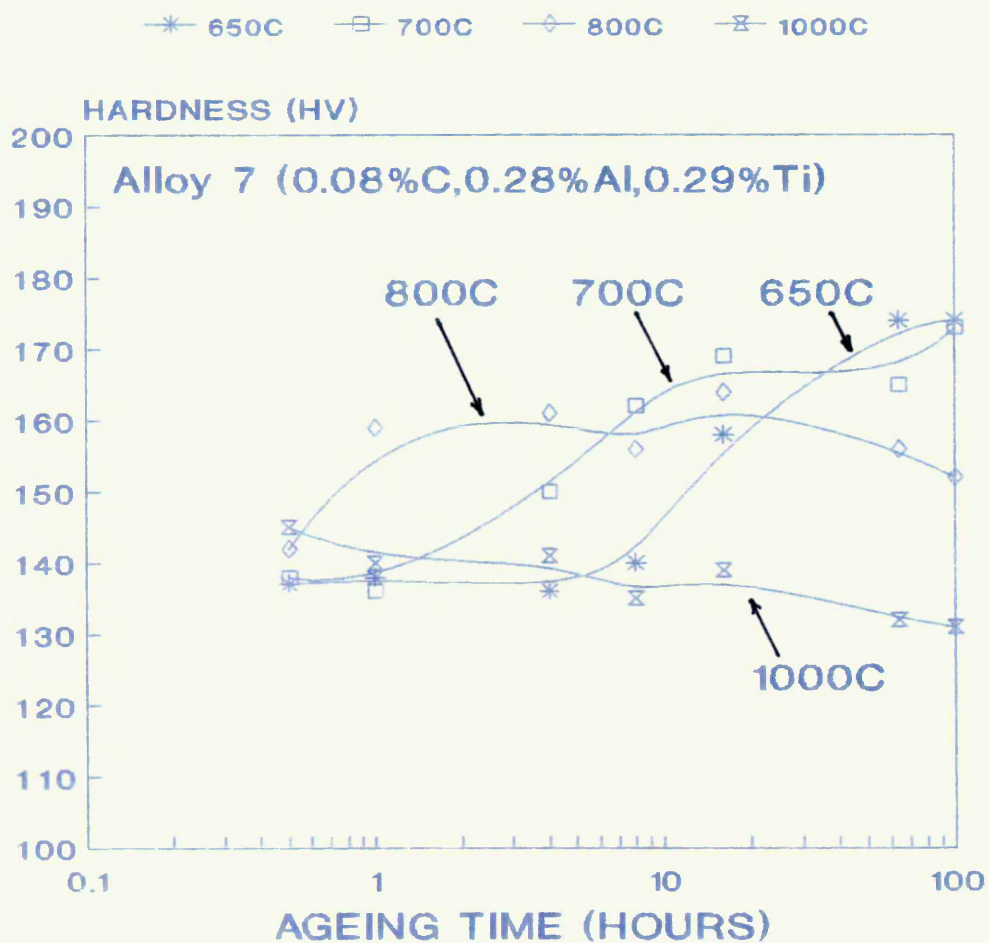
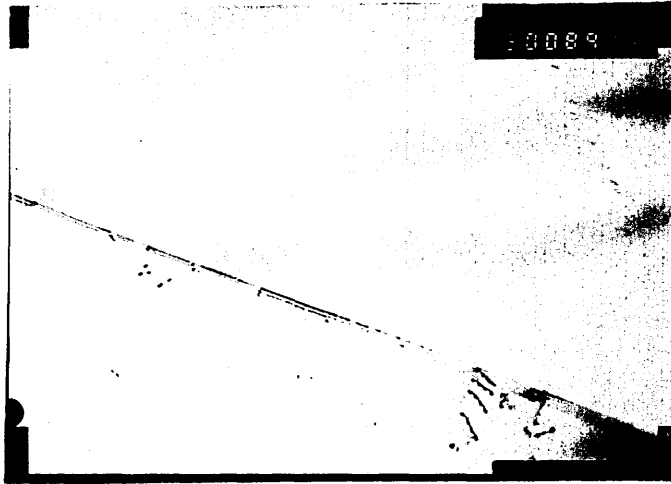


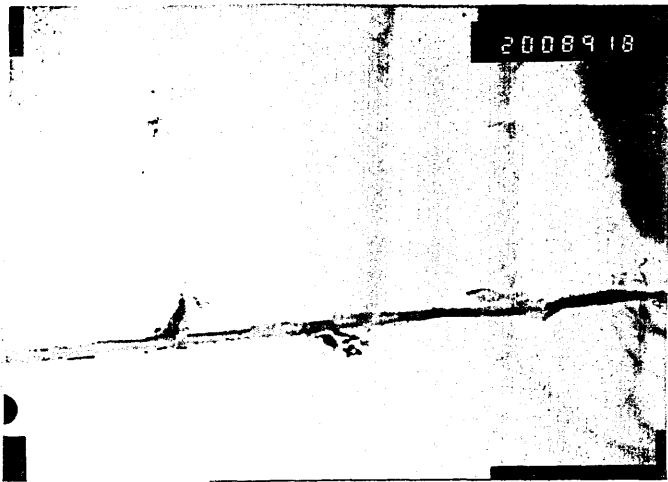
Figure 41 Effect of Thermal Ageing on the Hardness of Series II Alloy 7



1 μm

(a) Alloy 1B

Figure 42 Thin Foil Electron Micrographs of Series I
Alloys Solution Treated 1150°C, Water
Quenched



1 μm

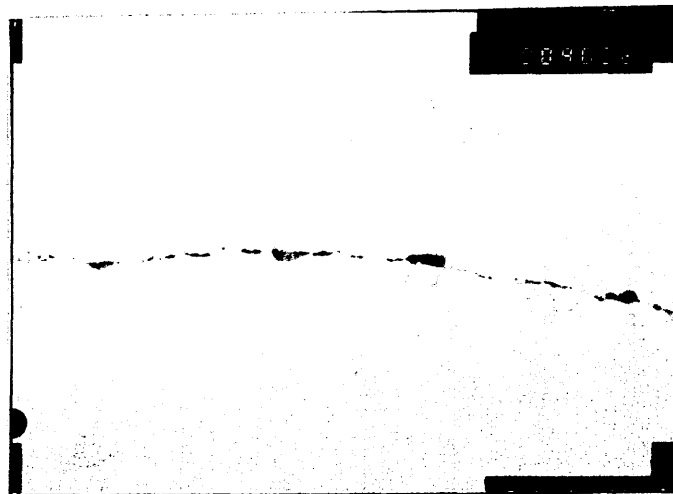
(b) Alloy 4



0.5 μ m

a) Alloy 1B, aged 650°C 1 hour. Onset of $M_{23}C_6$ precipitation on grain boundaries.

Figure 43 Thin Foil Electron Micrographs of Series I Alloys following Thermal Ageing



2 μ m

b) Alloy 4, aged 650°C 30 minutes. Onset of $M_{23}C_6$ precipitation on grain boundaries.



2 μ m

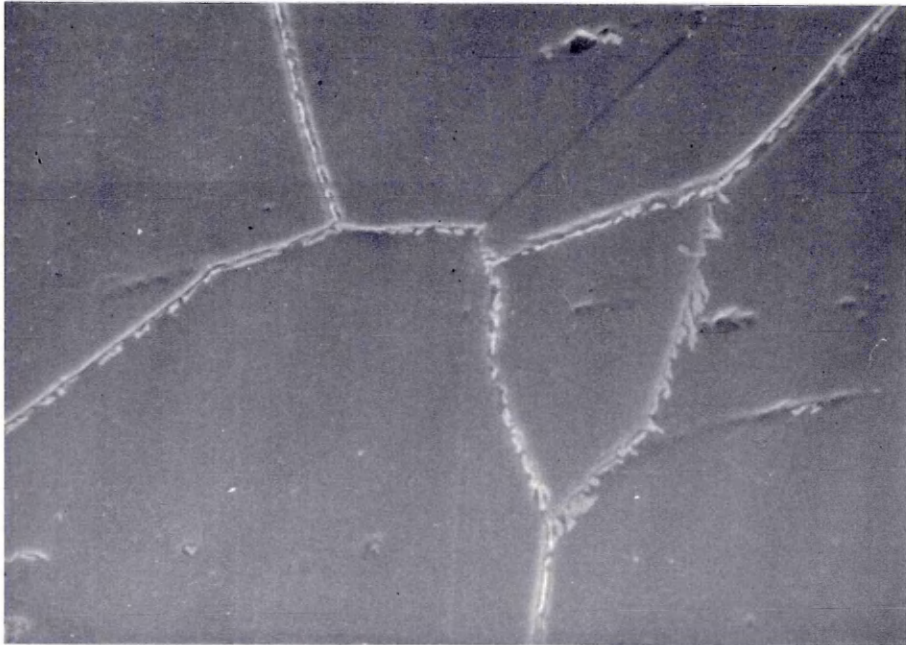
a) Alloy 1B, aged 650°C 16 hours. Growth of discrete grain boundary carbides.

Figure 44 Thin Foil Electromicrographs of Thermally Aged Series I Alloy 1B.



0.4 μ m

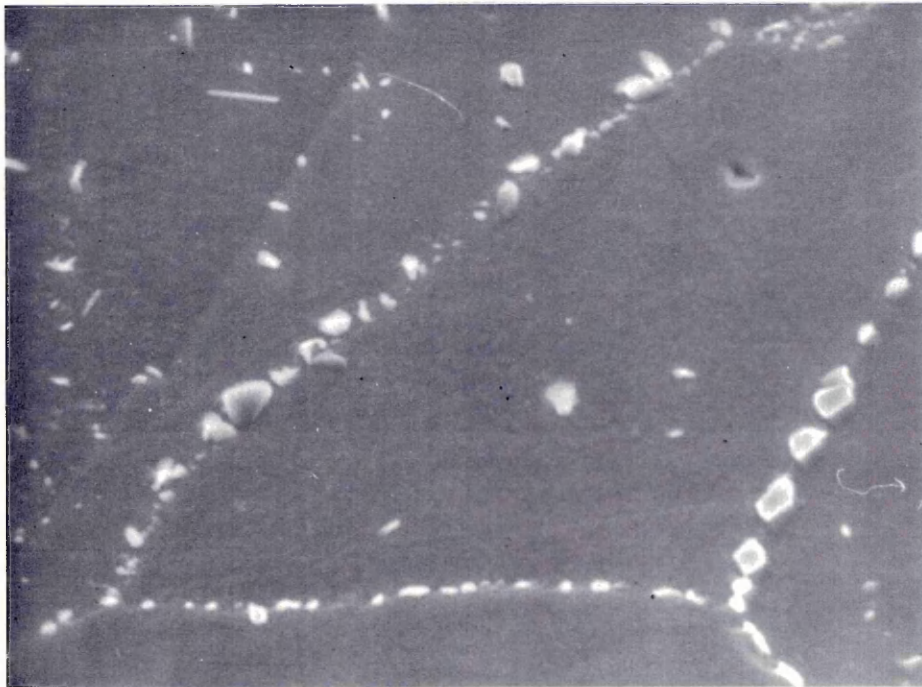
b) Alloy 1B, aged 700°C 4 hours.
Precipitation of 'rod like' grain boundary and discrete intragranular carbides



1 hr
700°C
(a)

1 μm

Figure 45 Effect of Thermal Ageing at 700°C On Carbide Precipitation in Alloy 4



100 hrs
700°C
(b)

1 μm



1 μm



0.25 μm



0.25 μm

Figure 46 Thin Foil Electron Micrographs for Series I
Alloy 4. Aged 650°C 100 hours.

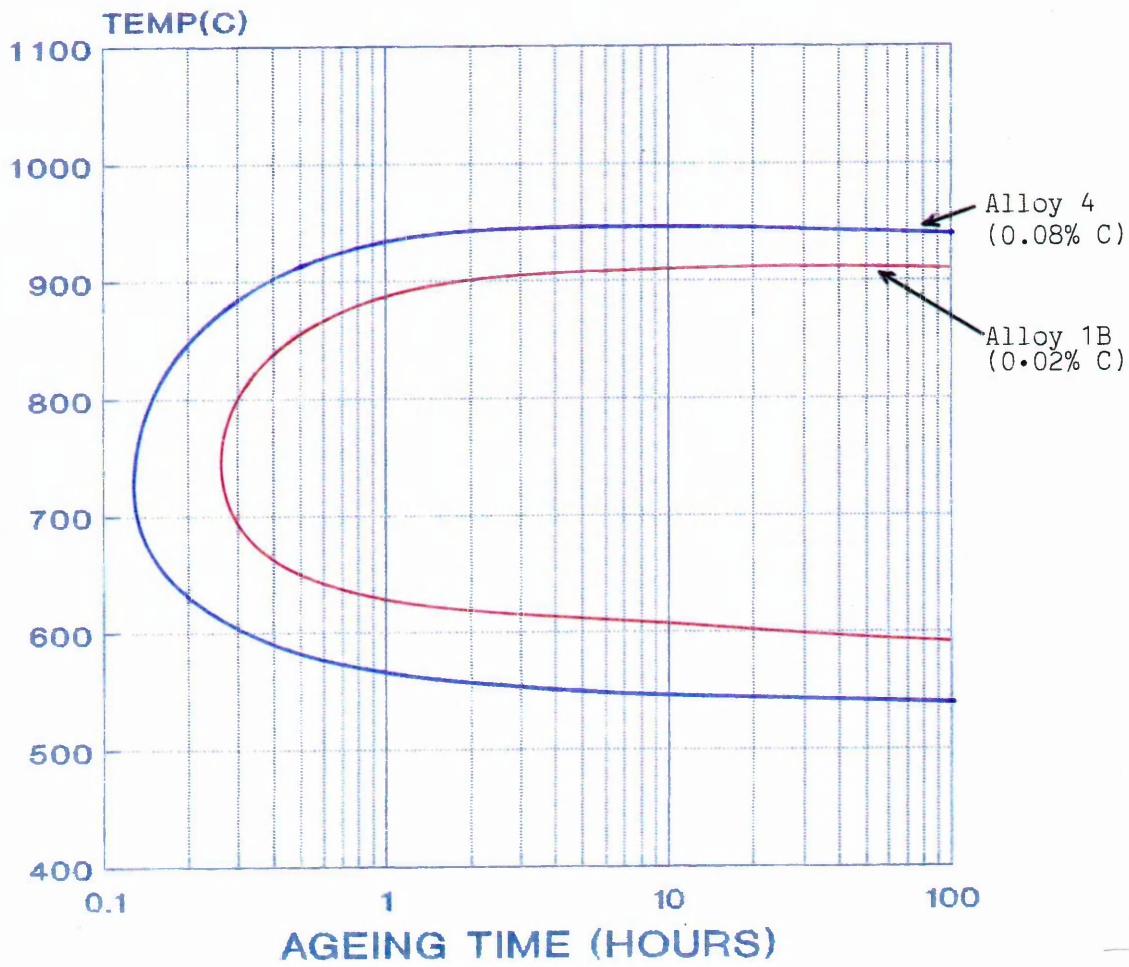
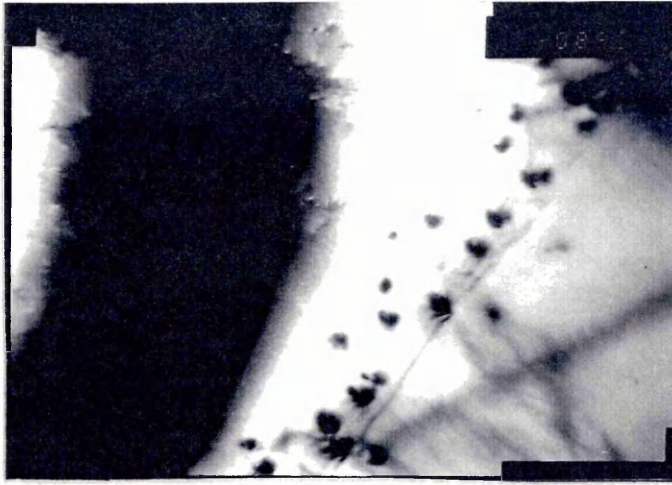


Figure 47 Series I Alloys : Precipitation C-Curves for 0% (Onset) of precipitation



0.5 μ m
Alloy 2682



0.25 μ m
Alloy 2697



1 μ m
Alloy 7

Figure 48 Thin Foil Electron Micrographs of Series II alloys solution treated 1150°C, water quenched

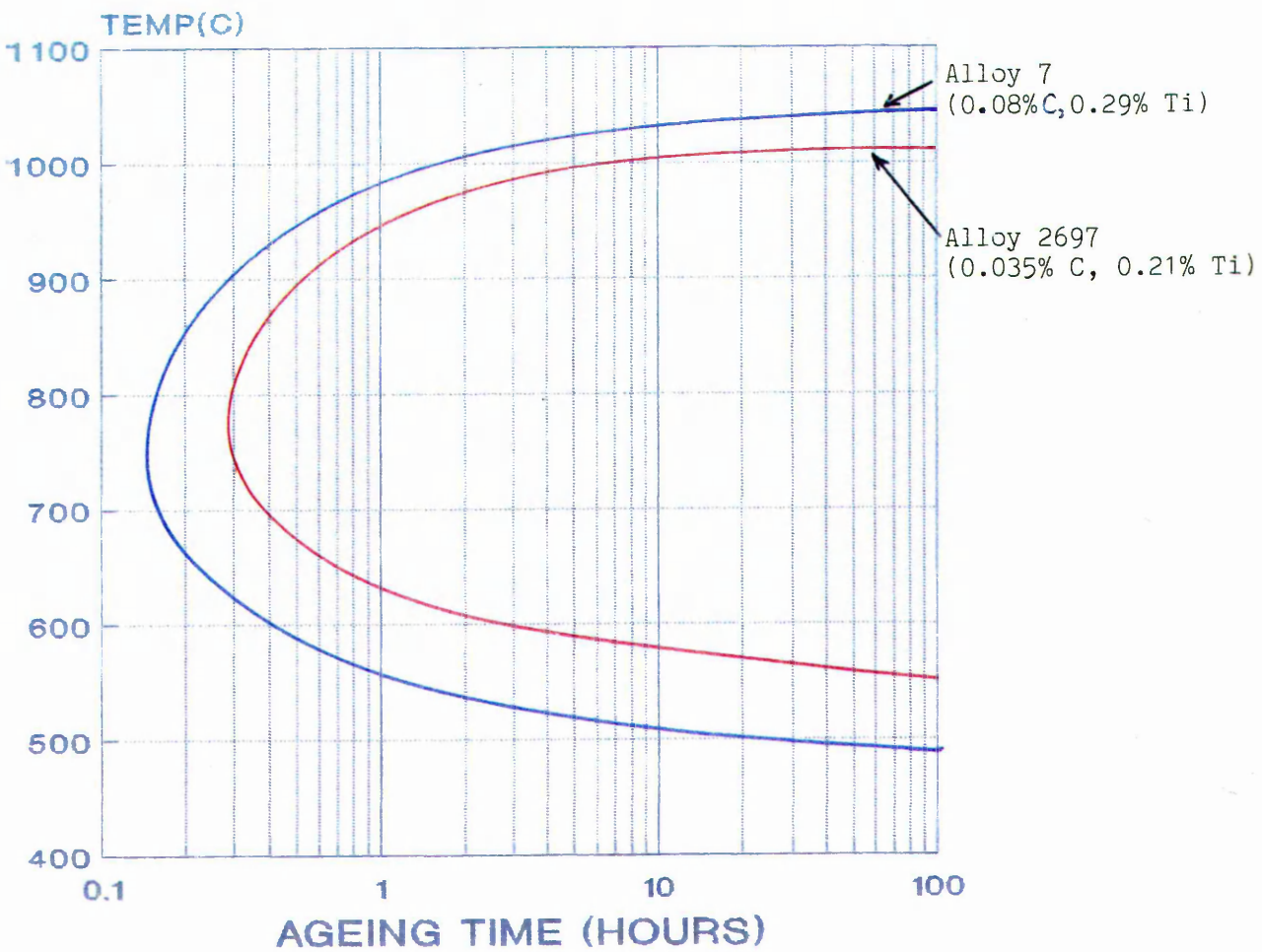


Figure 49

Series II Alloys : Precipitation
C-Curves are For 0% (Onset) of
Precipitation



0.25 μ m



0.25 μ m

Figure 50 Thin Foil Electron Micrographs for Series II alloy 7. Aged 650°C 100 hours.

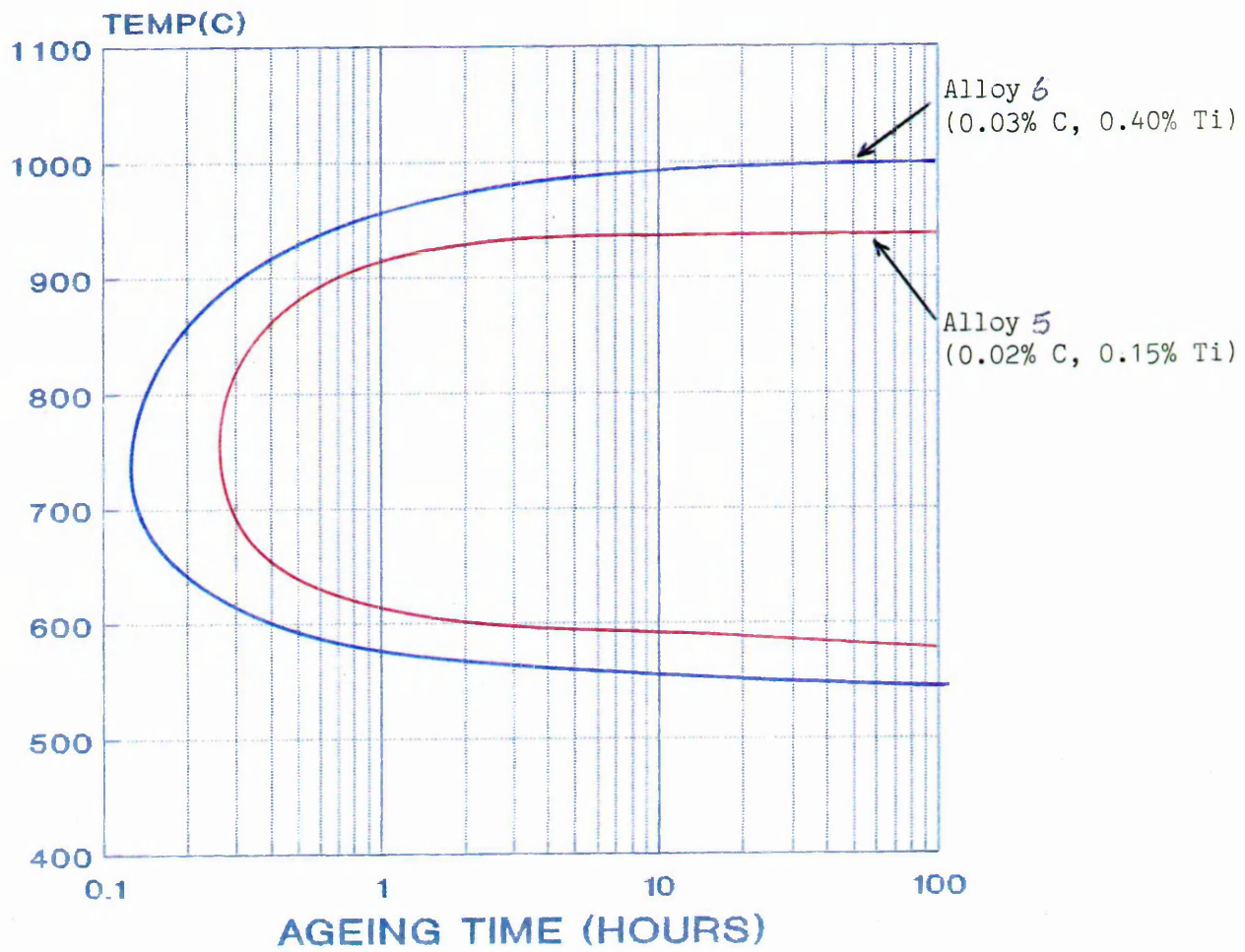
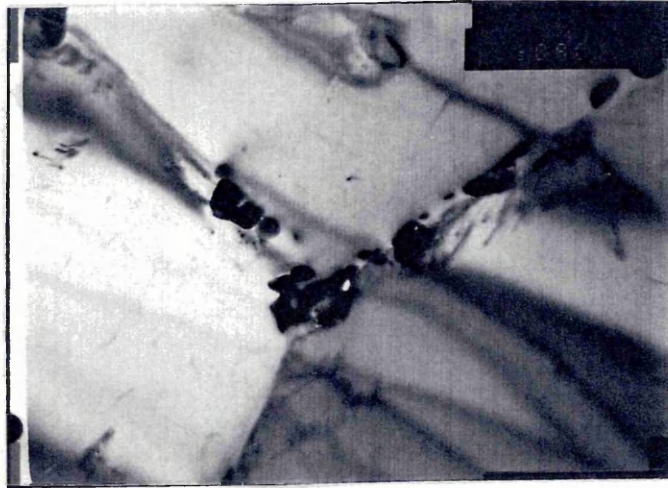
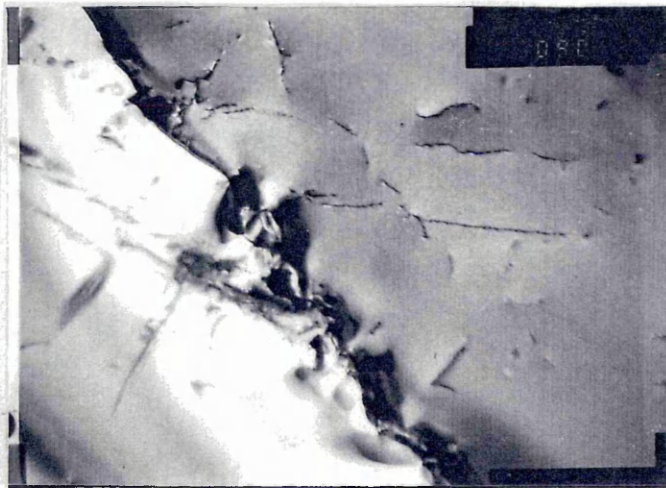


Figure 51 Series III Alloys : Precipitation
 C-Curves for 0% (Onset) of
 Precipitation

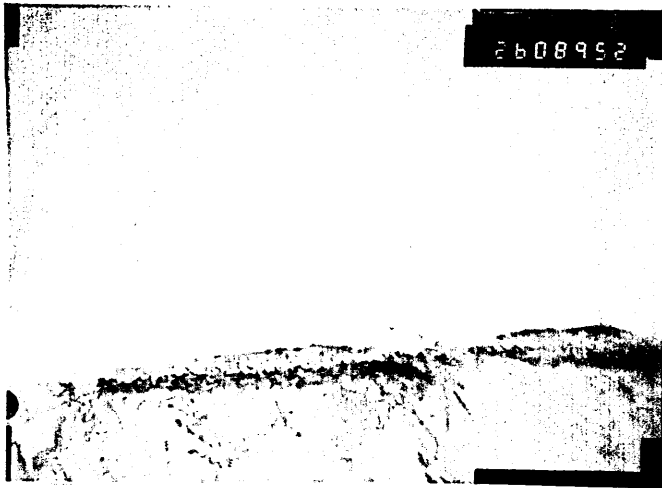


1μm

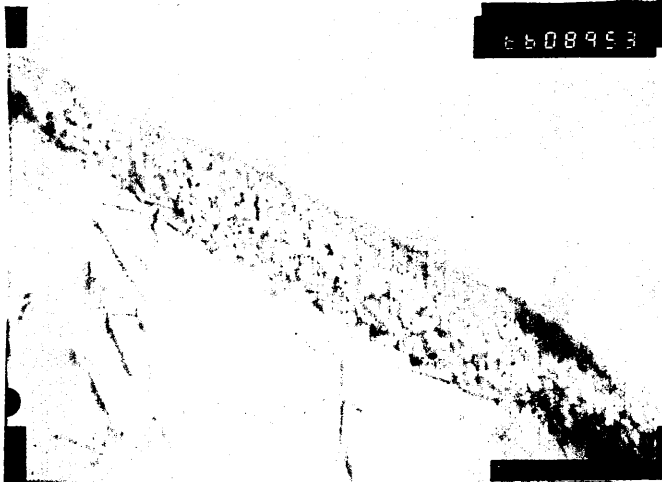


1μm

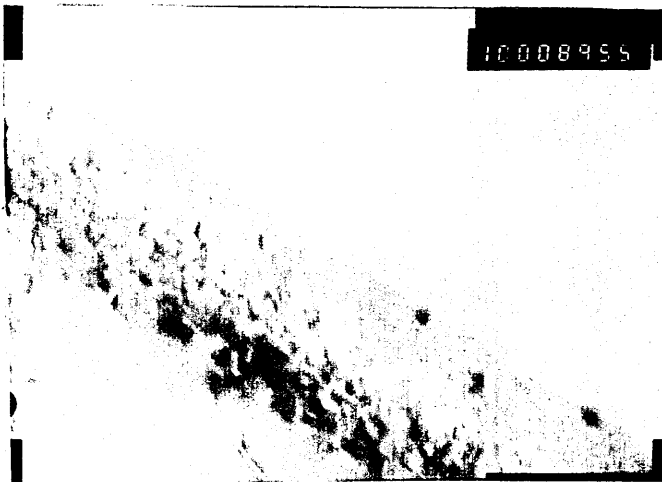
Figure 52 Thin Foil Electron Micrographs for Series III alloy 5. Aged 600°C 64 hours.



0.5 μ m



0.25 μ m



0.125 μ m

Figure 53 Thin Foil Electron Micrographs for Series III alloy 6. Aged 600°C 64 hours.

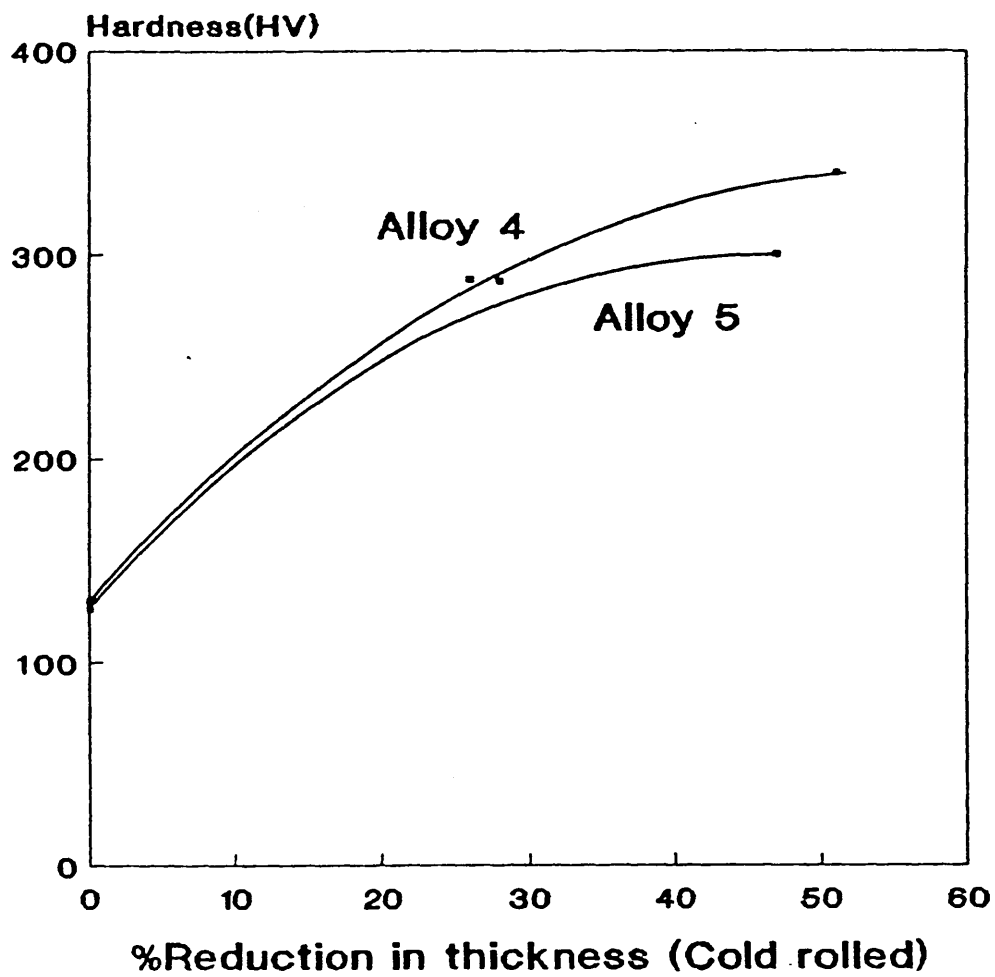


Figure 54 Effect of Cold Rolling on the Hardness of Alloys 4 And 5

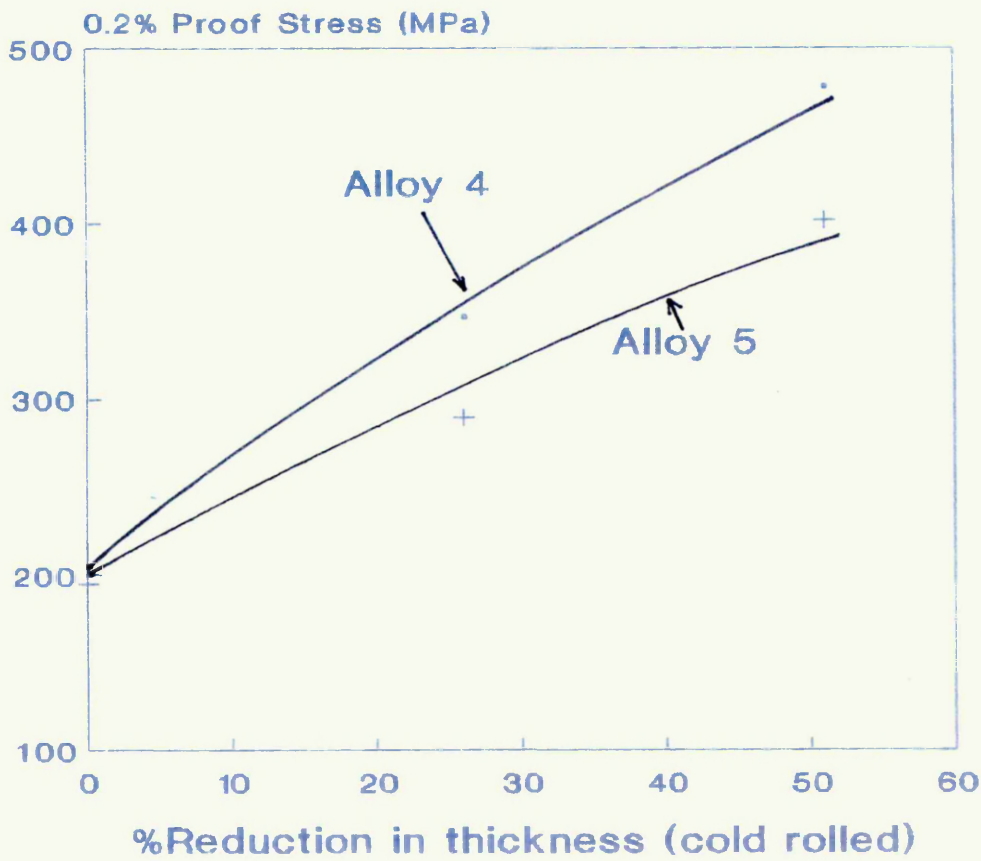
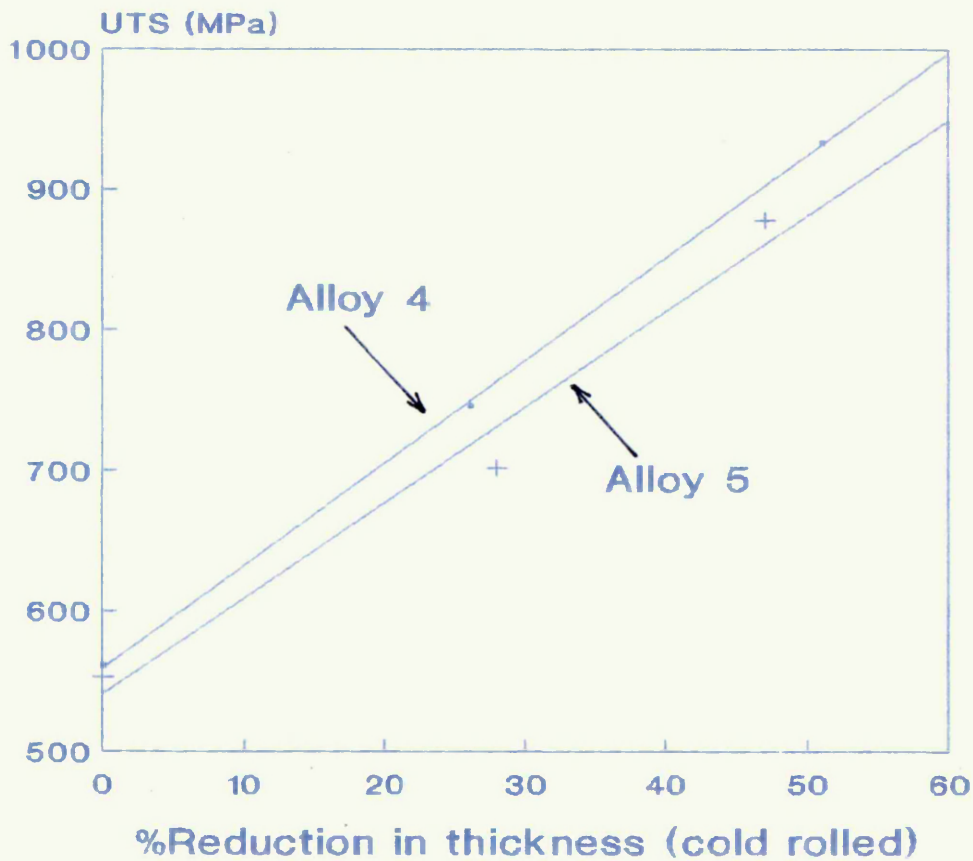


Figure 55 Effect of Cold Rolling on 0.2% Proof Stress and UTS of Alloys 4 and 5



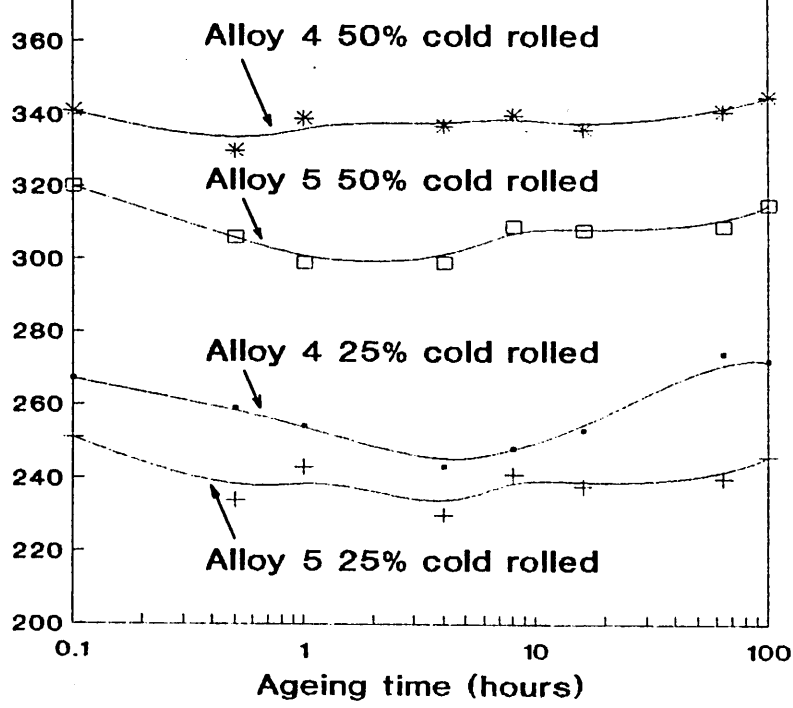


Figure 56 Effect of Ageing at 500°C on Cold Rolled Alloys 4 and 5

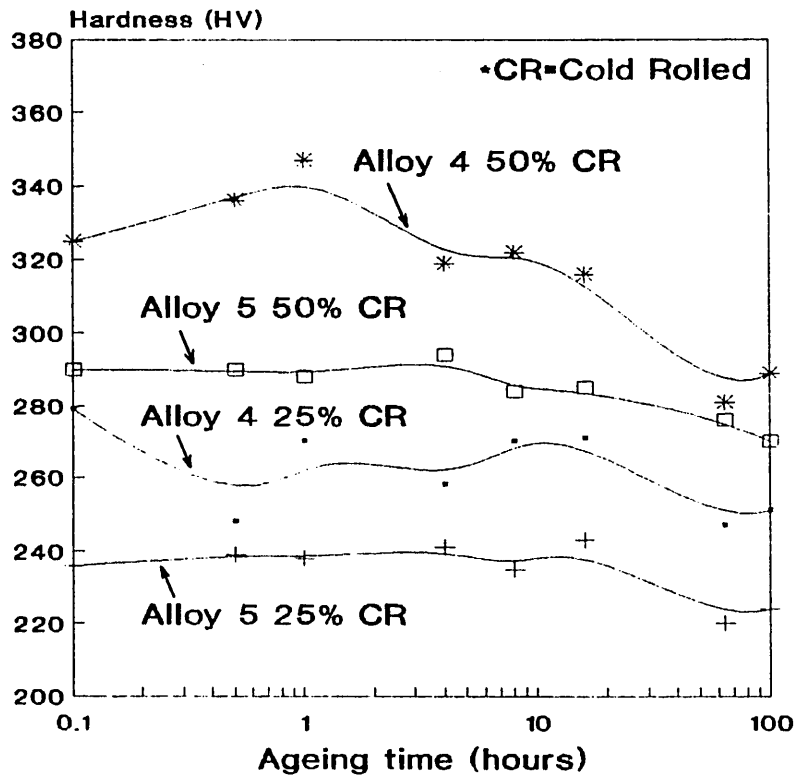


Figure 57 Effect of Ageing at 600°C on Cold Rolled Alloys 4 And 5

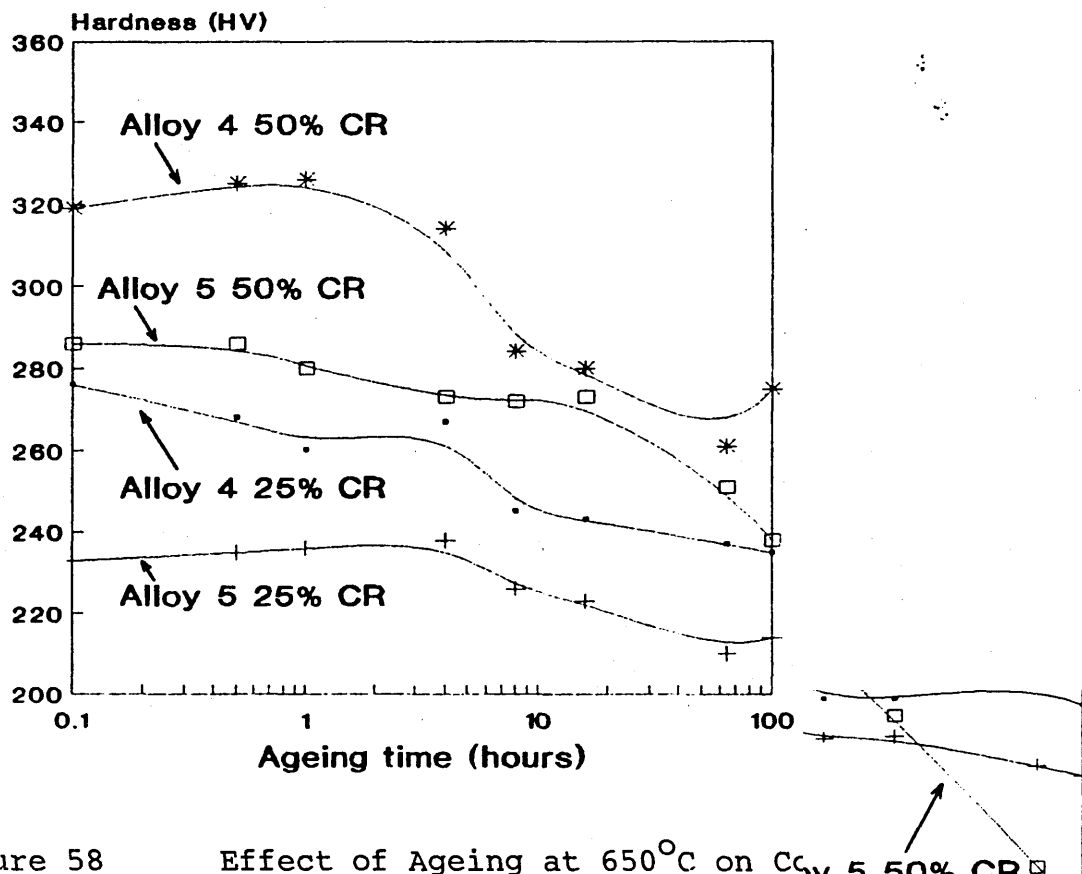


Figure 58 Effect of Ageing at 650°C on Cold Rolled Alloys 4 and 5

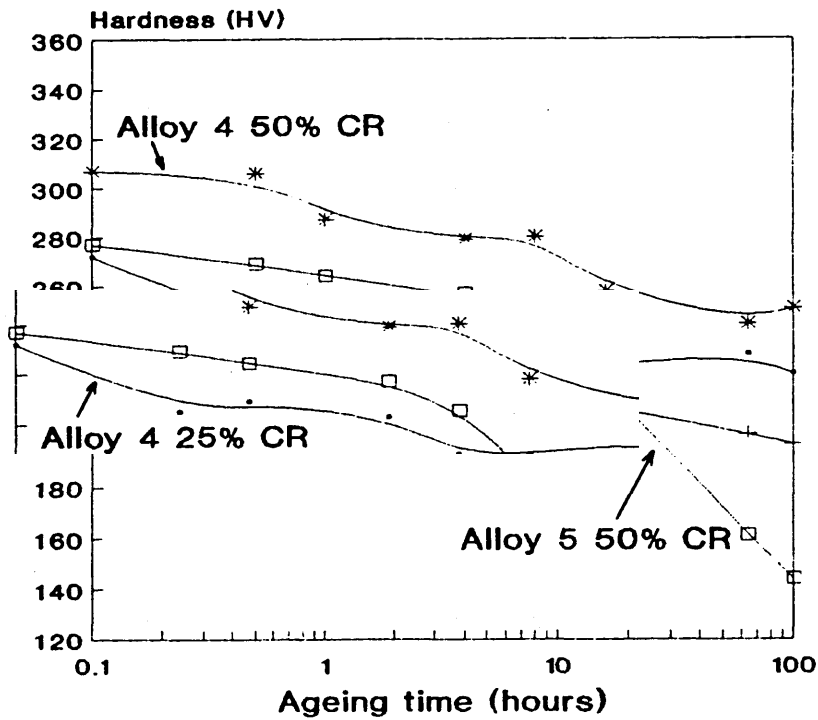


Figure 59 Effect of Ageing at 700°C on Cold Rolled Alloys 4 and 5

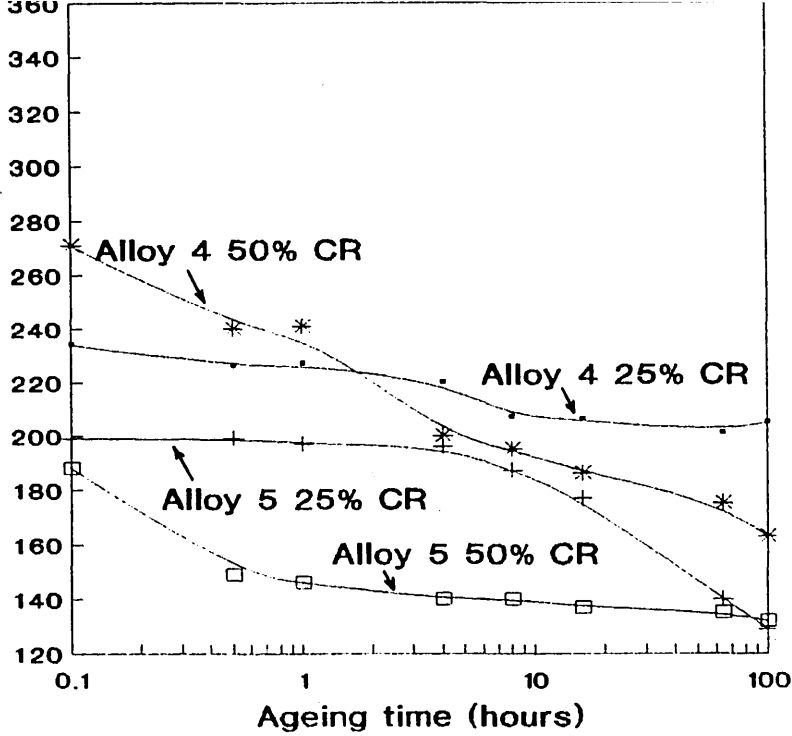


Figure 60 Effect of Ageing at 800°C Cold Rolled Alloys 4 and 5

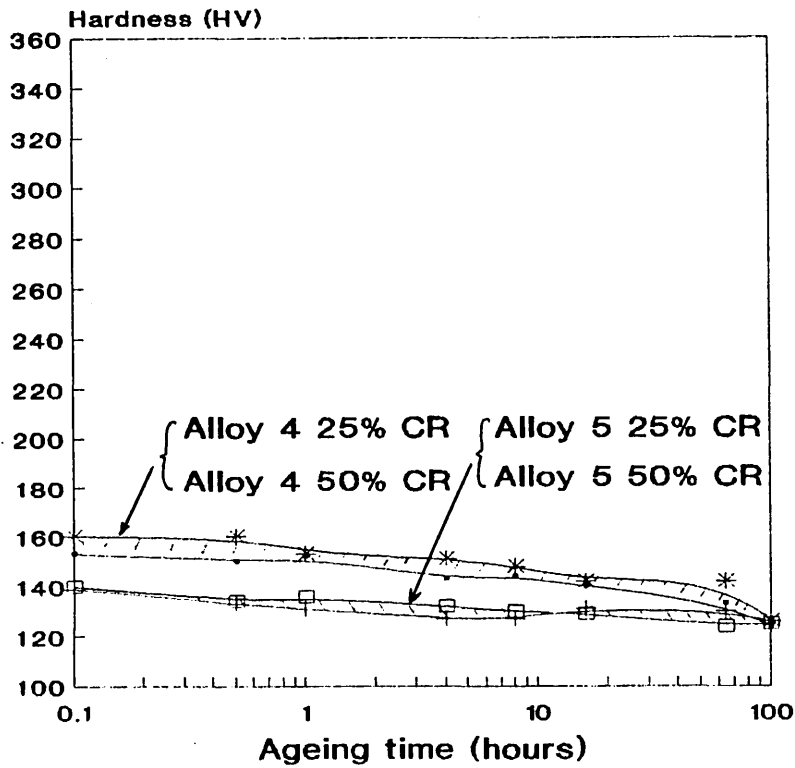
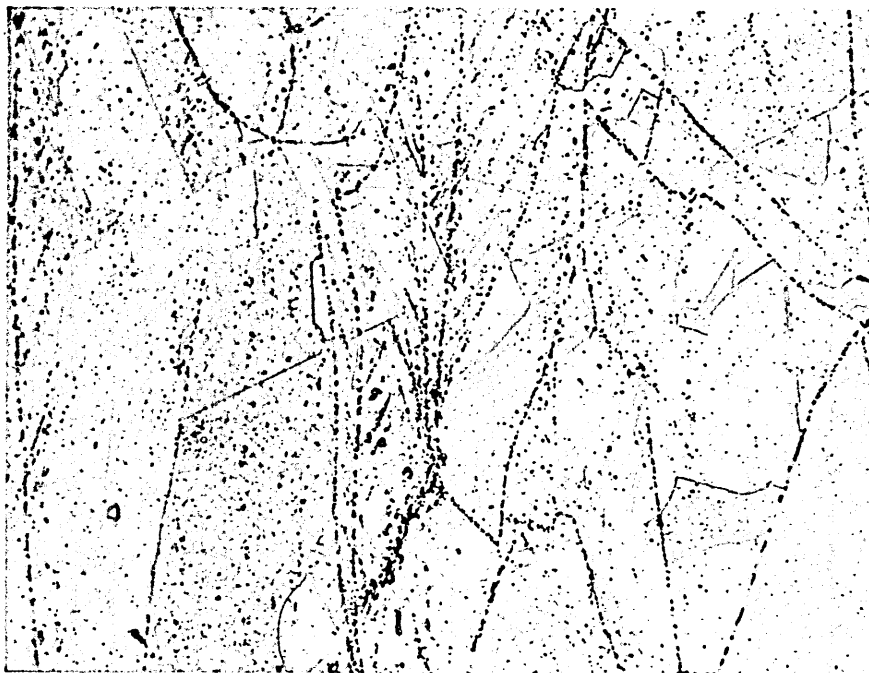


Figure 61 Effect Of Ageing At 900°C On Cold Rolled Alloys 4 And 5



x400

Figure 62

Photomicrograph typical of alloys 4 and 5 showing presence of precipitates on 'ghost' deformed grain boundaries. Material condition is fully recrystallised following ageing at 700°C for 64 hours.

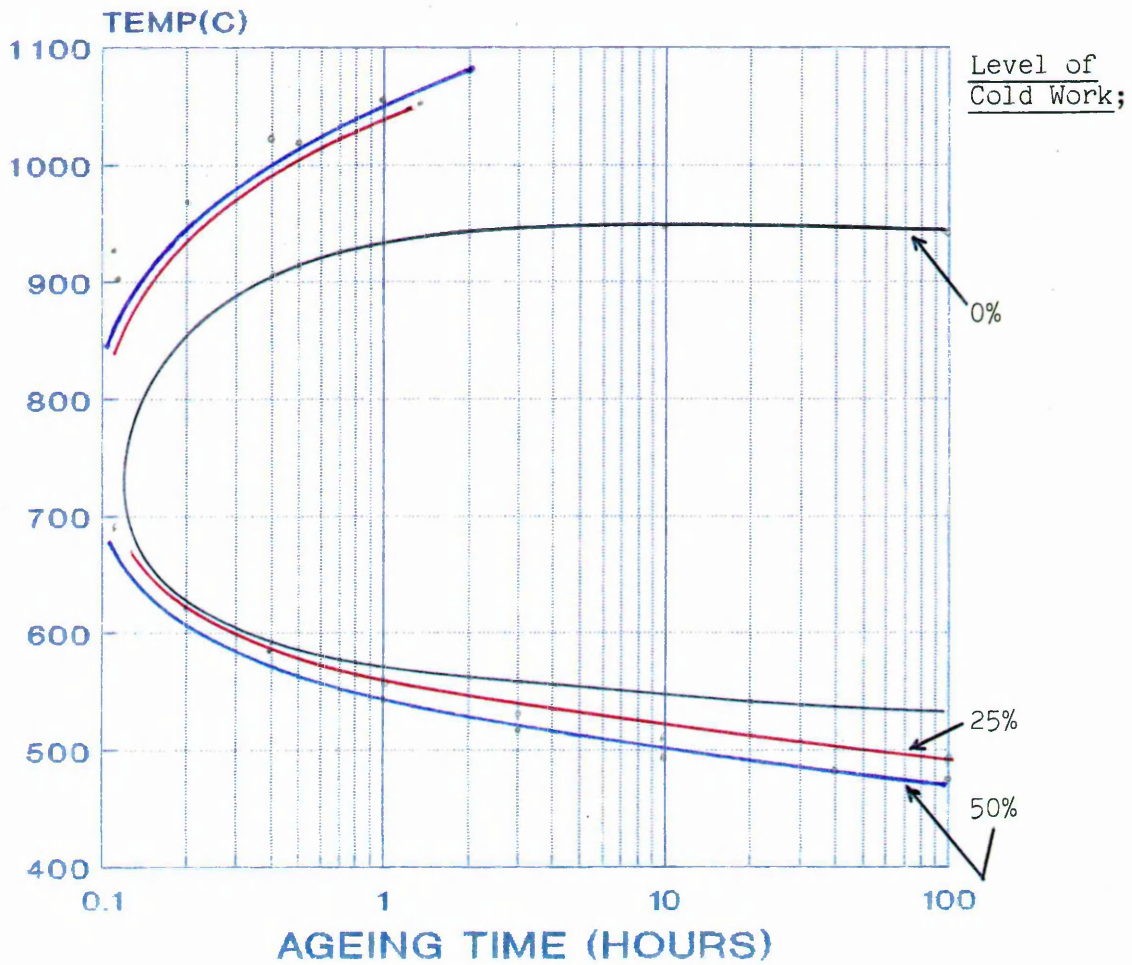


Figure 63

Precipitation C-Curves for Alloy 4
 Cold Rolled and Aged condition.
 Curves are for 0% (Onset) of
 Precipitation

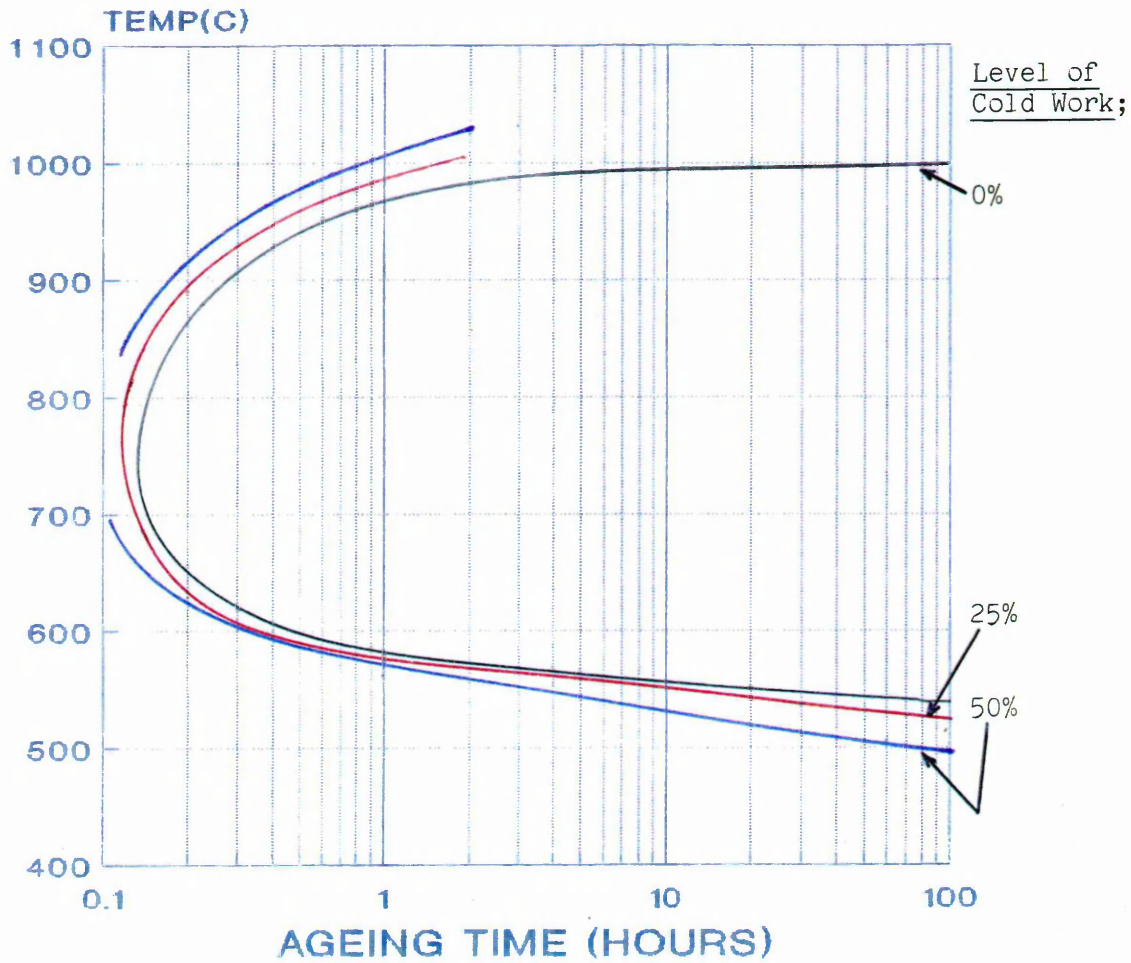


Figure 64 Precipitation C-Curve for Alloy 5 in Cold Rolled and Aged condition. Curves are for 0% (Onset) of Precipitation.

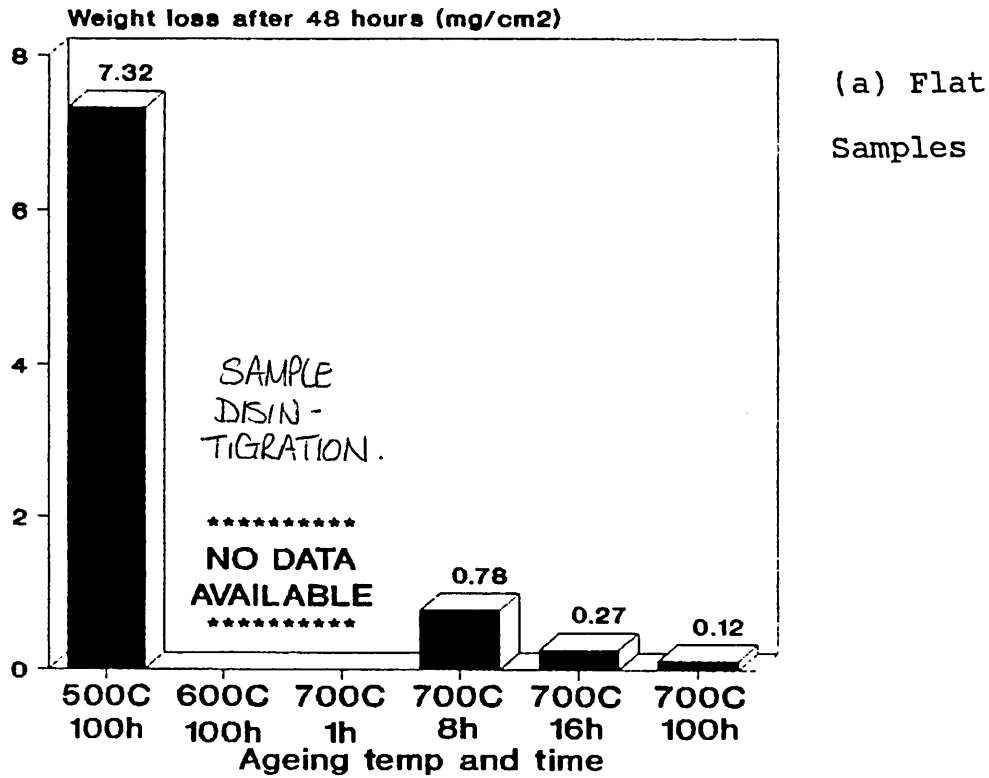
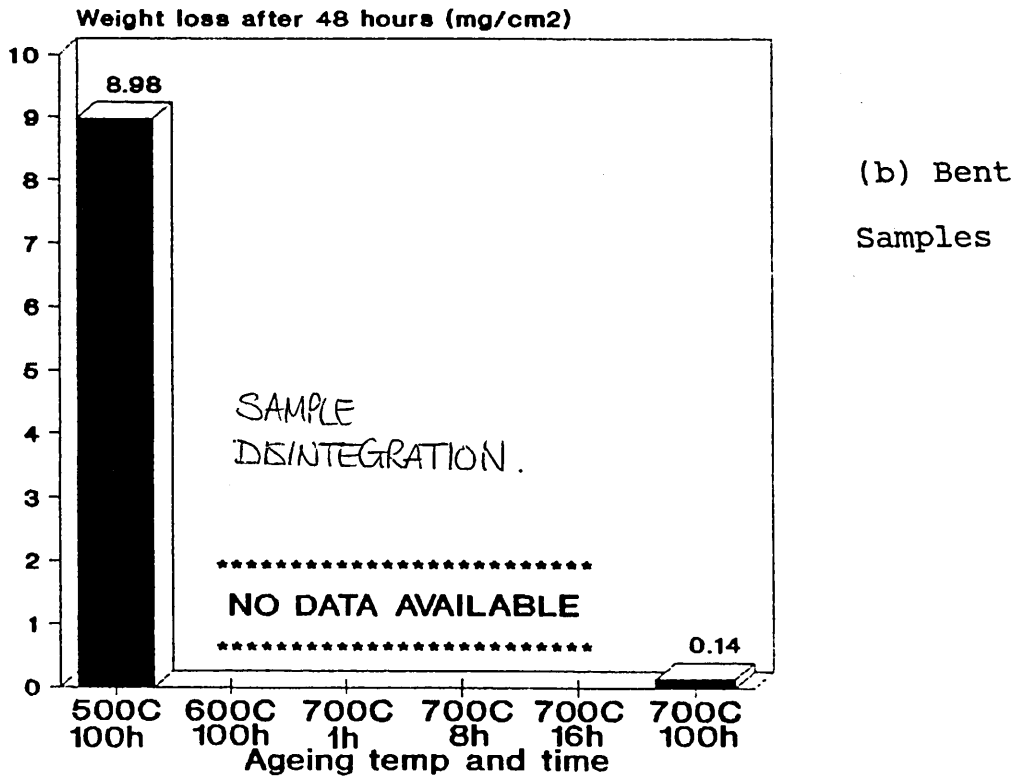


Figure 65 Effect of Thermal Ageing and Local Deformation on the Huey Test Weight Loss of Alloy 4



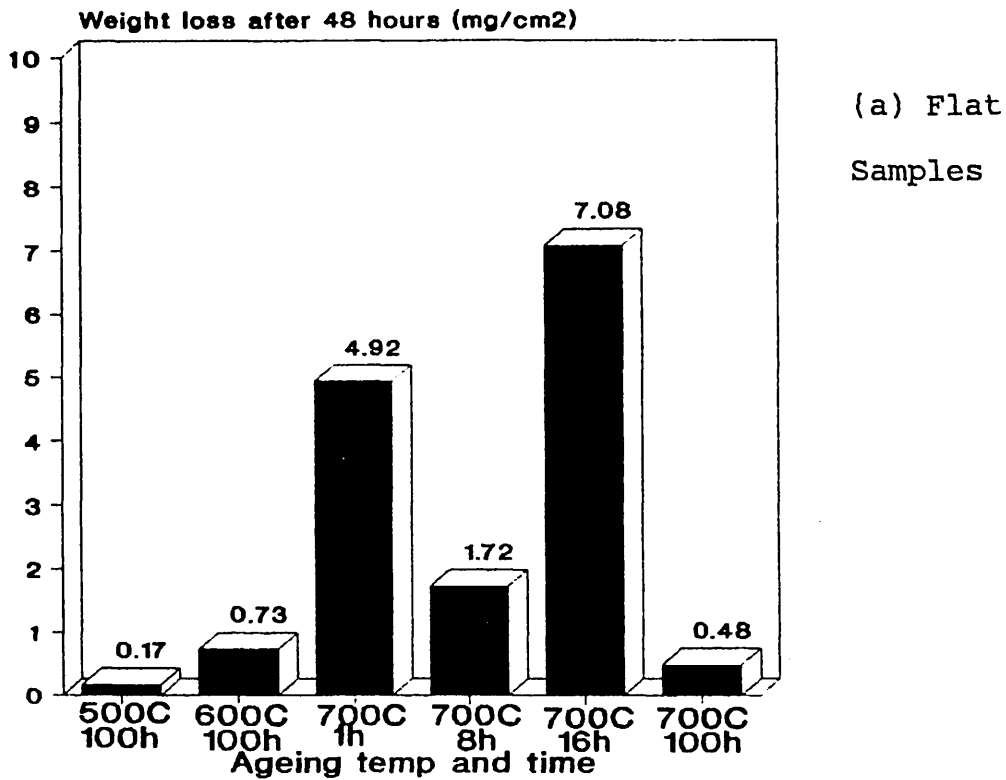
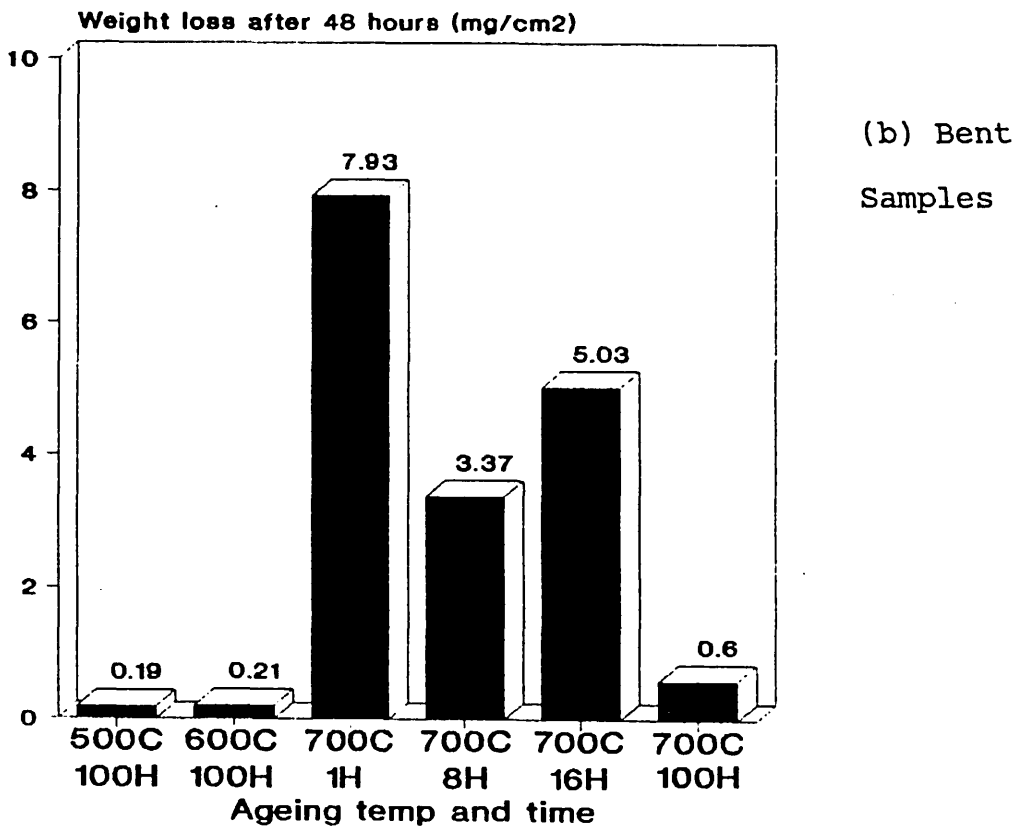


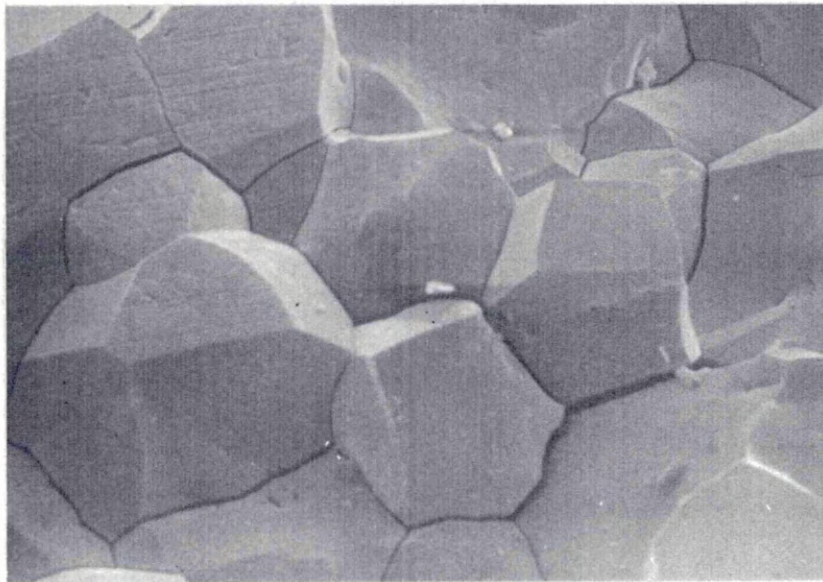
Figure 66 Effect of Thermal Ageing and Local Deformation on The Huey Test Weight Loss Of Alloy 5





x 104

Figure 67 Alloy 4 Aged 500°C 100 hours. Corrosion Crack in deformed region of bent sample following testing for 1 x 48 Hours.



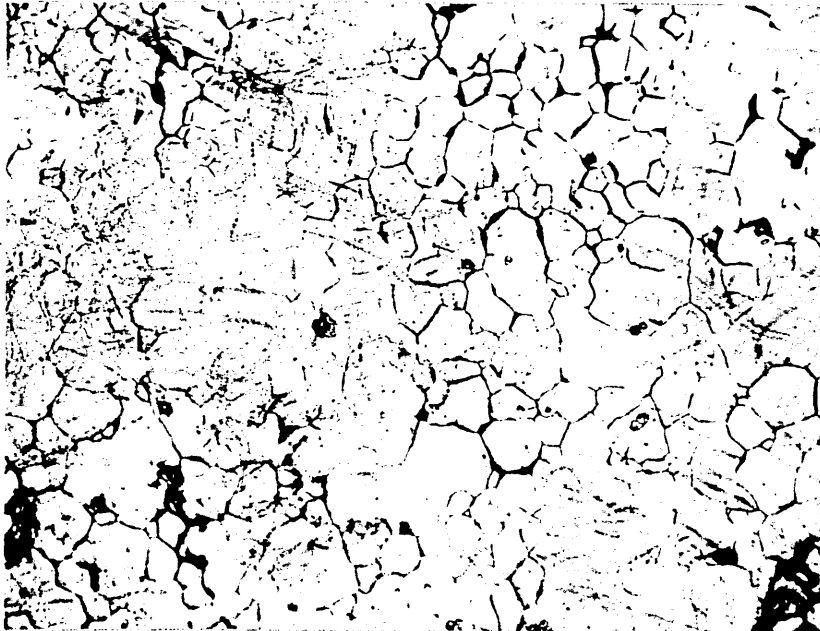
x800

Figure 68 Alloy 4 Aged 500°C 100 Hours. IGC evident in flat sample following testing for 1 x 48 Hours.



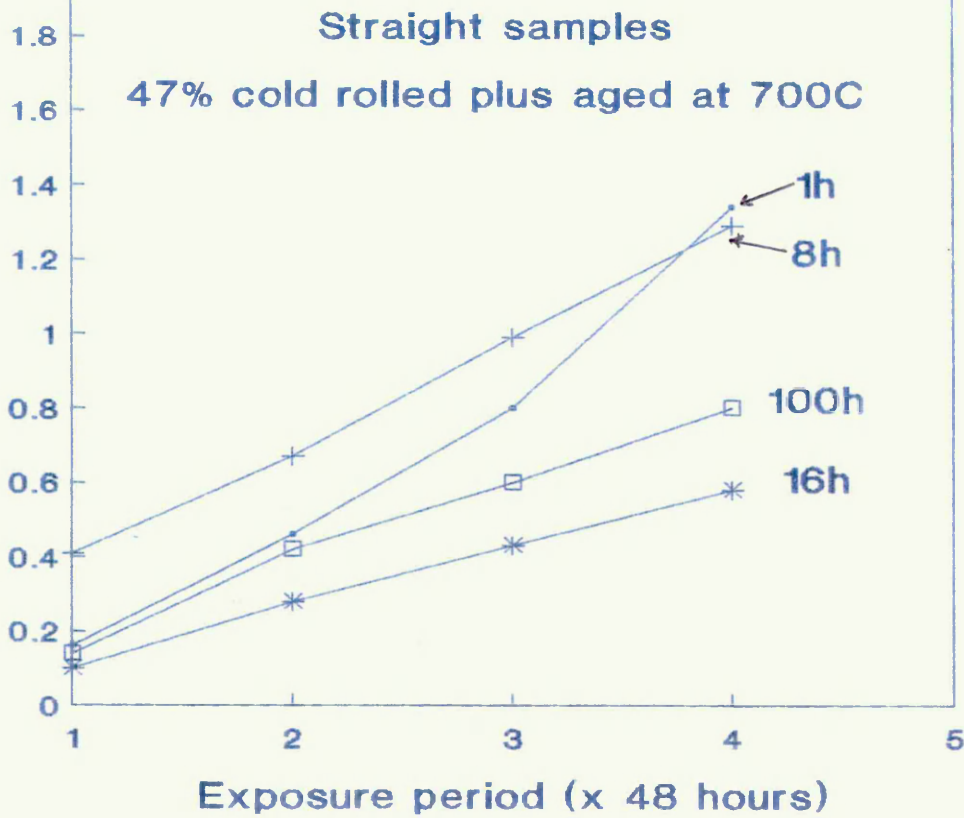
x 140

Figure 69 Alloy 5 Aged 500°C 100 Hours. Localised 'Finger' of Corrosion in flat sample following exposure for 1 x 48 hours



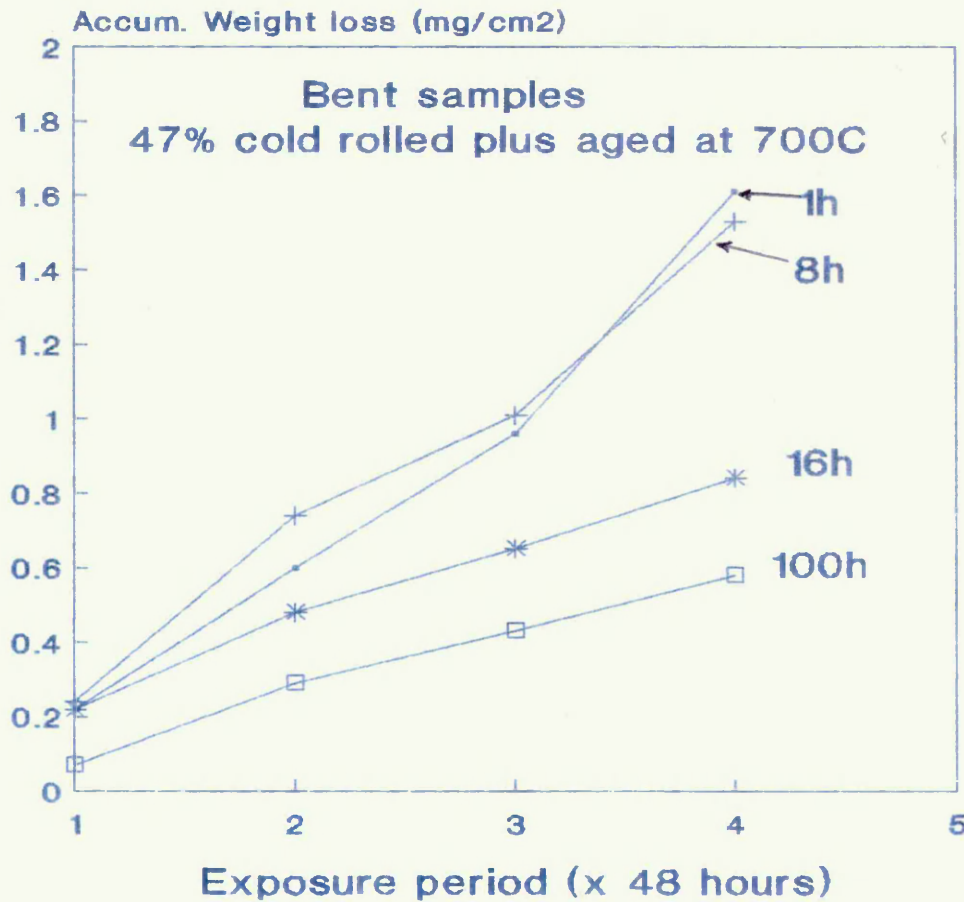
x 140

Figure 70 Alloy 5 Aged 500°C 100 hours. IGC in deformed region of bent sample following exposure for 1 x 48 hours.

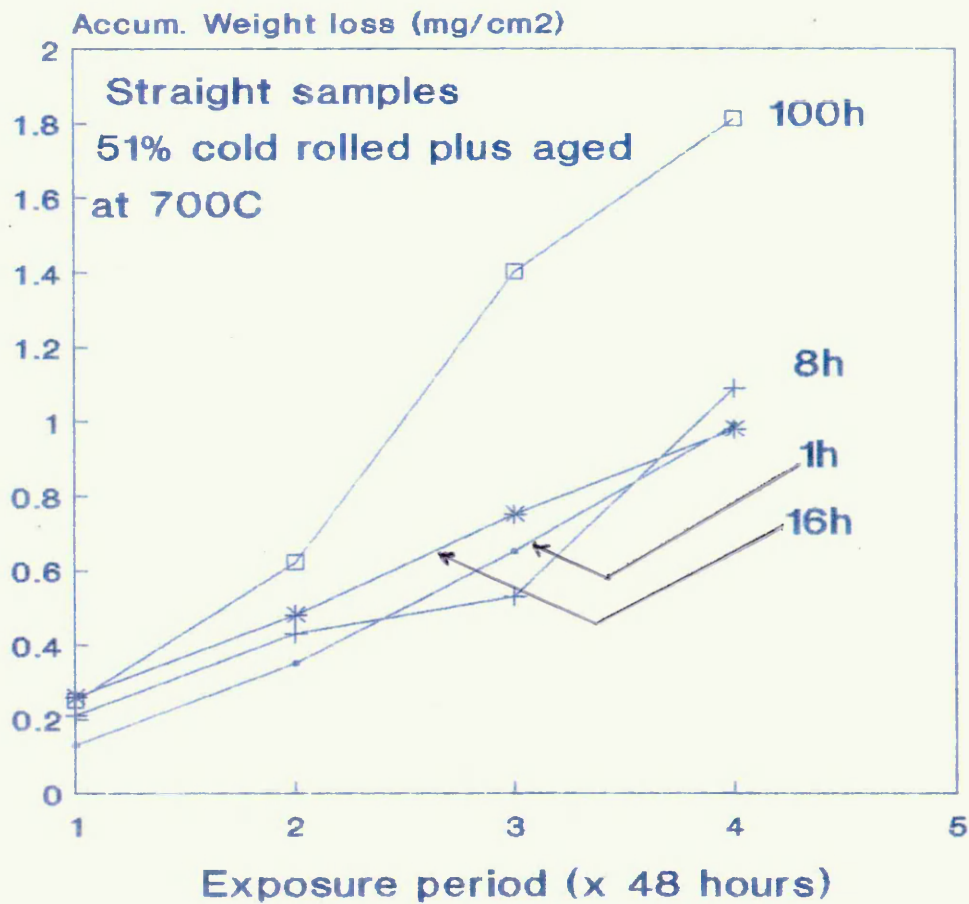


a)
Straight
Samples

Figure 71 Effect of Thermal Ageing and local deformation on Huey Weight Loss of cold worked Alloy 4.

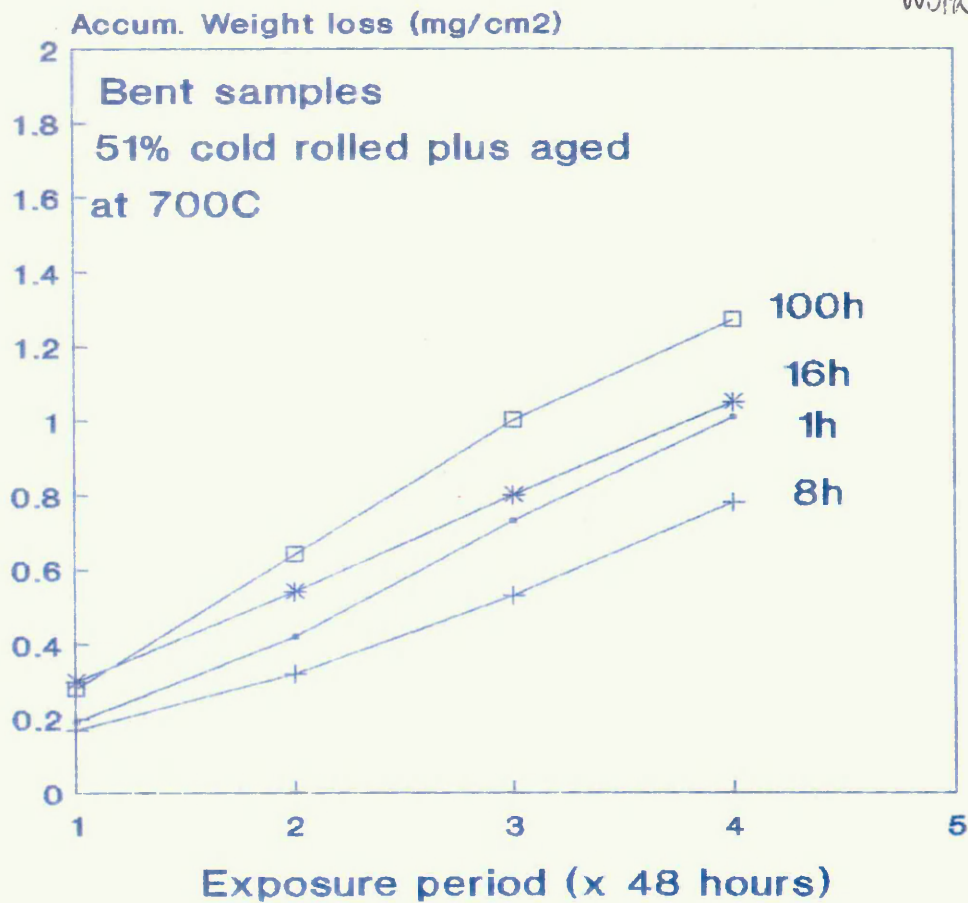


b) Bent
Samples



a)
Straight
Samples

Figure 72 Effect of Thermal Ageing and local deformation on Huey Weight Loss of cold Worked Alloy 5.



b) Bent
Samples

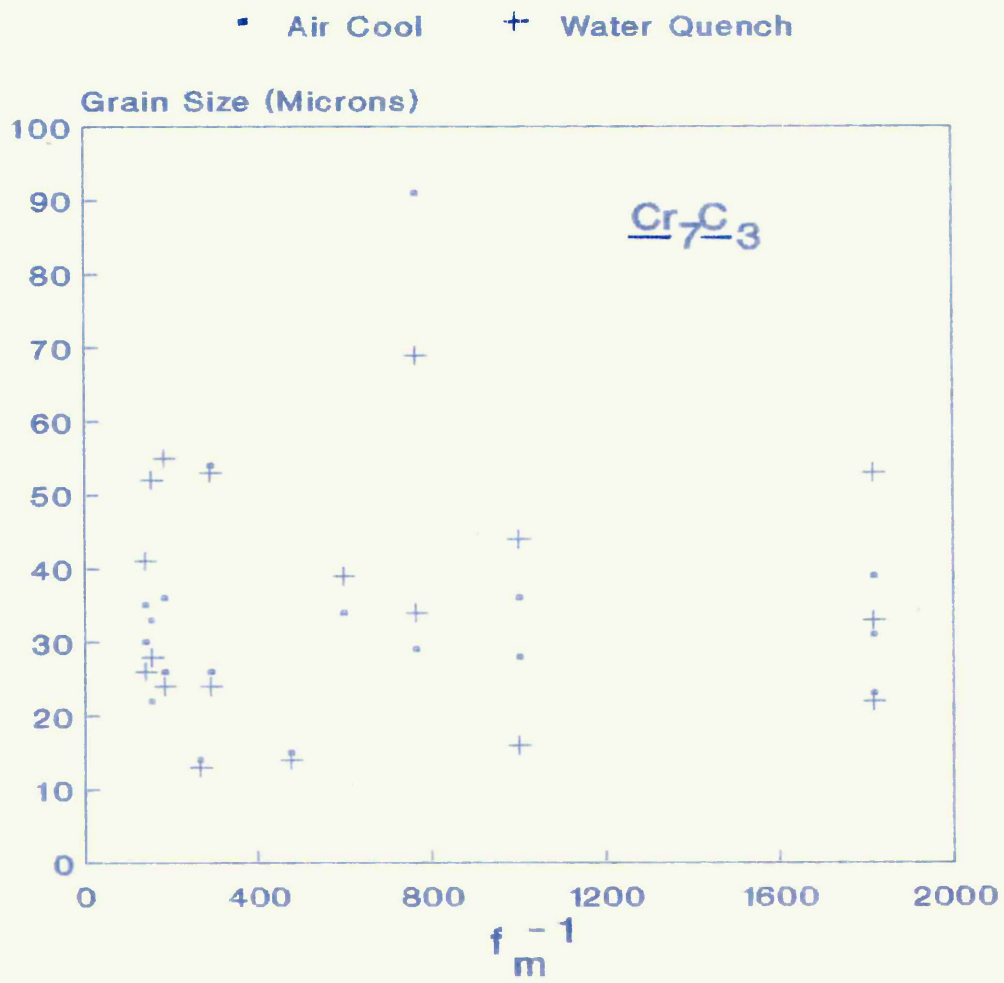


Figure 73 Effect of reciprocal of chromium carbide mass fraction on grain size

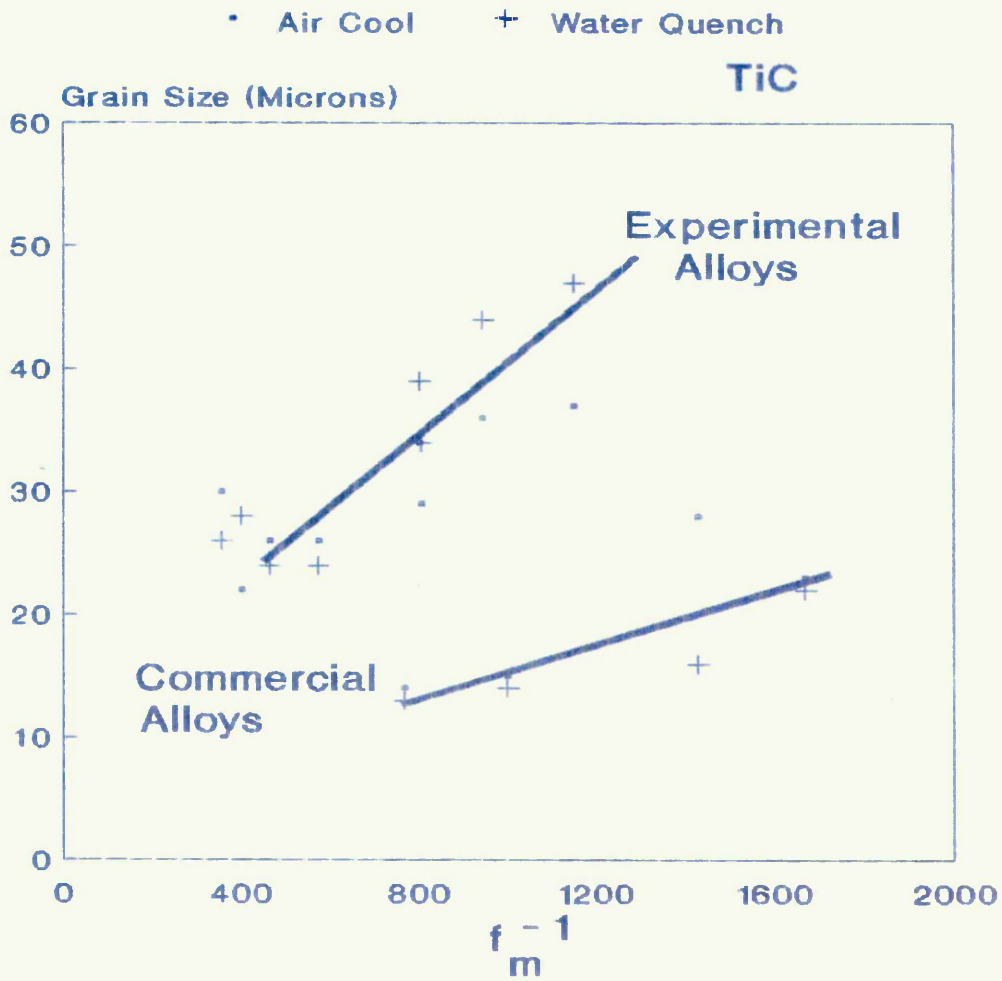


Figure 74 Effect of reciprocal of titanium carbide mass fraction on grain size

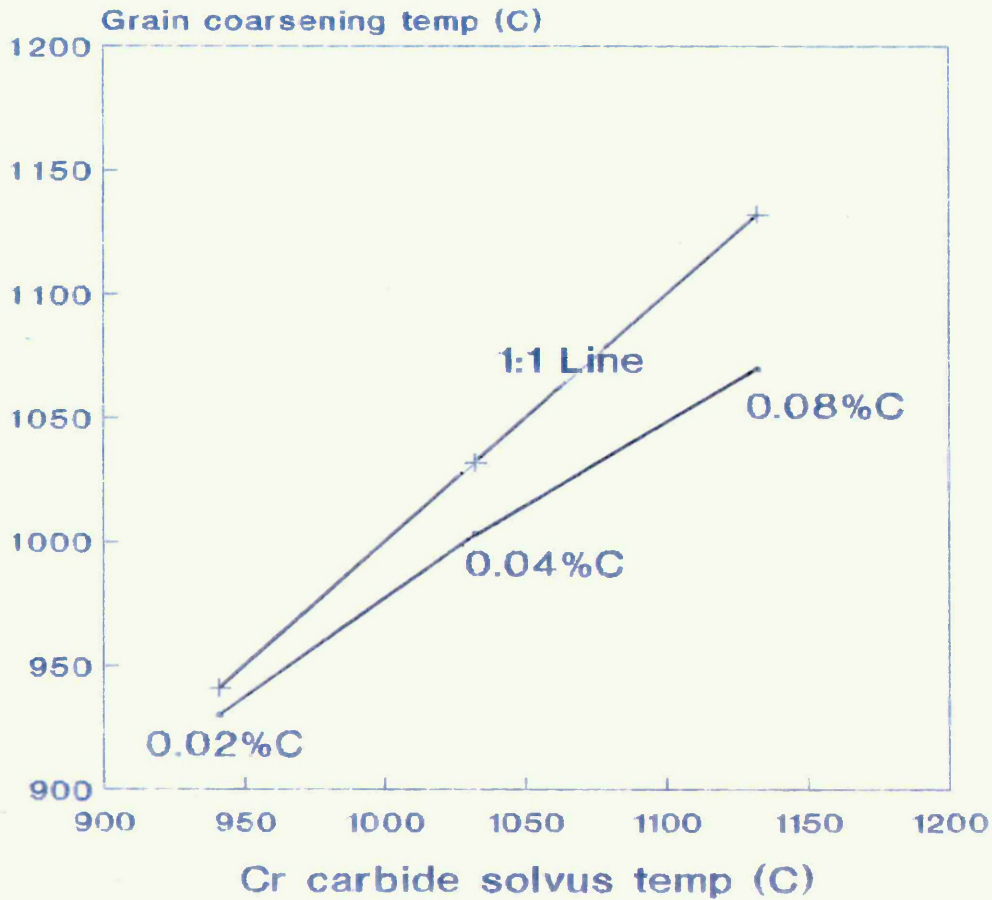


Figure 75

Comparison of actual Grain Coarsening Temperature with chromium carbide solvus temperature for Series II Alloys.

Note: Grain coarsening always begins before carbide solvus temperature is reached

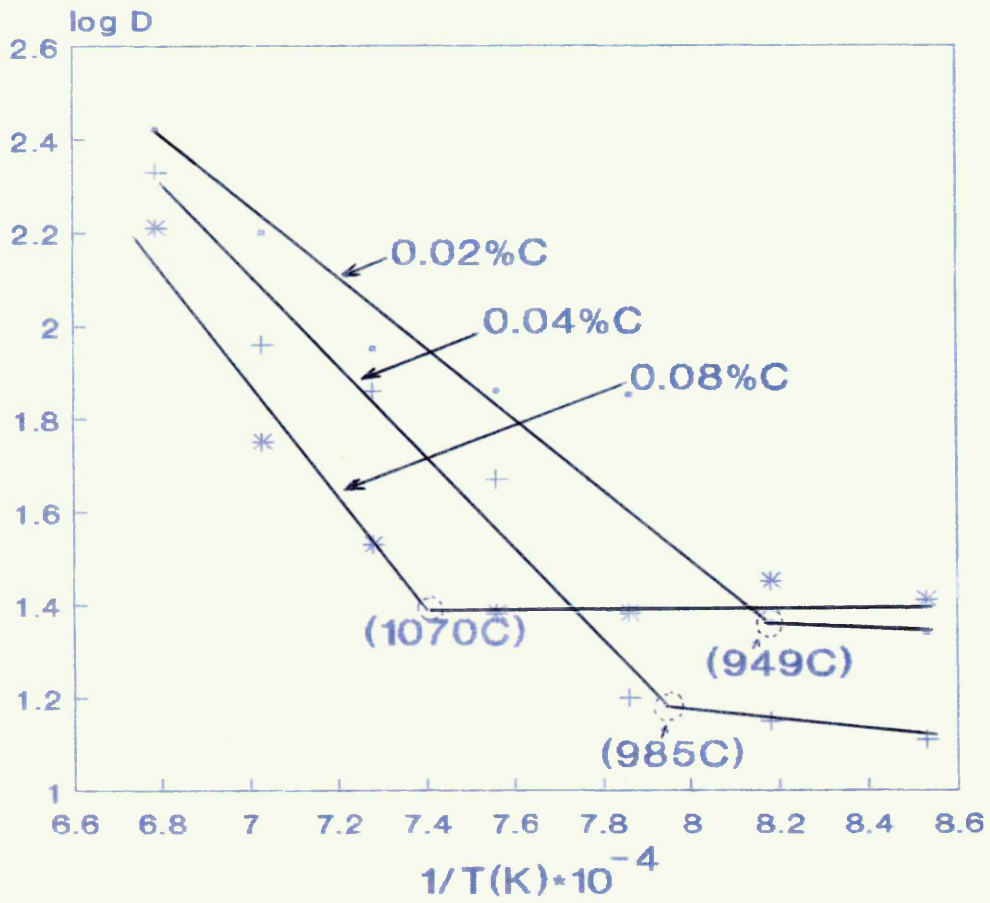


Figure 76 Temperature v Log grain size for
Series II Alloys

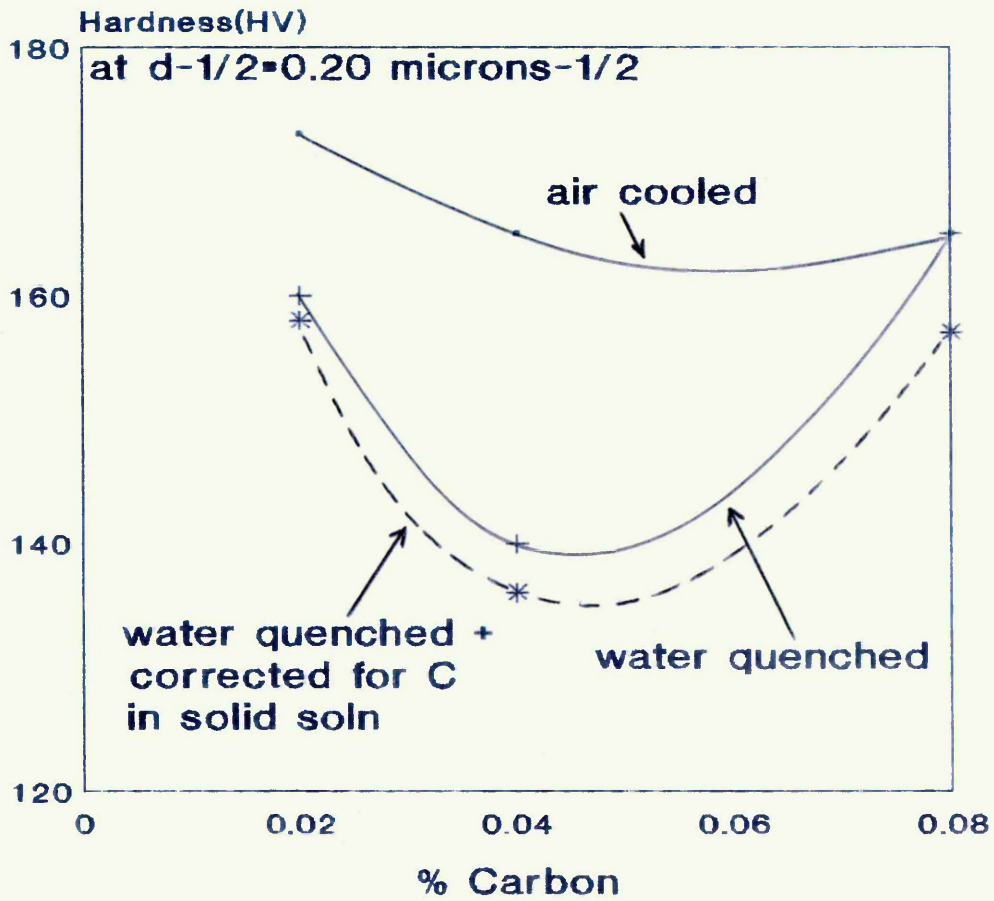


Figure 77 Effect of Carbon Content and Cooling Rate on the Hardness of Series II Alloys

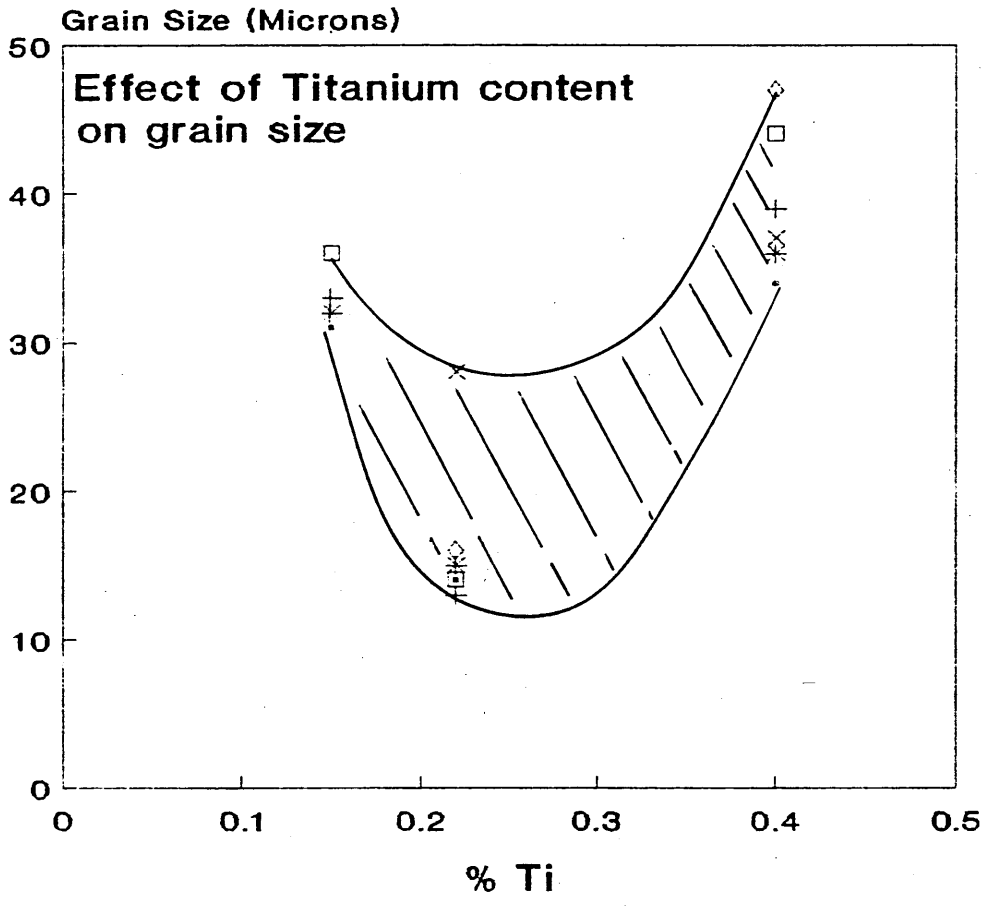


Figure 78 Effect Of Titanium content on Grain Size below the Grain Coarsening Temperature for Series ^{II} and ^{III} Alloys

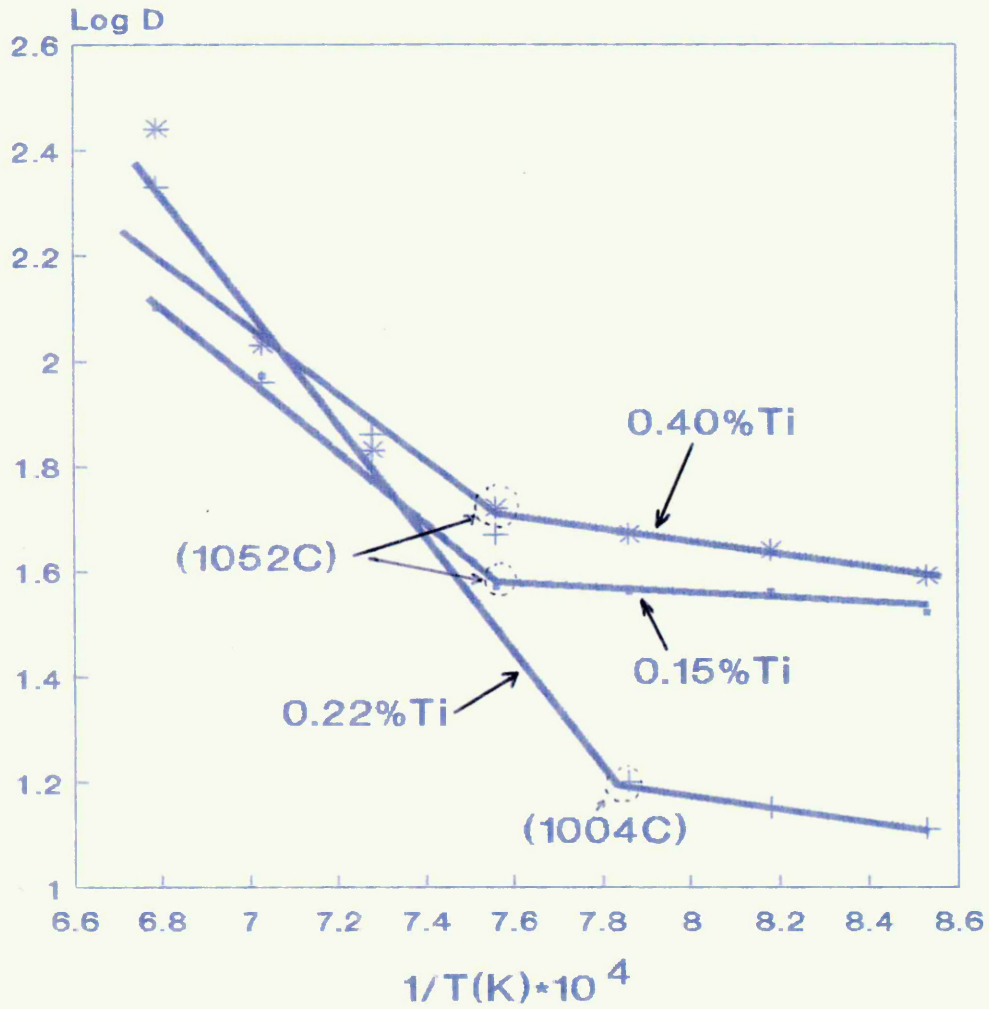


Figure 79 Temperature v Log Grain Size for Series III Alloys after Solution Treatment (WQ)

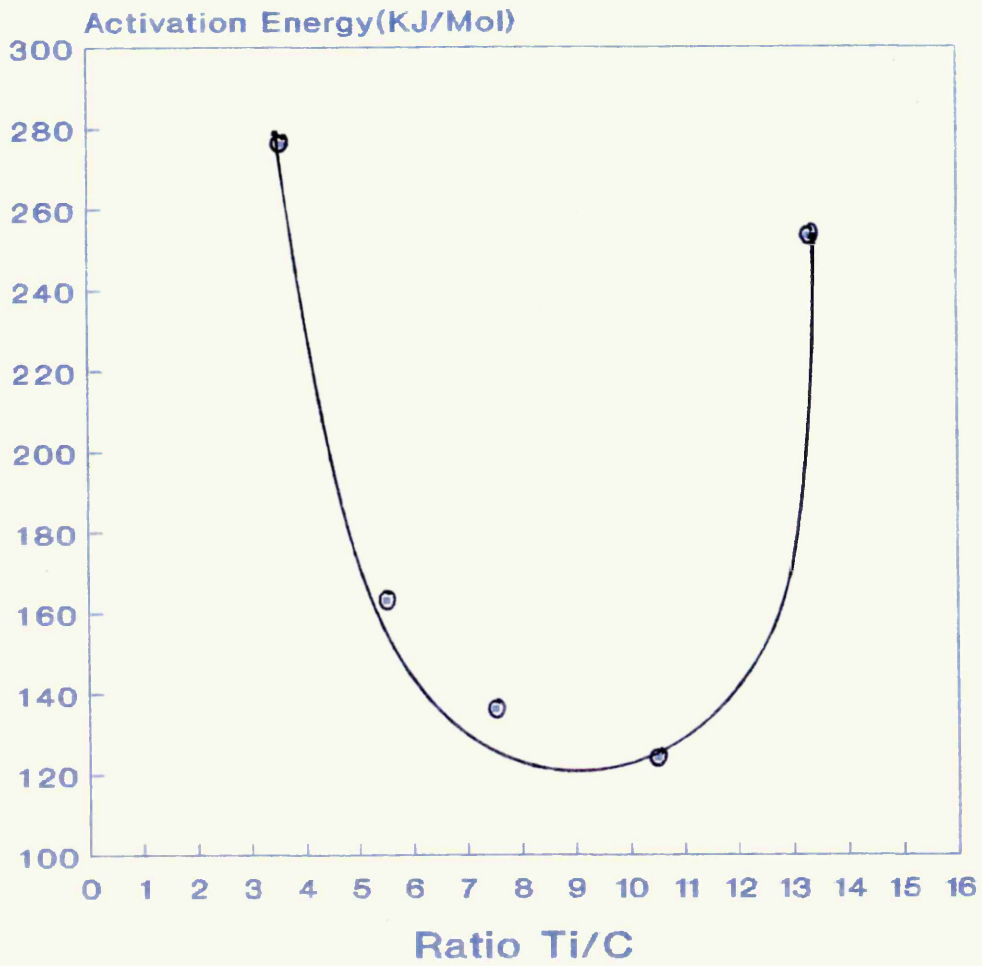


Figure 80 Effect of Ti/C Ratio on the Activation Energy for grain growth of Series ^{II and} III Alloys

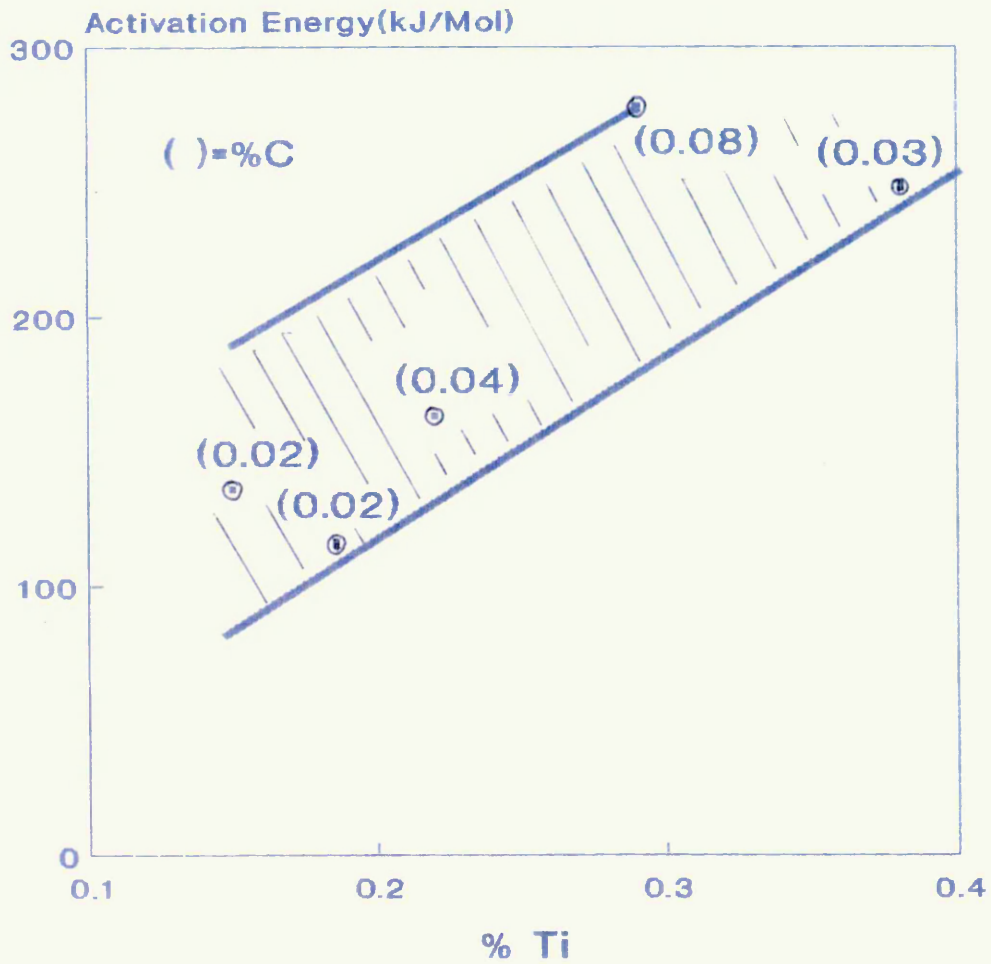


Figure 81 Effect of Titanium content on the
 Activation Energy for grain growth of
 Series ^{II} and ~~III~~ Alloys